

# NANOP

NANOPHOTONICS THE UBIQUITOUS SCIENCE

NANOPHOTONICS

AND

MICRO/NANO OPTICS

INTERNATIONAL CONFERENCE

/ OCT 1-3, 2018

ROME

BOOK OF ABSTRACTS

ISSN 2678-2987



Conferences, Events & Workshops

[premc.org/nanop](http://premc.org/nanop)

# Table of Contents

<b>Nanophotonics for a Green Internet</b>	<b>1</b>
<u>Prof. Dieter Bimberg</u>	
<b>Nano-Photonics of Super-Oscillations</b>	<b>2</b>
<u>Prof. Nikolay Zheludev</u>	
<b>Exciton diffusion of directed assembly of perovskite nanocrystals on patterned surfaces</b>	<b>3</b>
<u>Dr. Stefano Cabrini</u> , Dr. Erika Penzo, Dr. Alexander Weber Bargioni	
<b>Optical properties of metallic nanoparticles: from field enhancement to molecular detection</b>	<b>5</b>
<u>Prof. Lamy de la Chapelle Marc</u>	
<b>Three-dimensional disordered hyperuniform networks with a photonic bandgap</b>	<b>6</b>
<u>Dr. Jakub Haberkowicz</u> , Dr. Nicolas Muller, Dr. Catherine Marichy, Dr. Luis Froufe, Prof. Frank Scheffold	
<b>Linear and nonlinear optical properties of silicate oxide glasses containing metallic gold and silver nanoparticles</b>	<b>8</b>
<u>Dr. Krzysztof Dzierzega</u> , Dr. Nadia Pellerin, Ms. Aleksandra Gorczyca, Dr. Jean-philippe Blondeau, Dr. Witold Zawadzki, Dr. Stephane Pallerin, Mr. Babacar Diallo	
<b>Electrochemical investigation of plasmonic near-field and hot electron effects promoted by aluminium nanostructures</b>	<b>9</b>
<u>. Madasamy Thangamuthu</u> , Dr. Christian Santschi, Prof. Olivier Martin	
<b>On the use of Genetic Algorithm to Design and Optimize Graphene-based Absorbers</b>	<b>11</b>
<u>Mr. Hamidreza Taghvaei</u> , Dr. Sergi Abadal, Prof. Albert Cabellos-Aparicio, Prof. Eduard Alarcón	
<b>Novel Phenomena in Optical Manipulation due to Magnetic-Field-Induced Resonant States</b>	<b>12</b>
<u>Ms. Shulamit Edelstein</u> , Dr. R. M. Abraham Ekereth, Dr. P. A. Serena, Prof. J. J. Saenz, Dr. A. García-Martín, Prof. M. I. Marques	
<b>Light creation without pump: tuning plasmonic resonance for surface enhanced chemiluminescence</b>	<b>13</b>
<u>Mr. Daler Dadadzhanov</u> , Dr. Tigran Vartanyan, Dr. Alina Karabchevsky	
<b>Effects of manifold gaps on SERS enhancement in coupled plasmonic nanoantennas</b>	<b>14</b>
<u>Prof. Patrizio Candeloro</u> , Dr. Marialaura Coluccio, Dr. Gerardo Perozziello, Dr. Mario Russo, Prof. Enzo Di Fabrizio	
<b>Stimulated emission of dye molecules coupled to localized plasmons in Ag nanoparticles</b>	<b>16</b>
<u>Dr. Nikita Toropov</u> , Ms. Aisylu Kamaliev, Dr. Tigran Vartanyan	
<b>Influence of angular momentum of light on excitation of near field hot spots</b>	<b>17</b>
<u>Dr. Marco Allione</u> , Dr. Andrea Giugni, Dr. Bruno Torre, Prof. Enzo Di Fabrizio	
<b>Optical Waveguides in Oxidised Porous Silicon</b>	<b>18</b>
<u>Mr. Alexander Kellarev</u> , Prof. Shlomo Ruschin	

---

<b>SERS studies on DNA: optimization of experimental conditions.</b>	20
<u>Ms. Edyta Pyrak, Dr. Aleksandra Jaworska, Prof. Tomasz Wilanowski, Prof. Andrzej Kudelski</u>	
<b>Triple dyes-labeled polyelectrolyte microcapsules@gold nanoparticles for anthocyanins delivery as topical administration for tumor skin cells</b>	21
<u>Ms. Raluca Flavia Ghiman, Dr. Dumitrita Rugina, Dr. Monica Focsan, Ms. Andreea Campu, Prof. Adela Pintea, Prof. Simion Astilean</u>	
<b>Simple and Reliable Patterning of Plasmonic Nanostructures by Spontaneous Adhesion Lithography</b>	22
<u>Dr. Sihai Luo, Prof. Bård Helge Hoff, Prof. John De Mello</u>	
<b>Tunable degree of second order coherence for radiation of plasmonic structure excited by single photon source</b>	23
<u>Mr. Nikita Nefedkin, Dr. Evgeny Andrianov, Prof. Alexander Pukhov, Prof. Alexey Vinogradov</u>	
<b>An Intensity Enhanced High-Resolution Spectrometer In “Water Window”.</b>	24
<u>Mr. Zhuo Li, Dr. Bin Li</u>	
<b>Collective Enhanced IR Absorption plasmonic device for conformational studies of biomolecules in physiological conditions</b>	25
<u>Mr. Paolo Zucchiatti, Dr. Andrea Cerea, Dr. Marta Semrau, Dr. Giovanni Birarda, Dr. Andrea Toma, Dr. Paola Storici, Dr. Lisa Vaccari</u>	
<b>A 3D finite element model for waveguide-based plasmonic sensors</b>	27
<u>Dr. Guillaume Demesy, Prof. Gilles Renversez</u>	
<b>Decay-rate enhancement of spontaneous emitters coupled to Bloch Surface Waves on one-dimensional photonic crystals.</b>	29
<u>Dr. Angelo Angelini, Mr. Ugo Stella, Dr. Francesca Frascella, Dr. Natascia De Leo, Dr. Luca Boarino, Prof. Emiliano Descrovi</u>	
<b>Optimizing band-edge slow light in Silicon-On-Insulator grating waveguides</b>	30
<u>Prof. Lucio Andreani, Mr. Marco Passoni, Prof. Dario Gerace, Dr. Liam O’Faolain</u>	
<b>Ultra-Narrow Bandwidth Acousto-Optic Filter</b>	32
<u>Prof. Nikolai Petrov, Prof. Vladislav Pustovoit</u>	
<b>Influence of strains on the structural and optical properties of nanoheterostructures with quantum island arrays and quantum wells based on group IV elements Ge, Si and Sn</b>	34
<u>Dr. Vyacheslav Timofeev, Dr. Alexander Nikiforov, Dr. Vladimir Mashanov, Dr. Ivan Loshkarev, Ms. Natalia Baidakova</u>	
<b>Magnetic and optical properties of gold coated iron oxide nanoparticles</b>	35
<u>Mr. Alexander Omelyanchik, Ms. Maria Efremova, Mr. Maxim Abakumov, Dr. Alexander Majouga, Dr. Ilia Samusev, Dr. Natalya Myslitskaya, Mr. Andrey Zyubin, Dr. Valeria Rodionova</u>	
<b>Chromogen-free color interference-based biosensors for visual detection of viruses.</b>	36
<u>Ms. Ana Frosiniuk, Dr. Vladimir Vinogradov</u>	
<b>Upconversion metal oxide aerogels for diagnostics and sorption of toxicants</b>	37
<u>Mr. Daniil Ilatovskii, Dr. Pavel Krivoshapkin, Dr. Elena Krivoshapkina, Mr. Grigoriy Kiselev, Dr. Vladimir Vinogradov</u>	

---

---

<b>Diagnose of biomolecules using Raman interactions of the light</b>	<b>38</b>
Prof. Enachi Nicolae, <u>Dr. Turcan Marina</u> , Dr. Ristoscu Carmen, Prof. Mihailescu Ion	
<b>Nonlinear behavior of silver nano-films in cw regime</b>	<b>39</b>
<u>Prof. Husam Abu-Safe</u>	
<b>Enhancing, controlling and guiding light with high refractive index dielectric nanoantennas</b>	<b>40</b>
Ms. Angela I. Barreda, Dr. Toshihiko Shibamura, Prof. Stefan A Maier, Prof. Francisco Gonzalez, Prof. Fernando Moreno, <u>Dr. Pablo Albella</u>	
<b>On chip resonant optical sensors</b>	<b>42</b>
<u>Prof. Yves-Alain Peter</u>	
<b>Effect of local time-periodic perturbations on the topological edge mode of the SSH-model</b>	<b>44</b>
<u>Prof. Stefan Linden</u> , Mrs. Zlata Cherpakova	
<b>Encoded SERS nanotags for multiplex bioassays</b>	<b>45</b>
<u>Prof. Xiangwei Zhao</u>	
<b>Oxidation effects on the SERS response of silver nanoprism arrays</b>	<b>46</b>
Dr. Niccolò Michieli, <u>Dr. Roberto pilot</u> , Dr. Valentina Russo, Dr. Carlo Scian, Dr. Francesco Todescato, Prof. Raffaella Signorini, Prof. Stefano Agnoli, Prof. Tiziana Cesca, Prof. Renato Bozio, Prof. Giovanni Mattei	
<b>Raman of Nano-objects at subwavelength scales</b>	<b>47</b>
<u>Prof. bernard Humbert</u> , Dr. Angéline D'orlando, Dr. Maxime Bayle, Prof. Guy Louarn	
<b>Towards DNA biosensors: SERS studies on oligonucleotides</b>	<b>48</b>
<u>Dr. Aleksandra Jaworska</u> , Ms. Edyta Pyrak, Prof. Andrzej Kudelski	
<b>Optical paddle - a new microtool for optical tweezers</b>	<b>50</b>
<u>Ms. Weronika Lamperska</u> , Dr. Sławomir Drobczyński, Dr. Piotr Wasylczyk, Dr. Jan Masajada	
<b>2D nanomaterials enhanced surface plasmon resonance for sensing applications</b>	<b>51</b>
<u>Dr. Shuwen Zeng</u>	
<b>Nanoplasmonic NO<sub>2</sub> sensing with a Au-WO<sub>3</sub> Nanocomposite</b>	<b>52</b>
<u>Dr. Irem Tanyeli</u> , Dr. Olof Andersson, Prof. Christoph Langhammer	
<b>GFP-based Nanothermometry at the Mitochondria</b>	<b>53</b>
<u>Dr. Oleksandr A. Savchuk</u> , Dr. Oscar F. Silvestre, Mr. Ricardo M. R. Adão, Dr. Jana B. Nieder	
<b>Enhancing hydrodynamic nonlocal resonances in semiconductor plasmonics</b>	<b>55</b>
Ms. Tahereh Golestanizadeh, Dr. Johan Maack, Prof. N. Asger Mortensen, Dr. Tahmineh Jalali, Dr. Abbas Zarifi, <u>Dr. Martijn Wubs</u>	
<b>Transverse Anderson localization of channel plasmon polaritons</b>	<b>57</b>
<u>Dr. Jiří Petráček</u> , Dr. Vladimír Kuzmiak	
<b>Single-emitter and collective effects in light emission from ordered arrays of InGaN-GaN nanowires</b>	<b>59</b>
<u>Dr. Duncan Allsopp</u> , Dr. Chris Lewins, Dr. Szymon Lis, Dr. Simon O'kane, Dr. Pierre-marie Coulon, Dr. Emmanuel Le Boulbar, Dr. Margaret Hopkins, Dr. Philip Shields	

---

<b>Whispering gallery modes in novel silicon nanophotonic resonators</b>	<b>60</b>
<u>Dr. Sebastian Schmitt</u> , Dr. Klaus Schwarzburg, Mr. Christian Appelt, Dr. Hanno Kröncke, Mr. Sven Wiesner, Prof. Catherine Dubourdieu	
<b>Attojoule Modulators for Photonic Neuromorphic Computing</b>	<b>61</b>
Mr. Jonathan George, Mr. Amin Mehrabian, Mr. Rubab Armin, Prof. Tarek El-Ghazawi, Prof. Paul Prucnal, Prof. Volker Sorger	
<b>Nano-scale luminescence imaging and properties of radially-heterostructured III-V nanowires</b>	<b>63</b>
<u>Dr. PAOLA PRETE</u> , Prof. Nico Lovergine	
<b>Amplified spontaneous emission, Purcell effect, lasing, and light emitting diodes from perovskite nanocrystal films</b>	<b>64</b>
<u>Dr. Roman Krahne</u>	
<b>Nonlinear THz Plasmonics in Bi<sub>2</sub>Se<sub>3</sub> Topological Insulator</b>	<b>65</b>
<u>Dr. Paola Di Pietro</u> , Dr. Nidhi Adhlakha, Dr. Federica Piccirilli, Dr. Alessandra Di Gaspare, Prof. Seangshik Oh, Dr. Andrea Perucchi, Prof. Stefano Lupi	
<b>Structural and transport investigation of two different types of organic-inorganic halide perovskite structures.</b>	<b>66</b>
<u>Dr. Andrea Giugni</u> , Dr. Bruno Torre, Dr. Marco Allione, Dr. Ayan Zhumekenov, Prof. Osman Bakr, Mrs. Erlin Nurlianti, Prof. Jr-Hau He, Prof. Enzo Di Fabrizio	
<b>Light Controlled Assembly of Silver Nanoparticles</b>	<b>67</b>
<u>Mr. Ivan Shutsko</u> , Mr. Andreas Polywka, Mr. Christian Tückmantel, Prof. Patrick Görrn	
<b>Does location matter? Hot-electron driven selective photosynthesis of catalytic nanoparticles</b>	<b>68</b>
<u>Ms. Evgenia Kontoleta</u> , Dr. Sven Askes, Prof. Erik Garnett	
<b>Chiroptical Response of Geometrically Symmetric Nanoscopic Heterostructures</b>	<b>69</b>
<u>Mr. Rene Barczyk</u> , Dr. Sergey Nechayev, Dr. Peter Banzer	
<b>Possible polaritons-mediated light emission from nanostructured polyaniline with no external resonant microcavity</b>	<b>70</b>
<u>Prof. Jerzy J. Langer</u> , Ms. Ewelina Frąckowiak, Ms. Katarzyna Ratajczak	
<b>Carrier cooling dynamics in inorganic perovskites</b>	<b>72</b>
<u>Prof. Anna Vinattieri</u> , Dr. Fabio Gabelloni, Dr. Francesco Biccari, Dr. Giulia Andreotti, Dr. Nicola Calisi, Dr. Stefano Caporali	
<b>Nanopatterning of sol-gel derived luminescent thin films as a promising tool to enhance extraction efficiency in LEDs devices</b>	<b>73</b>
Dr. Jeff NYALOSASO, <u>Dr. Audrey Potdevin</u> , Dr. Rachid Mahiou, Dr. François Réveret, Prof. Pierre Disseix, Prof. Geneviève Chadeyron	
<b>Optical properties of III-V nanostructures for optoelectronic applications</b>	<b>74</b>
<u>Dr. Nabiha Ben Sedrine</u> , Mr. J. Cardoso, Dr. J. Rodrigues, Ms. J. P. Teixeira, Ms. A. Alves, Dr. R. Ribeiro-andrade, Prof. A. Gustafsson, Dr. P. M. P. Salomé, Prof. J. C. González, Mr. D. Nd. Faye, Dr. M. Belloeil, Prof. Bruno Daudin, Prof. M. Bockowski, Prof. V. Hoffmann, Prof. M. Weyers, Dr. Eduardo Alves, Prof. Katharina Lorenz, Prof. A. J. Neves, Prof. J. P. Leitão, Prof. M. R. Correia, Prof. Teresa Monteiro	

<b>Graphene to Graphite; a Layer by Layer Experimental and Simulation Investigation of Electric and Optical Properties</b>	<b>76</b>
<u>Prof. Maher Amer, Mr. Mohammed Mohammed, Prof. Udo Schwingenschloegl</u>	
<b>Structural studies of nonpolar (10-10) ZnO/ZnMgO monolithic multiquantum well structures</b>	<b>78</b>
<u>Prof. Adrian Kozanecki, Mr. Jacek Sajkowski, Dr. Eduardo Alves, Dr. Sergio Magalhaes, Dr. Serhii Kryvyi, Ms. Agnieszka Pieniazek, Ms. Anna Reszka, Mr. Dawid Jarosz, Dr. Marcin Stachowicz, Dr. Ewa Przewdziecka, Dr. Mieczyslaw Pietrzyk</u>	
<b>Ultra-broadband directive scattering of silicon nanoparticles in the optical range</b>	<b>79</b>
<u>Dr. Kseniia Baryshnikova, Mr. Pavel D. Terekhov, Mr. Hadi K. Shamkhi, Mr. Dmitry N. Gulkin, Mr. Benyimin Hadad, Dr. Vladimir O. Bessonov, Dr. Alina Karabchevsky, Dr. Andrey A. Fedyanin, Dr. Alexander S. Shalin</u>	
<b>Dynamic functional metasurfaces at optical frequencies</b>	<b>80</b>
<u>Dr. Ping Yu, Dr. Jianxiong Li, Prof. Shuang Zhang, Dr. Michael Hirscher, Prof. Na Liu</u>	
<b>Cavities of monolithic subwavelength grating VCSELs</b>	<b>81</b>
<u>Prof. Tomasz Czyszanowski, Dr. Marcin Gębski, Prof. James Lott</u>	
<b>Utilizing of holographic principles for efficient excitation of plasmonic waveguide</b>	<b>83</b>
<u>Prof. Alexander Merzlikin, Dr. Anton Ignatov</u>	
<b>From optical magnetism to second-order spatial dispersion in self-assembled metamaterials</b>	<b>84</b>
<u>Prof. Alexandre Baron, Dr. Quentin Flamant, Dr. Philippe Richetti, Prof. Serge Ravaine, Dr. Virginie Ponsinet, Dr. Philippe Barois, Mrs. Veronique Many, Prof. Etienne Duguet, Prof. Mona Treguer-delapierre, Mrs. Sara De Cicco, Dr. Jean-baptiste Salmon, Dr. Jacques Leng</u>	
<b>Size and host-medium effects on topologically protected surface states in bi-anisotropic 3D optical waveguides</b>	<b>85</b>
<u>Prof. Vasily Klimov</u>	
<b>All-semiconductor plasmonic metamaterials for mid-infrared perfect absorption and selective thermal emission</b>	<b>87</b>
<u>Dr. Franziska Barho, Dr. Fernando Gonzalez-Posada Flores, Dr. Laurent Cerutti, Prof. Thierry Taliercio</u>	
<b>Latest Progress in Spasers</b>	<b>89</b>
<u>Prof. Mark Stockman</u>	
<b>The DNA origami route for nanoplasmonics</b>	<b>90</b>
<u>Prof. Na Liu</u>	
<b>Quantum and non-linear optics with semiconductor microcavities</b>	<b>91</b>
<u>Prof. Aristide Lemaitre</u>	
<b>Semiconductor Hetero-Nanowires on Silicon for Photonic Applications</b>	<b>92</b>
<u>Prof. Gerhard Abstreiter</u>	
<b>Semiconductor plasmonic resonances in the mid-IR range adjusted by thermal annealing</b>	<b>93</b>
<u>Mr. Guilhem Pacot, Dr. Maria Jose Milla Rodrigo, Dr. Fernando Gonzalez-Posada Flores, Dr. Franziska Barho, Mr. Mario Bomers, Dr. Laurent Cerutti, Prof. Eric Tournié, Prof. Thierry Taliercio</u>	
<b>Shannon entropy and avoided crossings in optical microcavities</b>	<b>95</b>
<u>Dr. Park Kyuwon, Dr. Moon Songki, Dr. Shin Younghoon, Mr. Kim Jinuk, Dr. Jeong Kabgyun</u>	

<b>Plasmon enhanced generation of stimulated emission of laser dyes in pores of Al<sub>2</sub>O<sub>3</sub></b>	<b>97</b>
Prof. Aitbek Aimukhanov, Prof. <u>Niyazbek Ibrayev</u>	
<b>Near-field imaging of surface-plasmon vortex-modes on a gold film with a single elliptical nanohole</b>	<b>98</b>
Dr. <u>Claudia Triolo</u> , Prof. Salvatore Savasta, Dr. Sebastiano Trusso, Prof. Rosalba Saija, Dr. Nisha Agarwal, Prof. Salvatore Patanè	
<b>A Parametric Analysis of Phase-gradient Meta-tips for Label-free Sensing Applications</b>	<b>99</b>
Dr. <u>Maria Principe</u> , Prof. Marco Consales, Prof. Giuseppe Castaldi, Prof. Vincenzo Galdi, Prof. Andrea Cusano	
<b>Improved stability and sensitivity of plasmonics metal layers with MPTS adhesion layer and CVD grown graphene transfer in water</b>	<b>101</b>
Mr. <u>Quaid Zaman</u> , Mr. André Do Nascimento Barbosa, Dr. Omar Pandoli, Dr. Ricardo Queiroz Aucélio, Dr. Marco Cremona, Dr. Fernando Lázaro Freire Júnior, Dr. Tommaso Del Rosso	
<b>Fluorescence Magnetic Immunoassays Using Graphene Quantum Dots and Fe<sub>2</sub>O<sub>3</sub>@SiO<sub>2</sub> Composite for AFP Detection</b>	<b>103</b>
Ms. <u>Yun TENG</u> , Prof. Philip W. T. Pong	
<b>Strain sensitivity of surface plasmon-polaritons excitation by attenuated total reflection in graphene</b>	<b>105</b>
Mr. <u>Maksim Usik</u> , Dr. Dmitry Kuzmin, Prof. Igor Bychkov, Prof. Vladimir Shavrov	
<b>710 nm red light source based on cascaded nonlinear optical processes for use in biomedical application.</b>	<b>106</b>
Dr. <u>Juan Gonzalez</u> , Dr. Liliana Martinez, Dr. Roger Cudney, Dr. Jose Enriquez, Dr. Rurik Farias, Mr. Eduardo Melendez	
<b>Identification of bacteria using surface-enhanced Raman spectroscopy</b>	<b>107</b>
Dr. Dmitry Kopitsyn, Mr. Maksim Gorbachevskii, Dr. Ekaterina Botchkova, Ms. Maria Bychenko, Dr. Pawel Gushchin, Dr. <u>Andrei Novikov</u>	
<b>Rough silver films for surface plasmons generation and SERS optical properties study</b>	<b>108</b>
Dr. <u>Ilya Samusev</u> , Dr. Anna Tcibulnikova, Ms. Elizaveta Konstantinova, Mr. Andrey Zyubin, Dr. Vasily Slezhkin, Prof. Valery Bryukhanov, Ms. Polina Medvedskaya, Mr. Ivan Lyatun, Mr. Aleksandr Vinichenko, Dr. Maksim Demin	
<b>Numerical simulation of light extraction efficiency of GaN-based blue micro-LED structures</b>	<b>109</b>
Prof. <u>Han-Youl Ryu</u>	
<b>Planar focusing reflectors based on high contrast gratings</b>	<b>110</b>
Dr. <u>Paulina Komar</u> , Dr. Marcin Gębski, Dr. Maciej Dems, Prof. Tomasz Czyszanowski, Dr. Michał Wasiak	
<b>Observation of Surface Plasmons in Subwavelength Gratings</b>	<b>111</b>
Prof. <u>Nikolai Petrov</u> , Mr. Victor Danilov, Dr. Vladimir Popov, Mr. Boris Usievich	
<b>Enhanced Raman spectroscopy of proteins on native cell membranes stretched on super-hydrophobic surface.</b>	<b>112</b>
Dr. <u>Manola Moretti</u> , Dr. Marco Allione, Dr. Maria Teresa De Angelis, Prof. Giovanni Cuda, Prof. Enzo Di Fabrizio	
<b>Dynamic Metasurface based optical cavity for enhanced optical phase modulation</b>	<b>113</b>
Mr. <u>Tayyab Nouman</u> , Prof. Jae-hyung Jang, Mr. Ji Hyun Hwang, Mr. Gyejung Lee	
<b>Particle sizing and concentration through elastic light scattering at small angles</b>	<b>115</b>
Prof. <u>MIGUEL CASAS-RAMOS</u> , Dr. Eduardo Sandoval-romero	

<b>Hydrogel-based plasmonic sensor system</b>	<b>116</b>
<u>Mr. Christoph Kroh, Mr. Roland Wuchrer, Dr. David Ulkoski, Dr. Margarita Günther, Prof. Carmen Scholz, Prof. Thomas Härtling, Prof. Gerald Gerlach</u>	
<b>Thermoplasmonic maskless lithography assisted by gold nanostars</b>	<b>117</b>
<u>Dr. Eduardo Martínez, Prof. Ricardo Urbano, Prof. Carlos Rettori</u>	
<b>High efficiency gradient index GaN metasurfaces</b>	<b>119</b>
<u>Mr. Gauthier Briere, Mr. Nikolai Schmitt, Mr. Niklas Georg, Mr. Dimitrios Loukrezis, Dr. Patrice Genevet, Dr. Stéphane Lanteri, Prof. Ulrich Römer, Prof. Claire Scheid</u>	
<b>Raman scattering for InAsSb</b>	<b>120</b>
<u>Mr. Krzysztof Murawski, Dr. Kacper Grodecki, Mr. Krystian Michalczewski, Mr. Bogusław Budner, Prof. Piotr Martyniuk</u>	
<b>Numerical investigation on metamaterial side of epoxy resins at visible light</b>	<b>121</b>
<u>Ms. HANAN ALI</u>	
<b>Indirect nanoplasmonic sensing.</b>	<b>122</b>
<u>Dr. Benjamin Demirdjian, Dr. Igor Ozerov, Mr. Alain Ranguis, Mr. Frédéric Bedu, Dr. Claude R. Henry</u>	
<b>Numerical modelling of green and red emitting quantum dot based optical films by Monte Carlo ray tracing method for smartphone display applications</b>	<b>123</b>
<u>Mr. S. Efdal Mutcu, Dr. Güneş Aydınođan, Mr. Sezer Caynak, Mr. Sadra Sadeghi, Mr. Kivanç Karşlı, Prof. Sedat Nizamoglu</u>	
<b>Inkjet printing of anisotropic structures by cellulose nanocrystals</b>	<b>125</b>
<u>Ms. Elena Eremeeva, Prof. Alexandr Vinogradov, Prof. Vladimir Vinogradov</u>	
<b>Numerical computation of plasmonic resonances in dispersive media: Application to metallic gratings</b>	<b>126</b>
<u>Dr. Guillaume Demesy, Dr. Boris Gralak, Prof. André Nicolet</u>	
<b>Multipole analysis of metasurfaces composed of nanoparticles supporting electric and magnetic optical resonances</b>	<b>127</b>
<u>Dr. Andrey B. Evlyukhin</u>	
<b>Pixel-level Microsecond Electrical Switching of Infrared Transparent Phase Change Materials</b>	<b>128</b>
<u>Dr. Vladimir Liberman, Mr. Yifei Zhang, Dr. Mikhail Shalaginov, Mr. Paul Robinson, Dr. Christopher Roberts, Dr. Myungkoo Kang, Dr. Yadav Anupama, Prof. Kathleen Richardson, Prof. Juejun Hu, Dr. Jeffrey Chou</u>	
<b>Transitions between States in Topological Waveguide Systems by Time-Periodic Driving</b>	<b>130</b>
<u>Ms. Christina Jörg, Mr. Christoph Dauer, Mr. Fabian Letscher, Prof. Sebastian Eggert, Prof. Michael Fleischhauer, Prof. Georg Von Freymann</u>	
<b>Metamaterials for manipulating light polarization</b>	<b>132</b>
<u>Dr. Jakub Haberkow, Dr. Michal Nawrot, Dr. Lukasz Zinkiewicz, Dr. Piotr Wasylczyk</u>	
<b>Switchable Holographic Device Using Electrochemical Method</b>	<b>134</b>
<u>Dr. Seong M. Cho, Ms. Sujung Kim, Dr. Yong-Hae Kim, Dr. Tae-Youb Kim, Dr. Sang Hoon Cheon, Dr. Joo Yeon Kim, Dr. Chil Seong Ah, Ms. Juhee Song, Dr. Hojun Ryu, Dr. Chi-Sun Hwang, Dr. Jeong-Ik Lee</u>	



<b>Nanoparticles obtained via solid state dewetting of silver thin film</b>	<b>136</b>
Dr. Iryna Gozhyk, Dr. Paul Jacquet, Ms. Barbara Bouteille, Dr. Renaud Podor, Mr. Johann Ravaux, Mr. Joseph Lautru, Dr. Morten Kildemo, Dr. Romain Dezert, Dr. Alexandre Baron, Dr. Jacques Jupille, Dr. Rémi Lazzari, Dr. Jeremie Teisseire	
<b>Superradiant properties of Collective plasmon modes in ultra-dense film of silver nanoparticles</b>	<b>137</b>
Dr. Julien Laverdant, Mr. Gérard Colas Des Francs, Mr. Hugo Varguet, Dr. Jean-michel Benoit, Mr. Ruben Mascart, Dr. Jeremie Margueritat, <u>Dr. Alice Berthelot</u>	
<b>Fundamental Limits in the Coupling between Light and 2D Polaritons</b>	<b>138</b>
<u>Mr. Eduardo Brioso Dias</u> , Prof. Javier García de Abajo	
<b>Characterization of Airy Surface Plasmon Polaritons by Photoemission Electron Microscopy</b>	<b>139</b>
<u>Mr. Matthias Falkner</u> , Mr. Amit V. Singh, Dr. Goran Isic, Prof. Thomas Pertsch	
<b>Nonlinear semiconductor superlattices for the Gigahertz to the Mid Infrared ranges</b>	<b>140</b>
<u>Prof. Mauro Fernandes Pereira</u> , Dr. Apostolos Apostolakis, Mr. Vladimir Anfertev, Prof. Vladimir Vaks	
<b>Clusters of nanoparticles as isotropic Huygens sources for metasurfaces applications</b>	<b>142</b>
Mr. Romain Dezert, Dr. Philippe Richetti, <u>Prof. Alexandre Baron</u>	
<b>Plasmonic Luneburg lens characterization with phase detection</b>	<b>143</b>
<u>Dr. César E. García-Ortiz</u> , Dr. Rodolfo Cortés-Martínez, Dr. Jesus Gomez-Correa, Dr. Eduardo Pisano, Dr. Jacek Fiutowski, Dr. Victor Ruiz-cortes, Dr. Víctor M. Coello-Cárdenas	
<b>Polymer distributed Bragg reflectors: an old structure with unexpected sensing capabilities</b>	<b>146</b>
<u>Dr. Paola Lova</u> , Prof. Alberto Servida, Prof. Davide Comoretto	
<b>Imaging-based molecular barcoding with pixelated dielectric metasurfaces</b>	<b>148</b>
<u>Dr. Andreas Tittl</u> , Mr. Aleksandrs Leitis, Dr. Mingkai Liu, Dr. Filiz Yesilkoy, Prof. Duk-Yong Choi, Prof. Dragomir Neshev, Prof. Yuri Kivshar, Prof. Hatice Altug	
<b>Silver Nanoparticle Films with Highly Tunable Plasmon Properties: Tuning the Plasmon Resonance Band for X-Ray Detection</b>	<b>150</b>
<u>Dr. Eder Guidelli</u> , Prof. David Clarke, Prof. Oswaldo Baffa	
<b>Flexible SERS Membrane: a Universal Platform for Quantitative SERS Analysis</b>	<b>151</b>
<u>Dr. Qi Hao</u> , Dr. Libo Ma, Prof. Oliver G. Schmidt	
<b>LAB ON FIBER SERS OPTRODES BY NANOSPHERE LITHOGRAPHY</b>	<b>152</b>
Dr. Giuseppe Quero, Dr. Gianluigi Zito, Dr. Stefano Managò, Dr. Francesco Galeotti, <u>Dr. Marco Pisco</u> , Dr. Anna Chiara De Luca, Prof. Andrea Cusano	
<b>Hot carriers on organic semiconductors: relating mechanics and electronic properties.</b>	<b>154</b>
<u>Dr. Bruno Torre</u> , Dr. Andrea Giugni, Dr. Marco Allione, Ms. Xinyu Zhang, Prof. Enzo Di Fabrizio	
<b>Chiral coupling of atoms near plasmonic and photonic interfaces</b>	<b>155</b>
<u>Dr. Mihail Petrov</u> , Mr. Danil Kornovan, Dr. Ivan Iorsh	
<b>Nonlinear atom-plasmon interactions enabled by nanostructured graphene</b>	<b>157</b>
<u>Dr. Joel Cox</u> , Prof. Javier García De Abajo	
<b>Bright and Stable Single-Photon Emission from Single Molecules in Organic Nanocrystals</b>	<b>158</b>
<u>Mrs. Sofia Pazzagli</u>	

<b>Fine structure splitting energy correction for single quantum dot via quadrupole potential</b>	<b>159</b>
<u>Mr. Mohd Zeeshan</u> , Mr. Nachiket Sherlekar, Mr. Arash Ahmadi, Dr. Sandra Gibson, Prof. Michael Reimer	
<b>Quantum Nonlinear Optics in Nanoscale Waveguides</b>	<b>161</b>
<u>Dr. Hashem Zoubi</u>	
<b>Weak Measurement of the Dipolar Emitter Polarization State via its Far-Field Polarization Singularities</b>	<b>163</b>
<u>Dr. Sergey Nechayev</u> , Dr. Martin Neugebauer, Mr. Martin Vorndran, Prof. Gerd Leuchs, Dr. Peter Banzer	
<b>Urban Heat Island Mitigation with PbS quantum dots</b>	<b>164</b>
<u>Ms. Samira Garshasbi</u> , Prof. Mat Santamouris, Prof. Shujuan Huang	
<b>Revealing local material properties with high resolution optical microscopy</b>	<b>165</b>
Dr. Marius Van Den Berg, Mr. Tobias Koeninger, Mr. Yu-ting Chen, Dr. Anke Horneber, Prof. Alfred Meixner, <u>Dr. Dai Zhang</u>	
<b>Enhanced multimodal biosensing using plasmonic paper-based nanoplatfoms</b>	<b>166</b>
<u>Ms. Andreea Campu</u> , Mr. Filip Orzan, Dr. Frederic Lerouge, Prof. Stephane Parola, Prof. Simion Astilean, Dr. Monica Focsan	
<b>The SERS performance optimization with coupled modes and low-loss metals</b>	<b>167</b>
Mr. Kang Qin, Prof. Yongyuan Zhu, Prof. Yanqing Lu, <u>Prof. Xuejin Zhang</u>	
<b>Surface-enhanced Raman spectra and higher order scattering in Bi<sub>2</sub>O<sub>3</sub>-Ag nanoplasmonic eutectic composite</b>	<b>168</b>
<u>Dr. Piotr Piotrowski</u> , Mr. Kamil Szlachetko, Mr. Paweł Osewski, Dr. Katarzyna Sadecka, Dr. Dobrosława Kasprowicz, Prof. Dorota A. Pawlak	
<b>Probing out of-equilibrium optical excitations with fast electrons</b>	<b>170</b>
<u>Mr. Valerio Di Giulio</u> , Dr. Vahagn Mkhitaryan, Prof. Javier García de Abajo	
<b>Upgraded nanoparticle-based SERS substrates: superhydrophobicity and oxidative treatment</b>	<b>171</b>
<u>Dr. Andrei Novikov</u> , Mr. Maksim Gorbachevskii, Dr. Dmitry Kopitsyn, Dr. Mikhail Kotelev, Ms. Alexandra Kuchierskaya, Dr. Evgenii Ivanov, Prof. Vladimir Vinokurov	
<b>Two-Color Fluorescent Cross-Correlation Spectroscopy as a valuable tool to evaluate the loading efficiency of DNA liposome complexes to improve cell reprogramming</b>	<b>173</b>
<u>Dr. Aline Marie Fernandes</u> , Mr. Matej Siketanc, Dr. Ana Isabel Gómez Varela, Dr. Juliane Assis, Dr. Adelaide Miranda, Prof. Rafael Valverde, Prof. Marcelo Einicker Lamas, Dr. Pieter De Beule	
<b>Thermoplasmonics of Platinum nanoparticles</b>	<b>175</b>
<u>Dr. Akbar Samadi</u> , Dr. Henrik Klingberg, Dr. Liselotte Jauffred, Prof. Andreas Kjaer, Dr. Poul Martin Bendix, Prof. Lene B. Oddershede	
<b>Detecting plasmonic heating via liquid crystals thermometry</b>	<b>177</b>
<u>Dr. Luciano De Sio</u> , Dr. Ugo Cataldi, Dr. Alexa Guglielmelli, Prof. Thomas Bürgi, Dr. Nelson Tabiryan, Dr. Timothy J. Bunning	
<b>Light-Emitting Halide Perovskite Nanoantennas</b>	<b>178</b>
<u>Ms. Ekaterina Tiguntseva</u> , Mr. George Zograf, Prof. Anvar Zakhidov, Dr. Sergey Makarov, Prof. Yuri Kivshar	
<b>Plasmonic behavior of spherical core-shell structures in the tunneling regime</b>	<b>180</b>
<u>Dr. Muhammad Khalid</u> , Dr. Fabio Della Sala, Dr. Cristian Ciraci	

<b>Hybrid Longitudinal-Transverse Modes in Surface Phonon Polariton Systems</b>	<b>181</b>
<u>Dr. Christopher Gubbin, Dr. Simone De Liberato</u>	
<b>Plasmonic magneto-optical 1D nanostructure: Wood's anomaly and the Faraday rotation for biosensing</b>	<b>182</b>
<u>Mr. Alexey Shaymanov, Dr. Nikolay Orlikovsky, Mr. Eldar Khabushev, Mr. Alexander Zverev, Ms. Anastasiya Pishimova, Dr. Georg Sharonov, Dr. Georgii Yankovskii, Dr. Ilya Rodionov, Dr. Alexander Baryshev</u>	
<b>One-dimensional spherical photonic crystal</b>	<b>184</b>
<u>Mr. Lewis Asilevi, Mrs. Ségolène Péliisset, Ms. Myriam Bailly, Mrs. Leila Ahmadi, Prof. Emiliano Descrovi, Prof. Matthieu Roussey</u>	
<b>Plasmonic nanoparticle doping of the active layer for enhancing efficiency and stability in organic photovoltaic devices</b>	<b>185</b>
<u>Dr. Barbara Paci, Dr. Amanda Generosi, Dr. Emmanuel Stratakis, Dr. Emmanuel Kymakis</u>	
<b>Diode-like asymmetric transmission in hyperbolic epsilon-near-zero media</b>	<b>187</b>
<u>Dr. Carlo Rizza, Dr. Xin Li, Dr. Andrea Di Falco, Prof. Elia Palange, Dr. Andrea Marini, Dr. Alessandro Ciattoni</u>	
<b>Hybrid photonic-plasmonic devices for enhanced sensitivity biosensors</b>	<b>188</b>
<u>Dr. Lucia Fornasari, Dr. Paola Pellacani, Dr. Miguel Manso, Dr. Chloe Rodriguez, Dr. Vicente Torres-costa, Prof. Franco Marabelli</u>	
<b>Plasmonic Photodetector Incorporating SrTiO<sub>3</sub> Interfacial Layer</b>	<b>190</b>
<u>Dr. Takayuki Matsui, Dr. Yi Li, Prof. Rupert F Oulton, Prof. Lesley F Cohen, Prof. Stefan A Maier</u>	
<b>Preparation of plasmonic HfN nanoparticle arrays for hot-electron photochemistry</b>	<b>192</b>
<u>Dr. Sven Askes, Prof. Erik Garnett, Ms. Evgenia Kontoleta</u>	
<b>Random lasers for spectroscopy applications</b>	<b>193</b>
<u>Mrs. Alice Boschetti, Dr. Andrea Taschin, Dr. Paolo Bartolini, Dr. Lorenzo Pattelli, Prof. Renato Torre, Prof. Diederik Wiersma</u>	
<b>Efficient Generalized Mie Theory Analysis of Nano Silver Dimers for Optical Field Enhancement in the Plasmonic Photoconductive THz Antenna</b>	<b>194</b>
<u>Ms. Faezeh zarrinkhat, Prof. Jordi Romeu, Prof. Juan Rius, Prof. Lluís Jofre</u>	
<b>Controlling Light at the Atomic Scale</b>	<b>196</b>
<u>Prof. Javier García de Abajo</u>	
<b>Charge transfer in nanoplasmonics as an avenue for control of chemical SERS enhancement and molecular self-assembly</b>	<b>197</b>
<u>Prof. Stefan A Maier</u>	
<b>Plasmonics for high quality light sources</b>	<b>198</b>
<u>Prof. Femius Koenderink</u>	
<b>Polariton quantum fluids</b>	<b>199</b>
<u>Prof. Daniele Sanvitto</u>	
<b>Polarization state transfer and photon routing with discrete high-index dielectric nanowaveguides</b>	<b>200</b>
<u>Mr. Roman Savelev, Mr. Vitaly Yaroshenko, Mr. Danil Kornovan, Dr. Mihail Petrov</u>	

<b>Switching of surface plasmon-polariton transmittance through the graphene stub nanoresonator with quantum dot</b>	<b>201</b>
<u>Dr. Alexei Prokhorov, Dr. Mikhail Gubin</u>	
<b>Stabilization of quantum dots on modified natural aluminosilicate nanotubes for biological application</b>	<b>202</b>
<u>Dr. Anna Stavitskaya, Dr. Andrei Novikov, Dr. Elvira Rozhina, Mrs. Fereshtech Pouresmaeil, Mr. Danila Logvinenko, Dr. Pawel Gushchin, Prof. Rawil Fakhruilin, Prof. Yuri Lvov, Prof. Vladimir Vinokurov</u>	
<b>Passively Q-switched fiber laser using PtS<sub>2</sub> microflakes saturable absorber</b>	<b>203</b>
<u>Mr. Xinyu Wang, Mr. Ping Kwong Cheng, Mr. Chun Yin Tang, Mr. Wayesh Qarony, Dr. Yuen Hong Tsang</u>	
<b>Strong coupling between excitons in transition metal dichalcogenides and optical bound states in the continuum</b>	<b>204</b>
<u>Ms. Zarina Sadrieva</u>	
<b>Self-trapping of optical solitons in double Josephson junctions formed by spatially coupled soliton and surface-plasmons</b>	<b>206</b>
<u>Dr. Güneş Aydınođan, Prof. Kaan Güven</u>	
<b>Fabrication of Fluorescence Graphene Quantum Dots/CoFe<sub>2</sub>O<sub>4</sub>@SiO<sub>2</sub> Nanoparticles and Potential Application for Targeted Drug Delivery and Fluorescence Imaging of Cancer Cells</b>	<b>207</b>
<u>Ms. Yun TENG, Prof. Philip W. T. Pong</u>	
<b>Experimental Demonstration of the Purcell Effect in Silicon Mie-resonators with Embedded Ge(Si) Quantum Dots</b>	<b>209</b>
<u>Ms. Viktoriia Rutckaia, Dr. Mihail Petrov, Dr. Frank Heyroth, Dr. Alexey Novikov, Dr. Vadim Talalaev, Prof. Joerg Schilling</u>	
<b>Cellulose based photonic architectures</b>	<b>211</b>
<u>Ms. Camilla Dore, Dr. André Espinha, Mr. Cristiano Matricardi, Dr. Maria Isabel Alonso, Dr. Alejandro Goni, Dr. Johann Osmond, Dr. Agustin Mihi</u>	
<b>Ultrahigh Purcell factor achieved in a single sphere-gap-cone hybrid nanoantenna</b>	<b>213</b>
<u>Ms. Yali Sun, Dr. Sergey Makarov, Dr. Dmitry Zuev</u>	
<b>Dynamic plasmonic metasurface holograms</b>	<b>214</b>
<u>Dr. Jianxiong Li, Prof. Na Liu</u>	
<b>Temperature-dependent optical properties of plasmonic nanosystems</b>	<b>216</b>
<u>Mr. Michele Magnozzi, Ms. Marzia Ferrera, Dr. Francesco Bisio, Prof. Maurizio Canepa</u>	
<b>Tunable MIM plasmonic near-infrared transmissive metasurface</b>	<b>217</b>
<u>Mr. Arash Nemati, Prof. Minghui Hong, Dr. Jinghua Teng</u>	
<b>Development of a rapid measurement method of bacterial concentration by light-induced assembly based on photothermal effect</b>	<b>219</b>
<u>Mr. Yasuyuki Yamamoto, Prof. Shiho Tokonami, Prof. Takuya Iida</u>	
<b>Generation of shear waves in a soft medium by 2.1 <math>\mu\text{m}</math> light source based on periodically poled ferroelectric crystal</b>	<b>220</b>
<u>Dr. Liliana Martinez, Dr. Juan Gonzalez, Mr. Amaury Garcia, Dr. Luis Rios, Dr. Rurik Farias, Dr. Jose Enriquez</u>	

<b>Combined effect of Etched diameter and thickness of Reduced Graphene Oxide coating on the sensitivity of Fiber Bragg Grating sensors for DNA application</b>	<b>221</b>
<u>Mrs. Kavitha Srinivasan, Prof. Asokan Sundarrajan, Ms. Radhika Nambannor</u>	
<b>A new fluorescent 1,8-naphthalimide based chemosensor for detection of dinitrobenzene</b>	<b>223</b>
<u>Dr. Jiri Zednik, Prof. Vladimir Sedlarik, Dr. Diana Harea</u>	
<b>Nanostructured Si- and Al for advanced microLED imaging</b>	<b>224</b>
<u>Prof. Aliaksandr Smirnov, Dr. Andrey Stepanov, Mr. Yauhen Mukha, Mr. Boris Kazarkin, Mr. Ilya Zacharchenya</u>	
<b>Plasmon-enhanced Förster resonance energy transfer in Langmuir-Blodgett films based on organic dyes</b>	<b>225</b>
<u>Prof. Niyazbek Ibrayev, Dr. Evgeniya Selivertsova, Ms. Nazerke Zhumabay</u>	
<b>Improvement of the photoinduced birefringence in azopolymer PAZO doped with TiO<sub>2</sub> via thermal annealing</b>	<b>227</b>
<u>Mr. Georgi Mateev, Prof. Lian Nedelchev, Prof. Dimana Nazarova, Dr. Anton Georgiev</u>	
<b>Nonlinear optical behavior of metallic nanoparticle suspensions at high laser fluences</b>	<b>228</b>
<u>Ms. Stefanie Dengler, Dr. Bernd Eberle</u>	
<b>Assessment of the optical properties of two cover materials of greenhouse on the heat transfer</b>	<b>229</b>
<u>Dr. LALMI Djemoui</u>	
<b>Fundamental study of the size-dependent optical properties of periodic arrays of nanoscale semiconducting fin structures</b>	<b>230</b>
<u>Mr. Andrzej Gawlik, Dr. Janusz Bogdanowicz, Dr. Andreas Schulze, Prof. Jan Misiewicz, Prof. Wilfried Vander-vorst</u>	
<b>Coherent reflectance of light from confined nanocolloid films: Modeling, experiment and applications</b>	<b>231</b>
<u>Mr. Gesuri Morales-Luna, Dr. Augusto García-Valenzuela</u>	
<b>Optical and electrical properties of coupled silver nanocrystal based flexible transparent nano-mesh film</b>	<b>232</b>
<u>Ms. Mihyun KIM, Mr. Hyungmok Joh, Mr. Sunghoon Hong, Prof. Soong Ju Oh</u>	
<b>Application of portable nanogenerator using friction charging</b>	<b>233</b>
<u>Dr. Dongseob Kim</u>	
<b>Hydrogenated amorphous silicon for nano-photonic devices from visible to mid-infrared</b>	<b>234</b>
<u>Prof. Duk-Yong Choi</u>	
<b>Large Area Optics with Silver Nanoparticles</b>	<b>236</b>
<u>Mr. Ivan Shutsko, Mr. Maik Meudt, Mr. Andreas Polywka, Mr. Christian Tückmantel, Prof. Patrick Görrn</u>	
<b>Second harmonic generation from zero-diffraction-order AlGaAs metasurfaces</b>	<b>237</b>
<u>Dr. Giuseppe Marino, Mr. Carlo Gigli, Dr. Ivan Favero, Mr. Stéphan Suffit, Dr. Arnaud Garnache, Dr. Isabelle Sagnes, Prof. Giuseppe Leo</u>	
<b>Intersubband plasmons induced negative refraction at mid-IR frequency in heterostructured semiconductor metamaterials</b>	<b>238</b>
<u>Mr. Mario Ferraro, Dr. Miguel Montes Bajo, Mr. Julen Tamayo-Arriola, Prof. Massimo Giudici, Dr. Angela Vasanelli, Dr. Jean Michel Cheuveau, Dr. Adrian Hierro, Dr. Patrice Genevet</u>	

---

<b>Plasmonic Metasurface Absorber by Transfer Printing</b>	240
<u>Mr. Maik Meudt</u> , Mr. Timo Jakob, Mr. Andreas Polywka, Mr. Luca Stegers, Mr. Stefan Kropp, Mr. Simon Runke, Mr. Martin Zang, Prof. Markus Clemens, Prof. Patrick Görrn	
<b>Gain-loss hyperbolic plasmonic metasurfaces</b>	241
<u>Dr. Dmitry Kuzmin</u> , Prof. Igor Bychkov, Prof. Vladimir Shavrov, Dr. Vasily Temnov	
<b>Optical properties and reliability studies of gradient alloyed green and red emitting quantum dots for white light-emitting diodes</b>	242
Dr. Rachod Boonsin, Dr. Florian Donat, Dr. Damien Boyer, Prof. Raphael Schneider, Prof. Philippe Boutinaud, Dr. Rachid Mahiou, <u>Prof. Geneviève Chadeyron</u>	
<b>Plasmon-induced in-plane band gap engineering in hydrogenated dilute nitrides</b>	243
<u>Dr. Giorgio Pettinari</u> , Mr. Loris Angelo Labbate, Dr. Silvia Rubini, Prof. Antonio Polimeni, Dr. Marco Felici	
<b>Control of light emission by diamond nanoantennas</b>	245
<u>Ms. Anastasia Zalogina</u> , Mr. Dmitry Zuev, Mr. Roman Savelev, Prof. Ilya Shadrivov	
<b>Nanoplasmonic Sensing by Silver Nanoplates Generated by Pulsed Laser Ablation and Reirradiation in Liquids</b>	246
<u>Dr. vittorio scardaci</u> , Mr. Marcello Condorelli, Dr. Luisa D'urso, Prof. Orazio Puglisi, Prof. Giuseppe Compagnini	
<b>Self-assembling of nanomaterials via droplet manipulation for multifunctional optoelectronics</b>	247
<u>Dr. Meng Su</u>	
<b>Color centers in diamond: from single-photons to nanoscale sensing</b>	248
<u>Dr. Paolo Traina</u> , Dr. Ekaterina Moreva, Dr. Jacopo Forneris, Dr. Sviatoslav Ditalia Tchernij, Dr. Federico Piccolo, Dr. Ivo Degiovanni, Prof. Valentina Carabelli, Dr. Paolo Olivero, Dr. Marco Genovese	
<b>Designing plasmonic eigenstates for optical signal transmission and logic gates nanodevices.</b>	249
Mr. Upkar Kumar, Mrs. Sviatlana Viarbitskaya, Mr. Aurélien Cuche, Mr. Alexandre Bouhelier, Mr. Gérard Colas Des Francs, Mr. Christian Girard, <u>Mr. Erik Dujardin</u>	
<b>Phase-matching-free micron-sized parametric oscillators by two-dimensional media</b>	250
<u>Dr. Andrea Marini</u> , Dr. Alessandro Ciattoni, Dr. Carlo Rizza, Prof. Claudio Conti	
<b>Active dielectric nanoantennas for directional lasing</b>	251
Dr. Son Tung Ha, Dr. Yuan Hsing Fu, Dr. Naresh K. Emani, Dr. Zhenying Pan, Dr. Reuben M. Bakker, <u>Dr. Ramon Paniagua-Dominguez</u> , Dr. Arseniy I. Kuznetsov	
<b>Mixed Frequency Generation in a Gold Antenna enables Double Blind Ultrafast Pulse Characterization</b>	252
<u>Dr. Sylvain Gennaro</u> , Dr. Yi Li, Prof. Stefan A Maier, Prof. Rupert F Oulton	
<b>Superfluid Brillouin Laser</b>	254
<u>Dr. Andreas Sawadsky</u> , Dr. Christopher Baker, Mr. He Xin, Prof. Warwick Bowen	
<b>The role of corners in the second harmonic scattering origin response from silver nanocubes</b>	256
<u>Dr. christian jonin</u> , Dr. Isabelle Russier-antoine, Prof. Emmanuel Benichou, Prof. Pierre-françois Brevet, Prof. Hye Jin Lee, Dr. Alastair Wark, Dr. Jérémy Butet, Prof. Olivier Martin	
<b>Raman spectroscopy of a single gold nanoparticle dimer</b>	257
Dr. Adrien Girard, Dr. Hélène Gehan, Dr. Alain Mermet, Dr. Christophe Bonnet, Dr. Jean Lermé, Dr. Alice Berthelot, Dr. Emmanuel Cottancin, Dr. Aurélien Crut, <u>Dr. Jeremie Margueritat</u>	

---

<b>Dynamics of electric dipoles in fluctuating light fields: From gravity-like interactions to accelerated expansion</b>	<b>258</b>
<u>Prof. M. I. Marques, Dr. Jorge Luis-hita, Mr. Victor Jose Lopez Pastor, Dr. Nuno De Sousa, Dr. Luis Froufe, Prof. Frank Scheffold, Prof. Rafael Delgado-Buscalioni, Prof. J. J. Saenz</u>	
<b>Optical Modulation of Flexible Pre-Structured Metallo-Dielectric Films</b>	<b>260</b>
<u>Mr. Ali El-Hadi Zeineddine, Prof. Nazir Kherani</u>	
<b>Optomechanical Kerker effect</b>	<b>261</b>
<u>Dr. Alexander Poshakinskiy, Dr. Alexander Poddubny</u>	
<b>Light Control using Microlens Arrays</b>	<b>262</b>
<u>Prof. Nikolai Petrov, Mrs. Galina Petrova</u>	
<b>Surface profile 3D visualization from thickness map reconstruction of thin films using scattering of surface plasmon polaritons</b>	<b>264</b>
<u>Dr. Rodolfo Cortés-Martínez, Dr. César E. García-Ortiz, Dr. Raúl Hernández-Aranda, Dr. Felix Aguilar-Valdez, Dr. Víctor M. Coello-Cárdenas</u>	
<b>Nanodisk lasers for internalisation by live cells</b>	<b>265</b>
<u>Mr. Alasdair Fikouras, Dr. Marcel Schubert, Mr. Markus Karl, Dr. Dinesh Kumar, Dr. Simon Powis, Dr. Andrea Di Falco, Prof. Malte Gather</u>	
<b>Dust particles contamination monitoring in the backscattering light experiment for the LISA mission</b>	<b>267</b>
<u>Dr. Sibilla Di Pace, Dr. Arwa Dabbech, Mr. Vitalii Khodnevych, Dr. Michel Lintz, Dr. Nicoleta Dinu-jaeger</u>	
<b>Localized surface plasmon studies on Au@Ag cuboids by electron energy-loss spectroscopy (EELS). Application to SERS experiments.</b>	<b>269</b>
<u>Dr. Israa Haidar, Dr. Guillaume Radtke, Dr. Markus Krug, Dr. Andreas Hohneau, Dr. Viktor Kapetanovic, Prof. Joachim R. Krenn, Dr. Matthieu Bugnet, Prof. Gianluigi Botton, Dr. Leïla Boubekeur-lecaque, Prof. Nordin Felidj</u>	
<b>Time-resolved four-wave mixing using Laguerre-Gauss modes</b>	<b>270</b>
<u>Dr. Pierre Gilliot, Mr. Marc Ziegler, Prof. Bernd Hönerlage, Dr. Mathieu Gallart</u>	
<b>Trigonal symmetric plasmonic array of standing wires for broadband, polarization insensitive molecular sensing.</b>	<b>271</b>
<u>Dr. Andrea Giugni, Dr. Bruno Torre, Dr. Marco Allione, Dr. Giovanni Marinaro, Dr. Gobind Das, Prof. Jurgen Kosel, Prof. Enzo Di Fabrizio</u>	
<b>Low Frequency Raman spectroscopy of small gold clusters: limits of Lamb model ?</b>	<b>272</b>
<u>Mr. Quentin Martinet, Dr. Adrien Girard, Dr. Alice Berthelot, Dr. Baira Donoeva, Ms. Clothilde Comby-zerbino, Dr. Franck Bertorelle, Ms. Marte Van Der Linden, Dr. Nathalie Tarrat, Prof. Nicolas Combe, Dr. Jeremie Margueritat</u>	

---

# Nanophotonics for a Green Internet

---

Monday, 1st October @ 09:05: Plenary Speeches (AUDITORIUM) - Oral - Abstract ID: 100

---

***Prof. Dieter Bimberg***<sup>1</sup>

*1. TU Berlin and Chinese-German Center of Green Photonics of the CAS at CIOMP Chanchun*

The energy required to transmit information as encoded optical and electrical data bits within and between electronic and photonic integrated circuits, within and between computer servers, within and between data centers, and ultimately nearly instantly across the earth from any one point to another clearly must be minimized. This energy spans between typically tens of pJpb to well over tens of mJ for intercontinental distances. We seek to meet the exploding demand for information within the terrestrial resources available but more importantly as a common sense measure to reduce costs and to become stewards of a perpetual Green Internet. The concept of a Green Internet implies a collection of highly energy-efficient, independent, and ubiquitous information systems operating with minimal impact on the environment via natural or sustainable energy sources (1). A key enabling optical component for the Green Internet is the vertical-cavity surface-emitting laser (VCSEL).

We review our research work on energy-efficient VCSELs for application as light-sources for optical interconnects and optical fiber data communications between 850 and 1310 nm. We present VCSEL designs, design principles, and operating methods that enable data communication systems capable of  $10 \exp -12$  bit error-free operation at bit rates exceeding 50 Gbps in the range 850-980 nm with energy efficiencies approaching 100 fJpb. Bit rates exceeding 200 Gbps by wavelength multiplexing of NRZ signals are possible for single mode devices showing an output power of 3 mW. The large linearity of the L-U-characteristics enables also higher order modulation rates like PAM4 leading to still much larger bit rates (2).

(1) For a review on Green Photonics see: G.Eisenstein and D.Bimberg, eds. „Green Photonics and Electronics”, Springer, Cham 2017

(2) G. Larisch, R.Rosales, J.A.Lott, and D.Bimberg, Proc. ESLW Bari Sept. 2018



# Nano-Photonics of Super-Oscillations

---

Monday, 1st October @ 09:40: Plenary Speeches (AUDITORIUM) - Oral - Abstract ID: 540

---

***Prof. Nikolay Zheludev***<sup>1</sup>

*1. Nanyang Technological University, Singapore and University of Southampton, UK*

TBD

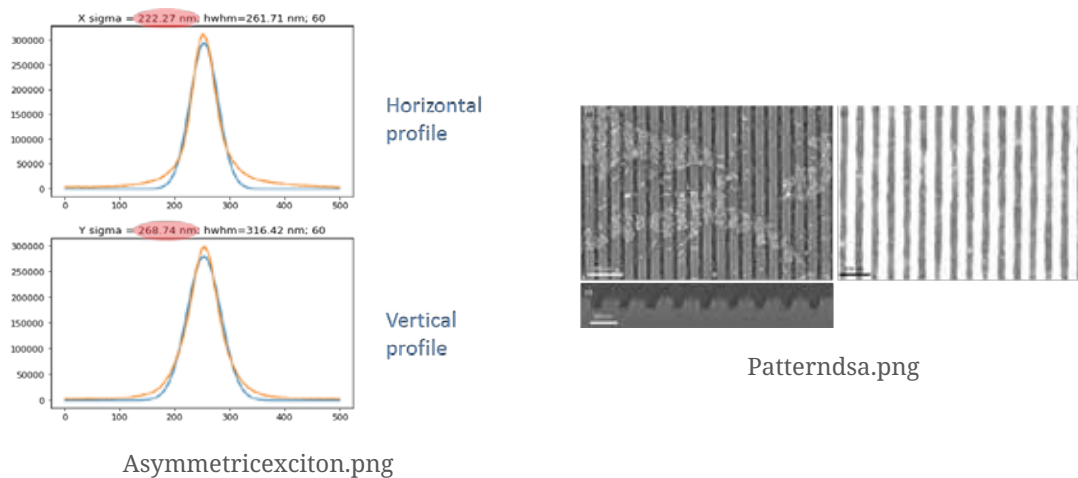
# Exciton diffusion of directed assembly of perovskite nanocrystals on patterned surfaces

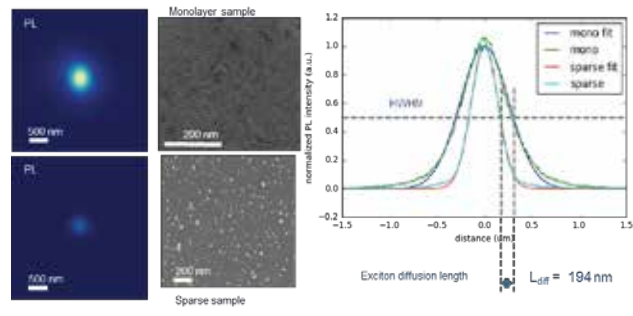
Monday, 1st October @ 10:45: Plenary Speeches (AUDITORIUM) - Oral - Abstract ID: 456

*Dr. Stefano Cabrini<sup>1</sup>, Dr. Erika Penzo<sup>1</sup>, Dr. Alexander Weber Bargioni<sup>1</sup>*

*1. Lawrence Berkeley National Laboratory*

Colloidal nanomaterials display a broad range of unique chemical and physical properties that make them prime candidates as nanoscale building blocks for the development of future technologies. Towards this goal, one of the main challenges resides in developing methods to manipulate these materials with a level of precision comparable with their small size; it requires a transition from solution phase to solid state. During this transition the system is brought from the random and dynamic spatial distribution to an ordered, static assembly. In this work we study the effects of topography and surface chemistry on the exciton diffusion properties of perovskite nanocrystals (PNCs). The PNCs subjects of this study are cubic in shape with side length of about 10 nm. They are surrounded by organic ligands terminating with apolar groups. The PNCs solution is deposited by spin-coating on silicon substrates. If the nanocrystals are arranged in a monolayer, we can excite them with a focused laser beam. These excited nanocrystals will fluoresce and we can record the intensity profile in the far field which will have approximately a gaussian shape. If the particles are close enough, the excitons can hop from one nanocrystal to the next in this 2d network of nanocrystals. The result of this process will be an expansion of excited state ensemble. Comparing PL intensity profiles, one without exciton diffusion and one with exciton diffusion we can obtain a direct measurement of the average exciton diffusion length in this system (figure 1). The PNCs solution is also deposited on substrates that are patterned with narrow trenches and which surface is chemically functionalized to change the degree of hydrophobicity. In Figure 2, trenches between 20 and 50 nm successfully confine PNCs into ordered lines as narrow as one or two PNCs and extending for hundreds of nanometers without gaps or defects. Arranging PNCs in such ordered, 1D-like features allows careful studies of the collective mechanisms of exciton diffusion and recombination in PNCs assemblies (figure 3), which in turn determine the optoelectronic behavior of the system and offer fundamental guidance in engineering new optoelectronic devices made of PNCs.





Excitondiffusion.png

# Optical properties of metallic nanoparticles: from field enhancement to molecular detection

---

Monday, 1st October @ 10:45: Plenary Speeches (AUDITORIUM) - Oral - Abstract ID: 542

---

***Prof. Lamy de la Chapelle Marc***<sup>1</sup>

*1. Université du Mans*

The metallic nanoparticles can strongly interact with light. They can provide some huge enhancement of the near field at the vicinity of the nanoparticle surface due to the excitation of the localised surface plasmon (LSP). Their plasmonic properties depend on the geometrical parameters (size, shape, coupling...) of the nanoparticles. By using electron beam lithography, we can produce some arrays of nanostructures with high reproducibility at the nanometer scale. With such arrays, we can provide a fine control of the plasmonic properties and tune the LSP resonance on a wide range of wavelength. We are also able to reach the highest enhancement of the near-field.[1]

In this presentation, we will discuss the relation between the LSP and the enhancement efficiency depending on the geometrical parameters of the nanostructures.[2] We will also present how to exploit these properties in several applications : sensor development, identification of biomolecules [3] and study of their structure [4], thermal effect [5], surface functionalisation [6]...

This work is supported by the grant PIRANEX project (ANR-12-NANO-0016), the Louise project (ANR-15-CE04-0001) and the Nanobiosensor project (ANR-15-CE29-0026) from the French National Research Agency (ANR).

[1] N. Guillot , M. Lamy de la Chapelle, JQSRT 113, 2321, 2012

[2] F. Colas, et al., J. Phys. Chem. C120 (25), 13675, 2016

[3] M. Cottat, et al., J. Phys. Chem. C 119 15532, 2015

[4] M. Cottat, et al., Scientific Reports 7, 39766, 2017

[5] G. Picardi, et al., J. Phys. Chem. C120 (45), 26025, 2016

[6] I. Tijunelyte, et al., Nanoscale 7/13, 7105, 2016

---

# Three-dimensional disordered hyperuniform networks with a photonic bandgap

---

Monday, 1st October @ 13:30: Poster Session (HALL & ROOM 3) - Poster - Abstract ID: 161

---

***Dr. Jakub Haberk***<sup>1</sup>, ***Dr. Nicolas Muller***<sup>2</sup>, ***Dr. Catherine Marichy***<sup>3</sup>, ***Dr. Luis Froufe***<sup>2</sup>, ***Prof. Frank Scheffold***<sup>2</sup>

*1. AGH University of Science and Technology, Faculty of Physics and Applied Computer Science, 2. University of Fribourg, Physics Department and Fribourg Center for Nanomaterials, 3. Université de Lyon, Laboratoire des Multimatériaux et Interfaces*

## **Introduction**

The term “hyperuniform” refers to point patterns, whose structure factor tends to zero for short wave-vectors, meaning the absence of long-wavelength density fluctuations. Apart from crystalline and quasi-crystalline patterns belonging to this class, there exist structures with no long-range order which also have this property. It has been shown that networks derived from such patterns can possess an isotropic photonic band-gap.

## **Methods**

We have generated 3D networks from a hyperuniform disordered point pattern by performing a Delaunay tessellation and connecting the centers of resulting tetrahedra with dielectric rods. We have been able to fabricate such three-dimensional networks by means of 3D laser nanolithography in a polymer photoresist and to prove by FIB-SEM, light scattering and optical microscopy that their geometry is correct [1-2]. These polymer networks were then used as templates and replicated in silicon on two different routes of single and double inversion, involving atomic layer deposition, high-temperature chemical vapor deposition and calcination [3-4]. FTIR measurements were performed to extract spectral features of our structures. Interaction of light with the networks was simulated using the finite difference time domain technique (FDTD).

## **Results and discussion**

We have shown that the resulting networks possess the expected spectral characteristics and specifically a dip in transmission, being a footprint of PBG. With a characteristic structural distance below 2  $\mu\text{m}$  it falls in the near-infrared regime. The spectroscopic results are in good quantitative agreement with our FDTD simulations, both in terms of position of the PBG on the frequency scale as well as isotropy.

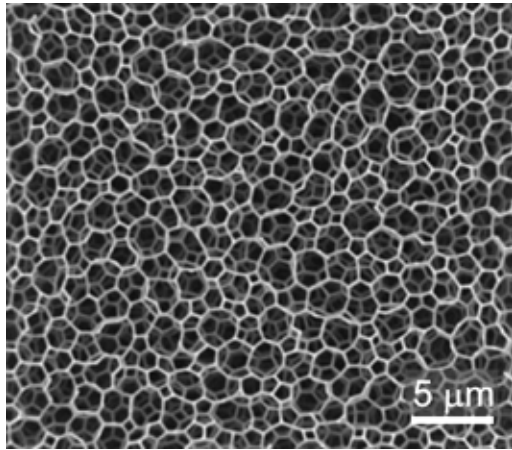
## **References**

[1] Opt. Ex. 21(1), 1057–1065 (2013)

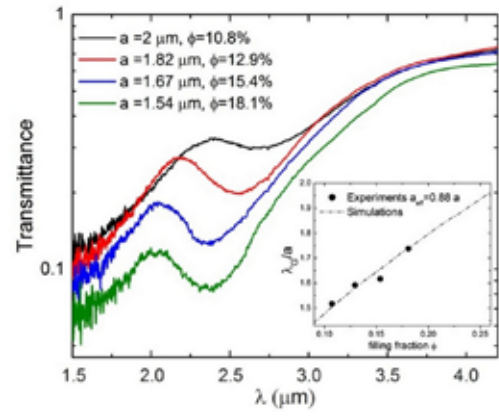
[2] Phys. Rev. A 88(4) 043822-1–043822-9 (2013)

[3] Adv. Opt. Mat. 2(2), 115–119 (2014)

[4] Optica 4 (3), 361–366 (2017)



3d hyperuniform network sem.jpg



3d hyperuniform network transmission.jpg

# Linear and nonlinear optical properties of silicate oxide glasses containing metallic gold and silver nanoparticles

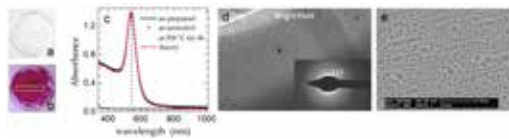
Monday, 1st October @ 13:30: Poster Session (HALL & ROOM 3) - Poster - Abstract ID: 251

**Dr. Krzysztof Dzierzega**<sup>1</sup>, **Dr. Nadia Pellerin**<sup>2</sup>, **Ms. Aleksandra Gorczyca**<sup>1</sup>, **Dr. Jean-philippe Blondeau**<sup>2</sup>, **Dr. Witold Zawadzki**<sup>1</sup>, **Dr. Stephane Pallerin**<sup>2</sup>, **Mr. Babacar Diallo**<sup>2</sup>

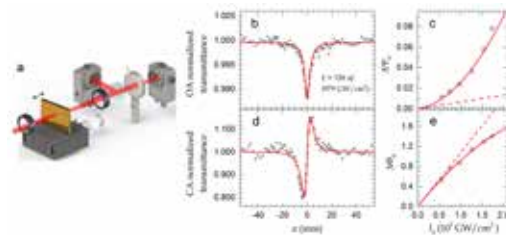
1. Institute of Physics, Jagiellonian University, 2. Universite d'Orleans

Glasses with metallic nanoparticles (NPs) are of great interest in photonics and plasmonics due to their unique linear and non-linear optical properties. These features directly arise from the localized surface plasmon resonance (LSPR) and the enhancement of the electric field in the vicinity of such nanoparticles.

We report on the embedded gold and silver nanoparticles in a standard silicate oxide glass. Au or Ag metallic compounds were introduced in vitreous oxide matrices as gold chloride (AuCl) or silver nitrate (AgNO<sub>3</sub>), respectively, together with some reducing agents in case of Au. The amorphous glass (Fig.1a) was obtained using the standard melt-quenching technique while metallic Au or Ag NPs were precipitated by thermal annealing of as-prepared glass plates in reducing atmosphere or in air (Fig.1b). Measurements of the absorbance spectra of the prepared samples in the UV-VIS range revealed the existence of the LSPR at expected wavelengths of 420 nm and 540 nm for Ag and Au NPs (Fig.1c), respectively. Moreover, the modeling of these spectra, using the Drude model, the Mie theory as well as the Maxwell-Garnet theory of the effective medium, allowed to determine the size (on the order of several nm) and the filling factor (on the order of 10<sup>-5</sup>) of embedded NPs. Further proofs are given by analysis of TEM micrographs. The non-linear optical properties of samples, originating from the optical Kerr effect and multiphoton absorption, were investigated with the Z-scan method (Fig.2a) using the 35 fs laser pulses at 813 nm which were generated by a mode-locked Ti:sapphire laser system at a repetition rate of 1 kHz. The open (Fig.2b) and closed aperture (Fig.2d) z-scan curves for the as-annealed glass with dispersed Au nanoparticles were fitted with the standard Z-scan theory and the nonlinear absorption  $\beta$  and refractive index  $n_2$  coefficients are determined. The measured nonlinear absorption and nonlinear phase shift for different energy of the incident laser pulse are shown in Fig.2c,e. Our studies clearly show the increase in the non-linearities in comparison to the samples without metallic NPs.



Tem abs au.png



Z-scan.png

# Electrochemical investigation of plasmonic near-field and hot electron effects promoted by aluminium nanostructures

Monday, 1st October @ 13:30: Poster Session (HALL & ROOM 3) - Poster - Abstract ID: 408

. *Madasamy Thangamuthu*<sup>1</sup>, *Dr. Christian Santschi*<sup>1</sup>, *Prof. Olivier Martin*<sup>1</sup>

*1. Swiss Federal Institute of Technology Lausanne (EPFL)*

## Electrochemical investigation of plasmonic near-field and hot electron effects promoted by aluminium nanostructures

### Introduction

Recently, plasmonic nanostructures have been employed for harvesting solar energy for photovoltaics and photocatalytic chemical reactions. Their efficient use requires a close investigation of the involved plasmonic mechanisms. In the present work, plasmonic near-field and hot electron effects promoted by aluminium nanotriangles (AlNTs) were investigated in different configurations using electrochemical photocurrent measurements.

### Methods

Three different configurations were developed and fabricated, using colloidal lithography, to study i) plasmonic hot electrons (ITO-AlNTs) ii) near-field coupling to a semiconductor (ITO-AlNTs-TiO<sub>2</sub>) and iii) hot electron transfer to a semiconductor (ITO-TiO<sub>2</sub>-Pt-AlNTs). A 40 nm Al and 100 nm TiO<sub>2</sub> films were deposited using electron beam evaporation whereas atomic layer deposition was used to deposit a uniform Pt layer. The optical response of the photoelectrodes were explored using UV-vis-NIR spectrometry and subsequently compared with numerical simulations. Electrochemical photocurrent measurements were performed in a three electrode photoelectrochemical cell using amperometric technique. A collimated narrow banded LED beam with its central wavelength at  $\lambda = 365$  nm was used to irradiate the photoelectrodes.

### Results and Discussion

A SEM image of the AlNTs and their size distribution are shown in Fig. 1. The UV-Vis-NIR extinction spectra matches well with the numerical simulations showing a plasmonic peak around 365 nm (Fig. 2). Numerical simulations revealed the highest plasmonic electric field intensities at the edges of the AlNTs (inset, Fig. 2). Fig. 3 shows the photocurrent responses of the a) ITO-AlNTs, b) ITO-TiO<sub>2</sub>, c) ITO-AlNTs-TiO<sub>2</sub> electrodes under illuminated conditions. The AlNTs on ITO does not show significant current due to the fast recombination of hot electrons. The bare TiO<sub>2</sub> photoelectrode shows a photocurrent of  $I = 33.2 \mu\text{A}$  corresponding to an external quantum efficiency (EQE) of 1.12 %. The photocurrent increases to  $78 \mu\text{A}$  when AlNTs are brought close to the TiO<sub>2</sub> (ITO-AlNTs-TiO<sub>2</sub>) that corresponds to an EQE, 2.7 %. Hence, plasmonic near-field coupling enhances the photocurrent  $\sim 2.4$  fold. An additional 2 nm thin Pt layer forming a Schottky barrier prevents efficient recombination of the electron/hole pairs at the metal/semiconductor interface and favours hot electron injection into TiO<sub>2</sub>.

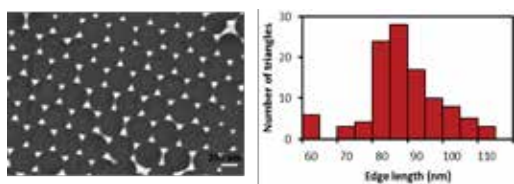


Figure 1.png

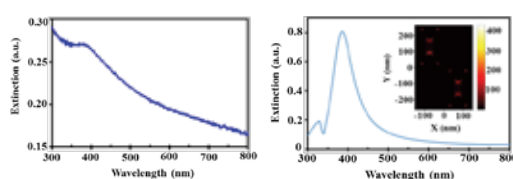


Figure 2.png



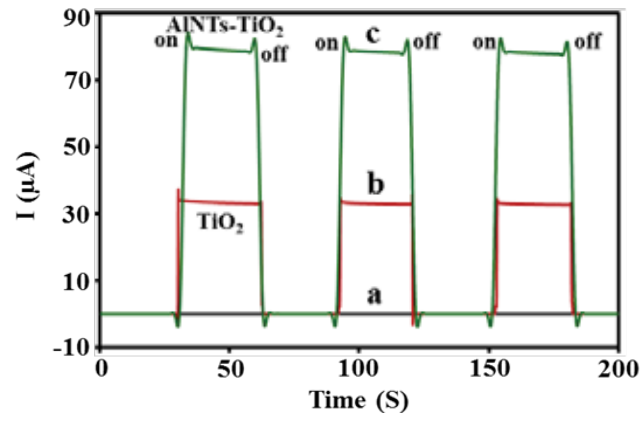


Figure 3.png

# On the use of Genetic Algorithm to Design and Optimize Graphene-based Absorbers

Monday, 1st October @ 13:30: Poster Session (HALL & ROOM 3) - Poster - Abstract ID: 466

**Mr. Hamidreza Taghvaei<sup>1</sup>, Dr. Sergi Abadal<sup>1</sup>, Prof. Albert Cabellos-Aparicio<sup>1</sup>, Prof. Eduard Alarcón<sup>1</sup>**

*1. NaNoNetworking Center in Catalunya (N3Cat), Universitat Politècnica de Catalunya*

Absorbers are widely used in diverse applications such as antenna pattern shaping, stealth technology and mid-infrared converters. Recently, metamaterials have been introduced to design microwave absorbers [1]. Enabled by graphene's electrical tunability, THz absorbers have also been developed [2]. Most designs are limited to concept proofs and, as we will see, are not ultimately optimized [3].

In this communication, we propose the use of Genetic Algorithm (GA) to find optimal topologies for metamaterial-like absorbers with graphene-based unit cells. The main idea is to break down the unit cell into a matrix of pixels and use the GA to iteratively improve the topology. The GA is coupled to a full-wave solver to evaluate the absorption bandwidth (BW), and the topology evolves until an optimal solution is reached.

We first prove the validity of the idea by optimizing an already existing design. We take [3] as an example and maintain its chemical potential, relaxation time and dimensions. Then, we apply our approach to find a topology that maximizes the 90% absorption BW. Fig. 1 shows that the 90% absorption BW increases from the original 39% to our 59%, with a unit cell topology reassembling the original ring resonator.

We secondly prove the versatility of the GA-based methodology by designing a microwave absorber from scratch. In this case, we assume a lossless substrate (e.g. air) to model the worst-case scenario for an absorber. Fig. 2 shows the design of an absorber with a 1.2-mm thick lossless substrate and a PEC ground plane. Even in such adverse conditions, our method achieves a BW of 65%. It is worth noting that, with lithographic methods, fabrication of such apparently complex patterns is possible.

This method is executable for designing not only ultra-wideband absorbers, but also for any other metamaterial. Getting advantage of tunable materials like graphene for the control of unit cell, along with the GA, diverse objectives such as cloaking and beam steering can be approached optimally.

[1] H. Taghvaei, et al., ICEEM 2014.

[2] HR. Taghvaei, et al., Opt. Commun. 383, 11-16, 2017.

[3] Chang Liu, et al., AIP Advances 8, 015301, 2018.

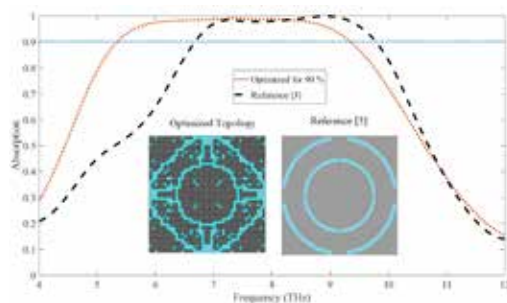


Figure 1 comparison of the results between previous design and the optimized topology for maximum bw.png

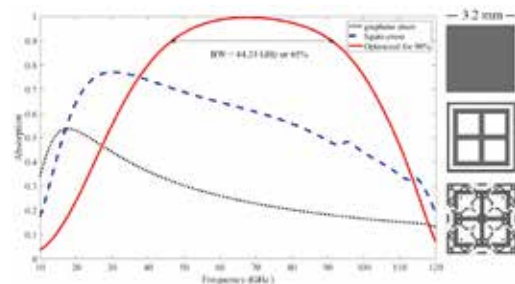


Figure 2 design of a wideband absorber without any substrate.png

# Novel Phenomena in Optical Manipulation due to Magnetic-Field-Induced Resonant States

Monday, 1st October @ 13:30: Poster Session (HALL & ROOM 3) - Poster - Abstract ID: 200

**Ms. Shulamit Edelstein**<sup>1</sup>, **Dr. R. M. Abraham Ekeroth**<sup>2</sup>, **Dr. P. A. Serena**<sup>1</sup>, **Prof. J. J. Saenz**<sup>3</sup>, **Dr. A. García-Martín**<sup>4</sup>, **Prof. M. I. Marques**<sup>5</sup>

1. Instituto de Ciencia de Materiales de Madrid (ICMM-CSIC), Campus de Cantoblanco, 28049 Madrid, Spain, 2. Instituto de Física Arroyo Seco, Universidad Nacional del Centro de la Provincia de Buenos Aires, Pinto 399, 7000 Tandil, Argentina, 3. Donostia International Physics Center, 4. Instituto de Micro y Nanotecnología IMN-CNM, CSIC, CEI UAM+CSIC, Isaac Newton 8, Tres Cantos, Madrid 28760, Spain, 5. Departamento de Física de Materiales, Condensed Matter Physics Center (IFIMAC) and Instituto Nicolás Cabrera, Universidad Autónoma de Madrid, Madrid 28049, Spain

We study the effect of optical forces [1] on a spherical isotropic magneto-optical nanoparticle [2]. Bringing together the two fields of optical forces and magneto-optics, we find three novel and intriguing phenomena: (i) Inducing an optical torque on an isotropic, spherical particle usually requires a circularly or elliptically polarized wave; we show that it is possible to induce a permanent torque using a linearly polarized plane wave. (ii) We also show that it is possible to generate a conservative optical lattice with non-interfering incoming fields and (iii) to exert radiation pressure, whose intensity can be actively modified, using electromagnetic fields with zero average value of the Poynting vector.

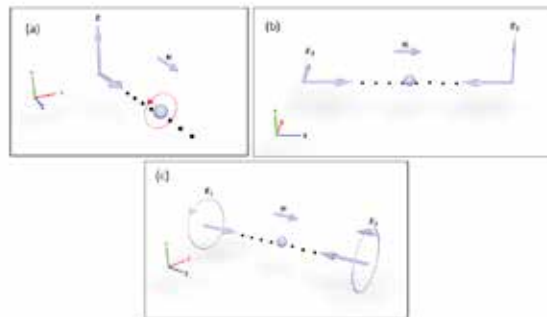


Figure 1: Schematic representation of (a) the spin torque of a nanoparticle induced by the incidence of a linearly polarized plane wave propagating in a direction parallel to the external magnetic field (z direction). (b) Two linearly polarized waves, propagating in opposite directions, while a constant magnetic field is applied in the y direction, generate a conservative optical lattice. And (c) two circularly polarized waves with same helicities, vector propagating in a direction parallel to the external magnetic field, exert radiation pressure on a nanoparticle.

Schematic representation of 3 novel phenomena.png

# Light creation without pump: tuning plasmonic resonance for surface enhanced chemiluminescence

Monday, 1st October @ 13:30: Poster Session (HALL & ROOM 3) - Poster - Abstract ID: 275

**Mr. Daler Dadadzhanov<sup>1</sup>, Dr. Tigran Vartanyan<sup>2</sup>, Dr. Alina Karabchevsky<sup>3</sup>**

1. Ben-Gurion University/ITMO University, 2. ITMO University, 3. Ben-Gurion University of the Negev

Chemiphores are entities, which exhibit wide-band light emission without any external light source but just due to the chemical reaction resulting in the chemiluminescence effect. Since the chemiphores usually have low quantum efficiency, chemiluminescence is a weak optical effect. Surface plasmon resonance in metallic nanoparticles (NP), however, can enhance the chemiluminescence of molecules due to the acceleration of radiative transitions. To enhance the chemiphores-particles interaction, metal NP has to be placed at the optimum distance from the chemiphores. The shape and material of the particles has to be accurately chosen to ensure the overlapping of their plasmonic band with the emission band of the chemiphores.

The proof of concept experiment was carried out in a microfluidic chip. Although the commercially available NP with non-optimized position of the plasmon resonance were employed, considerable enhancement of the chemiluminescence intensity was obtained [1]. To test the opportunities for further chemiluminescence enhancement we studied the optical properties of silver NP of different shape and size.

According to our calculations, optimum overlapping with the luminol emission bands at 452 and 489 nm is achieved for hemispherical NP with diameter of 18 and 73 nm on a quartz substrate as shown in Figure 1. The feasibility of obtaining of such NP arrays is confirmed by the extinction spectra of the ensembles of NP on quartz substrates fabricated via physical vapor deposition. Figure 2 plots the corresponding extinction spectra of granular silver films with equivalent thicknesses of 3 and 9 nm [2]. Contrary to that optical properties of NP obtained via laser ablation in liquids is less tunable. The red wing of the plasmon band peaked at 400 nm overlaps with the luminol luminescence bands. In addition, the arrangement of particles on the surface of transparent dielectric material makes it possible to control the distance between NP and chemiphores and opens up the possibility of integrating the substrates modified with the NP into the flowing microfluidic systems. [1] A. Karabchevsky et al., 'Tuning the chemiluminescence of a luminol flow using plasmonic nanoparticles', *Light Sci Appl.* 5, e16164 (2016).

[2] Leonov et al. *Opt. Spectrosc.* (2015) 119: 450. <https://doi.org/10.1134/S0030400X15090179>

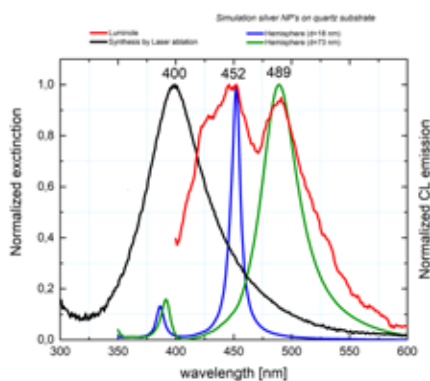


Figure 1.png

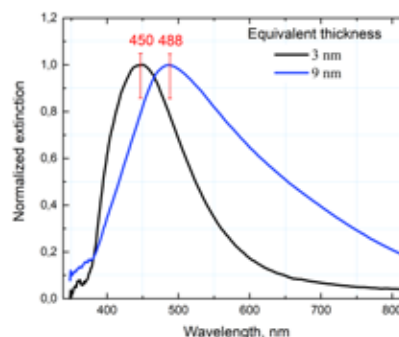


Figure 2.png

---

# Effects of manifold gaps on SERS enhancement in coupled plasmonic nanoantennas

---

Monday, 1st October @ 13:30: Poster Session (HALL & ROOM 3) - Poster - Abstract ID: 355

---

***Prof. Patrizio Candeloro***<sup>1</sup>, ***Dr. Marialaura Coluccio***<sup>1</sup>, ***Dr. Gerardo Perozziello***<sup>1</sup>, ***Dr. Mario Russo***<sup>1</sup>,  
***Prof. Enzo Di Fabrizio***<sup>2</sup>

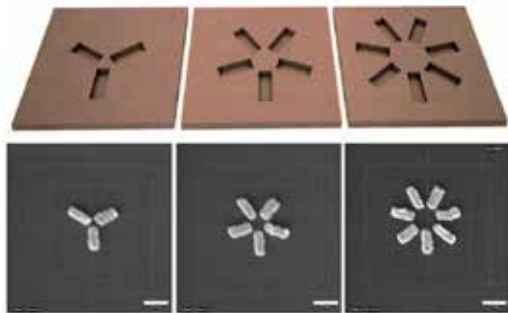
1. Dept. of Experimental and Clinical Medicine, University of Catanzaro, 2. KAUST

Since a couple of decades, surface-enhanced Raman scattering (SERS) is playing a crucial role for high-sensitive label-free detection in several research fields, from biophysics and molecular biology up to materials science [1-2]. Even single molecule detection regimes have been reported [3-4], thanks to very high enhancing factors accomplished with specific experimental conditions. In order to make SERS results as reliable and reproducible as possible, large efforts have been also dedicated to the study of plasmonic resonances conditions in nanostructures. Coupled plasmonic elements, like circular dimers and rod-shaped nanoantennas where plasmonic resonances are tuned by geometrical features [5], have been widely investigated and proposed as SERS nanosensors.

In this work we investigate three different kinds of nanostructures in the shape of trimers (3-arms), pentamers (5-arms) and eptamers (7-arms). All the arrays of nanostructures are fabricated over Si substrates by electron beam lithography in combination with thermal metal deposition and electroless Ag deposition. The geometrical parameters relevant for plasmonic resonances are kept constant through all kinds of nanostructures, more in details all the arms are 160nm×60nm while all the gaps between arms are 20nm wide. Rhodamine (R6G) is deposited over the samples before micro-Raman measurements, in order to probe their SERS capabilities. Keeping constant all the experimental conditions, the largest Raman signals are achieved on the 5-arms nanostructures (pentamers), even if the 7-arms ones have a larger number of SERS active spots.

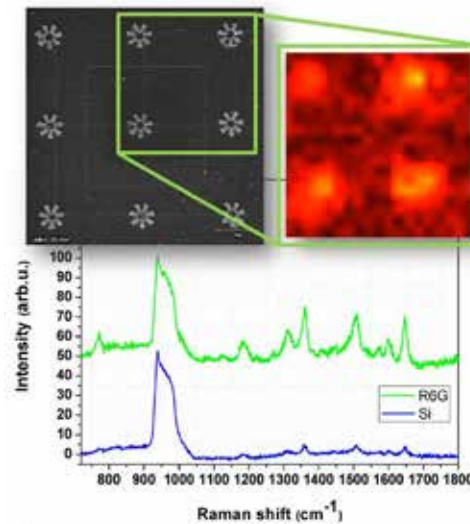
This result suggests that plasmonic resonances occurring in these nanogaps is not relying on the single gap behavior only, but that a potential coupling effect between neighboring gaps could lead to a further enhancing factor. Obviously the inter-gap enhancement would strongly rely on spacing between gaps, and further improvements in SERS sensitivity could be achieved by proper design of nanostructures with manifold gaps.

1. K. Kneipp et al., J. Phys.: Condens. Matter (2002), 14:R597–R624
2. J. Chao et al., Journal of Materials Chemistry B (20 16), 4:1757-1769
3. K. Kneipp et al., Phys. Rev. Lett. (1997), 78:1667-1670
4. S. Nie et al., Science (1997), 275:1102-1106.
5. O.L. Muskens et al., Optics Express (2007) 15:17736-46



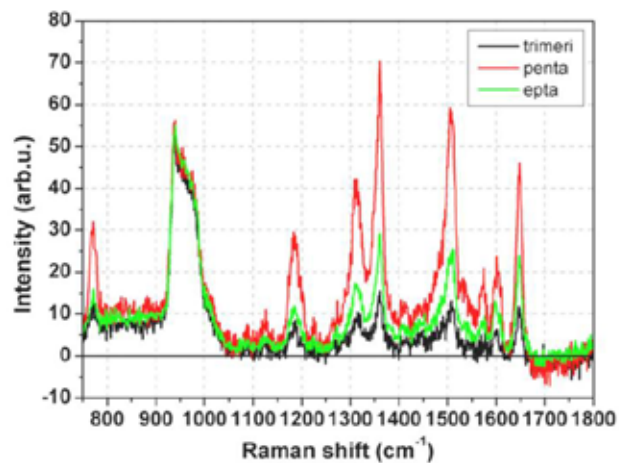
**Figure 1:** Fabricated plasmonic nanoantennas in the shape of trimers (3-arms), pentamers (5-arms) and eptamers (7-arms). All the arms are 200nm×60nm and the gaps are 20nm wide. (Scale bar is 200nm)

Figure1.jpg



**Figure 2:** Raman mapping over eptamers nanostructures after Rhodamine (R6G) deposition. Typical R6G peaks (green spectrum) are observed in SERS active regions which reproduce exactly the array spatial pitch. The broad band at approximately 950cm<sup>-1</sup> is due to Si substrate.

Figure2.jpg



**Figure 3:** Average Raman spectra measured over trimers (black curve), pentamers (red) and eptamers (green). All curves are normalized to the Si substrate band at 950cm<sup>-1</sup> for comparison. The largest signal is achieved with pentamers nanostructures, even if eptamers have a larger number of hot-spots (gaps).

Figur3.jpg

---

## Stimulated emission of dye molecules coupled to localized plasmons in Ag nanoparticles

---

Monday, 1st October @ 13:30: Poster Session (HALL & ROOM 3) - Poster - Abstract ID: 441

---

***Dr. Nikita Toropov*<sup>1</sup>, *Ms. Aisylu Kamaliev*<sup>2</sup>, *Dr. Tigran Vartanyan*<sup>2</sup>**

*1. ITMO University and Aston University, 2. ITMO University*

Optical properties of silver nanoparticles are determined by the excitation of localized plasmon oscillation. These oscillations result in the appearance of strong local electromagnetic fields near the nanoparticles. Of particular interest is the possibility of creating coherent nanosized light sources such as a spaser. In this contribution, lasing properties of the structures based on organic dye layer and 2D silver nanoparticles ensemble are explored.

The fluorescence spectra of the organic coumarin thin films with and without silver nanoparticles were measured at excitations by pulses of the third harmonic of a Nd-YAG laser at different energy. While at low pump energies fluorescence intensity was proportional to the pump energy in both samples, at larger pump energies their behavior was completely different. The fluorescence intensity of the dye layer was saturated. Contrary to that the fluorescence intensity of dye with silver nanoparticles was not saturated. Moreover, after a threshold, it grew even faster than at smaller pump pulse energies. Also, in the presence of silver nanoparticles, strong narrowing of the fluorescence band with the growing pumping energy was observed.

Thus, two basic features of stimulated emission, namely the spectral line narrowing and the superlinear non-saturated dependence of the luminescence intensity on the pumping energy had been observed.

---

# Influence of angular momentum of light on excitation of near field hot spots

---

Monday, 1st October @ 13:30: Poster Session (HALL & ROOM 3) - Poster - Abstract ID: 465

---

***Dr. Marco Allione*<sup>1</sup>, *Dr. Andrea Giugni*<sup>1</sup>, *Dr. Bruno Torre*<sup>1</sup>, *Prof. Enzo Di Fabrizio*<sup>1</sup>**

*1. King Abdullah University of Science and Technology (KAUST), 23955-6900, Thuwal KSA*

Realization of plasmonic nanostructure which show hot spots with a strong enhancement of the local near field has been a strong field of research in the last decades, for either fundamental interest as well as for applications such as Surface Enhance Raman Scattering (SERS). To this purpose, we have used FDTD simulation methods to analyze the field profiles in different concentric structures, upon excitation with radially polarized light sources having different orders of Orbital Angular Momentum (OAM), and compared with the response to normal linearly polarized and circularly polarized light. Among the structure used there are mainly circular arrangement of radially distributed plasmonic antennas and concentric tapered plasmonic structures. Our interest has been mainly devoted to the structure and intensity of the near field hot spots in the small metallic gaps in the center of the different structures. Our simulations show a strong dependence on the OAM order of the field profile at the gaps in the center of the structure. In particular, due to the phase mismatch in the oscillation of the different plasmonic components in the structure, the near field hot spots in the structure shift, with a strong intensity dependence on the OAM of excitation source. Comparison with other type of excitation are also interesting. In particular, excitation with circularly polarized light lead to results which are much closer to those obtained with  $OAM > 0$ , a result which is in accordance with literature results that support the evidence of a mixing of spin and orbital angular momentum of light in plasmonic structures. These results can lead to an important optimization of the intensity of the hot spots used in SERS by exploiting the angular momentum of the excitation source as an alternative degree of freedom to control the excitation of nanostructured samples, and they might have application in optimization of specific high-sensitivity detection of bio-molecules on nanopatterned samples. Further work is currently ongoing in our lab to simulate other structures as well as to experimentally realize and test for Raman and SERS applications some of the devices we have simulated.



---

# Optical Waveguides in Oxidised Porous Silicon

---

Monday, 1st October @ 13:30: Poster Session (HALL & ROOM 3) - Poster - Abstract ID: 239

---

***Mr. Alexander kellarev*<sup>1</sup>, *Prof. Shlomo Ruschin*<sup>1</sup>**

*1. Tel Aviv University*

## **Introduction**

Currently creation of waveguides and other planar optical elements is performed using relatively sophisticated methods, which involve complex apparatus, and often requires making multiple lithography masks and growing of additional structure layers. An alternative method of creation of such elements is patterning in a porous substrate by pore filling. [1] This process is relatively simple and can be used to create regions with desired refractive index when applied with a mask or other patterning techniques. Porous silicon (PSi) is an optical metamaterial, which possesses a high ability to absorb other substances. PSi with specific refractive index can be created by means of electrochemical etching of Si wafer.

## **Methods**

To create the light-guiding structures we used an oxidised Si wafer with two porous layers of different refractive indices, where the bottom layer serves as cladding. KDP salt solution was applied to fill the pores by two methods: printing and through a photoresist mask. After the pore filling the wafer was cleaved to allow access to the sides of the layers.

Propagation was examined at wavelengths 1.064 $\mu\text{m}$  and 1.550 $\mu\text{m}$ . Laser light was inserted into the waveguides using a lensed fiber. Transmitted light and light scattered from the top surface were acquired by means of imaging. The acquired images were used to analyse the spatial distribution of the transmitted light and to estimate the propagation loss.

## **Results**

We created straight waveguides, tapered waveguides, waveguides with S-bends and Y-splitters by means of the method described above. As an example, part of the top surface is presented in Figure 1, showing a waveguide and a Y-splitter. We successfully measured light propagation through all the created structures. Examples of the acquired images are presented in Figure 2. At  $\lambda=1.064\mu\text{m}$  we obtained multimode propagation for waveguides designed with 30-micron width while waveguides designed with 3-micron width support 2 propagated modes. Preliminary best measured losses were around 3.4dB/cm ( $\lambda=1.064\mu\text{m}$ ) and 0.2dB/cm ( $\lambda=1.550\mu\text{m}$ ).

## **Discussion**

We demonstrated the possibility of creation of optical elements in PSi by pore filling. The measured losses are competitive to recently published reports for patterned waveguides in PSi.

[1] Optical Materials, vol.85, 2018, pp.113-120

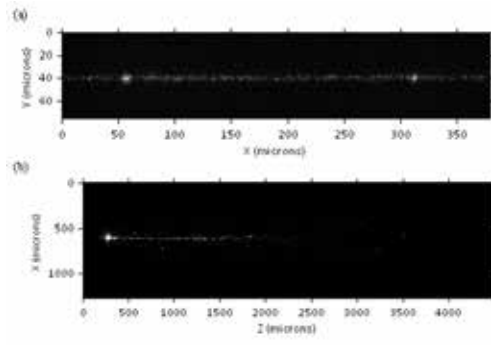


Figure 1-top surface of the porous silicon.png

Figure 2-images of transmitted a and scattered b light acquired from y-splitter.png

---

## SERS studies on DNA: optimization of experimental conditions.

---

Monday, 1st October @ 13:30: Poster Session (HALL & ROOM 3) - Poster - Abstract ID: 97

---

**Ms. Edyta Pyrak**<sup>1</sup>, **Dr. Aleksandra Jaworska**<sup>2</sup>, **Prof. Tomasz Wilanowski**<sup>3</sup>, **Prof. Andrzej Kudelski**<sup>4</sup>

1. Faculty of Chemistry, University of Warsaw, ul. Pasteura 1, 02-093 Warsaw, Poland; Nencki Institute of Experimental Biology of Polish Academy of Sciences, Warsaw, Poland, 2. Faculty of Chemistry, University of Warsaw, ul. Pasteura 1, 02-093 Warsaw, Poland, 3. Nencki Institute of Experimental Biology of Polish Academy of Sciences, Warsaw, Poland, 4. Faculty of Chemistry, University of Warsaw, ul. Pasteura 1, 02-093 Warsaw

Nowadays, a great research effort is put into the development of techniques enabling early diagnosis of genetic disorders, including different types of cancer [1]. Among those techniques, polymerase chain reaction or different types of blotting are mostly used for DNA mutation detection as a part of cancer treatment [2]. However, those methods lack of sensitivity and can detect DNA mutations only in advanced stage of the disease. Therefore, new detection tools are needed as alternatives to the techniques which are used routinely, in order to improve the early detection in diagnostics. One of the promising technique developing very fast in the field of cancer diagnosis is surface enhanced Raman spectroscopy (SERS). This method, discovered in 1974 by Fleischmann, is based on a huge enhancement of the Raman signal (up to 14 orders of magnitude) when the molecule is adsorbed on the rough metal surface [3]. The most commonly used metal substrate is colloidal gold and silver, because of relatively easy way of preparation and repeatable results [4]. SERS spectroscopy, because of its ultrasensitive detection limits, is a perfect method for detection of biomolecules at very low concentrations.

The idea of SERS-based sensors for DNA detection is quite simple: capture DNA, complimentary to target DNA, is immobilized on metal surface, then target DNA is added and this hybrid is labeled with another single stranded DNA modified with an organic dye [5].

Immobilization of capture DNA on the metal surface is a crucial moment influencing effectiveness of the sensor. Here we present the optimization of the formation of ssDNA monolayer on SERS substrate taking into consideration: type of metal surface, pH, presence of small molecules between ssDNA (6-mercapto-1-hexanol) and how these conditions influence the hybridization process.

Acknowledgement: Work implemented as a part of Operational Project Knowledge Education Development 2014-2020 cofinanced by European Social Fund.

References:

[1] J.Wang, Biosensors and Bioelectronics 21 (2006) 1887; [2] X.Zhu et al., Biosens.Bioelectron. 74 (2015) 113; [3] M.Fleischmann et al., Chem.Phys.Lett. 26 (1974) 163; [4] G. Frens, Nature Phys Sci. (1973) 241, 20; [5] F. Peng et al., Acc.Chem.Res., 47 (2014) 2, 612

---

# Triple dyes-labeled polyelectrolyte microcapsules@gold nanoparticles for anthocyanins delivery as topical administration for tumor skin cells

---

Monday, 1st October @ 13:30: Poster Session (HALL & ROOM 3) - Poster - Abstract ID: 397

---

***Ms. Raluca Flavia Ghiman*<sup>1</sup>, *Dr. Dumitrita Rugina*<sup>2</sup>, *Dr. Monica Focsan*<sup>3</sup>, *Ms. Andreea Campu*<sup>1</sup>, *Prof. Adela Pinte*<sup>2</sup>, *Prof. Simion Astilean*<sup>4</sup>**

*1. Babes-Bolyai University, Faculty of Physics, 2. University of Agricultural Science and Veterinary Medicine, 3. Nanobiophotonics and Laser Microspectroscopy Center, Interdisciplinary Research Institute on Bio-Nano-Sciences, 4. Babes-Bolyai University, Nanobiophotonics and Laser Microspectroscopy Center, Interdisciplinary Research Institute on Bio-Nano-Sciences and Biomolecular Physics Department*

Over the past decades a great incidence of melanoma was recorded, maybe also because the atmosphere loses more and more of its protective filter function and more solar UV radiation reaches the Earth's surface.

Anthocyanins are natural pigments with remarkable health benefits against cancer. Unfortunately, anthocyanins are very sensitive to environmental conditions, such as alkaline pH, light or oxygen and therefore are easily degraded. To increase their stability and obtain an efficient release, a novel multifunctional delivery system targeted towards tumor skin cells should be urgently designed.

Herein, triple dyes-labeled polyelectrolyte microcapsules were firstly obtained through layer by layer assembly technique with nearly spherical shape and a diameter of  $1 \pm 0.1 \mu\text{m}$ , as proved by dynamic light scattering results and transmission electron microscopy observation. Subsequently, gold nanoparticles (like spheres, bipyramids and rods) were employed to be encapsulated into shells of microcapsules for an efficient release of the loaded drug under laser radiation.

The encapsulation efficiency of anthocyanins was confirmed through the chromatography technique coupled with mass spectrometry (LC-ESI(+)-MS).

The as-designed microcapsules were then labeled with a pH insensitive fluorophore as rhodamine B isothiocyanate or two pH sensitive fluorophores as Oregon Green isothiocyanate and fluorescein isothiocyanate, to establish their specific localization inside the tumor skin cells.

Notably, our proposed delivery system for anthocyanins locally administration proved do not reduce cell viability, according to WST-1 viability assay performed. More importantly, the intracellular tracking of the triple dyes-labeled microcapsules was evaluated by fluorescence imaging microscopy (FLIM), an ideal non-invasive tool to probe their local internalization inside B16F10 melanoma cells.

Taken together, our results could contribute and enlarge the research knowledge in the pharmaceutical and healthcare industry, leading to a real breakthrough on the sustained and targeted locally delivery therapies.

---

# Simple and Reliable Patterning of Plasmonic Nanostructures by Spontaneous Adhesion Lithography

---

Monday, 1st October @ 13:30: Poster Session (HALL & ROOM 3) - Poster - Abstract ID: 185

---

***Dr. Sihai Luo***<sup>1</sup>, ***Prof. Bård Helge Hoff***<sup>1</sup>, ***Prof. John De Mello***<sup>2</sup>

*1. Norwegian University of Science and Technology, 2. Imperial College London*

Nanoscale gaps in noble metal films can locate surface plasmons. Molecules positioned within such metallic nanogaps significantly enhance light-matter interactions, increasing absorption, emission, and, most notably, surface-enhanced Raman scattering (SERS). However, the reliable and reproducible fabrication of ultranarrow gaps (< 20 nm) for real applications is still challenging. Here, we show a method to fabricate simply and reliably sub-20-nm metallic gap arrays with aspect ratios in excess of 100,000. This method exploits the ability of selected self-assembled monolayers to attach conformally to a pre-patterned metal layer and thereby weaken adhesion to a subsequently deposited metal film. The method can be carried out under ambient conditions via a simple mechanically induced process that involves no intricate alignment procedures and high-cost instruments. With this method, we fabricated densely packed gold nanostructures of varying geometries separated by ultras-small gaps. Optical and SERS measurements on the patterned structures show that this technique has promising applications in the fabrication of tunable plasmonic nanostructures with nanogaps.

# Tunable degree of second order coherence for radiation of plasmonic structure excited by single photon source

Monday, 1st October @ 13:30: Poster Session (HALL & ROOM 3) - Poster - Abstract ID: 229

**Mr. Nikita Nefedkin**<sup>1</sup>, **Dr. Evgeny Andrianov**<sup>1</sup>, **Prof. Alexander Pukhov**<sup>2</sup>, **Prof. Alexey Vinogradov**<sup>3</sup>

1. Dukhov Research Institute for Automatics, 2. Institute for Theoretical and Applied Electromagnetics RAS, 3. Institute of Theoretical and Applied Electrodynamics

Currently, a substantial progress has been achieved in creating nano-sized sources of coherent radiation. Radiation sources for quantum information transmission lines in addition to high temporal coherency must also have a desirable correlation function of the second order ( $g^2$ ). Usually, single-photon sources (SPS) are required. To increase the speed of SPSs, single molecules, NV centers or quantum dots interacting with plasmonic structures are used. However, in such systems, due to the Purcell effect, the  $g^2(0)$  function of radiation is modified. Thus, it is necessary to create sources with required  $g^2(0)$  and the high radiation rate.

We suppose that SPS is a two-level system (TLS) and choose the one mode of the plasmonic structure interacting with TLS. To find the statistical properties of radiation and the radiation rate of the SPS coupled with plasmonic structure we use the Lindblad master equation formalism. The SPS is excited by incoherent continuous pumping. Both components of the system are surrounded by the medium with non-zero temperature.

We consider the  $g^2(0)$  function of electromagnetic field emitted by plasmonic structure which is excited by SPS, and show that it strongly depends both on Rabi constant of interaction and temperature of surrounding medium. In the case of high temperature, at low pumping rates of the SPS, the second order correlation function,  $g^2(0)$ , equals two as it takes place for black-body radiation (see Fig. 1). However, in the opposite case, when Rabi constant is much larger than temperature, the  $g^2(0)$  function equals zero as for radiation of a single TLS, Fig. 1. We show that the reason of such behavior is non-linear dependence of Rabi-splitting on the occupation number of plasmonic mode. At high pumping rates in both cases the  $g^2(0)$  function tends to unity as in laser above threshold (Fig. 1). Note that the single-photon regime in this system is available at room temperature and the radiation rate of the system greatly exceeds the radiation rate of a single SPS due to Purcell effect (Purcell factor can reach  $10^3$ ), which is of great interest for the applications in sphere of quantum information processing.

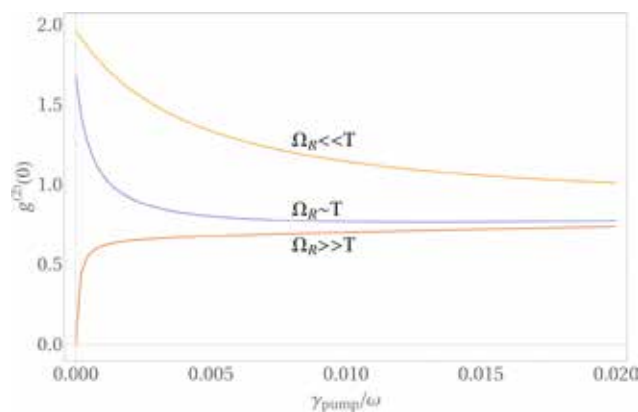


Fig1.png

# An Intensity Enhanced High-Resolution Spectrometer In “Water Window”.

---

Monday, 1st October @ 13:30: Poster Session (HALL & ROOM 3) - Poster - Abstract ID: 232

---

***Mr. Zhuo Li<sup>1</sup>, Dr. Bin Li<sup>2</sup>***

*1. Shanghai Institute of Applied Physics, Shanghai / University of Chinese Academy of Sciences /, 2. Shanghai Institute of Applied Physics, Shanghai/ University of Chinese Academy of Sciences/School of Physical Science and Technology, ShanghaiTech University*

An original and novel design scheme of a grazing incidence spectrometer is introduced. The optical properties of the system are investigated and optimized, to create an excellent meridional flat field in its detector domain to deliver the desired spectral resolution throughout the full designated spectral range, while eliminate the sagittal astigmatism to enhance the spectral intensity simultaneously (see Figure.1). We demonstrated within the “water window” (i.e. 2-5nm wavelength range), the resolving power of 6000-15000 could be achieved at the effective meridional source size of 200 $\mu$ m (rms) (see Figure.2); and it would be further enhanced to 10600-24000 if a pre-convex mirror is inserted into the system (see Figure.3). The design parameters of the original and enhanced spectrometer are shown in Table.1. This scheme owns universal adaptability, which could be easily extended in much broader photon-energy (or wavelength) range through appropriate modification to the design parameters. And it is also feasible to utilize the scheme to develop a high-performance grating monochromator simply by putting a fine slit right across the focal spectrograph of the diffraction beam.

---

# Collective Enhanced IR Absorption plasmonic device for conformational studies of biomolecules in physiological conditions

---

Monday, 1st October @ 13:30: Poster Session (HALL & ROOM 3) - Poster - Abstract ID: 351

---

**Mr. Paolo Zucchiatti**<sup>1</sup>, **Dr. Andrea Cerea**<sup>2</sup>, **Dr. Marta Semrau**<sup>3</sup>, **Dr. Giovanni Birarda**<sup>3</sup>, **Dr. Andrea Toma**<sup>2</sup>, **Dr. Paola Storici**<sup>3</sup>, **Dr. Lisa Vaccari**<sup>3</sup>

1. University of Trieste, Elettra-Sincrotrone Trieste, Istituto Italiano di Tecnologia, 2. Istituto Italiano di Tecnologia, 3. Elettra-Sincrotrone Trieste S.C.p.A.

## *Introduction:*

Collective Enhanced IR Absorption (CEIRA) microscopy is a well-known method for increasing FTIR sensitivity by taking advantage from the collective resonant excitation of nanoantennas' arrays, that provides a huge electromagnetic field enhancement on the nano-scale [1]. Infrared signals of molecules located in these fields are enhanced by orders of magnitude, enabling a spectroscopic detection with unprecedented sensitivity [2].

Here, we present a multipurpose device made by adjacent gold nanoantennas arrays which allows the investigation of biomolecules in the entire MIR range. As a first application, we present a study on two model proteins, Bovine Serum Albumin (BSA) and Concanavalin-A (ConA), and one of biomedical interest: the Epithelial Growth Factor Receptor (EGFR)

## *Methods:*

CEIRA substrates were fabricated by electron beam lithography. The repeating units of the arrays were centrosymmetric crosses, a geometry which permits to couple the antennas with both polarization of the light. Finite-difference time-domain simulations were used to calculate far-field and near-field signal profiles of the arrays. Proteins were immobilized onto the gold surfaces by taking advantage from the gold/thiols chemistry. CEIRA substrates were integrated in fluidic devices in order to work in buffer and preserve protein native conformation. FTIR resonance spectra were acquired in reflection.

## *Results:*

We benchmarked the performances of our devices using monolayers of reference proteins: BSA and Con A (Figure 1): model proteins were bonded to the surface via ammine coupling. Results confirmed the capabilities of our devices to discern the different conformation of the two proteins .

Then, EGFR was measured, a protein of particular interest since most of its mutations leads to lung cancer. EGFR was modified by adding to the original construct a His-tag, which was used for induce its selective binding in solution, without chemically modify the protein. In this way, we had the possibility to follow in real-time the binding of the molecule (Figure 2).

We believe that a platform with this sensitivity, few hundreds of molecules, has really the potentialities to become an advance high-throughput tool.

## *References:*

[1] R. Adato *et al.* Nat.Commun. 2013, 4, 2154.[2] F. Neuberech *et al.* Chem.Rev. 2017,117, 5110-5145.



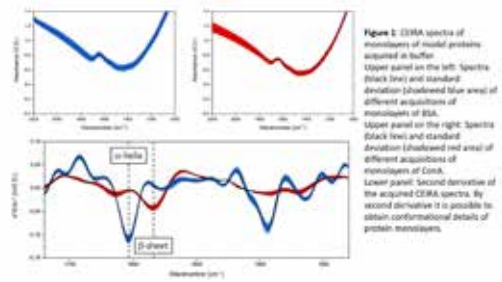


Figure 1.jpg

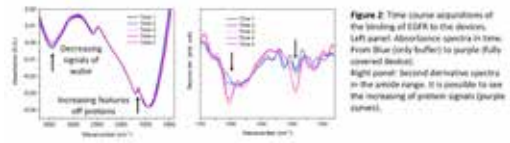


Figure 2.jpg

---

# A 3D finite element model for waveguide-based plasmonic sensors

---

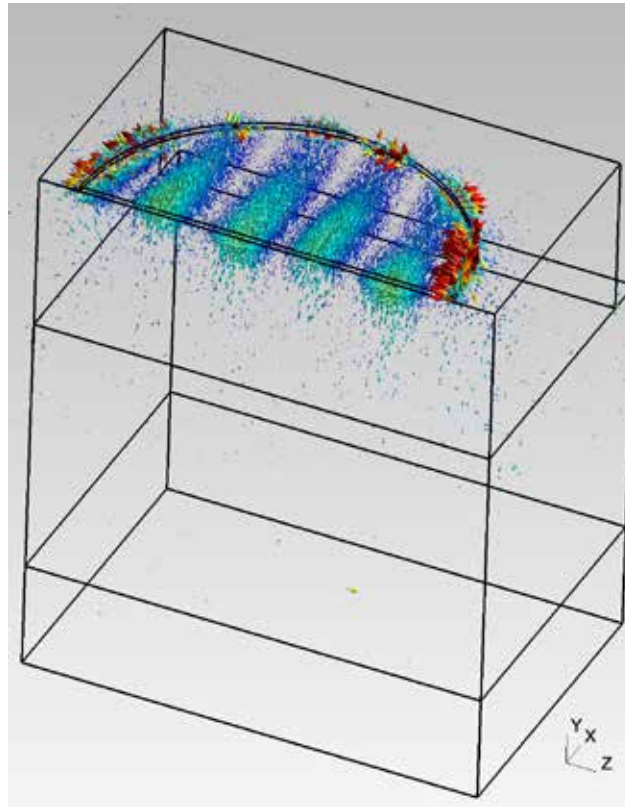
Monday, 1st October @ 13:30: Poster Session (HALL & ROOM 3) - Poster - Abstract ID: 113

---

*Dr. Guillaume Demesy*<sup>1</sup>, *Prof. Gilles Renversez*<sup>1</sup>

*1. Institut Fresnel*

The context of this theoretical and numerical study is the design of efficient plasmonic waveguides for infrared sensing. The device configuration is fully integrated and based on a ridge waveguide upon which metallic scattering nano-objects will ensure the coupling between the guided modes and superstrate of the device. Chalcogenide glasses are chosen for the main layers due to their high transparencies for infrared wavelengths. Ultimately, the metallic scatterers are planned to be functionalized in order to react to the targeted chemical species. In order to model the response of the resulting 3D guiding structure, we adopt a diffracted field formulation consisting of two sequential steps, the output of first step being the input of the second one. First, we determine the guided leaky modes for a fixed frequency, corresponding to the 7.7micron wavelength of interest, of the unperturbed 2D waveguide (without the plasmonic nanostructures). This is a ridge waveguide made of chalcogenide layers on a silicon substrate, assumed to be invariant along its propagation axis. We use usual vector FEM method with the Galerkin approach to solve the associated eigenvalue problem. This first step provides both the propagation constants (eigenvalues) and the associated modes profiles (eigenvectors). Second, these guided modes are used as incident fields for the full 3D problem (i.e. with the metallic nanostructures). The electromagnetic problem to solve for this second step is then a scattering problem. It is finally possible to define a proper energy balance (transmission and reflexion into the ridge guide, absorption taking place into the plasmonic rods, radiation losses) allowing to characterize the efficiency of the device as a plasmonic sensor. Our method allows to compute all the required energy-related quantities to investigate quantitatively the behavior of the full structure including the impact of the metal nanoparticles located on the top of the waveguide and to take into account the way it is excited by the selected propagating mode. We provide a study of the influence of the nano-particle parameters on the output field as well as a study of more complex nano-structuration on top of the ridge waveguide consisting of arrays of metallic particles.



Etot.png

# Decay-rate enhancement of spontaneous emitters coupled to Bloch Surface Waves on one-dimensional photonic crystals.

Monday, 1st October @ 13:30: Poster Session (HALL & ROOM 3) - Poster - Abstract ID: 142

*Dr. Angelo Angelini*<sup>1</sup>, *Mr. Ugo Stella*<sup>1</sup>, *Dr. Francesca Frascella*<sup>1</sup>, *Dr. Natascia De Leo*<sup>2</sup>, *Dr. Luca Boarino*<sup>2</sup>, *Prof. Emiliano Descrovi*<sup>1</sup>

1. Politecnico di Torino, 2. Istituto Nazionale di Ricerca Metrologica

## Introduction

The ability of engineering the radiative properties of spontaneous emitters is one of the main targets in nanophotonics. In this framework, plasmonic cavities and nano-antennas have gained particular attention, due the large number of photonic states confined in subwavelength volumes accessible from the external environment. [1] Unfortunately, plasmonic resonant structures working at visible wavelengths are affected by intrinsic high losses of metals that broaden the resonances reducing the quality factors.

Here we propose a fully dielectric structure exhibiting a resonant surface mode with well-defined dispersion relation (Bloch Surface Wave -BSW-). [2] By properly patterning the surface with a periodic structure we show a band gap opening in the dispersion relation of BSW and a defect state acting as a resonant cavity able to modify the spontaneous emission of fluorescent molecules located at the mode maxima

## Methods

A dielectric multilayer composed by 10 pairs of SiO<sub>2</sub> (n=1.45, thickness 137 nm) and Ta<sub>2</sub>O<sub>5</sub> (n=2.1, thickness 95 nm) thin films sustains resonant surface modes at the truncation interface. We fabricated 75 nm thick PMMA (n=1.48) concentric ring structures surrounding a central disk acting as a resonant cavity (Fig 1a) at the surface.

## Results and Discussion

The ring structure acts as a resonant cavity surrounded by a Distributed Bragg Reflector (DBR). In Figure 1b a wide-field image shows the fluorescence radiation coupled to the fundamental cavity mode at the center of the inner spacer (fig. 1b). Excitation is provided by a 10ps pulsed laser, at . Fluorescence lifetime measurements performed collecting only the light coming from the cavity region through a pinhole show a decay rate enhancement of about one order of magnitude (fig. 1c). Moreover, the analysis of the emission spectrum, reported in figure 1d, reveals clearly the coupling to the resonant mode of the cavity, with the possibility to tune the resonant condition by modifying the grating period and the inner spacer.

In conclusion, we present a purely dielectric photonic structure capable of controlling the emissive properties of fluorescent molecules both in terms of frequency emitted and decay rate.

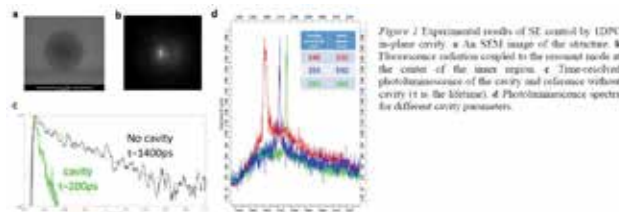


Figura1.png

# Optimizing band-edge slow light in Silicon-On-Insulator grating waveguides

Monday, 1st October @ 13:30: Poster Session (HALL & ROOM 3) - Poster - Abstract ID: 342

**Prof. Lucio Andreani<sup>1</sup>, Mr. Marco Passoni<sup>1</sup>, Prof. Dario Gerace<sup>1</sup>, Dr. Liam O'Faolain<sup>2</sup>**

1. University of Pavia, 2. Cork Institute of Technology

Silicon-based Photonic Integrated Circuits (PICs) are of great interest for the photonics community. Slow-light devices institute an important building block for such circuits, allowing the enhancement of light-matter interaction for a traveling wave. Typical examples are Mach-Zehnder interferometers used in electro-optical modulators. Various ways of realizing such devices have been studied, with different levels of complexity and performance.

In this work, we focus on the slow-light effect arising in 1D periodically patterned waveguides near the edge of the band-gap region, where the dispersion becomes naturally flat (Figs. 1, 2). The periodic pattern is inserted in a conventional silicon ridge waveguide (400 x 310 nm Si on SiO<sub>2</sub>) by a simple modulation of the width. The advantages of this approach are the ease of fabrication and the low losses involved, which is crucial for prospective applications in PICs.

We present a theoretical analysis of the band dispersion and slow light effect in such grating waveguides [1]. By a combination of numerical simulations by the aperiodic Fourier-modal method and perturbation theory, we are able to explore a broad space of parameters and to identify those that maximize the slow light bandwidth. We find that the slow-light bandwidth improves when increasing the modulation width and decreasing the thickness of silicon in the cladding region, reaching the optimal solution when the modulation is complete and the waveguide reduces to a lattice of trenches (Fig. 3). The fully modulated structure is, however, not convenient when considering insertion losses, which should be minimized by including an adiabatic taper that cannot be realized for the lattice of trenches. A viable solution is to use a deep grating, i.e., a structure in which the internal width is small but not zero. We show that this configuration is able to maintain performances neat the optimal ones, while being compatible with insertion of a taper. Finally, we demonstrate a slow-light design with a group index  $n_g > 10$  over a bandwidth of about 10 nm, which can be connected by a low-loss adiabatic taper to a standard silicon rib waveguide (Fig. 4).

[1] M. Passoni et al, Optics Express 26, 8470 (2018).

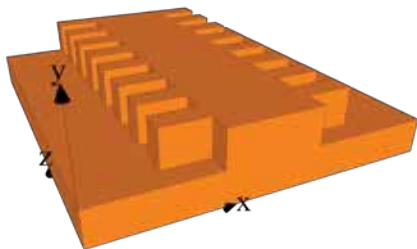


Fig1-structure.png

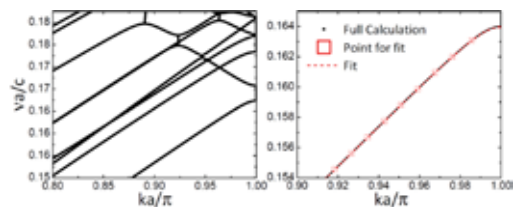


Fig2-band-edge-slow-light.png

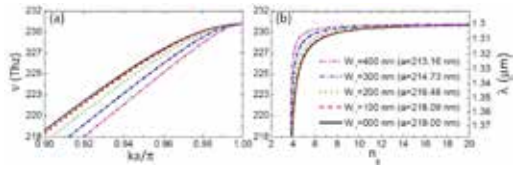


Fig3-group-index.png

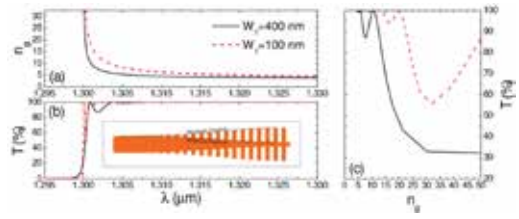


Fig4-adiabatic-taper.png

---

# Ultra-Narrow Bandwidth Acousto-Optic Filter

---

Monday, 1st October @ 13:30: Poster Session (HALL & ROOM 3) - Poster - Abstract ID: 365

---

***Prof. Nikolai Petrov*<sup>1</sup>, *Prof. Vladislav Pustovoit*<sup>1</sup>**

*1. Scientific and Technological Center of Unique Instrumentation of Russian Academy of Sciences*

Periodic structures created in crystals by an acoustic wave have a number of advantages compared to conventional devices based on diffraction gratings [1, 2]. They allow changing the period of a volume grating, modulating its characteristics, and high spectral resolution to be achieved.

In the present paper the resonator formed by two spatially-distributed “mirrors” is studied theoretically. The influence of different apodization functions on diffraction curves of reflection and transmission is studied. The effects of light absorption and moving gratings on the spectral resolution are evaluated. Influence of random changes of the dielectric constant of the medium on the reflection and transmission spectra of AO filter is investigated numerically. Significant increase in spectral resolution of acoustooptic filter due to spatial variation of refractive index of medium is shown.

The line width of the transmittance can reach very small values (Fig. 1). In transparent crystals with low absorption coefficients, the resolution of the filter is  $\Delta\lambda/\lambda \approx 10^{-11}$ , which is by 5-6 orders of magnitude higher than the resolution of the conventional filters with the same crystal thickness.

Complete elimination of sidelobes and a significant suppression of the “tails” of a diffraction reflection curve are demonstrated. Creation of high contrast optical filters with suppressed spurious sidelobes is important for various applications. This problem is particularly acute in Raman spectroscopy, when there is a need for suppression of laser radiation to measure very weak Raman scattering.

Acousto-optic filters with metamaterial inclusions opens up opportunities to create devices of infrared (IR) and terahertz technology, inaccessible to ordinary crystals. Note that a one-dimensional photonic bandgap structure with plasmonic inclusions can be used in a refractive index sensor in terahertz domain for optofluidics [3].

The results are of practical interest and can be used in the development of new diffraction acousto-optic modulators, AO filters and spectrometers, and also in the measurements of gravitational waves.

## References

- [1] V. I. Pustovoit, *Doklady Physics* **44**, 132-136 (1999).
- [2] N. I. Petrov and V. I. Pustovoit, *Laser Physics Letters* **14**, 115702 (2017).
- [3] J. Jose, *Optics Letters* **42**, 470-473 (2017).

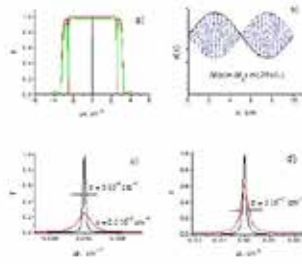


Fig. 1. The dependence of the reflection coefficient (a) for different absorption coefficients  $\alpha=10^{10} \text{ cm}^{-1}$  (black),  $\alpha=10^{11} \text{ cm}^{-1}$  (red),  $\alpha=10^{12} \text{ cm}^{-1}$  (green) and transmittances (c, d) on the value of the density of the resonator (b) - change of the dielectric constant  $\epsilon(x)$  depending on  $x$  (not to scale).

Refl trans coef.jpg



# Influence of strains on the structural and optical properties of nanoheterostructures with quantum island arrays and quantum wells based on group IV elements Ge, Si and Sn

Monday, 1st October @ 13:30: Poster Session (HALL & ROOM 3) - Poster - Abstract ID: 455

Dr. Vyacheslav Timofeev<sup>1</sup>, Dr. Alexander Nikiforov<sup>1</sup>, Dr. Vladimir Mashanov<sup>1</sup>, Dr. Ivan Loshkarev<sup>1</sup>,  
Ms. Natalia Baidakova<sup>2</sup>

1. A.V. Rzhhanov Institute of Semiconductor Physics SB RAS, 2. Institute for Physics of Microstructures RAS

At present, photodetectors, light-emitting diodes and lasers with optical pumping have been realized using GeSn and GeSiSn compounds. The Sn addition in Ge or GeSi matrix can result in direct bandgap materials, which could be applied in Si photonics, plasmonics and microelectronics.

The multilayer periodic structures with the GeSiSn/Si, GeSiSn/Ge heterojunctions, including the quantum island arrays and quantum wells, were grown. The method of the control for the 2D-3D transition and superstructures was the reflection high-energy electron diffraction (RHEED). The study of strains, the content and heterointerfaces was performed by the X-ray diffraction. The sample optical properties were studied by photoluminescence (PL) spectroscopy.

We present our studies on the initial stages of the  $\text{Ge}_{1-x-y}\text{Si}_x\text{Sn}_y$  film growth on the Ge and Si substrates and discuss the data on the structural properties of multilayer structures with the  $\text{Ge}_{1-x-y}\text{Si}_x\text{Sn}_y/\text{Ge}$  and  $\text{Ge}_{1-x-y}\text{Si}_x\text{Sn}_y/\text{Si}$  heterojunctions. The phase diagrams for the Sn deposition on Si(100) at room temperature and 200 °C are demonstrated in figure 1. The (7×1), (8×1) and (10×1) superstructures were first obtained on the Sn surface. New results on the appearance of Sn superstructures on Si(100) and Ge(100) templates were obtained, which allow controlling the Sn segregation phenomenon during the  $\text{Ge}_{1-x-y}\text{Si}_x\text{Sn}_y/\text{Si}$  and  $\text{Ge}_{1-x-y}\text{Si}_x\text{Sn}_y/\text{Ge}$  heterostructure growth. The rocking curves obtained by the X-ray diffraction from the multilayer structures containing the GeSiSn layers with the Sn content up to 14 % on the Ge and Si substrates demonstrate the pseudomorphic GeSiSn film state, sharp interfaces, as well as the conservation of the periodicity and content in all periods. The photoluminescence in mid-infrared region for the multilayer periodic GeSiSn/Si structures was detected. The blue shift with the excitation power increase is observed suggesting the presence of a type II heterostructure. It is possible to achieve a direct-band gap material replacing the Si substrate by the Ge substrate.

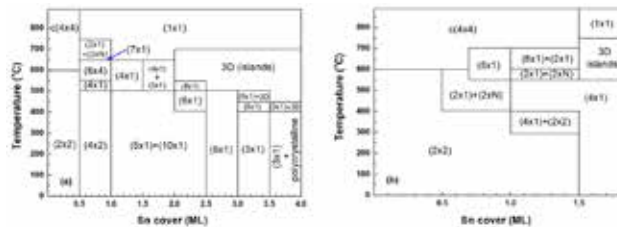


Figure1.jpg

---

# Magnetic and optical properties of gold coated iron oxide nanoparticles

---

Monday, 1st October @ 13:30: Poster Session (HALL & ROOM 3) - Poster - Abstract ID: 530

---

**Mr. Alexander Omelyanchik**<sup>1</sup>, **Ms. Maria Efremova**<sup>2</sup>, **Mr. Maxim Abakumov**<sup>3</sup>, **Dr. Alexander Majouga**<sup>4</sup>, **Dr. Ilia Samusev**<sup>1</sup>, **Dr. Natalya Myslitskaya**<sup>5</sup>, **Mr. Andrey Zyubin**<sup>1</sup>, **Dr. Valeria Rodionova**<sup>1</sup>

*1. Immanuel Kant Baltic Federal University, 2. Lomonosov Moscow State University, 3. National University of Science and Technology MISiS, 4. D. Mendeleev University of Chemical Technology of Russia, 5. Kaliningrad State Technical University*

Magnetic nanoparticles (MNPs) are in branch of interest due to their unique magnetic properties, which have potential in applications, for example in biomedicine [1]. Among magnetic materials, iron oxide MNPs are most promising because of the magnetization saturation high value and moderate cytotoxicity effect on human cells. However, they are difficult to functionalize and with prolonged exposure to the body they produce free radicals. To overcome these limitations, the MNPs can be covered with some materials as polymers, oxides, and metals forming core/shell structures. Fe<sub>3</sub>O<sub>4</sub>/Au MNPs are the most commonly used due to the possibility of bioconjugation and good biocompatibility [2]. Moreover, when gold-covered, some new optical functions to MNPs occur, in particular, to combine the both therapy and diagnostic agency in single vehicle [3]. In this work the core of iron oxide was prepared with co-precipitation route and shell of gold was build up by reduction of AuCl<sup>4-</sup> on the surface of cores to assemble Fe<sub>3</sub>O<sub>4</sub>/Au core/shell structure in form of electrostatic stabilized suspension as reported earlier [4]. Hydrodynamic radius expected from photon correlation spectroscopy (PCS) method was 17±2 nm for naked iron oxide and 26±6 nm for gold-coated MNPs. In order to distinguish the impact of the gold shell, the UV-Vis and Raman spectroscopy techniques were performed for naked and gold-coated MNPs. Magnetic properties were studied with SQUID magnetometer and superparamagnetic state of MNPs at room temperature was confirmed for both systems.

The reported study was funded by RFBR according to the research project № 17-32-50202.

[1] Kolhatkar, A.G., et al. *Int. J. Mol. Sci.* 14 (2013)

[2] Salihov, S.V., et al. *J. Magn. Mag. Mat.* 394. 173-178 (2015)

[3] Vinhas, R., et al. *Nanobiosensors Dis. Diagnosis.* Doi:10.2147/NDD.S60285 (2015)

[4] Majouga, A., et al. *Colloids Surf. B Biointerfaces.* 125. 104-109 (2015)

# Chromogen-free color interference-based biosensors for visual detection of viruses.

Monday, 1st October @ 13:30: Poster Session (HALL & ROOM 3) - Poster - Abstract ID: 532

*Ms. Ana Frosiniuk<sup>1</sup>, Dr. Vladimir Vinogradov<sup>1</sup>*

*1. ITMO University, International Laboratory "Solution Chemistry of Advanced Materials and Technologies"*

An optical biosensor is a miniature analytical device. It converts the information about an analyte in a complex sample into the analytical signal in real time. Such sensors provide non-destructive analysis and at the same time can be miniaturized down to nanometer-size that is why they became perspective instrument of quantitative microanalysis.

Here we demonstrate, new conception for simple visual detection of bio-analytes in solutions. Towards the achievement of that goal we describe the strong interference in sol-gel titania films which change a color after interaction with virus-like structures and show that the developed approach can also be used for qualitative and quantitative analyses even with naked eye.

**Figure1.** Schematic illustration of interference in thin films, where  $R$  — incident light beam;  $R^*$  — light beam reflected from interface;  $I$  — combination of reflected beams (coloring effect). Calibration curve, average analytical signal as a function of bacteriophage concentration.

We show theoretically and experimentally how interference in thin films can be used as analytical signal for optical sensors. Due to inkjet printing the sensor substrates present good reproducibility, which makes it possible to scale the production for integrating into the industrial manufacturing process. Analytical applicability was approved on the *Staphylococcus aureus* bacteriophage. Due to specificity of interference optical signal, two new methods of experimental data interpretation were proposed. It is expected that presented optical sensor system will allow to conduct several analyses simultaneously in one sample, particularly by applying multiple antibodies on different sections of a sensor array.

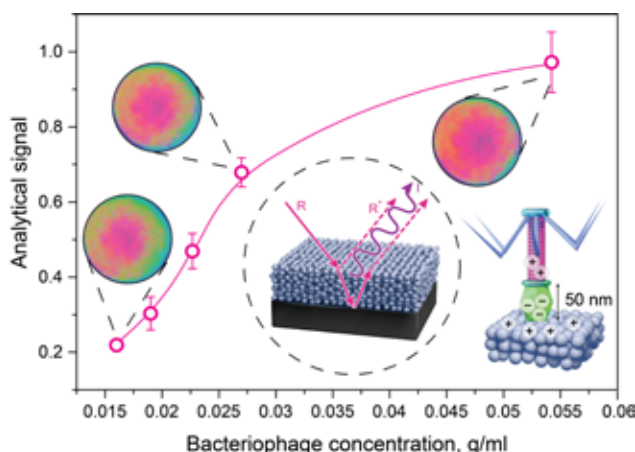


Figure 1.png

---

# Upconversion metal oxide aerogels for diagnostics and sorption of toxicants

---

Monday, 1st October @ 13:30: Poster Session (HALL & ROOM 3) - Poster - Abstract ID: 533

---

***Mr. Daniil Ilatovskii*<sup>1</sup>, *Dr. Pavel Krivoshapkin*<sup>1</sup>, *Dr. Elena Krivoshapkina*<sup>1</sup>, *Mr. Grigoriy Kiselev*<sup>1</sup>,  
*Dr. Vladimir Vinogradov*<sup>2</sup>**

*1. ITMO University, 2. ITMO University, International Laboratory "Solution Chemistry of Advanced Materials and Technologies"*

## **Introduction**

The drugs, which are applied in modern methods of cancer and thrombosis treatment, are often lead to fatal outcome of patients because of toxic effect of these. Consequently, the development of materials for both diagnostics (imaging, biodetection) and sorption of toxicants from blood is highly actual challenge of today. Aerogels are interesting matrix for such an application, because their surface area is giant, which is suitable for the role of adsorbent. Next, it was decided to produce aerogels with upconversion luminescence in order to provide diagnostic property based on ability to transform, for instance, NIR radiation to visible and UV regions via a nonlinear optical process. ZrO<sub>2</sub>, HfO<sub>2</sub> and Ta<sub>2</sub>O<sub>5</sub> (preliminary doped by Er<sup>3+</sup> and Yb<sup>3+</sup> ions for upconversion effect) were chosen as substrates thanks to their biocompatibility and ability to form stable gels.

## **Methods**

ZrO<sub>2</sub>, HfO<sub>2</sub> and Ta<sub>2</sub>O<sub>5</sub> aerogels were obtained by controlled hydrolysis and polycondensation of corresponding precursors, followed by drying on supercritical CO<sub>2</sub> extractor. Materials were characterized by HR TEM, XRD, FTIR, N<sub>2</sub> sorption and AFM methods. The optical and upconversion properties of aerogels monoliths were studied, doxorubicinum sorption was measured.

## **Results and Discussion**

Stable metal oxide aerogels doped by Er<sup>3+</sup> and Yb<sup>3+</sup> ions where produced. The samples demonstrated upconversion luminescence due to the fact, that rare-earth ions built in crystalline structure of matrices. The materials have also shown high surface area, which resulted in good sorption of doxorubicinum in the corresponding experiment. Overall, it was proved, that upconversion aerogels are perspective candidate for bioimaging, biodetection and adsorption both *in vitro* and *in vivo*.

---

# Diagnose of biomolecules using Raman interactions of the light

---

Monday, 1st October @ 13:30: Poster Session (HALL & ROOM 3) - Poster - Abstract ID: 75

---

**Prof. Enachi Nicolae<sup>1</sup>, Dr. Turcan Marina<sup>1</sup>, Dr. Ristoscu Carmen<sup>2</sup>, Prof. Mihailescu Ion<sup>2</sup>**

*1. Quantum Optics and Kinetic Processes Laboratory, Institute of Applied Physics (IFA), 2. Laser-Surface-Plasma Interactions Laboratory, National Institute for Lasers, Plasma and Radiation Physics (INFLPR)*

It is particularly important by now to apply the light in processing and development of modern diagnostic. Here with, two basic aspects of the interaction of light with the substance are discussed: the nonlinear one of light interaction with the environment, and the cooperative aspect of interaction of photons with matter (atoms or biomolecules). One should mention the use of metamaterials for tissue decontamination where the specific form of contact surface plays an important role. Another goal of the present work is the study and use of the cooperative effects of bacteria and viruses located in the evanescent field of biomaterials during Raman interaction of light in ultraviolet region. A model is proposed based upon existing experiments which takes into account the local symmetry of biomolecules. New models emerging from the non-linear interaction of the atomic (molecular) subsystem and the electromagnetic field of cavity could be elaborated. The photons statistic is proposed for the diagnosis of the new collective processes.

**Acknowledgment:** This paper is supported by the projects: NATO EAP-SFPP 984890, No. 15.817.02.07F and No. 18.80012.50.33A.

## References

- [1] N. Enaki, S. Bazgan; N. Ciobanu, M. Turcan, T. Paslari, C. Ristoscu; A. Vaseashta, I. N. Mihailescu, "Improvement in Ultraviolet Based Decontamination rate Using Metamaterials", *Applied Surface Science*, 2017, Volume 417, 30 September, P. 40-47, 2017.
- [2] T. Rosca, S. Bazgan, G. Dorcioman, C. Ristoscu, G. Popescu-Pelin, N. Enaki, I. N. Mihailescu, Temperature control of crystalline status and phenomenological modes, *Rom. Rep. in Phys.*, Volume 68, No. 1, P. 241-248, 2016.
- [3] M. Turcan, N.A. Enaki, "Cooperative generation of entanglement states by Raman conversion of photons in nano-Fibers", *Rom. Rep. in Phys.*, Volume 67, No. 4, P. 1334-1340, 2015.

# Nonlinear behavior of silver nano-films in cw regime

Monday, 1st October @ 13:30: Poster Session (HALL & ROOM 3) - Poster - Abstract ID: 121

***Prof. Husam Abu-Safe***<sup>1</sup>

*1. German Jordanian University*

Transmission Z-scan measurements of silver nano-films in the cw regime were carried out to investigate the local response in the films' nano particles. The films were evaporated onto glass substrates at room temperature. The dependence of the far-field intensity on the sample position due to intensity-dependent optical nonlinearities was examined based on the Gaussian decomposition analysis of Shiek-Bahae model (SBM) and the thermal-lens model (TLM). In prefocal region, the experimental data were fitted with the SBM, whereas in the postfocal region the data were better fitted with the TLM. The thermal-lens model is nonlocal in space and time, whereas the Gaussian decomposition model is based strictly on local response. I discuss this behavior based on the context of the two models.

## Introduction

A major difference between the thermally induced nonlinearities and those induced by the local interaction is in the material's response time. Recently, there have been reports about ultrafast thermal nonlinearities in nanocomposite materials due to plasmonic effects. From the context of these reports, it was interesting to ask if the local model used to interpret z-scan measurements could be utilized to interpret the ultrafast thermal nonlinearities in these nanomaterials based on some sort of local behavior that arises from confining effects of the radiation fields in nano-volumes and shed some light on the cause of this behavior.

## Results

The thermal load from the laser source that produced the nonlinear behavior was manipulated by an optical chopper with 11% duty cycle. Fig. 1 shows the fitting of the measured data points with the SBF and TLM curves without using the optical chopper. The local model was excellent in the pre-focal region whereas the data were better fitted with the thermal model in the post-focal region. Fig. 2 shows the results of the SBF fitting when the optical chopper was used. Here, good agreement between the measured data and the SBF calculated curves suggest that the nonlinear response in the fabricated films is local which means it is in the ultrafast scale.

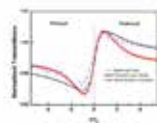


Fig. 1: The closed aperture z-scan for a 2 nm silver film. The open circles are the measured data. The connected stars are the SBF fitting curve, and the solid line is for TLM fitting curve.

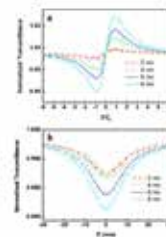


Fig. 2: The fitting of the SBF transmittance of the measured datapoints for the a) closed aperture runs. b) open aperture runs.

Slide1.jpg

Slide2.jpg

---

# Enhancing, controlling and guiding light with high refractive index dielectric nanoantennas

---

Monday, 1st October @ 14:30: Enhanced spectroscopy and sensing (ROOM 1) - Oral - Abstract ID: 354

---

**Ms. Angela I. Barreda <sup>1</sup>, Dr. Toshihiko Shibanuma <sup>2</sup>, Prof. Stefan A Maier <sup>2</sup>, Prof. Francisco Gonzalez <sup>1</sup>, Prof. Fernando Moreno <sup>1</sup>, Dr. Pablo Albella <sup>1</sup>**

*1. University of Cantabria, 2. Imperial College London*

Optical antennas can transform light from freely propagating waves into highly localized excitations that interact strongly with matter. These nanoantennas are usually made of metallic nanostructures and employed to obtain strong light-matter interactions at subwavelength size scales (plasmonics). Metals show some limitations due to their inherent ohmic losses, leading to temperature increase in the nanoantenna and its surroundings. Another limitation of metals is the difficulty to generate optical magnetic response.

Nanoantennas made of High Refractive Index Dielectric (HRID) materials with low losses in the VIS and NIR ranges, can produce both, high near field enhancements and good scattering efficiencies, while showing magnetic response and low heat radiation. Here, we will show how HRID nanoantennas can act as basic units for the development of efficient light emitting devices aimed at integrated photonics, sensing and surface enhanced spectroscopic applications[1-2]. Also, we will discuss another key aspect of these nanostructures, which is the presence of coherent effects between electric and magnetic resonances. Then, by conveniently designing their shape and size, they can arbitrarily interfere to direct light towards a desired direction[3-5]. This opens new paths to control the way light propagates at the nanoscale, such as steering (on-chip wireless communications)[4-6], building operational switching devices[7], designing novel metamaterials[8], enhancing nonlinear effects[9] or improving the performance of solar cells[10-11].

1. Albella, P. et al. J.Phys.Chem. C 117, 13573 (2013).

2. Caldarola, M. et al. Nat. Commun. 6, 7915 (2015).

3. Geffrin, J. M. et al. Nat. Commun. 3, 1171 (2012).

4. Albella, P., Shibanuma, T. & S. A. Maier. Sci. Rep. 5, 18322 (2015).

5. Barreda, A. I., Gutiérrez, Y., Sanz, J. M., González, F. & Moreno, F. Sci. Rep. 7, 11189 (2017).

6. Shibanuma, T. et al. ACS Photonics 4, 489 (2017).

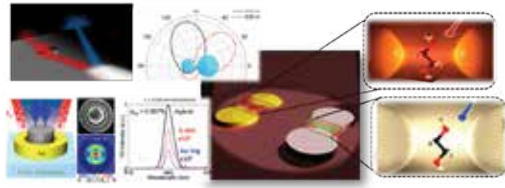
7. Barreda, A. I. et al. Nat. Commun. 8, 13910 (2017).

8. Shibanuma, T. Maier, S. A. & Albella, P. APL 112, 063103 (2018).

9. Shibanuma T., Grinblat, G., Albella, P. & Maier, S. A. Nano Lett. 17 (4), 2647 (2017)

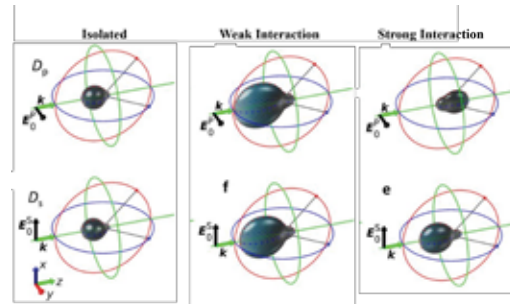
10. Shibanuma, T., Albella, P. & Maier, S. A. Nanoscale 8, 14184 (2016).

11. Barreda, A. I. et al. Sci. Rep., 8, 7976 (2018).



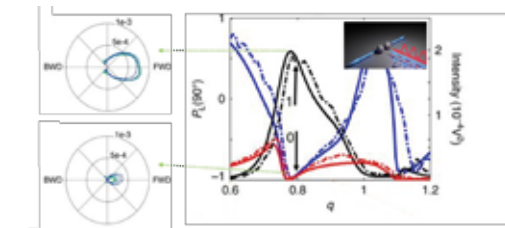
Hot spot with low heat radiation (right), efficient third harmonic generation with hybrid structures (bottom left) and light steering with HRID nanoantennas (top left).

Fig 1.png



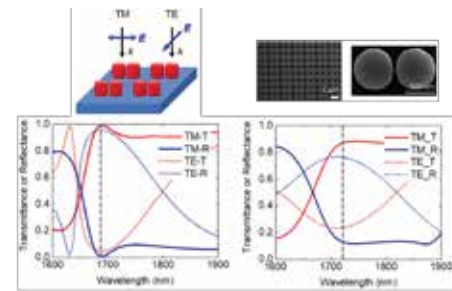
Isolated structure: no switching effect shown. Center and right columns show the no switching and switching effects for weak and strong interactions, respectively.

Fig 2.png



Switching effect. Scattered intensity diagrams for p- (top) and s-incident polarizations (bottom) at the wavelengths around the switching frequency ( $q=0.77$ ). Spectral behavior of the scattered intensity for p- (black line) and s- incident polarizations (red line) and the linear polarization degree (blue line) at  $90^\circ$ .

Fig 3.png



Calculated and measured transmission (red lines) and reflection (blue lines) spectra of a Si dimer array under the illumination of TM (solid lines) and TE (broken lines) polarizations.

Fig 4.png



---

## On chip resonant optical sensors

---

Monday, 1st October @ 14:30: Optical sensing from solid state to bio-medicine (ROOM 2) - Oral - Abstract ID: 201

---

***Prof. Yves-Alain Peter***<sup>1</sup>

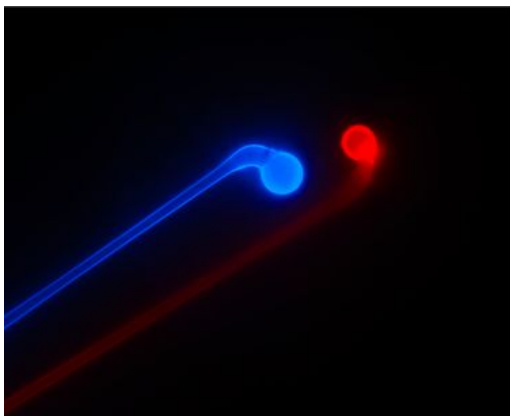
*1. Polytechnique Montréal*

On chip optical microresonators [1, 2] are compact, robust and can be integrated with micro electro-mechanical components as well as microfluidics. They can efficiently sense acceleration [3], forces [4], gases [5], refractive index of liquids [6], living cells [7], and bacteria [8], as well as tune lasers [9, 10].

I will report several sensors and tunable devices based on different types of optical microresonators, such as in-plane Fabry-Perot cavities, whispering gallery mode resonators and 2D photonic crystals.

### References

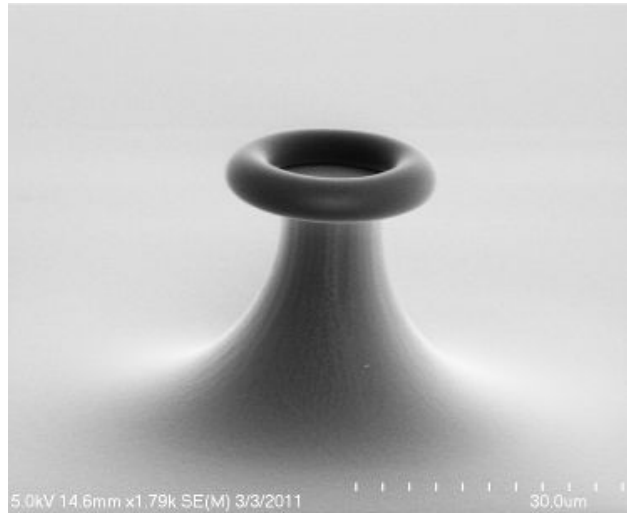
- [1] R. St-Gelais, A. Poulin, Y.-A. Peter, *Journal of Lightwave Technology* **30**, 1900 (2012)
- [2] S. Bergeron, S. Saïdi, Y.-A. Peter, *Optics Express* **18**, 16797 (2010).
- [3] K. Zandi, J.A. Bélanger, Y.-A. Peter, *Journal of Microelectromechanical Systems* **21**, 1464 (2012)
- [4] A. Poulin, R. St-Gelais, A. L. Eichenberger, L. Thévenaz, Y.-A. Peter, *Journal of Microelectromechanical Systems* **22**, 884 (2013)
- [5] R. St-Gelais, G. Mackey, J. Saunders, J. Zhou, A. Leblanc-Hotte, A. Poulin, J. A. Barnes, H.-P. Looock, R. S. Brown, Y.-A. Peter, *Sensors & Actuators B: Chemical* **182**, 45 (2013)
- [6] R. St-Gelais, J. Masson, Y.-A. Peter, *Applied Physics Letters* **94**, 243905 (2009)
- [7] A. Leblanc-Hotte, G. Chabot-Roy, L. Odagiu, M. Richaud, S. Lesage, J.-S. Delisle, Y.-A. Peter, *Sensors & Actuators B: Chemical*, (2018)
- [8] H. Ghali, H. Chibli, P. Bianucci, J. L. Nadeau, Y.-A. Peter, *Biosensors* **6**, 20 (2016)
- [9] F. Vanier, M. Rochette, N. Godbout, Y.-A. Peter, *Optics Letters* **38**, 4966 (2013)
- [10] J. Masson, R. St-Gelais, A. Poulin, Y.-A. Peter, *J. Quantum Electron.* **46**, 1313 (2010)



1.jpg



2.jpg



3.jpg

# Effect of local time-periodic perturbations on the topological edge mode of the SSH-model

Monday, 1st October @ 14:30: Optical properties, photonic & plasmonic nanomaterials (AUDITORIUM) - Oral - Abstract ID: 41

*Prof. Stefan Linden<sup>1</sup>, Mrs. Zlata Cherpakova<sup>1</sup>*

*1. University of Bonn*

The Su-Schrieffer-Heeger (SSH) model [1] is the prototypical system of a 1D topological insulator. It consists of a chain of identical sites coupled via alternating strong and weak bonds and features two topologically distinct dimerizations. Each interface between the two different dimerizations supports a topologically protected edge mode.

Here, we study the effect of time-periodic perturbations on this topological edge mode. We use arrays of evanescently coupled dielectric-loaded surface plasmon polariton waveguides to implement the SSH model (Fig. 1). Alternating strong and weak bonds with couplings  $J$  and  $J'$  were realized by choosing two different separations between neighboring waveguides. Periodic temporal fluctuations were implemented by fabricating a meandering waveguide at the interface between two domains. The SPP evolution was monitored by leakage radiation microscopy.

Figure 2 a depicts the real-space intensity distribution for a static interface [2]. Excitation of the central waveguide results in a localized mode at the interface. The corresponding momentum resolved spectrum (Fig. 2 b) reveals a mode in the center of the band gap.

The effect of the time-periodic driving on the topological edge mode depends on the driving frequency  $\omega$ . We observe both for fast modulations (Fig. 2 c) as well as for slow modulations (Fig. 2 g) a localized mode at the interface between the two dimerizations. In contrast to this, the intensity spreads over the whole array for intermediate modulation frequencies (Fig. 2 e).

The experimental results can be interpreted as follows. Modulation of the central waveguide with frequency  $\omega$  creates Floquet-replicas of the edge mode, which are shifted in energy by  $\pm n\omega$ . For  $\omega > |J+J'|$  (fast modulation) and  $\omega < |J-J'|$  (slow modulation), the first replicas do not energetically overlap with the two SSH bands (see arrows in momentum resolved spectrum in Fig. 2 d and e). However, for  $|J-J'| < \omega < |J+J'|$  the replicas can couple to bulk modes resulting in delocalization. This interpretation is supported by numerical calculations. In summary, our experiments show that time-periodic perturbations can destroy topological protection.

[1] W. P. Su et al., Phys. Rev. B **22**, 2099 (1983).

[2] F. Bleckmann et al., Phys. Rev. B **96**, 045417 (2017).

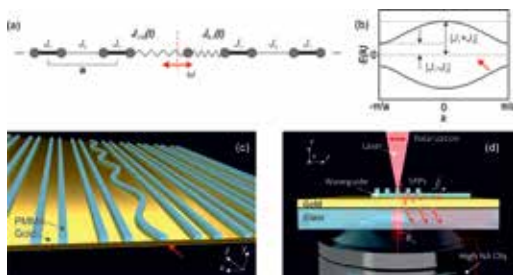


Figure 1.jpg

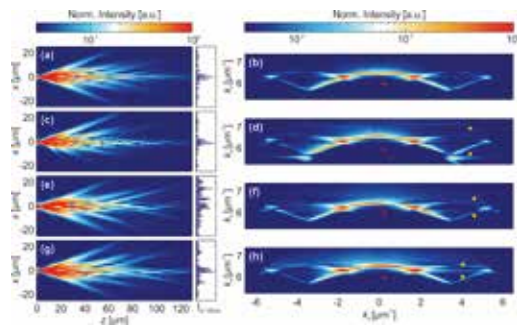


Figure 2.jpg

## Encoded SERS nanotags for multiplex bioassays

---

Monday, 1st October @ 15:00: Enhanced spectroscopy and sensing (ROOM 1) - Oral - Abstract ID: 103

---

***Prof. Xiangwei Zhao***<sup>1</sup>

*1. Southeast University*

Multiplex bioassays with high throughput sequencing and high throughput screening have drawn more and more attention for the development of novel analytical techniques, which are valuable for acquisition techniques of bioinformation of precision medicine. However, detection of proteins in a wide concentration range from fg mL<sup>-1</sup> to sub mg mL<sup>-1</sup> is a challenge in the high throughput analysis of precision medicine. Furthermore, the ultrasensitive detection of the extremely low concentration of multiplex analytes is challenging. With the rapid development of plasmonics, surface enhanced Raman scattering (SERS) has shown its promise in biomolecular analysis as a multifunctional modality. In this talk, SERS nanotags with fingerprinting molecular vibrational spectra as coding elements for multiplex assays will be introduced as well as their applications in practical applications with regards to the linear dynamic range (LDR), repeatability and limit of detection (LOD). Our results showed that SERS nanotags are desirable alternatives for commonly used fluorescence labels.

# Oxidation effects on the SERS response of silver nanoprism arrays

Monday, 1st October @ 15:17: Enhanced spectroscopy and sensing (ROOM 1) - Oral - Abstract ID: 471

**Dr. Niccolò Michieli**<sup>1</sup>, **Dr. Roberto Pilot**<sup>2</sup>, **Dr. Valentina Russo**<sup>1</sup>, **Dr. Carlo Scian**<sup>1</sup>, **Dr. Francesco Todescato**<sup>1</sup>, **Prof. Raffaella Signorini**<sup>1</sup>, **Prof. Stefano Agnoli**<sup>1</sup>, **Prof. Tiziana Cesca**<sup>1</sup>, **Prof. Renato Bozio**<sup>1</sup>, **Prof. Giovanni Mattei**<sup>1</sup>

1. University of Padova, 2. Consorzio INSTM and University of Padova

Silver nanostructures are widely employed for Surface Enhanced Raman Scattering (SERS) characterizations owing to their excellent properties of field confinement in plasmonic resonances. However, the strong tendency to oxidation at room temperature of these substrates may represent a major limitation to their performances.[1] In the present work, we investigated in detail the effects of oxidation on the SERS response of a peculiar kind of Ag nanostructured substrates, i.e., bi-dimensional ordered arrangements of Ag nanoprisms synthesized by nanosphere lithography. Particularly, wavelength-scanned SERS measurements were performed on Ag nanoprism arrays (NPA) oxidized at three different levels (non-oxidized, mildly and strongly oxidized) and thereafter functionalized with benzenethiol, in order to determine the SERS enhancement curves as a function of the excitation wavelength around the dipolar plasmonic resonance of the arrays. The experimental results were compared with those obtained by finite elements method simulations. With this approach, we were able to decouple the effects of spectral shift and decrease of the maximum value of the SERS enhancement observed for the different oxidation conditions.[2] From a practical standpoint we can state that the tendency of silver towards oxidation does not preclude the use

of Ag NPAs as platforms for SERS sensing with thiol- terminated molecules. Benzenethiol was found to effectively bind to the oxidized NPA surface as it does to the metallic NPAs: the SERS enhancement reduction demonstrated in

the oxidized samples amounts only to a factor of 2.5 and therefore does not alter significantly the NPA performances required for applications. As an example, in the Figure below we show the extinction spectrum (blue line), the experimental SERS enhancement profile (dots) and its fit (orange line) for the non-oxidized sample. Figure. Non-oxidized sample: absorption spectrum (blue line), experimental SERS enhancement profile (dots) and its fit (orange line).

[1] Y. Han et al.; *Anal. Chem.*, (2011), 83, 5873.

[2] N. Michieli, R. Pilot et al.; *RSC Adv.* (2017), 7, 369.

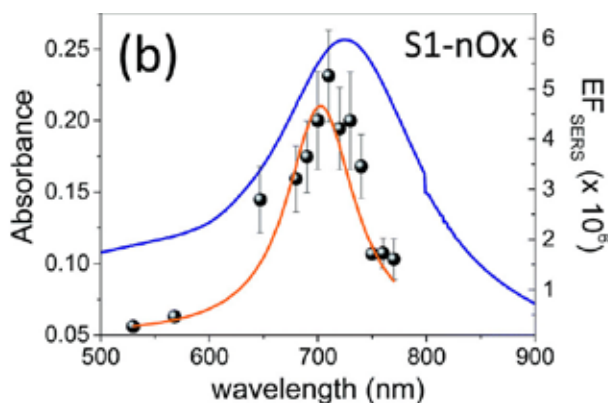


Figure.jpg

---

## Raman of Nano-objects at subwavelength scales

---

Monday, 1st October @ 15:34: Enhanced spectroscopy and sensing (ROOM 1) - Oral - Abstract ID: 422

---

***Prof. bernard Humbert*<sup>1</sup>, *Dr. Angéline D'orlando*<sup>2</sup>, *Dr. Maxime Bayle*<sup>1</sup>, *Prof. Guy Louarn*<sup>1</sup>**

*1. IMN J Rouxel-Univ Nantes, 2. INRA Nantes*

Our group develops an original approach combining an Atomic Force Microscope and a confocal-Raman microscope, where AFM microscope is used either to image and to manipulate nano-particles under the confocal optical microscope coupled at the Raman spectrometer or to enhance local electric field by plasmonic effects. Moreover, our optical device allows us to scan the resonance effects by tuning the wavelengths of excitation. This presentation will show the results obtained with some symmetric structures of assembling of metallic nano-particles, in the vicinity of a single and isolated nanoobject. We will investigate the consequence on the spatial super-resolved Raman spectra and as a function of the different sub-wavelength-scale geometries of aggregates. We will discuss the different interactions between nano-particles, including their impact on resonance effects. In particular, we will focus on the enhancement of the local electrical field by metallic nano-structures to probe single objects. These experimental data are interpreted according to finite element models of far and local electromagnetic fields. Thus, on one hand, we achieve to a better understanding about the tunability of plasmon resonance modes of home-tailored nanostructures, including sensitive breaks symmetry modes. On the other hand, the consequences of their interactions with a substrate or molecule dipole moment, depending on the excitation wavelength (especially in the case of the inelastic scattering), are studied. All this allows us to understand and predict the experimental observation

---

# Towards DNA biosensors: SERS studies on oligonucleotides

---

Monday, 1st October @ 15:51: Enhanced spectroscopy and sensing (ROOM 1) - Oral - Abstract ID: 96

---

***Dr. Aleksandra Jaworska*<sup>1</sup>, *Ms. Edyta Pyrak*<sup>2</sup>, *Prof. Andrzej Kudelski*<sup>1</sup>**

*1. Faculty of Chemistry, University of Warsaw, ul. Pasteura 1, 02-093 Warsaw, 2. Faculty of Chemistry, University of Warsaw, ul. Pasteura 1, 02-093 Warsaw; Department of Cell Biology, Nencki Institute of Experimental Biology of Polish Academy of Sciences, Warsaw*

Early diagnosis of cancer is vital to successful treatment. Unfortunately, many malignancies are detected at a stage of progression beyond when surgical resection or other interventions can be effectively implemented. New detection tools are therefore needed that overcome the poor levels of detection and/or high costs symptomatic of many of the approaches in use today.

One of the techniques that might help overcome these limitations is surface-enhanced Raman spectroscopy (SERS)<sup>1</sup>. SERS is a very sensitive and powerful tool for molecular detection upon adsorption on metal nanoparticles (colloids, electrodes and other surfaces). It relies on the plasmonically amplified electric fields that are excited upon irradiation of with optically resonant light.

With its limit of detection, SERS technique can help overcome obstacles appearing in routinely used methods, such as poor sensitivity, selectivity or false positive results caused by complicated preparation process required in advanced modifications of PCR methods.

SERS biosensors with the use of labels are based on high cross section on Raman scattering of certain organic molecules called Raman reporters (RR) /nanoprobes (especially dyes). The idea of a sensor is quite simple. Briefly, single stranded capture DNA (cDNA) is immobilized on a metal surface forming a monolayer where the empty gaps are filled in with spacer molecules (e.g., mercaptohexanol). Then, a small amount of sample containing target ssDNA is placed on this structure. Together with ssDNA it forms dsDNA during the hybridization process, and then it can be covered by another layer of ssDNA (rDNA), complimentary to tDNA and labelled with RR molecules enabling recording SERS signal<sup>2</sup>. The effectiveness of this type of sensors strongly depends on the structure of the layer of capture DNA (cDNA), selectivity of hybridization process, enhancement of the Raman signal by metal surface and RR molecule. Here we test different metal surfaces, methods of preparation of ssDNA monolayer and conditions of hybridization to optimize conditions to be able to detect single base mutation.

## Acknowledgements

This work was supported by the National Center of Science, Poland (grant FUGA UMO-2016/20/S/ST4/00148).

## References:

[1] M.Fleischmann et al., Chem.Phys.Lett.26(1974)163, [2] Y.Cao et al., Science297(2002)5586

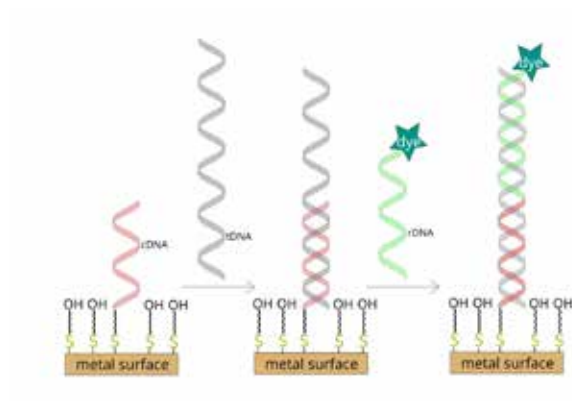


Figure 1. scheme of the basic sers-based nanosensor for dna mutation detection..jpeg



---

## Optical paddle - a new microtool for optical tweezers

---

Monday, 1st October @ 15:00: Optical sensing from solid state to bio-medicine (ROOM 2) - Oral - Abstract ID: 20

---

***Ms. Weronika Lamperska<sup>1</sup>, Dr. Sławomir Drobczyński<sup>1</sup>, Dr. Piotr Wasylczyk<sup>2</sup>, Dr. Jan Masajada<sup>1</sup>***

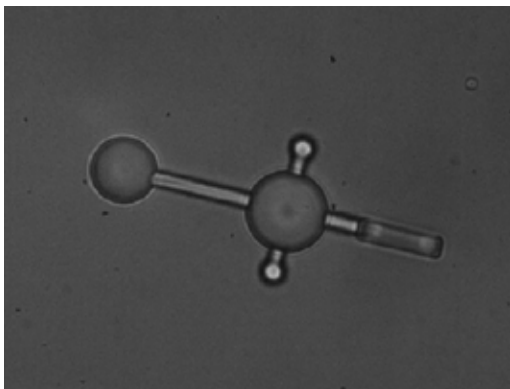
*1. Wrocław University of Science and Technology, 2. University of Warsaw*

Optical tweezers are the device which makes use of tightly focused laser light to optically trap and precisely manipulate the specimen in microscale. The examined object can be either trapped itself or studied with an additional tool. Since spherical shapes undergo the most stable trapping, so-called microbeads of various sizes and materials became a natural solution. They can be used as a probe, a handle, a marker, etc. Nevertheless, their simple shape is both an advantage and a limitation.

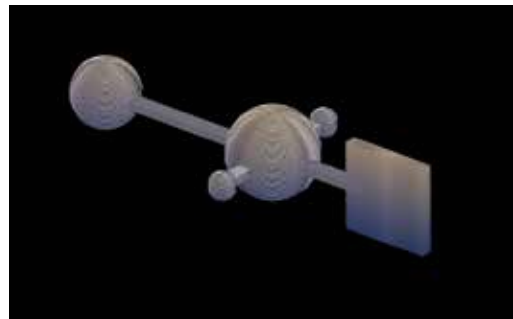
In this work, we propose a novel microtool which we called the optical paddle (see figures). It consists of two spheres, acting as handles, with a bar between them and a square 'blade' on the end. There are also two smaller spheres at both ends of a perpendicular arm which provide extra stabilization. The total length of this microtool is 45 $\mu$ m whereas the blade is 10x10 $\mu$ m. The optical paddle was 3D printed with the two-photon polymerization technique and then immersed in a chamber filled with water.

We use optical paddles in two different optical tweezers (OT) setups – a holographic and non-holographic version. Both consist of a laser source, a high-numerical aperture microscope objective (NA=1.3), and a CMOS camera. The difference lies in the way of steering the laser beam. While the holographic OT use spatial light modulator (SLM), the second setup uses galvanic mirrors. As a result, the experiments benefit from both the unlimited number of available optical traps and high stiffness of the trap.

We present new possibilities that arise from introducing optical paddles to the OT system. Firstly, the microtools were tested for sensitivity to forces even below single piconewtons. This included e.g. exposing the paddle to weak hydrodynamic flow produced by oscillating microbead or pressing one paddle against the other. The response of the tool was measured as a displacement of the rear handle from the trap center. Finally, having confirmed the sufficient sensitivity, an experiment with human spermatozoa pushing onto the paddle was performed in order to estimate their force. In our work we demonstrate these experiments and discuss further applications of optical paddles.



Optical paddle fig1.jpg



Optical paddle fig2.png

## 2D nanomaterials enhanced surface plasmon resonance for sensing applications

---

Monday, 1st October @ 15:17: Optical sensing from solid state to bio-medicine (ROOM 2) - Oral - Abstract ID: 214

---

***Dr. Shuwen Zeng**<sup>1</sup>*

*1. XLIM Research Institute, UMR 7252 CNRS, France*

Surface plasmon resonance sensors are commonly used an effective tool for real-time monitoring biomolecular interactions. The sensing mechanism is based on the evanescent field perturbation at the metallic sensing substrate induced by the binding of chemical and biological molecules. Molecular binding interactions could be measured from the signal of reflected light, under the condition that the surface plasmon resonance is excited by the incident light. In this talk, we will present the use of hybrid 2D nanomaterials-based metasurface nanostructure as an enhanced sensing substrate. The thickness of the plasmonic sensing substrate is tuned in an atomic scale and optimized to improve the sensing capability. Here, both a sharp phase signal change and phase-related Goos-Hänchen signal shift were achieved due to the strong resonance at the surface of the sensing film. The enhanced plasmonic sensitivities of 2D nanostructures were systematically investigated. It is worth noting that the tunability of atomic layer led to the sensing substrate optimized with a narrow scale < 1 nm. Through a precise engineering of the metasurface substrates, 3 orders of magnitude improvement of the sensitivity were demonstrated compared to the one with pure gold sensing substrate. This hybrid 2D nanomaterial-based metasurfaces would provide a good opportunity for developing portable theranostic devices in clinical applications.

---

# Nanoplasmonic NO<sub>2</sub> sensing with a Au-WO<sub>3</sub> Nanocomposite

---

Monday, 1st October @ 15:34: Optical sensing from solid state to bio-medicine (ROOM 2) - Oral - Abstract ID: 272

---

***Dr. Irem Tanyeli*<sup>1</sup>, *Dr. Olof Andersson*<sup>2</sup>, *Prof. Christoph Langhammer*<sup>1</sup>**

*1. Chalmers University of Technology, 2. Insplorion AB*

Air pollution is one of the largest environmental risk factors causing severe health problems all over the world. In order to take a fast and decisive action against this serious threat, real-time monitoring is desirable. Presently, conventional instrumentation for highly accurate air quality monitoring exists, however it is expensive, stationary and complex. Here, we are presenting an air quality sensor based on indirect nanoplasmonic sensing [1], with the potential to enable real time monitoring of air pollutants at the ppb level. Our sensor is initially optimized for NO<sub>2</sub> detection, since NO<sub>2</sub> is identified as one of the most toxic and corrosive pollutants. In our present design, an array of Au nanodisks is used as plasmonic signal transducer and a thin sputtered WO<sub>3</sub> thin film on top as the active and selective layer. In our study, we investigated the effects of microstructure and thickness of the WO<sub>3</sub> layer, as well as the size of the plasmonic particles, on the sensitivity towards NO<sub>2</sub>. In order to mimic a realistic sensing environment, we also conducted our measurements in the presence of CO, CO<sub>2</sub> and humidity. Our results show that with materials grown under optimized conditions our sensors exhibit an NO<sub>2</sub> detection limit in the ppb range, as well as very low cross-sensitivity towards CO, CO<sub>2</sub> and H<sub>2</sub>O.

[1] Larsson E. M. et al Science 2009, 326, 1091-1094.

---

## GFP-based Nanothermometry at the Mitochondria

---

Monday, 1st October @ 15:51: Optical sensing from solid state to bio-medicine (ROOM 2) - Oral - Abstract ID: 434

---

***Dr. Oleksandr A. Savchuk*<sup>1</sup>, *Dr. Oscar F. Silvestre*<sup>1</sup>, *Mr. Ricardo M. R. Adão*<sup>1</sup>, *Dr. Jana B. Nieder*<sup>1</sup>**

*1. Nanophotonics Department, Ultrafast Bio- and Nanophotonics group, INL - International Iberian Nanotechnology Laboratory*

Temperature plays a crucial role for the biological functioning of all living organisms. Thus, accurate and spatially resolved information on internal temperature can make an important contributions to cell biology and biomedical field [1]. In this context, luminescence nanothermometry that uses small luminescent thermometers to measure temperature has attracted a lot of attention due to its non-invasive nature, high spatial and thermal resolution [2]. However, it is challenging to control intracellular specific locations of nanothermometers, since some are taken up by endocytosis, and many others require microinjection. Another important drawback of existing luminescent nanothermometers is a need of complicated synthesis procedure and potential toxicity of the luminescent material or unwanted aggregation.

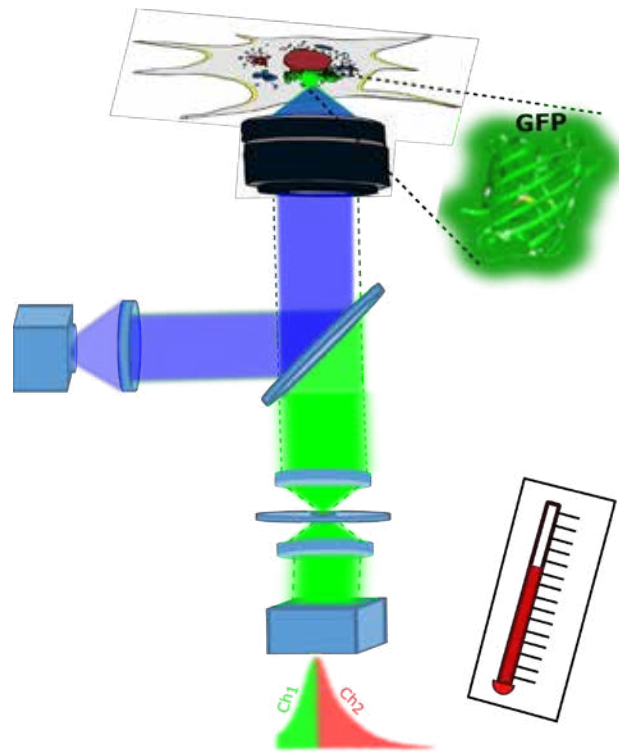
Here, we show how intracellular temperature can be measured using commercial available green fluorescence protein (GFP) attached to specific proteins in the cell. We show that a ratiometric approach applied to the analysis of the fluorescence emission spectrum of GFP can be used to determine temperature. First, we demonstrate the capability of wt-GFP for solution-based nanothermometry. Then, in vitro studies were performed with genetically transfected HeLa cells using a GFP agent associated to the mitochondria of the cells. Thermal images were recorded by means of confocal microscopy, where fluorescence emission is separated into two spectral wavelength ranges using a diffractive grating and selected subarrays of the 32 channel GaAsP detector.

High intracellular thermal resolution and sensitivity of around 0.26 °C and 2.5 °C<sup>-1</sup>, respectively were achieved [3]. Moreover, the specific organelle association of the protein based nanothermometer at the mitochondria allowed observing temperature increase induced by a chemical uncoupling reagent. We believe that our method will facilitate basic research on cellular biological processes and furthermore may find practical application in hyperthermia therapy allowing temperature feedback during treatments.

[1] K. Okabe, R. Sakaguchi, B. Shi, and S. Kiyonaka. *Pflugers Arch. Eur. J. Physiol.*, vol. 470, no. 5, pp. 717–731, 2018.

[2] H. Zhou, M. Sharma, O. Berezin, D. Zuckerman, and M. Y. Berezin. *ChemPhysChem*, vol. 17, no. 1, pp. 27–36, 2016.

[3] O.A. Savchuk, O. F. Silvestre, R. M. R. Adão, J. B. Nieder\*, submitted (2018).



Illustrative representation of the gfp-based intracellular temperature method.png

---

# Enhancing hydrodynamic nonlocal resonances in semiconductor plasmonics

---

Monday, 1st October @ 15:00: Optical properties, photonic & plasmonic nanomaterials (AUDITORIUM) - Oral - Abstract ID: 396

---

**Ms. Tahereh Golestanizadeh**<sup>1</sup>, **Dr. Johan Maack**<sup>2</sup>, **Prof. N. Asger Mortensen**<sup>3</sup>, **Dr. Tahmineh Jalali**<sup>4</sup>,  
**Dr. Abbas Zarifi**<sup>5</sup>, **Dr. Martijn Wubs**<sup>2</sup>

*1. Technical University of Denmark and Yasouj University, 2. Technical University of Denmark, 3. University of Southern Denmark, 4. Persian Gulf University, 5. Yasouj University*

We study the breakdown of the bulk plasmonic model of semiconductors as we reduce their size. For metallic nanostructures in the few-nm range it is well known that the usual description breaks down since nonlocal-response and spill-out effects start to play a role, both of which can be described by the semiclassical hydrodynamic Drude model or by more microscopic theories. On the other hand, the smallest semiconductor structures such as quantum wells or dots are described by particle-in-a-box quantum mechanics, while larger semiconductors get a bulk plasmonics description.

Recently we proposed that an intermediate size regime for semiconductor nanostructures should exist where a semiclassical hydrodynamic Drude description replaces the classical Drude-like response; deviations from classical plasmonics will occur for larger-sized structures than for metals and nonlocal effects will be even more pronounced than for metals [1]. For example, we predicted the existence of hydrodynamic standing bulk plasmons which have no classical analogue. Interestingly, their experimental observation has recently been reported [2].

Further novel hydrodynamic plasmonic effects can be expected in semiconductors where two or more species of charge carriers co-exist, for example in intrinsic or p-doped semiconductors. While classically the effect of two or more such ‘fluids’ is rather trivial, in the hydrodynamic theory, the collective resonances of the two plasma’s can lead to novel resonances including an acoustic resonance at low frequencies which has no analogue in classical plasmonics [3].

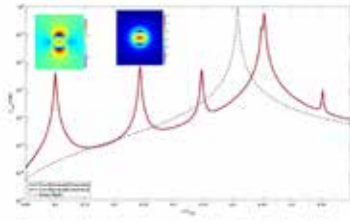
To facilitate the observation of two-fluid hydrodynamic effects, we currently investigate plasmonic nanostructures for which the nonlocal responses are most pronounced [4]. To that end we have numerically implemented the two-fluid hydrodynamic model and found fine agreement with Mie calculations in a benchmark problem (Fig1). We report nonlocal effects in rectangular waveguide structures and study the two-fluid acoustic modes in plasmonic dimers (Fig2). Our analytical and numerical study paves the way for experimental confirmation of rich hydrodynamic plasmonics in various semiconductor nanostructures.

[1] J.R. Maack et al., EPL 119, 17003 (2017).

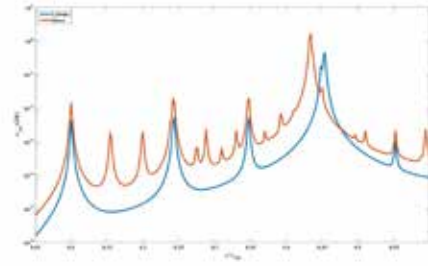
[2] D. de Ceglia et al., Sci. Rep. 8, 9335 (2018).

[3] J.R. Maack et al., PRB 97, 115415 (2018).

[4] T. Golestanizadeh et al., in preparation (2018).



Golestanizadeh fig1 benchmark extinction cross section with mie versus comsol for two fluid plasmonic cylinder 1 .jpg



Golestanizadeh fig2 extinction cross section for two fluid plasmonic cylinder versus its dimer.jpg

---

# Transverse Anderson localization of channel plasmon polaritons

---

Monday, 1st October @ 15:17: Optical properties, photonic & plasmonic nanomaterials (AUDITORIUM) - Oral - Abstract ID: 37

---

***Dr. Jiří Petráček<sup>1</sup>, Dr. Vladimír Kuzmiak<sup>2</sup>***

*1. Brno University of Technology, Institute of Physical Engineering, Technická 2896/2, 616 69 Brno, 2. The Czech Academy of Sciences, Institute of Photonics and Electronics, Chaberska 57, 182 51, Praha 8*

Photonic lattices and coupled waveguide arrays represent convenient systems in which the evolution of the waves in complex structures can be studied. It has been shown that by engineering of the propagation constants of the individual waveguides and their mutual couplings one can explore a rich variety of quantum-optical analogies. In this paper we investigate the transverse Anderson localization (TAL) of the surface plasmon polaritons induced by an off-diagonal disorder. Our system consists of a metallic (silver) surface perturbed by  $N$  parallel rectangular grooves with the same width  $w$  and depth  $d$  cut into the planar surface of a metal. The off-diagonal disorder is introduced by uniform random variation of the separation distance  $s$  between the neighboring grooves in the range  $[s_0 - \Delta s, s_0 + \Delta s]$ . Each groove supports bound surface electromagnetic wave - channel plasmon polariton (CPP). Solving the Maxwell equation for the array of grooves represents a full 3D problem, however, the spatial evolution of the CPP beam along the system ( $z$ ) can be conveniently described by the coupled mode theory (CMT). The two key parameters of the structure, coupling coefficient  $C$  and the change in the CPP propagation constant  $\Delta\beta$ , that enter the CMT model and their dependencies on  $s$  are rigorously evaluated (Comsol). The power distribution of the CPP beam for a periodic system ( $\Delta s = 0$ ) exhibits a diffractive spreading with increasing the transverse distance into the array of grooves. A transition from this ballistic regime to TAL is observed with increasing the disorder strength  $\Delta s$  (see Fig. 1, parameters:  $w = 100$  nm,  $d = 350$  nm, wavelength = 600 nm,  $s_0 = 100$  nm,  $N = 300$ , the results are averaged over 200 realizations). Fig. 2 shows an effective longitudinal length  $L_{\text{eff}}$  (the shortest propagation distance at which the beam width becomes approximately constant) for various  $s_0$  and  $\Delta s$  compared with the CPP propagation length  $L_p$ . Clearly, the Ohmic losses and the effect of relative disorder strength  $\Delta s/s_0$  on the coupling between the grooves play a central role in realization of the TAL. We suggest two strategies which are beneficial for its observation and discuss a potential impact of randomness on beam steering in the plasmonic nanodevices.



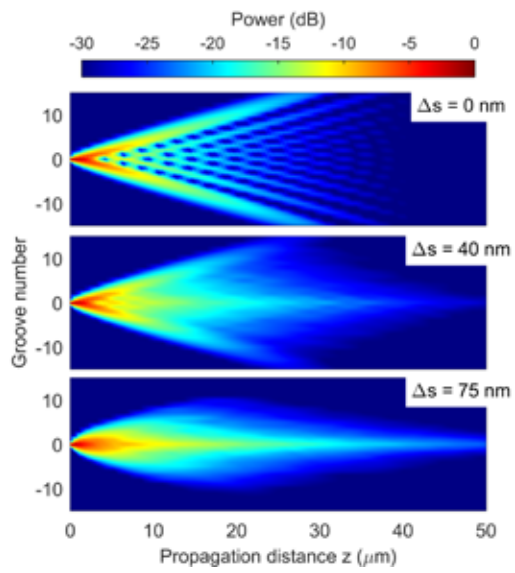


Fig1 power vs distance.png

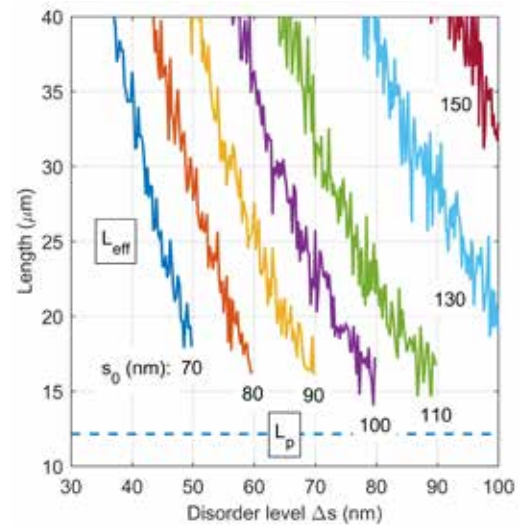


Fig2 longitudinal effective length vs disorder level.png

# Single-emitter and collective effects in light emission from ordered arrays of InGaN-GaN nanowires

Monday, 1st October @ 15:34: Optical properties, photonic & plasmonic nanomaterials (AUDITORIUM) - Oral - Abstract ID: 111

***Dr. Duncan Allsopp<sup>1</sup>, Dr. Chris Lewins<sup>1</sup>, Dr. Szymon Lis<sup>1</sup>, Dr. Simon O'kane<sup>1</sup>, Dr. Pierre-marie Coulon<sup>1</sup>, Dr. Emmanuel Le Boulbar<sup>1</sup>, Dr. Margaret Hopkins<sup>1</sup>, Dr. Philip Shields<sup>1</sup>***

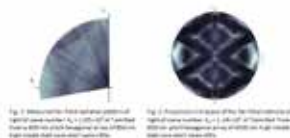
*1. University of Bath*

It is widely known that the size of a light emitting devices (LED) has a profound effect on their emissive properties. In particular, wire-shaped nanostructures have been proposed for increasing the external quantum efficiency of light emitters and for controlling the direction of their emission. Yet achieving such benefits is not straightforward because of intricate interactions between the light source and the realized geometry of a nanowire. Also, the constraints of nanofabrication can limit the separation between adjacent devices when ordered arrays of emissive nanowires are required. This paper describes an investigation of the roles of single nano-device emission and collective effects on the emissive properties of ordered arrays InGaN-GaN light emitting nanowires.

InGaN-GaN nano-LEDs were fabricated in two ways: (a) arrays of 200-450 nm diameter nanowires were etched from pre-grown InGaN-GaN epitaxial layers containing a single InGaN quantum well (QW); or (b) from GaN homo-epitaxial layers and then over-grown with a single InGaN-GaN QW by metalorganic vapour phase epitaxy. The angle dependence of resonantly excited room temperature photoluminescence (PL) was measured using a goniometer system.

The angle dependence of the PL from a hexagonal array (600 nm pitch) of short (850 nm high) core-shell nano-LEDs (Fig.1) shows traditional diffraction behaviour. However, increasing the height of the core-shell nanowires causes a dramatic change in the angular distribution of the radiation (Fig.2).

Measurements of free-space wave number ( $k_o$ ) versus lateral wave-vector ( $k_{||}$ ) of the type of diffraction feature seen in Fig. 2 revealed their origin is the formation of the partial bandgaps of a two-dimensional photonic crystal fabricated on a high index substrate, due to only weak coupling of light propagating laterally in an array of tall (4000 nm high) nanowires to the underlying substrate. Maps of  $k_o$  versus  $k_{||}$  of other emissive nanowire array structures revealed that features characteristic of the emission of light from single nanowires are typically superimposed on diffraction patterns of the types shown in Figs. 1 and 2. The impact of these nano-photonic emission effects and on the properties of nano-LED devices, including ring-shaped nanostructures, and light trapping in the substrate will be discussed.



# Whispering gallery modes in novel silicon nanophotonic resonators

Monday, 1st October @ 15:51: Optical properties, photonic & plasmonic nanomaterials (AUDITORIUM) - Oral - Abstract ID: 278

***Dr. Sebastian Schmitt*<sup>1</sup>, *Dr. Klaus Schwarzburg*<sup>1</sup>, *Mr. Christian Appelt*<sup>1</sup>, *Dr. Hanno Kröncke*<sup>1</sup>, *Mr. Sven Wiesner*<sup>1</sup>, *Prof. Catherine Dubourdieu*<sup>1</sup>**

*1. Helmholtz Zentrum Berlin für Materialien und Energie*

The emerging research field of silicon (Si) nanophotonics is pointing out promising ways towards revolutionary new lighting and modulator devices that rely on the nonlinear interaction of light with Si nanostructures. We provide a detailed understanding of photonic modes hosted in monolithic silicon nanophotonic resonators of a novel geometry (inverse half ellipsoid). Cathodoluminescence (CL) spectra were acquired along the height of the resonators. The intensity distributions were found to precisely match the numerically predicted distributions of hosted whispering gallery modes (WGMs). This enabled the derivation of an analytical design rule that describes the mode alignment in the resonators. We also show that a precise mode modulation can be performed via the application of a thin dielectric oxide cladding ( $\text{Al}_2\text{O}_3$  or  $\text{HfO}_2$ ).

Samples were prepared using cryogenic reactive ion etching and CL measurements were performed in a scanning electron microscope (SEM). For the numerical mode analysis, finite difference time domain (FDTD) simulations were used and for each emission peak the position and shape of the corresponding WGM was determined.  $\text{Al}_2\text{O}_3$  or  $\text{HfO}_2$  coatings were deposited by thermal atomic layer deposition (ALD) at 200°C. The wavelength shifts of the photonic modes were detected by micro-photoluminescence (PL) spectrometry.

Fig. 1a shows an SEM image in 90° tilt view of a typical Si nano-resonator under study. CL measurements permit a selective excitation of the photonic modes as indicated by the spectra shown in Fig. 1b. The spectra, collected at two positions along the nanostructure (see Fig. 1a), clearly exhibit spectrally coinciding peaks with a different distribution of intensities and permit to predict the position of the modes in the structures. X-Y cross sectional energy density ( $E^2$ ) maps obtained by FDTD simulations for two specific modes are given as insets. Fig. 2b shows a cross section image of a nanostructure conformally coated with alumina. As can be seen from the graph in Fig. 2a, the ALD coating induces peak shifts. The shifts are shown to be precisely tunable by the thickness and the refractive index of the applied optical cladding.

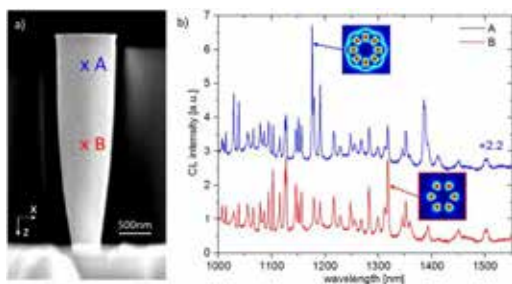


Figure 1.jpg

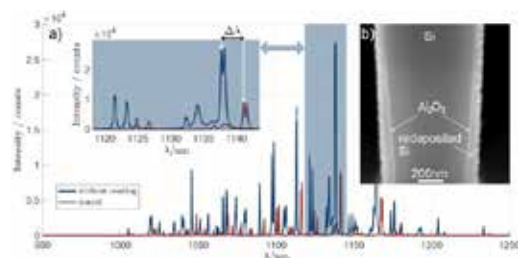


Figure 2.jpg

# Attojoule Modulators for Photonic Neuromorphic Computing

Monday, 1st October @ 16:35: Strong light-matter interactions at the nanoscale (ROOM 1) - Oral - Abstract ID: 367

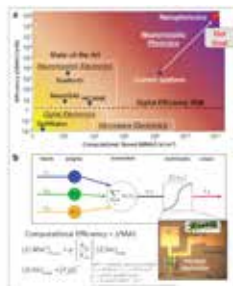
**Mr. Jonathan George<sup>1</sup>, Mr. Amin Mehrabian<sup>1</sup>, Mr. Rubab Armin<sup>1</sup>, Prof. Tarek El-Ghazawi<sup>1</sup>, Prof. Paul Prucnal<sup>2</sup>, Prof. Volker Sorger<sup>1</sup>**

1. George Washington University, 2. Princeton University

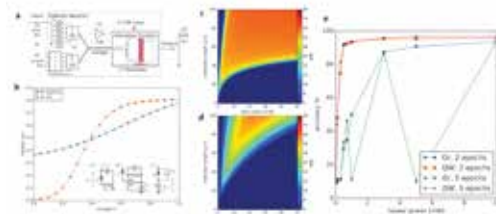
Neuromorphic networks are computational algorithms and network models inspired by signal processing in the brain with societal-relevant applications in machine-learning such as speech and image recognition, non-linear optimization, and real-time simulation. Recent progress by both industry and academia has demonstrated compute efficiencies surpassing the digital efficiency wall set by von-Neumann compute architectures. An artificial neural network consists of a set of input artificial neurons connected to both the hidden- and the output layer. Within each layer, information propagates by a linear combination such as matrix multiplication followed by the application of a nonlinear activation function. Optical neural network (ONN) implementations offer unique advantages over microelectronics because the linear transformation (e.g. matrix multiplication) can be executed in the optically with temporal response times  $<10\text{ps}$ .

Neural networks require both a weighting of inputs and a nonlinear activation function operating on their sum. Neural network weighting has been demonstrated in integrated photonics with both interferometric and ring-based wavelength division multiplexing. While direct nonlinearity in optics is difficult to achieve without high optical powers, an electro-optic nonlinearity can be created by directly coupling a photodiode to electro-optic modulator. The low capacitance of directly coupling the components results in operating speeds  $>10\text{GHz}$  with relatively low power consumption. Here we present a closed form equation for the activation functions created by graphene and quantum well electro-optic absorption modulators capacitive coupled to photodiodes. Our modulator-geometry based and thermal-noise analysis shows that such electro-optic neurons produce SNRs around 60. Performing an MNIST classification inference test on an AlexNet-based neural network with these electro-optic nodes, with accuracies of about 95% starting a laser power level around 3mW and 10mW for the QW and Graphene-based modulator, respectively. Our findings show regions of realistic operating performance of future optical and photonic neural networks using electro-optic analogue (non-spiking) neurons.

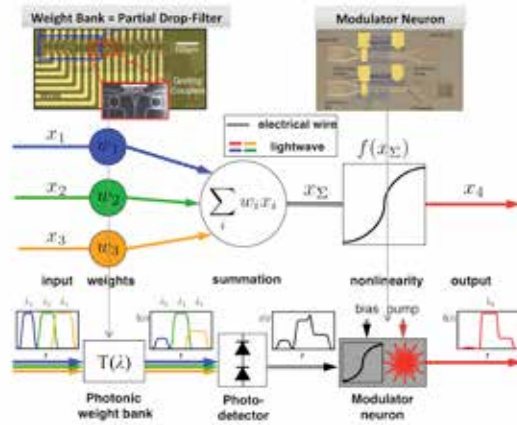
We report on using the transfer function of electrooptic absorption modulators as nonlinear activation functions of photonic neurons and show 95% accuracy of MNIST classification inference on an AlexNet in optical artificial neural networks.



Neuro-eam- fio fig1.png



Neuro-eam- fio fig2.png



Neuro-eam- fio fig3.png

---

# Nano-scale luminescence imaging and properties of radially-heterostructured III-V nanowires

---

Monday, 1st October @ 16:35: Optical properties of nanostructures (ROOM 2) - Oral - Abstract ID: 119

---

***Dr. PAOLA PRETE*<sup>1</sup>, *Prof. Nico Lovergine*<sup>2</sup>**

*1. CNR-IMM Lecce, Italy, 2. Università del Salento*

III-V compounds nanowires (NWs) have gathered considerable research interests in recent years, due to their potential applications to novel nano-scale photonic devices, such as nano-lasers, photodetectors and solar cells. Radial modulation of NW composition to form core-(multi)shell heterostructures promises to impact such nano-devices by adding new degrees of freedom (due to quantum confinement) to their design. However, strict control over the self-assembly of radially heterostructured NWs and detailed insights of their nano-scale (structural, radiative) properties are crucial for their exploitation in future nano-photonic devices.

We report on the nano-scale spectroscopic characterization of GaAs-AlGaAs core-shell and core-(multi)shell NWs grown by metal-catalysed metalorganic vapour phase epitaxy. High spatial resolution cathodo-luminescence (CL) spectroscopy measurements performed inside a field-emission scanning electron microscope enabled us to study the radiative properties of single core-(multi)shell NW structures in great details, and correlate them to the nanostructure dimensions. CL measurements were performed at low-temperature (7K) on single GaAs-AlGaAs core-shell NWs and GaAs-AlGaAs quantum well tube (QWT) structures. This allowed to study the free-exciton emission of GaAs core in GaAs-AlGaAs core-shell NWs and its energy shift with the heterostructure relevant size (namely, the shell thickness to core radius ratio), this being afterwards compared with the strain-shifted values of heavy- and light-hole excitons calculated for GaAs assuming an elastic energy equilibrium model in the NW. By comparing CL results with photoluminescence (PL) spectra collected from dense NW arrays, we further demonstrated the combined effect of strain-induced band-shift and the occurrence of a space-charge region (associated with materials unintentional doping) at the GaAs/AlGaAs interface, as the origin of red-shift of GaAs excitons in the PL emission of these core-shell NWs.

CL imaging of single GaAs-AlGaAs core-multishell NWs allowed to spatially resolve different contributions found in CL (and PL) spectra, namely (i) AlGaAs emission channels related to unintentional formation of Al-rich alloys within the nanostructure (a result of NW specific growth mechanism), and (ii), spatial inhomogeneity of the GaAs QWT emission, further ascribed to thickness gradient/fluctuations of the QWT along the NW axis. The results will be further discussed based on our current knowledge of the nano-scale structural properties of present NWs.

# Amplified spontaneous emission, Purcell effect, lasing, and light emitting diodes from perovskite nanocrystal films

Monday, 1st October @ 16:35: Metamaterials (AUDITORIUM) - Oral - Abstract ID: 68

**Dr. Roman Krahne**<sup>1</sup>

*1. Italian Institute of Technology*

Inorganic perovskite nanocrystals have recently emerged as a highly promising material in light emission due to color tunability by chemical composition and quantum confinement, and bright emission from nanocrystal films with photoluminescence quantum yields up to unity has been demonstrated. [1,2] In this talk the photo-physical properties of perovskite nanocrystal in solution and in thin films will be discussed. [3] We will show that a novel synthetic approach based on benzoyl halides leads to high PLQY and extremely low ASE thresholds (Fig. 1a,b). [4] Quantum confinement in CsPbBr<sub>3</sub> nanoplatelets results in blue emission and films with 25 % PLQY are obtained by spin-coating. The nanoplatelets in such films can be transformed to green emitting nanobelts by high intensity UV light exposure, as illustrated in Figure 1c-d. The transformed films manifest extremely stable emission and are robust to treatment with different solvents, which enables the fabrication of all-solution processed light emitting diodes. [5] Furthermore, the plasmonic resonances of metal/dielectric multilayers can be used to enhance the emission and radiative rate of the fluorophore that is spincoated on their surface. We demonstrate four-fold emission enhancement of a film of CsPbBr<sub>3</sub> nanocubes deposited on such planar metamaterial structures, and highlight how the plasmonic resonances can be tuned to the emission and absorption bands of the emitter (Fig. 2).

## References

- [1] L. Protesescu, S. Yakunin, M. I. Bodnarchuk, F. Krieg, R. Caputo, C. H. Hendon, R. X. Yang, A. Walsh, and M. V. Kovalenko, *Nano Lett.* **15**, 3692 (2015).
- [2] S. Yakunin *et al.*, *Nat. Commun* **6**, 8056 (2015).
- [3] F. Di Stasio, M. Imran, Q. A. Akkerman, M. Prato, L. Manna, and R. Krahne, *J. Phys. Chem. Lett.* **8**, 2725 (2017).
- [4] M. Imran, V. Caligiuri, M. Wang, L. Goldoni, M. Prato, R. Krahne, L. De Trizio, and L. Manna, *J. Am. Chem. Soc.* **140**, 2656 (2018).
- [5] J. Shamsi, P. Rastogi, V. Caligiuri, A. L. Abdelhady, D. Spirito, L. Manna, and R. Krahne, *ACS Nano* **11**, 10206 (2017).

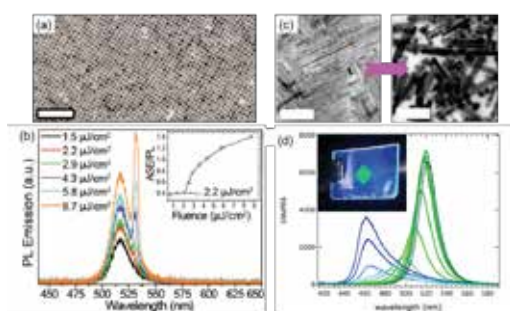


Figure 1. TEM image (a) and ASE (b) from CsPbBr<sub>3</sub> nanocubes. (c-d) Transformation by UV light exposure of blue emitting perovskite nanoplatelets to green emitting nanobelts.

Nanop fig1.png

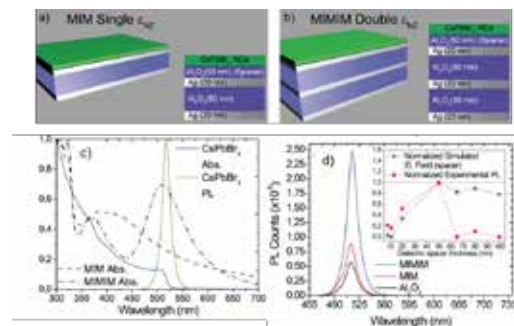


Figure 2. (a-b) Schemes of the metal/dielectric multilayers. (c) Matching of the plasmonic resonances of the MIM and MIMM to the absorbance and emission of the perovskite nanocrystal dye. (d) Emission enhancement.

Nanop fig2.png

---

# Nonlinear THz Plasmonics in Bi<sub>2</sub>Se<sub>3</sub> Topological Insulator

---

Monday, 1st October @ 17:05: Strong light-matter interactions at the nanoscale (ROOM 1) - Oral - Abstract ID: 46

---

**Dr. Paola Di Pietro**<sup>1</sup>, **Dr. Nidhi Adhlakha**<sup>1</sup>, **Dr. Federica Piccirilli**<sup>2</sup>, **Dr. Alessandra Di Gaspare**<sup>3</sup>, **Prof. Seangshik Oh**<sup>4</sup>, **Dr. Andrea Perucchi**<sup>1</sup>, **Prof. Stefano Lupi**<sup>5</sup>

1. Elettra-Sincrotrone Trieste S.C.p.A., 2. CNR-IOM Trieste, 3. NEST, Istituto Nanoscienze, CNR, Scuola Normale Superiore., 4. Department of Physics and Astronomy Rutgers, State University of New Jersey, 5. CNR-IOM Dip. di Fisica, Università di Roma Sapienza

Topological insulators are a class of materials which have raised a great interest over the last decade, thanks to their intriguing conduction properties. Indeed, they are insulating in the bulk and metallic at the surface. Moreover, these metallic surface states have linear Dirac dispersion as in the case of graphene [1,2].

Bi<sub>2</sub>Se<sub>3</sub> is among the most promising topological insulators, since its band structure provides only one Dirac cone, while the bulk gap is pretty large (about 300 meV) [3].

It has been demonstrated that by terahertz-infrared spectroscopy it is possible to detect the Dirac surface state by patterning thin films of Bi<sub>2</sub>Se<sub>3</sub> with ribbons of width from 2 to 20 μm. In this way, a Dirac plasmon is excited and its dispersion recovers very well the theoretical dispersion, calculated by using the parameters of the Dirac carriers [4].

In this scenario, we present here our investigation on the nonlinear regime of patterned films of Bi<sub>2</sub>Se<sub>3</sub> with ribbons of width of 4 and 20 μm. By exploiting the intense THz electric field of the TeraFERMI beamline at the FEL (Free Electron Laser) Fermi in Trieste [5], we were able to induce a nonlinear behaviour of the Dirac plasmon. Indeed, we observed a redshift of the plasmonic peak as the incoming THz electric field increases (up to MV/cm).

## References

- [1] L. Fu, C. L. Kane, and E. J. Mele, 2007 *Phys. Rev. Lett.* 98, 106803.
- [2] Y. Xia et al. 2009 *Nature Physics* 5, 398.
- [3] P. Di Pietro et al. 2012 *Phys. Rev B* 86, 045439.
- [4] P. Di Pietro et al. 2013 *Nature Nanotechnology* 8, 556.
- [5] P. Di Pietro et al. 2017 *Synchrotron Radiation News* 30, 4.



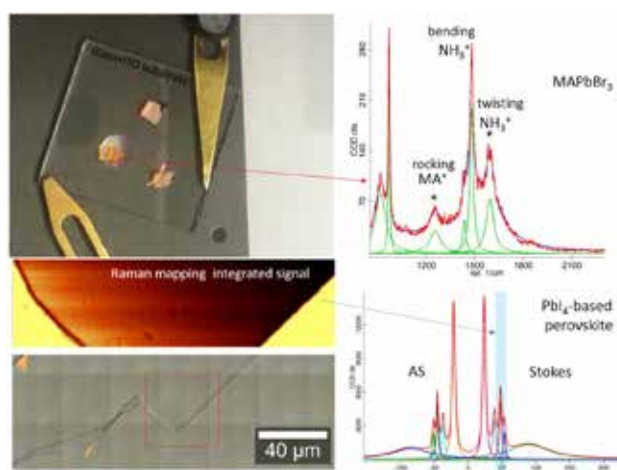
## Structural and transport investigation of two different types of organic–inorganic halide perovskite structures.

Monday, 1st October @ 17:22: Strong light-matter interactions at the nanoscale (ROOM 1) - Oral - Abstract ID: 470

**Dr. Andrea Giugni<sup>1</sup>, Dr. Bruno Torre<sup>1</sup>, Dr. Marco Allione<sup>1</sup>, Dr. Ayan Zhumekenov<sup>1</sup>, Prof. Osman Bakr<sup>1</sup>, Mrs. Erlin Nurlianti<sup>1</sup>, Prof. Jr-Hau He<sup>1</sup>, Prof. Enzo Di Fabrizio<sup>1</sup>**

*1. King Abdullah University of Science and Technology (KAUST), 23955-6900, Thuwal KSA*

The exciting intrinsic properties of single crystals metal halide perovskites intimately correlate with the metal and cation species and the structural arrangement reached during the crystallization. The mechanisms driving the solidification, the actual deficiencies that prevent long-term stability, and the humidity-related effects that impact the unique behavior of these material, are still poorly understood resulting to be the current bottlenecks towards single crystal-based optoelectronics and stable photovoltaic material. Here we compare experimentally two new different types of thin film perovskite single crystals, to evidence their structural and optoelectronic common and peculiar properties. The first, MAPbBr<sub>3</sub>, was obtained exploiting the role of surface tension by rapid synthesis of single perovskite crystals with the innovative inverse temperature crystallization method, the other, a new kind of PbI<sub>4</sub>-based material, was obtained by slow crystallization in solution, allowing the generation of a 2D layered structure. We used micro Raman spectroscopy as a useful technique for selectively studying the vibrational configuration and structural dynamics allowing the characterization of the samples quality and crystal structure. Both materials display substantial homogeneity, as can be evaluated for example considering the ratio of MA<sup>+</sup> rocking mode (1248 cm<sup>-1</sup>) and the twisting mode (1589 cm<sup>-1</sup>) of the NH<sub>3</sub><sup>+</sup> ions, highly sensitive to the environment. Negligible amount of defects or crystal structure impurities characterize the first, which reaches cm size scale quickly in the triclinic crystal structure, while the second solidifying in a compact 2D-layered well-ordered phase structure freeze the thermal orientation disorder associated to the organic cation, even at ambient temperature. Sharp and well defined low-frequency Stokes and AS peaks allow the complete characterization of the crystal that displays superior photo exposure resistance. Such results have been cross-correlated with AFM topography and electric force microscopy characterization at the nanoscale.



Perovskites raman study.jpg

---

# Light Controlled Assembly of Silver Nanoparticles

---

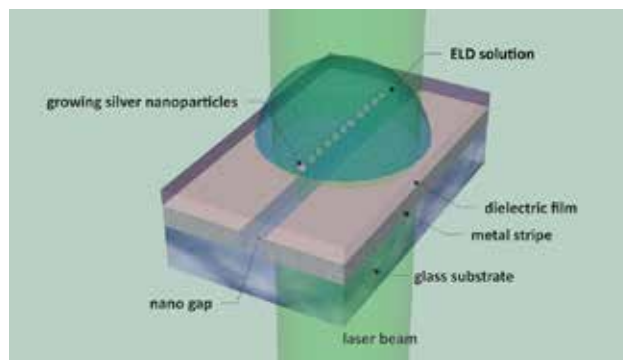
Monday, 1st October @ 17:39: Strong light-matter interactions at the nanoscale (ROOM 1) - Oral - Abstract ID: 271

---

***Mr. Ivan Shutsko*<sup>1</sup>, *Mr. Andreas Polywka*<sup>1</sup>, *Mr. Christian Tückmantel*<sup>1</sup>, *Prof. Patrick Görrn*<sup>1</sup>**

*1. Chair of Large Area Optoelectronics, University of Wuppertal*

Strong interaction of light with free electrons in metals makes it possible to localize and manipulate electromagnetic waves far beyond sub-wavelength dimensions. Enhanced absorption and scattering properties of metal nanoparticles enable light controlled growth and alignment with nanometer accuracy positioning. Here, we show the light controlled alignment of silver nanoparticles from liquid phase on a plane glass substrate with an estimated accuracy of well below 20 nm. During that alignment process, nanoparticles growth occurs in the position of maximum local intensity. In this way, an interdependency of light influencing the nanostructure and the nanostructure influencing the light is observed, leaving a unique fingerprint of used wavelength, polarisation and incident angle of the incoming electromagnetic wave on the grown nanostructure. Moreover, by introducing a light confining structure we were able to pattern the silver nanoparticles at the areas of local maximum intensity of counter-propagating dielectric modes excited at a nano gap in a metal stripe. The experimentally and theoretically proven approach combines the accurate positioning of top-down approaches with the benefits of bottom-up fabrication with an emphasis on facile processing under vacuum free conditions.



Setup of the photoinduced growth of the silver nanoparticles.png

# Does location matter? Hot-electron driven selective photosynthesis of catalytic nanoparticles

Monday, 1st October @ 17:56: Strong light-matter interactions at the nanoscale (ROOM 1) - Oral - Abstract ID: 376

*Ms. Evgenia Kontoleta*<sup>1</sup>, *Dr. Sven Askes*<sup>1</sup>, *Prof. Erik Garnett*<sup>1</sup>

*1. Center for Nanophotonics, AMOLF*

It is well known that plasmonic gold nanostructures feature extraordinary capability of absorbing visible light and concentrating the excitation energy in subwavelength volumes. Recently, they have also been proposed as promising candidates for the production of chemical fuels from sunlight. Upon excitation of these nanostructures, the energy is transferred to single electrons that for a brief period of time become highly energetic. Recent scientific advances demonstrate that these highly energetic, “hot” electrons can be extracted and used to drive chemical reactions, such as the conversion of protons to molecular hydrogen. However, to greatly improve the production rate, expensive and rare cocatalysts such as platinum are required.

In order to make effective use of as little catalyst material as possible, it is therefore important to localize the cocatalyst at the places where it is best coupled to the photogenerated hot electrons. To this end, we use the hot electrons themselves to deposit the cocatalyst and to construct photocatalytically active nanostructures. Briefly, a photocathode consisting of ITO-gold nanoislands-TiO<sub>2</sub> was illuminated with red light in presence of PtCl<sub>6</sub>, which resulted in the local deposition of platinum nanoparticles on the gold nanoislands. We furthermore compare the photocatalytic performance of these photocathodes, where the platinum nanoparticles were selectively deposited, with those that were fabricated by random-deposition techniques such as electrodeposition and e-beam evaporation.

Overall, these results demonstrate that plasmonic hot electron chemistry can be used for fabricating photocatalytic nanostructures with sub-wavelength control over localization. This careful design of photoelectrodes with nanoscale precision, could open up a new way for higher photocatalytic efficiencies as well as lower fabrication costs.

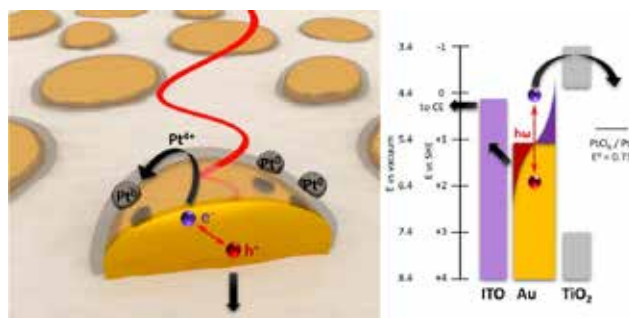


Illustration of the formation of platinum catalytic nanoparticles with hot-electrons generated after the excitation of gold nanoislands..jpg

# Chiroptical Response of Geometrically Symmetric Nanoscopic Heterostructures

Monday, 1st October @ 18:13: Strong light-matter interactions at the nanoscale (ROOM 1) - Oral - Abstract ID: 256

***Mr. Rene Barczyk<sup>1</sup>, Dr. Sergey Nechayev<sup>1</sup>, Dr. Peter Banzer<sup>1</sup>***

*1. Max Planck Institute for the Science of Light*

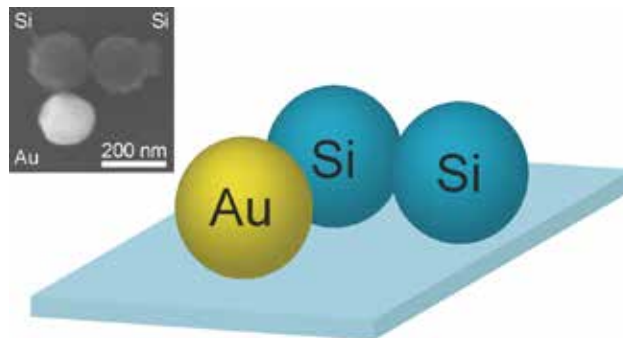
Chiral objects lack geometric mirror symmetry and thus can exist in two mirror-imaged forms, called enantiomers, distinguishable via their interaction with circularly polarized light [Nature **222**, 426–431 (1969)].

Recently, we proposed a novel concept for inducing a chiroptical response by breaking the in-plane symmetry of a nanostructure by a heterogeneous material composition, rather than geometry [Nat. Commun. **7**, 13117 (2016)]. We investigated an individual ensemble of three equally sized spherical nanoparticles of different materials (“trimer”, Fig. 1) fabricated using a custom-developed pick-and-place technique [10.1364/CLEO\_SI.2014.STu1H.1]. This geometrically mirror symmetric heterostructure shows differential absorption of normally incident circularly polarized light of opposite handedness.

Here, with the aid of k-space polarimetry, we perform complete Mueller matrix spectroscopy of this individual nanostructure. Employing full polarimetric analysis allows for quantifying the contributions of circular birefringence and circular dichroism to the chiroptical response, separated from linear dichroism and linear birefringence. We theoretically and experimentally demonstrate that the interaction of an individual geometrically mirror-symmetric heterostructure with a substrate transforms the morphology of the system from 2D to 3D chiral.

In summary, we elucidate chiroptical effects of resonant heterostructures in theory and experiment [arXiv:1804.04056]. Our findings open new avenues for designing novel chiral media with a material degree of freedom to precisely tailor the chiroptical response over a broad spectral range. In this perspective, we envision the impact of our results on studies of chiral response of molecules and nanostructures, immobilized on substrates.

Fig. 1: Sketch of the heterogeneous trimer composed of gold and silicon nanospheres, deposited on a glass substrate (inset: SEM image).



Trimer.png

# Possible polaritons-mediated light emission from nanostructured polyaniline with no external resonant microcavity

Monday, 1st October @ 18:30: Strong light-matter interactions at the nanoscale (ROOM 1) - Oral - Abstract ID: 548

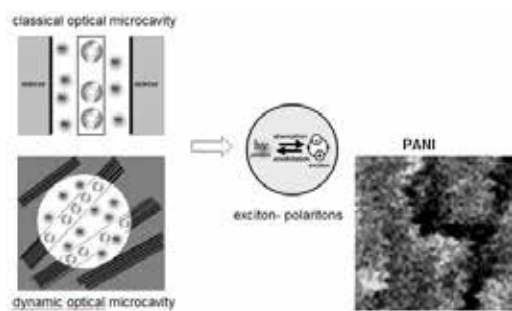
**Prof. Jerzy J. Langer**<sup>1</sup>, **Ms. Ewelina Frąckowiak**<sup>2</sup>, **Ms. Katarzyna Ratajczak**<sup>2</sup>

1. Adam Mickiewicz University in Poznan, 2. Adam Mickiewicz University

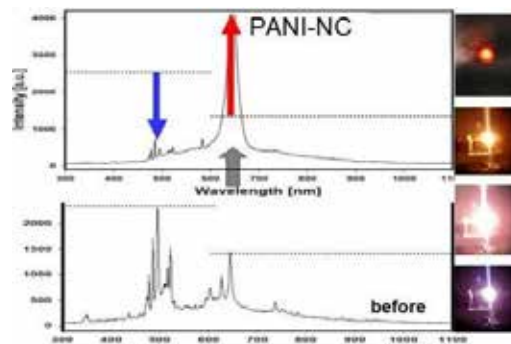
A new concept of the mechanism of light emission, induced by the electric current in polyaniline micro- and nanostructures is presented. The process includes formation of excitons, exciton-polaritons and finally the exciton-polariton condensate, what leads to the laser-like emission. This is observed in a system with intrinsic randomly formed and distributed microcavities, which is composed of interacting conducting polymer nanowires - polyaniline, the material strongly absorbing light. Here we report the results of experiments, indicating possible exciton-polariton condensation (EPC) and the action of the exciton-polariton polymer laser (directly electrically powered), without predefined external the resonant microcavity.

References

1. Kalisz, M. et al. Laser action induced in a nanostructured polyaniline LED, *J. Mater. Chem. C*, **4**, 6634-6640 (2016).
2. Langer, J. J. et al. Non-linear optical effects (SRS) in nanostructured polyaniline LED. *J. Mater. Chem.* **20**, 3859–3862 (2010).
3. Graf, A., et al. Electrical pumping and tuning of exciton-polaritons in carbon nanotube microcavities. *Nature Materials* (2017) on-line, doi:10.1038/nmat4940.



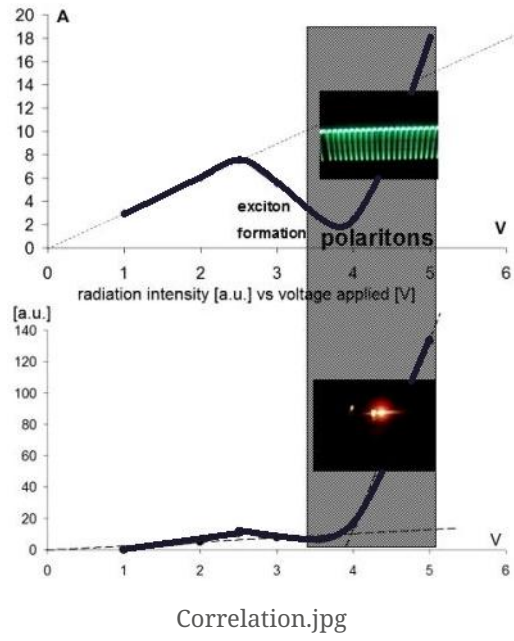
Dynamic microcavity scheme.jpg



Spectrum1a.jpg



Dynamic emission.jpg



Correlation.jpg

# Carrier cooling dynamics in inorganic perovskites

Monday, 1st October @ 17:05: Optical properties of nanostructures (ROOM 2) - Oral - Abstract ID: 128

**Prof. Anna Vinattieri<sup>1</sup>, Dr. Fabio Gabelloni<sup>1</sup>, Dr. Francesco Biccari<sup>1</sup>, Dr. Giulia Andreotti<sup>1</sup>, Dr. Nicola Calisi<sup>2</sup>, Dr. Stefano Caporali<sup>3</sup>**

1. University of Florence, Dept of Physics and Astronomy, 2. University of Florence, Dept of Chemistry, 3. University of Florence, Dept of Industrial Engineering

Inorganic perovskites represent a very promising alternative to hybrid organic-inorganic perovskites, given their better long-term stability and impressive radiative yield. In fact, such materials are extremely attracting not only for tandem photovoltaic cells but also for manufacturing efficient LEDs and lasers, allowing to cover a spectral range from NUV to NIR depending on the material composition. Despite the huge activity in this hot research field, quite incomplete and fragmentary is the knowledge on fundamental physics aspects, in particular concerning the relaxation rates of carriers and excitons. In this contribution, we present a detailed experimental investigation of the photoluminescence (PL) dynamics at the picosecond and nanosecond time-scale of carriers and excitons in CsPbBr<sub>3</sub> thin films and microstructures, deposited on different substrates (glass and metals), and also single crystals.

Non-resonant and resonant excitation are used to bring evidence of the different thermalization conditions and provide quantitative information of the characteristic time-scale of the thermalization process. Time-resolved PL spectra, varying several parameters (temperature, excitation density and wavelength) are discussed (see as example Fig.1). Our results show the occurrence of a very slow cooling process, which manifests itself even at very low excitation density, and then cannot be ascribed to Auger recombination or to screening of the electron-phonon interaction. The experimental data give evidence that recombination heating plays a fundamental role in the slowing down of the carrier thermalization.

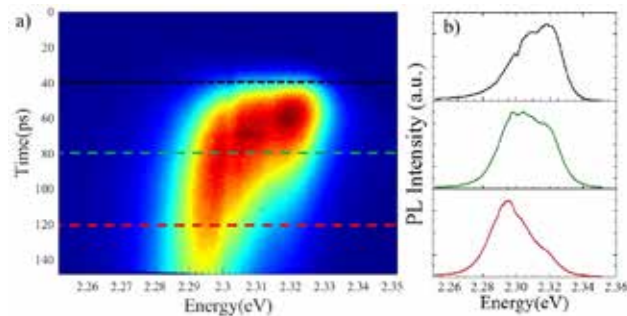


Fig. 1 TR spectra at 10 K of a CsPbBr<sub>3</sub> single crystal

Fig1 vinattieri.jpg

# Nanopatterning of sol-gel derived luminescent thin films as a promising tool to enhance extraction efficiency in LEDs devices

Monday, 1st October @ 17:22: Optical properties of nanostructures (ROOM 2) - Oral - Abstract ID: 80

**Dr. Jeff NYALOSASO<sup>1</sup>, Dr. Audrey Potdevin<sup>1</sup>, Dr. Rachid Mahiou<sup>1</sup>, Dr. François Réveret<sup>2</sup>, Prof. Pierre Disseix<sup>2</sup>, Prof. Geneviève Chadeyron<sup>3</sup>**

**1.** Université Clermont Auvergne, CNRS, SIGMA Clermont, ICCF, F-63000 Clermont-Ferrand, France, **2.** Université Clermont Auvergne, CNRS, Institut Pascal, F-63000 Clermont-Ferrand, France, **3.** Université Clermont Auvergne, CNRS, SIGMA Clermont, Institut de Chimie de Clermont-Ferrand (ICCF) – 63000-Clermont-Ferrand

Energy-saving lighting devices based on Light-Emitting Diodes (LEDs) combine a semiconductor chip emitting in the ultraviolet or blue wavelength region to one or more phosphor(s) deposited in the form of coatings. The most common ones combine a blue LED with the yellow phosphor  $\text{Y}_3\text{Al}_5\text{O}_{12}:\text{Ce}^{3+}$  (YAG:Ce) and a red phosphor. Even if these devices are characterized by satisfying photometric parameters (Color Rendering Index, Color Temperature) and good luminous efficiencies, further improvements can be carried out to enhance light extraction efficiency (increase in phosphor forward emission). One of the possible strategies is to pattern the phosphor coating. Most of the papers on the topic use layers of foreign materials as photonic crystals ( $\text{SiO}_2$ ,  $\text{TiO}_2$ ,  $\text{SiN}_x$ ) since YAG matrix is very harsh to pattern because of its good mechanical strength. These foreign materials could be eroded or fall off sooner or later, reducing the lifetime of these nanostructures. The strategy we have developed allows direct nanopatterning the YAG matrix by using the colloidal lithography combined with the Langmuir-Blodgett technique. The main interest of this procedure is that it can be applied to all luminescent matrices derived from the sol-gel process (oxides, fluorides ...). As a model system, nanopatterned YAG:Tb luminescent coatings have been elaborated. The obtained nanostructuration is a hexagonal network of YAG:Tb<sup>3+</sup> film (Figure 1) capable of modifying the light path, avoiding energy loss by the phenomenon of internal reflection within a given substrate. To determine the benefit of nanopatterning, conventional and angular-resolved photoluminescence were investigated on both unpatterned and patterned samples. Thanks to the nanostructuration, the extraction efficiency has been improved by 26 % and 131% depending on the sample nature (Figure 2). Noticeably, nanostructuration was found to have an influence on the angular distribution of photoluminescence whose intensity has been evaluated to its maximum at 0° with respect to the incident light. This work opens up the possibility either to reduce the phosphor quantity for the same device quality (reduction of rare-earth consumption) or to improve the light efficiency using the same quantity of phosphors.

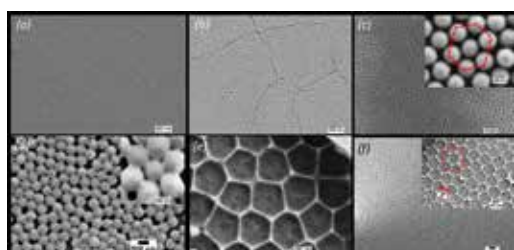


Figure 1.jpg

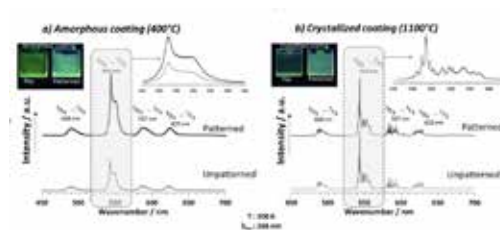


Figure 2.jpg



# Optical properties of III-V nanostructures for optoelectronic applications

Monday, 1st October @ 17:39: Optical properties of nanostructures (ROOM 2) - Oral - Abstract ID: 479

**Dr. Nabiha Ben Sedrine**<sup>1</sup>, **Mr. J. Cardoso**<sup>1</sup>, **Dr. J. Rodrigues**<sup>1</sup>, **Ms. J. P. Teixeira**<sup>1</sup>, **Ms. A. Alves**<sup>1</sup>, **Dr. R. Ribeiro-andrade**<sup>2</sup>, **Prof. A. Gustafsson**<sup>3</sup>, **Dr. P. M. P. Salomé**<sup>4</sup>, **Prof. J. C. González**<sup>5</sup>, **Mr. D. Nd. Faye**<sup>6</sup>, **Dr. M. Belloeil**<sup>7</sup>, **Prof. Bruno Daudin**<sup>7</sup>, **Prof. M. Bockowski**<sup>8</sup>, **Prof. V. Hoffmann**<sup>9</sup>, **Prof. M. Weyers**<sup>9</sup>, **Dr. Eduardo Alves**<sup>10</sup>, **Prof. Katharina Lorenz**<sup>11</sup>, **Prof. A. J. Neves**<sup>1</sup>, **Prof. J. P. Leitão**<sup>1</sup>, **Prof. M. R. Correia**<sup>1</sup>, **Prof. Teresa Monteiro**<sup>12</sup>

1. Departamento de Física e I3N, Universidade de Aveiro, Portugal, 2. INL – International Iberian Nanotechnology Laboratory, Braga, Portugal & Departamento de Física, Universidade Federal de Minas Gerais, Brazil, 3. Solid State Physics and NanoLund, Lund University, Sweden, 4. INL – International Iberian Nanotechnology Laboratory, Braga, Portugal, 5. Departamento de Física, Universidade Federal de Minas Gerais, Brazil, 6. IPFN, Instituto Superior Técnico, Campus Tecnológico e Nuclear, Bobadela LRS, Portugal, 7. Univ. Grenoble Alpes & CEA, INAC-PHELIQS Nanophysics & semiconductors group, Grenoble, France, 8. Institute of High Pressure Physics, Polish Academy of Sciences, Warsaw, Poland, 9. Ferdinand-Braun-Institut, Leibniz-Institut für Höchstfrequenztechnik, Germany, 10. Instituto Superior Técnico, Universidade de Lisboa, 11. IPFN, Instituto Superior Técnico, Campus Tecnológico e Nuclear, Bobadela LRS, Portugal & INESC-MN, Instituto de Engenharia de Sistemas de Computadores, Lisboa, Portugal, 12. Universidade de Aveiro

## Introduction

Since the successful development of quantum well lasers in the 1970s, one of the richest areas of application of semiconductor nanostructures is the area of optoelectronics, such as lasers and detectors. The most widely used semiconductors for optoelectronic applications are the compounds formed by group III and group V elements. For instance, GaAs and related compounds are mostly used for optical fiber communications, near infra-red and visible light emitting diodes (LEDs) as well as laser diodes. While, GaN and AlGaIn are used for LEDs, solid-state lasers and color displays, in the short wavelength range. Furthermore, optoelectronic devices based on novel semiconductor nanostructures are foreseen to revolutionize nowadays technology in terms of superior performance and efficiency, as well as the reduction of costs and material consumption.

## Methods

The use of semiconductor nanostructures integrated in devices is governed by the realization and control of p-n junctions, obtained by p- and n-type doping of the base materials. In addition to n and p-type doping, the semiconductor nanostructure emission can be tuned by incorporating rare earth ions by implantation and post-growth annealing. Doping can be performed by intentionally adding dopants during the growth (*in-situ*) or after the growth (*ex-situ*) by diffusion and ion implantation. However, several issues and controversies still need to be investigated in order to access/control semiconductor properties at the nanoscale level.

## Results and Discussion

We present our recent results on semiconductor nanostructures such as: *i)* Al<sub>x</sub>Ga<sub>1-x</sub>N (0 ≤ x ≤ 1) nanowires grown by molecular beam epitaxy on Si (111) substrate implanted with europium (Eu) ions and subject to rapid thermal annealing, *ii)* AlGaIn/GaN superlattice-based diode structures grown by metalorganic chemical vapor deposition implanted with two Eu fluences and subject to high temperature and high pressure annealing (Figure 1) demonstrating optical activation of Eu ions, and *iii)* silicon-doped GaAs nanowires with different nominal silicon doping levels (Figure 2) demonstrating that WZ/ZB polytypism is predominant for the lowest doping level.

The optical and vibrational properties of these nanostructures, of utmost importance for optoelectronic applications, will be assessed mainly using contactless spectroscopy techniques such as: photoluminescence, photo-

luminescence excitation, cathodoluminescence and micro-Raman spectroscopy.

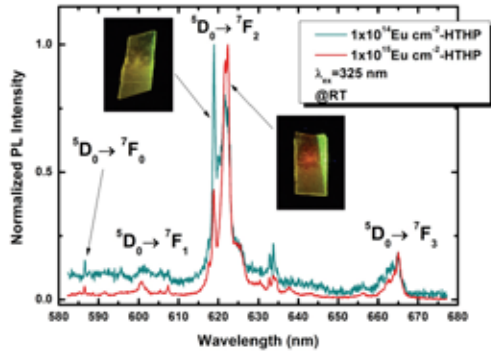


Fig1.png

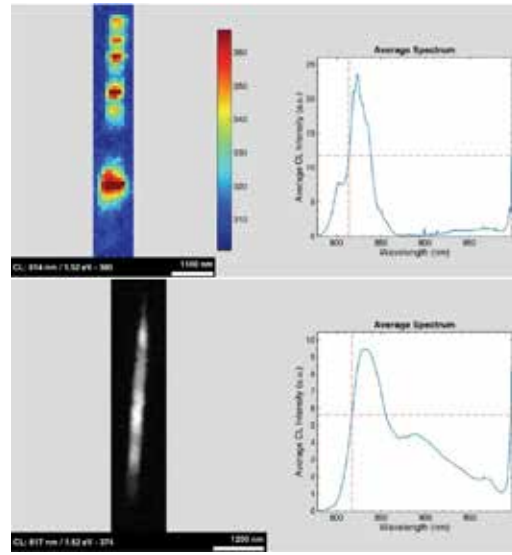


Fig2.png

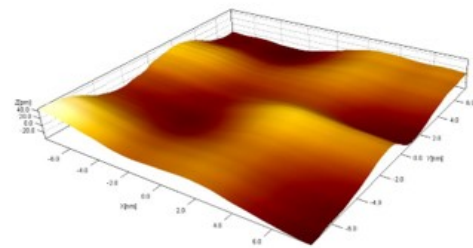
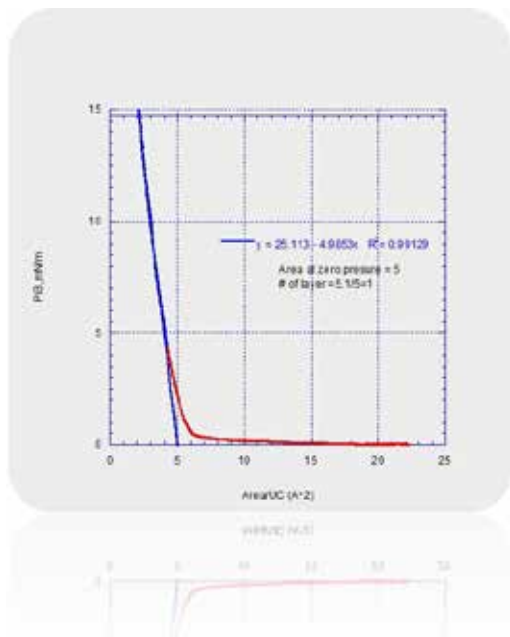
# Graphene to Graphite; a Layer by Layer Experimental and Simulation Investigation of Electric and Optical Properties

Monday, 1st October @ 17:56: Optical properties of nanostructures (ROOM 2) - Oral - Abstract ID: 129

**Prof. Maher Amer<sup>1</sup>, Mr. Mohammed Mohammed<sup>2</sup>, Prof. Udo Schwingenschloegl<sup>3</sup>**

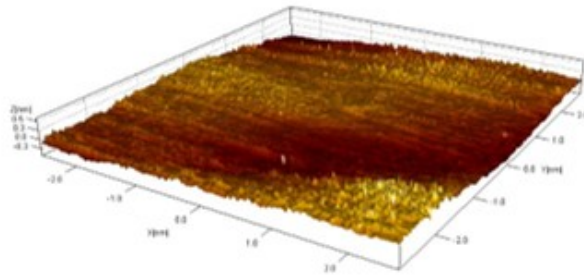
1. Wright State UNiversity/KAUST, 2. Wright State UNiversity, 3. KAUST

The unique and superior opto-electric properties of graphene have attracted much attention for its importance in many opto-electric applications. This, however, necessitates an answer to the question that at which number of graphene layers such unique material would no longer possess such superior properties and would turn into common graphite. Using Langmuir-Blodgett technique, we managed to deposit a mono-layer of graphene flakes on silica glass substrates. We experimentally measured the electric conductivity and UV-VIS spectra for samples with 1 to 20 layers of graphene. Both experimental results and density function theory (DFT) simulation agreed that electrical conductivity decreases exponentially with increasing the graphene number of layers and that the graphene turns into graphite at as little as 18 layers.



Stm-1.jpg

Isotherm.jpg



Stm-2.jpg

# Structural studies of nonpolar (10-10) ZnO/ZnMgO monolithic multiquantum well structures

Monday, 1st October @ 18:13: Optical properties of nanostructures (ROOM 2) - Oral - Abstract ID: 54

**Prof. Adrian Kozanecki<sup>1</sup>, Mr. Jacek Sajkowski<sup>1</sup>, Dr. Eduardo Alves<sup>2</sup>, Dr. Sergio Magalhaes<sup>2</sup>, Dr. Serhii Kryvyi<sup>1</sup>, Ms. Agnieszka Pieniazek<sup>1</sup>, Ms. Anna Reszka<sup>1</sup>, Mr. Dawid Jarosz<sup>1</sup>, Dr. Marcin Stachowicz<sup>1</sup>, Dr. Ewa Przewdzicka<sup>1</sup>, Dr. Mieczyslaw Pietrzyk<sup>1</sup>**

*1. Institute of Physics of the Polish Academy of Sciences, 2. Instituto Superior Técnico, Universidade de Lisboa*

## Introduction

Superlattices (SLs) of ZnO/ZnMgO are interesting for future applications in advanced optoelectronic devices such as polaritonic lasers. In this work nonpolar ZnO/ZnMgO multiquantum well structures were grown on (10-10) m-plane ZnO substrates by molecular beam epitaxy. The structures were composed of 10-20 pairs of ZnO and ZnMgO layers and the thicknesses of the individual layers varied from 10 nm to 50 nm. The Mg content in ZnMgO layers was ~30-70%, depending on the growth conditions.

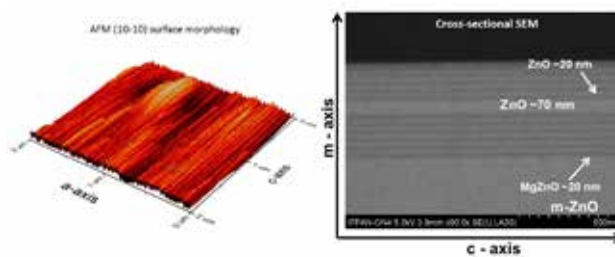
## Methods

The structures were characterized using a scanning electron microscope (SEM) in secondary electrons mode, cathodoluminescence (SEM-CL), photoluminescence (PL) and X-ray diffraction (XRD). Atomic Force Microscope (AFM) was used to monitor surface morphology. Rutherford backscattering and channeling (RBS/C) of 2 MeV He<sup>+</sup> ions were applied to determine the composition and quality of the structures. Channeling angular dependence of the backscattering yield was measured to obtain information about strain in the layers. For thick, ~50 nm layers, the RBS/C gives a unique opportunity not only to control the composition and thickness of the layers, but also to determine strain at each individual ZnO/ZnMgO and ZnMgO/ZnO interfaces.

## Results and discussion

XRD measurements revealed satellite lines up to the 7th order related to the existence of SLs, thus confirming their very good crystalline quality and coherent growth. The figure below shows typical AFM and SEM images for a SL grown on m-ZnO. The stripes seen in the AFM image are along the c-axis. The SEM image of the structure cross section was taken along the c-axis. SEM imaging revealed that ZnO/ZnMgO interfaces are well defined. Low temperature SEM-CL maps taken in panchromatic and monochromatic modes show the spatial distribution of the total luminescence intensity and individual lines. It has been found that even for a 50 nm/50 nm SL the luminescence comes predominantly from ZnO layers and the maximum intensities are observed near the interfaces. Analysis of experimental RBS spectra and numerical simulations revealed some gradient of Mg across the structures. It suggests a slight instability of the Mg flux during the long time growth process.

Acknowledgements: The work supported by the NCN project DEC-2014/15/B/ST3/04105.



Afm-sem.jpg

# Ultra-broadband directive scattering of silicon nanoparticles in the optical range

Monday, 1st October @ 18:30: Optical properties of nanostructures (ROOM 2) - Oral - Abstract ID: 92

**Dr. Kseniia Baryshnikova**<sup>1</sup>, **Mr. Pavel D. Terekhov**<sup>2</sup>, **Mr. Hadi K. Shamkhi**<sup>1</sup>, **Mr. Dmitry N. Gulkin**<sup>3</sup>,  
**Mr. Benyimin Hadad**<sup>2</sup>, **Dr. Vladimir O. Bessonov**<sup>3</sup>, **Dr. Alina Karabchevsky**<sup>2</sup>, **Dr. Andrey A. Fedyanin**<sup>3</sup>,  
**Dr. Alexander S. Shalin**<sup>1</sup>

1. ITMO University, 2. Ben-Gurion University of the Negev, 3. Lomonosov Moscow State University

Optical properties of high-refractive-index dielectric nanoparticles have attracted great scientific interest during the past several years [S. Jahani and Z. Jacob. *Nat. Nanotechnol.* 11, 23–36 (2016)]. These subwavelength scatterers can support the excitation of electric and magnetic multipolar resonances which enhance the light-matter interaction in a controllable manner. Control can be organized by changing the nanoparticles size, geometry, and material. Directive scattering of standalone high-refractive nanoparticles is of high interest within the frameworks of modern nanophotonics. Nanoparticles with controllable scattering pattern can be used as effective re-translators of light, as meta-atoms of metamaterials and so on. One of the most known cases of nanoparticles' directive scattering is a Kerker effect when most parts of energy scatter in the direction of incident light wave propagation, and backward scattering is almost zero [M. Kerker, D.-S. Wang and C. L. Giles. *J. Opt. Soc. Am.* 73, 765–767 (1983)]. Using nanoparticles with Kerker type scattering it is possible to construct fully invisible metasurfaces [M. Decker et al. *Adv. Opt. Mater.* 3, 813–820 (2015)]. Recently Kerker-type scattering was investigated for the silicon nanoparticles placed in the free space [S. Person et al. *Nano Lett.* 13, 1806–1809 (2013)] or on the substrate [K. V Baryshnikova, M. I. Petrov, V. E. Babicheva and P. A. Belov. *Sci. Rep.* 6, 22136 (2016)]. Kerker effect was achieved at certain frequencies where dipole moments of the nanoparticle are satisfied special conditions. Here we consider silicon nanoparticles placed in the homogeneous media with a refractive index different from the unity. Using method of multipole analysis, we show that for this system band of the effect can be effectively increased. Figure 1 illustrates how scattering pattern of cubical silicon nanoparticles changes in the optical spectral range. Multipole decomposition of scattering cross-section is also shown. Further, results of the experiment in the optical range, where silicon nanoparticles were placed in the glass media, is also discussed.

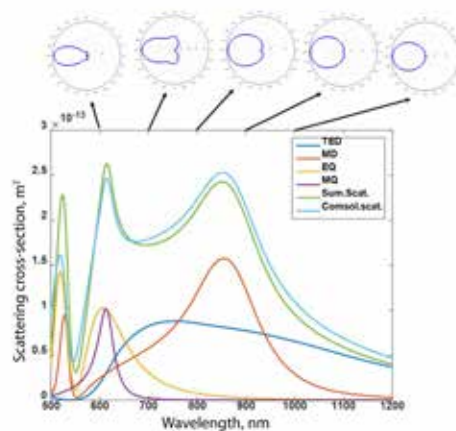


Figure 1.jpg

---

# Dynamic functional metasurfaces at optical frequencies

---

Monday, 1st October @ 17:05: Metamaterials (AUDITORIUM) - Oral - Abstract ID: 48

---

**Dr. Ping Yu<sup>1</sup>, Dr. Jianxiong Li<sup>1</sup>, Prof. Shuang Zhang<sup>2</sup>, Dr. Michael Hirscher<sup>1</sup>, Prof. Na Liu<sup>1</sup>**

1. Max Planck Institute for Intelligent Systems, 2. University of Birmingham

Metasurfaces have been widely used in a variety of optical device applications due to their remarkable ability to modify the phase, amplitude and polarization of light.[1] Recently, switchable metasurfaces have attracted a lot of attention due to their flexibility in controlling the optical fields at a designer's wish. To achieve the switching functions, helicity multiplexed metasurfaces have been used to generate alternative holographic patterns through polarization control.[2] Interesting materials such as  $\text{Ge}_3\text{Sb}_2\text{Te}_6$  have also been used to endow metasurfaces with switching functions.[3] However, so far a straightforward approach is missing to realize optical metasurfaces with versatile dynamic functions in a broad spectral range.

In this work, we demonstrate a novel approach to achieve dynamic functional metasurfaces at optical frequencies by employing the hydriding phase transition in magnesium (Mg).[4] Different optical functionalities can be dynamically switched upon hydrogenation/dehydrogenation of Mg metasurfaces without polarization manipulation. Our results show a great potential for metasurface applications in optical information encryption and provide a new route to design compact multifunctional optical devices.

## References

- [1] Yu, N. *et al.* Light Propagation with phase discontinuities: generalized laws of reflection and refraction. *Science* **334**, 333–337 (2011).
- [2] Wen, D. *et al.* Helicity multiplexed broadband metasurface holograms. *Nat. Commun.* **6**, 8241 (2015).
- [3] Yin, X. *et al.* Beam switching and bifocal zoom lensing using active plasmonic metasurfaces. *Light Sci. Appl.* **6**, e17016 (2017).
- [4] Duan, X. *et al.* Dynamic plasmonic colour display. *Nat. Commun.* **8**, 14606 (2017).

# Cavities of monolithic subwavelength grating VCSELs

Monday, 1st October @ 17:22: Metamaterials (AUDITORIUM) - Oral - Abstract ID: 374

**Prof. Tomasz Czyszanowski**<sup>1</sup>, **Dr. Marcin Gębski**<sup>2</sup>, **Prof. James Lott**<sup>3</sup>

1. Institute of Physics, Lodz University of Technology, ul. Wólczańska 219, 90-924 Łódź, Poland., 2. 1. Institute of Physics, Lodz University of Technology, ul. Wólczańska 219, 90-924 Łódź, Poland. 2. Institute of Solid State Physics, Center of Nanophotonics, Technical University of Berlin, Hardenbergstraße 36, 10632 Berlin, Germany., 3. Institute of Solid State Physics, Center of Nanophotonics, Technical University of Berlin, Hardenbergstraße 36, 10632 Berlin, Germany

Monolithic subwavelength gratings (MSGs) can be implemented in any material of a real refractive index larger than 1.75 without the need of the combination of low and high refractive index materials as it is in high-contrast gratings (HCGs). Recently, we achieved the first continuous-wave lasing of electrically-injected vertical-cavity surface-emitting lasers (VCSELs) that use a GaAs MSG mirror. VCSELs with one or both MSG mirrors have great prospects in application to monolithically integrated phosphide- and nitride-based VCSELs that lack monolithically integrated materials of high refractive index contrast. MSG replacing top DBR in arsenide-based VCSELs results in reduced size of the VCSEL by 30-50 % and two MSGs replacing both DBRs would enable a radical 90% or greater reduction thus potentially reducing the VCSEL manufacturing costs.

MSG however provides phase change of reflected light being depended on geometrical parameters of MSG. On the one hand side, makes the fabrication control of this type of structures more complicated, and on the other hand side, it provides additional degree of freedom enabling tuning the properties of the resonating light. We perform numerical analysis based on plane wave admittance method of the resonant cavities embedded between mirrors in the configurations: MSG – MSG and MSG – DBR. Quality ( $Q$ ) factor of MSG VCSELs is not related to the power reflectance of the mirrors with simple relationship as it is in conventional VCSELs. As an example dependence of  $Q$ -factor (Fig. 1), power reflectance (Fig. 2) and resonant wavelength (Fig. 3) of VCSEL composed of top and bottom 20 stripes MSGs of the same parameters:  $L$  – period and  $F$  – duty cycle. For the sake of comparison  $Q$ -factor of standard VCSEL with 21 pairs of top DBR is  $\sim 10^{4.5}$ , corresponding power reflectance of top DBR is 0.9993. Such high  $Q$ -factor of MSG VCSEL can be achieved in broad range of MSG parameters (green region in Fig. 1) which relates to significantly lower ( $\sim 0.99$ ) power reflectance of MSG mirrors (Fig. 2). Additionally MSG VCSELs offer resonant wavelength tuning by modification of lateral parameters of MHCG (Fig. 3) in the range of 40 nm for  $Q > 10^{4.5}$ .

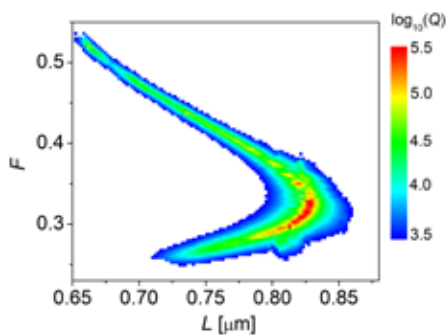


Fig1.png

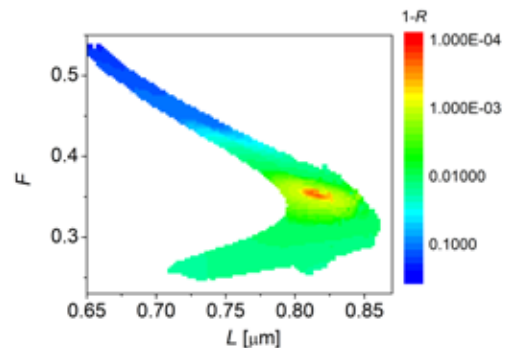


Fig2.png



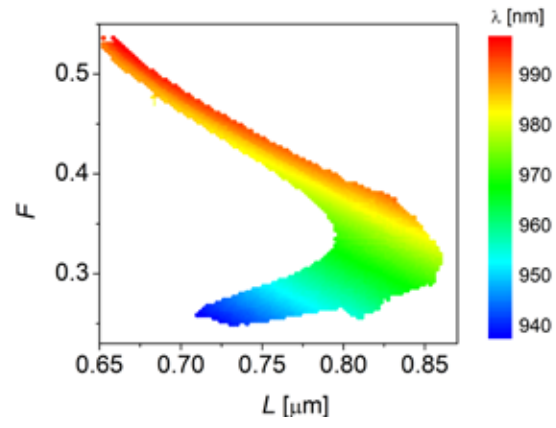


Fig3.png

---

# Utilizing of holographic principles for efficient excitation of plasmonic waveguide

---

Monday, 1st October @ 17:39: Metamaterials (AUDITORIUM) - Oral - Abstract ID: 313

---

***Prof. Alexander Merzlikin*<sup>1</sup>, *Dr. Anton Ignatov*<sup>1</sup>**

*1. All-Russia Research Institute of Automatics*

Plasmonic and surface wave optics are actively developing fields of modern optics. They are widely applicable for Raman spectroscopy, chemical- and biosensing, and integrated optics (optical interconnects, modulators, waveguide resonators, couplers, filters, etc.) where special interest is focused on the highly localized waves.

Studies and applications of surface waves and plasmonic waves with high degree of transverse mode localization encounter the problem of efficient mode excitation with far field. This difficulty is caused by the mismatch between the field distribution of the waveguide mode, which is localized on a subwavelength scale, and the field of the exciting radiation, the transverse localization of which is not less than a few wavelengths. The problem of efficient optical excitation of plasmonic waveguides is still far from final solution.

In this report we present the investigation of application of the holographic principle to excitation of various surface waves and plasmonic waves, in particular to excitation of plasmonic waveguides. We show that the excitation by use of surface or volume holograms can be several times more efficient than usage of excitation systems based on periodic diffraction gratings. Holograms help us to get the best phase matching and thus they help to match the field distribution of the waveguide mode with the field distribution of the incident wave.

# From optical magnetism to second-order spatial dispersion in self-assembled metamaterials

Monday, 1st October @ 17:56: Metamaterials (AUDITORIUM) - Oral - Abstract ID: 334

**Prof. Alexandre Baron<sup>1</sup>, Dr. Quentin Flamant<sup>1</sup>, Dr. Philippe Richetti<sup>1</sup>, Prof. Serge Ravaine<sup>1</sup>, Dr. Virginie Ponsinet<sup>1</sup>, Dr. Philippe Barois<sup>1</sup>, Mrs. Veronique Many<sup>1</sup>, Prof. Etienne Duguet<sup>1</sup>, Prof. Mona Treguer-delapierre<sup>1</sup>, Mrs. Sara De Cicco<sup>1</sup>, Dr. Jean-baptiste Salmon<sup>1</sup>, Dr. Jacques Leng<sup>1</sup>**

*1. University of Bordeaux*

The magnetic susceptibility of all natural materials is vanishingly small at high frequencies [1]. The metamaterials community has shown that optical magnetism could be realized using top-down fabricated structures, though at the expense of a high degree of anisotropy. We have shown experimentally that isotropic bulk optical magnetism can be produced by self-assembling dense materials made of magnetic meta-atoms composed of spherical plasmonic nanoclusters of well-controlled morphology [2]. These meta-atoms are composed of dielectric cores surrounded by metallic satellites that are either spheres or patches. Our bottom-up hierarchical approach permits the chemical synthesis of meta-atoms with tailored magnetic dipole moments characterized by polarization-resolved static light scattering spectroscopy, followed by microfluidic assembly of dense metamaterials that exhibit a resonance of the magnetic permeability at optical frequencies, characterized by variable-angle spectroscopic ellipsometry. Numerical simulations guide all our investigations. Figure 1(a-d) are scanning electron micrographs of the assembled metamaterial arranged into microfluidic channels. Figure 1(e) shows the experimental measurement of the real part of the magnetic permeability in the visible regime. The magnetism observed arises from circulating polarization currents within the meta-atom analogous to atomic circulating currents that arise from the angular momentum of the orbiting electron in the classical picture. This magnetic response originates from second-order spatial dispersion and is only valid in the case of divergent-free solutions (when the divergence of the electric field is null).

A full description of the optical properties of our metamaterials actually requires taking the locally non-zero divergence of the electric-field into account. This description requires three electromagnetic parameters.

In this talk, we shall review the realizations of optical magnetism based on the bottom-up approach of material chemistry and describe the emergence of a third nonlocal parameter required to fully describe our metamaterials.

[1] L. D. Landau and E.M. Lifshitz. *Electrodynamics of Continuous Media*, Pergamon Press. Oxford, 1960.

[2] S. Gomez-Grana, A. Le Beulze, ..., A. Baron, D. Torrent, and P. Barois, "Hierarchical self-assembly of a bulk metamaterial enables isotropic magnetic permeability at optical frequencies", *Materials Horizons*, 3(6), 596-601 (2016).

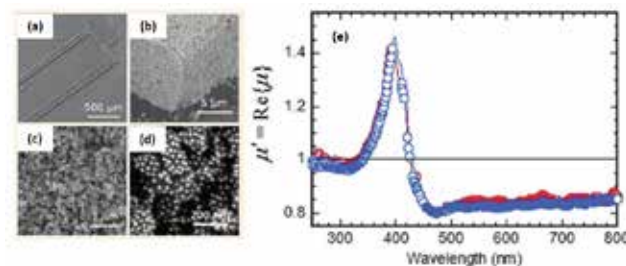


Fig abaron selfassembled magnetic metamaterial.png

# Size and host-medium effects on topologically protected surface states in bi-anisotropic 3D optical waveguides

Monday, 1st October @ 18:13: Metamaterials (AUDITORIUM) - Oral - Abstract ID: 21

*Prof. Vasily Klimov*<sup>1</sup>

*1. Lebedev Physical Institute*

Development of chip to chip optical interconnects is of great importance for reducing the energy consumption of heavy computations. Now it is widely believed that optical nanowaveguides with topologically protected surface states can help to achieve this goal. This is rather complicated from physical point of view and most of researchers deal with simplified geometries of waveguides which are far from practical. We study [1] the optical properties of 3D bi-anisotropic optical waveguides with nontrivial topological structure in wavevector space, placed in an ordinary dielectric matrix. We derive an exact analytical description of the eigenmodes of the systems with arbitrary parameters that allows us to investigate topologically protected surface states (TPSS) in details. In particular, we have found that the TPSS in the waveguides would disappear if their radius is smaller than a critical radius due to the dimensional quantization of azimuthal wavenumber (see Fig.1), and also (2) if the permittivity of the host-medium exceeds a critical value.

Fig.1. TPSS positions for the bi-anisotropic waveguides with different radii (black crosses) together with equifrequency curves of bulk bi-anisotropic medium (solid black lines). Fig.1a:  $k_0R=5$ , Fig.1b:  $k_0R=2.5$ , Fig.1c:  $k_0R=0.5$ . Note that when  $k_0R \leq 0.5$  there are no TPSS at all.

Interestingly, we also find that the TPSS in the waveguides have negative refraction for some geometries. We have found a TPSS phase diagram that will pave the way for development of the topological waveguides for optical interconnects and devices. Our results rise the general question about domains of applicability of topological protection and bulk-edge correspondence in topological photonics.

Reference:

[1] V. V. Klimov, D. V. Guzatov, I. V. Zabkov, H.-C. Chan, and G.-Y. Guo, Size and host-medium effects on topologically protected surface states in bi-anisotropic 3D waveguides, Phys. Rev. B **98** (2018) 075433

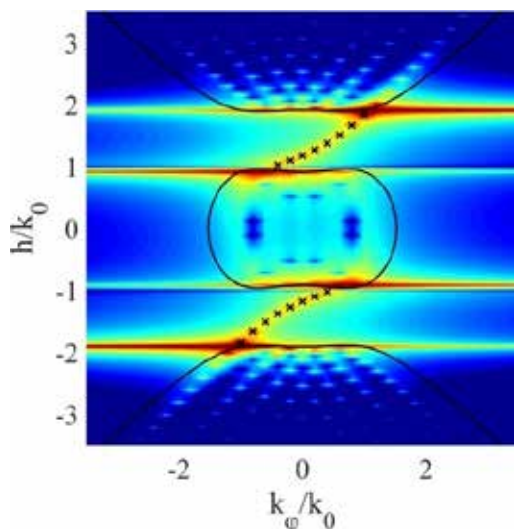


Fig1a.jpg

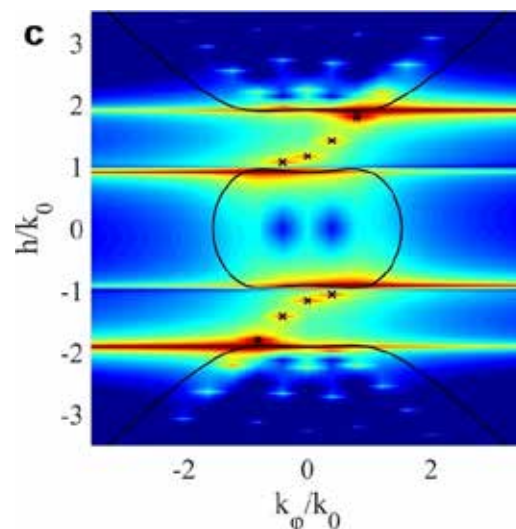


Fig1b.jpg

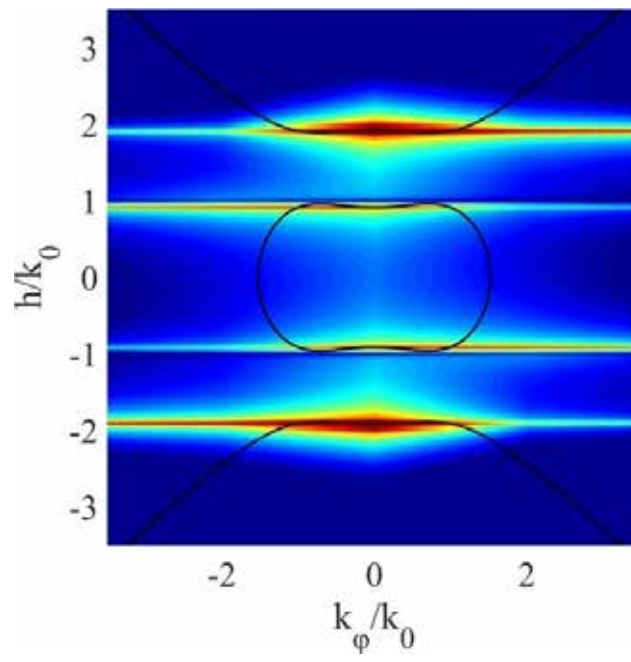


Fig1c.jpg

---

# All-semiconductor plasmonic metamaterials for mid-infrared perfect absorption and selective thermal emission

---

Monday, 1st October @ 18:30: Metamaterials (AUDITORIUM) - Oral - Abstract ID: 255

---

***Dr. Franziska Barho*<sup>1</sup>, *Dr. Fernando Gonzalez-Posada Flores*<sup>1</sup>, *Dr. Laurent Cerutti*<sup>1</sup>, *Prof. Thierry Taliercio*<sup>1</sup>**

*1. IES, University of Montpellier, CNRS*

## Introduction

Since the advent of metamaterial science, resonant perfect absorbers (PA) with sub-wavelength thickness have been of interest for electromagnetic wave control in various spectral ranges [1]. Perfect absorbers are based on suppressed transmission due to a metallic ground plane and simultaneous suppression of the reflected beam, by impedance matching to free space owing to effective material parameters [2]. In this work, we present PA metamaterials using a layer system of dielectric and highly doped semiconductor (HDSC) materials. Plasmonic and cavity resonances can be excited in this layer system when the topmost layer is patterned with nanoantennas. The strong absorptivity is equal to good thermal emission properties, making the perfect absorbers ideal candidates for narrowband selective thermal sources.

## Methods

InAsSb:Si/GaSb/InAsSb:Si layer structures were grown lattice-matched by solid-source molecular beam epitaxy. The topmost layer was patterned using UV or laser interference lithography followed by reactive ion etching (ICP-RIE) and wet chemical etching to obtain a sharp interface between the HDSC and the dielectric spacer. The PA samples were characterized by FTIR spectroscopy in reflectance and transmission mode. The experimental results were corroborated by electromagnetic simulations using the rigorous coupled wave analysis (RCWA). Furthermore, the thermal emission of the PA samples was measured.

## Results and discussion

We evaluate the thickness of the spacer layer as one of the key parameters to determine the interaction of the plasmonic and cavity resonances supported by the structure. Structures with different spacer thicknesses were optically characterized before and after fabrication of the nanoantennas. For an adapted spacer thickness, reflectivity as low as 0.5% is achieved. In addition, PA structures were tested as highly sensitive surface enhanced infrared absorption (SEIRA) spectroscopy substrates, using 20 nm thin films of polymethyl-methacrylate (PMMA) as test analyte. Finally, we show that the emissivity deduced from the thermal emission spectra of the samples is in agreement with Kirchhoff's law compared to the samples' reflectivity. Based on these results, we propose a novel surface enhanced sensing technique using the thermal emission of the near-perfect absorbers.

## References

- [1] Watts *et al.* Adv. Mater. 2012, 24, OP98-OP120.
- [2] Landy *et al.* PRL 2008, 100, 207402.

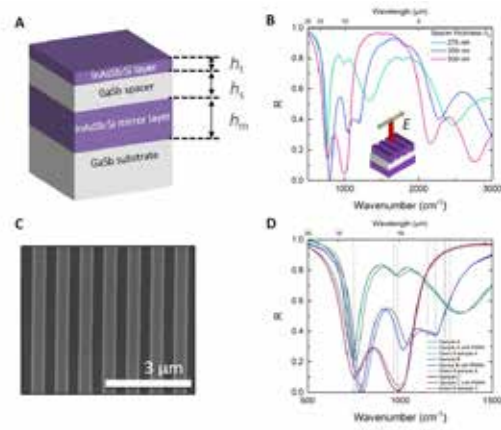


Figure 2: A. Schematic of the epitaxially grown structure. The InAs<sub>0.53</sub>Sb<sub>0.47</sub> layers act as mid-infrared mirrors. B. Reflectance spectra for different spacer layer thicknesses, obtained with the electric field vector perpendicular to the grating structure patterned into the topmost layer, as illustrated in the inset. C. SEM image of an exemplary grating. D. Reflectance spectra of the three samples shown in B (same polarization), coated with 20 nm PMMA as test analyte. For comparison, the spectra of the bare samples and smoothed curves excluding the vibrational features of the analyte molecule are also shown. Dashed vertical lines indicate the wavenumbers of vibrational features of PMMA. Sample A: 275 nm spacer, Sample B: 350 nm spacer, Sample C: 500 nm spacer.

Hdsc-perfect-absorber.jpg

## Latest Progress in Spasers

---

Tuesday, 2nd October @ 09:00: Plenary Speeches (AUDITORIUM) - Oral - Abstract ID: 8

---

***Prof. Mark Stockman***<sup>1</sup>

*1. Georgia State University*

Nanoplasmonics deals with collective electron excitations at the surfaces of metal nanostructures, called surface plasmons. The surface plasmons localize and nano-concentrate optical energy creating highly enhanced local fields. Nanoplasmonics has numerous applications in science, technology, biomedicine, environmental monitoring, and defense. There is an all-important need in active devices capable of generating and amplifying coherent optical fields on the nanoscale analogous to lasers and amplifiers of the conventional optics or transistors of microelectronics. Such an active device is the spaser (surface plasmon amplification by stimulated emission of radiation), also called plasmonic nanolaser. We focus on the newest ideas and review the latest experimental progress in spasers, which presently generate in a wide optical spectrum from IR to UV. We will present a recent breakthrough in ultrasensitive detection, in particular, on sensing of explosives vapors using the spaser. Another recent breakthrough to be presented is an application of the spaser as an ultrabright nanolabel and an efficient theranostic (therapeutic and diagnostic) agent in biomedicine (cancer diagnostics and treatment).



## The DNA origami route for nanoplasmonics

---

Tuesday, 2nd October @ 09:00: Plenary Speeches (AUDITORIUM) - Oral - Abstract ID: 539

---

***Prof. Na Liu***<sup>1</sup>

*1. Max Planck Institute for Intelligent Systems*

A prerequisite to build advanced plasmonic architectures is the ability to precisely control the organization of metal nanoparticles in space. To this end, DNA origami represents an ideal construction platform owing to its unique sequence specificity and structural versatility. I will present sequentially a diverse set of DNA-assembled plasmonic nanostructures according to their characteristic optical properties. I will also discuss about the inevitable evolution from static to dynamic plasmonic systems along with the fast development of this inter-disciplinary field. Finally, possible future directions and perspectives on the challenges are elucidated.

---

# Quantum and non-linear optics with semiconductor microcavities

---

Tuesday, 2nd October @ 10:45: Plenary Speeches (AUDITORIUM) - Oral - Abstract ID: 541

---

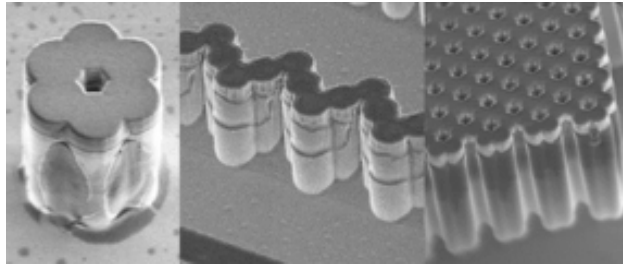
***Prof. Aristide Lemaitre***<sup>1</sup>

*1. CNRS C2N*

Semiconductor microcavities have shown their unique potential to play with light in the solid-state. Among the numerous phenomena encountered in these objects, cavity polaritons exhibit fascinating properties. These objects are hybrid light-matter quasi-particles, with mixed photonic and excitonic parts. Hence, they propagate like light but also strongly interact with their solid-state environment (electronic excitations). They constitute (quantum) fluids of light with striking particularities, which have been uncovered over the years, like polariton condensation, superfluidity, quantized vortices...

Over the last few years, at C2N, we have developed a polaritonic platform, by sculpting microcavities at the micro-scale. This creates a new playground to emulate quantum systems and Hamiltonians.

In this talk, I will show a few examples of our recent developments: a photonic benzene molecule for chiral photon emission, a photonic polyacetylene chain for topological lasing and a honeycomb lattice for the implementation of Dirac physics



Nanop18.png

---

# Semiconductor Hetero-Nanowires on Silicon for Photonic Applications

---

Tuesday, 2nd October @ 11:25: Plenary Speeches (AUDITORIUM) - Oral - Abstract ID: 147

---

***Prof. Gerhard Abstreiter***<sup>1</sup>

*1. Technische Universität München*

Semiconductor nanowires (NWs) can be combined with CMOS compatible technologies and provide much promise for optimized field-effect-transistors, efficient delivery and detection of light, and also sensing with ultrahigh detectivity. This is made possible especially with sophisticated core shell hetero-NW geometries.

I will discuss the fabrication of complex Ga(In,Al)As(P) based core-shell NWs grown by molecular beam epitaxy on pre-patterned Si substrates. The light emission can be tuned from about 1.6 eV down to about 0.4 eV, depending on composition and NW diameter, thus covering also the wavelength regime for optical fiber communication. The luminescence efficiency is increased by several orders of magnitude when the nanowires are passivated with appropriate thin shells. In this way we have achieved optically pumped infrared lasing up to room temperature from individual GaAs-AlGaAs core shell NWs with remarkably low threshold pump power densities. Our results show that by carefully designing NW materials composition profile high performance III-V near infrared NW lasers can be directly grown on Si substrates and thus open a path towards infrared photonic applications on a Si platform.

This work was performed in close collaboration with Gregor Koblmüller and Jonathan Finley together with various PhD- and master students at the Walter Schottky Institute of TUM. We acknowledge financial support from the Deutsche Forschungsgemeinschaft via SFB 631, the cluster of excellence “Nanosystems Initiative Munich”, and the Focus group “Nanophotonics” of the TUM Institute for Advanced Study.

---

# Semiconductor plasmonic resonances in the mid-IR range adjusted by thermal annealing

---

Tuesday, 2nd October @ 13:30: Poster Session (HALL & ROOM 3) - Poster - Abstract ID: 244

---

**Mr. Guilhem Pacot <sup>1</sup>, Dr. Maria Jose Milla Rodrigo <sup>1</sup>, Dr. Fernando Gonzalez-Posada Flores <sup>1</sup>, Dr. Franziska Barho <sup>1</sup>, Mr. Mario Bomers <sup>1</sup>, Dr. Laurent Cerutti <sup>1</sup>, Prof. Eric Tournié <sup>1</sup>, Prof. Thierry Taliercio <sup>1</sup>**

*1. IES, University of Montpellier, CNRS*

## Introduction

Mid-IR Biosensing, using surface enhanced infrared absorption, relies on resonant light absorption of molecules at certain characteristics wavelengths enhanced with plasmonic resonators. The tunability of plasmonic antenna resonances is achieved mainly by their geometry, size or interaction. [1] With highly doped semiconductors, the doping level is an additional parameter to tune the plasma frequency [2], a noble-metal material constant. In this work, we investigate rapid thermal annealing of the semiconductor as a mean to fine tune the resonance wavelength to the molecular absorption features.

## Methods

Highly Si-doped InAsSb films were epitaxially grown on GaSb substrates. Plasmonic resonators were fabricated by large-area surface patterning with UV lithography and selective chemical etching. Subsequent rapid thermal annealing were performed at temperatures from 500 to 650°C with different protective cover masks of InAs or GaSb at the same for as-grown and nanostructured samples. The plasma wavelength was measured by FTIR spectroscopy in the Brewster configuration. [3] The localized surface plasmon resonances (LSPR) were measured by FTIR spectroscopy in reflection configuration.

## Results and discussion

Both as-grown and nanostructured samples show a red-shift of the plasma wavelength and the LSPR respectively, as the temperature increases, indicating a reorganization of dopants in the epitaxial structure. The GaSb cover during the annealing renders a stable surface up to 650°C in comparison to only 590°C with the InAs cover. The maximum shifts obtained are 109 and 158  $\text{cm}^{-1}$  for the plasma wavelength and the LSPR respectively. Moreover, no geometrical degradations were seen in scanning electron microscope images, correlated to an almost constant resonance full width half maximum of the LSPR. However, with the InAs cover mask, material droplets appear between the resonators and their surface density increases with the annealing temperature. Energy dispersive spectroscopy indicates a droplet composition of In and As for an annealing temperature above 545°C, in correlation to a LSPR intensity decrease. At 590°C, the final distortion of the plasmonic resonances corresponds to the resonators disintegration.

## References

- [1] F. Barho et al. *Nanophotonics* 7, 507 (2018)
- [2] M.J. Milla et al. *Nanotechnology* 7, 425201 (2016)
- [3] T. Taliercio et al., *Opt. Exp.* 22, 24294, (2014)

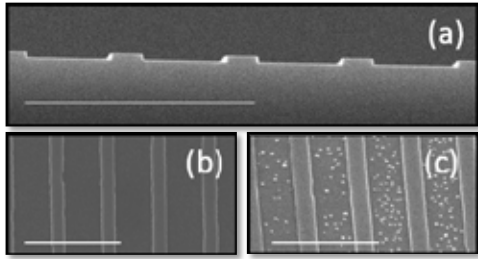


Figure 1: Scanning electron images of the nanostructures fabricated in the surface before the RTA side view (a) top view (b) and (c) after the RTA at 530 °C with an InAs cover mask. Scale bars are 4 μm.

Figure 1.png

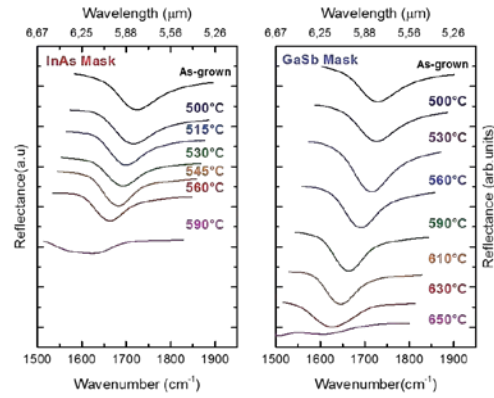


Figure 2: Reflectance measurement in the Brewster mode configuration evolution with the annealing temperature with InAs and GaSb mask for the as-grown samples

Figure 2.png

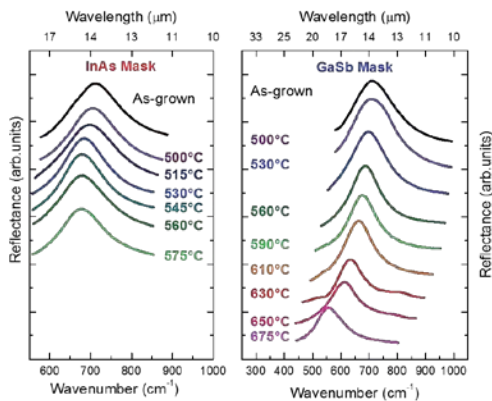


Figure 3: Reflectance measurement in the FTIR evolution with the annealing temperature with InAs and GaSb mask for the nanostructured samples

Figure 3.png

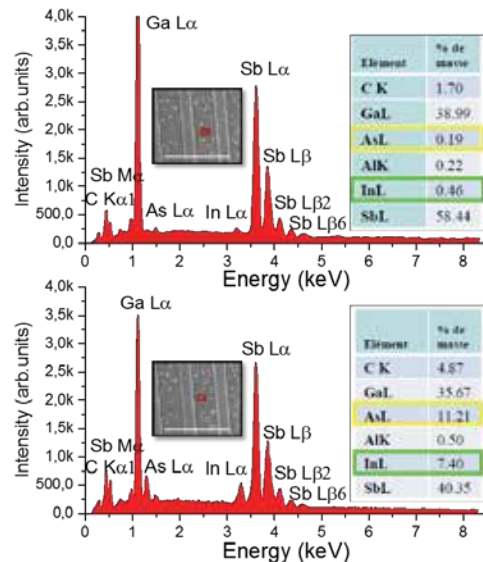


Figure 4: Energy dispersive spectroscopy for an InAs cover nanostructured sample (see SEM image inset. Scale bar 4μm) for a droplet (up) and between nanostructures (down). Both tables correspond to the mass percentage analysis taking into account the principal spectroscopic lines.

Figure 4.png

# Shannon entropy and avoided crossings in optical microcavities

Tuesday, 2nd October @ 13:30: Poster Session (HALL & ROOM 3) - Poster - Abstract ID: 285

**Dr. Park Kyuwon**<sup>1</sup>, **Dr. Moon Songki**<sup>2</sup>, **Dr. Shin Younghoon**<sup>3</sup>, **Mr. Kim Jinuk**<sup>1</sup>, **Dr. Jeong Kabgyun**<sup>4</sup>

1. School of Physics and Astronomy, Seoul National University, Seoul., 2. School of Physics and Astronomy, Seoul National University, Seoul, 3. Samsung Electronics, 4. IMDARC, Department of Mathematical Sciences, Seoul National University, Seoul

We investigated the relation between Shannon entropy and avoided crossings under strong coupling in optical microcavities. Before our work, the relation between Shannon entropy and avoided crossing was investigated in atomic physics, and the result was opposite to ours, i.e., Shannon entropy for an electron decreases due to electron ionization as we move close to the center of the avoided crossing. On the contrary, Shannon entropy of the probability density for optical microcavities (quantum billiards) increases due to the coherent superposition of wave functions as the center of the avoided crossing is approached, but both cases show exchanges of Shannon entropy as well as mode exchanges. Shannon entropy of the probability density for a closed elliptic billiard changes little with the eccentricity, while Shannon entropy of the probability density for an open elliptic billiard is maximized at the center of the avoided crossing. This maximization and exchange of Shannon entropy in an open elliptic billiard comes from the collective Lamb shift, which is an energy-level shift due to the interaction of energy levels with each other via the bath, and it can also induce an avoided crossing and coherent superposition of wave functions. In a closed quadrupole billiard, Shannon entropy is also maximized as the center of the avoided crossing is approached with both exchange of Shannon entropies as well as mode patterns. This maximization and exchange of Shannon entropy in a closed quadrupole billiard comes from the nonlinear dynamical effects in a chaotic system. Irrespective of the origin of the avoided crossings, the open elliptic cavity and the closed quadrupole cavity show similar behaviors to Shannon entropy. That is, the collective Lamb shift of open quantum systems and the symmetry breaking in the closed chaotic quantum systems have equivalent effects on the Shannon entropy.

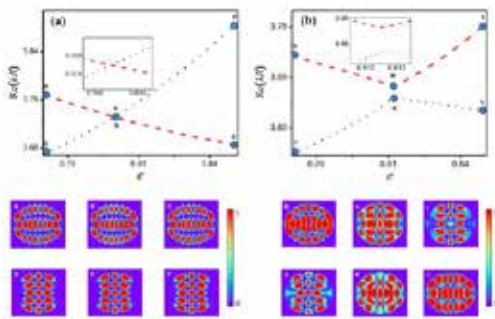


Fig1.jpg

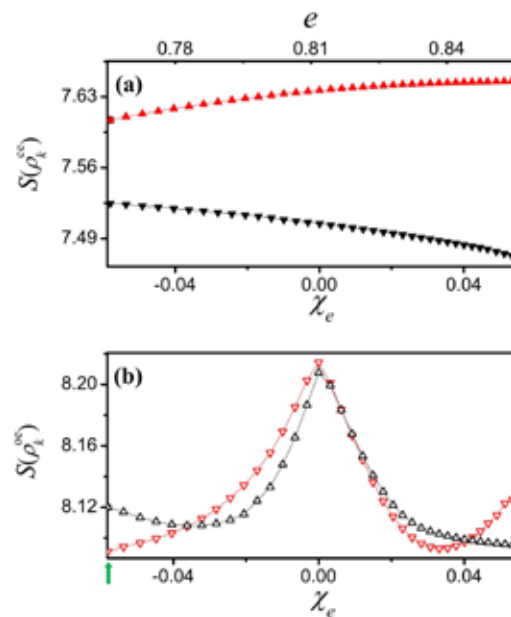


Fig2.jpg

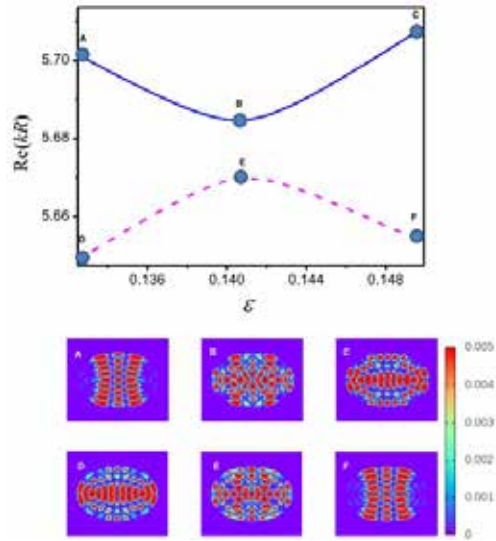


Fig3.jpg

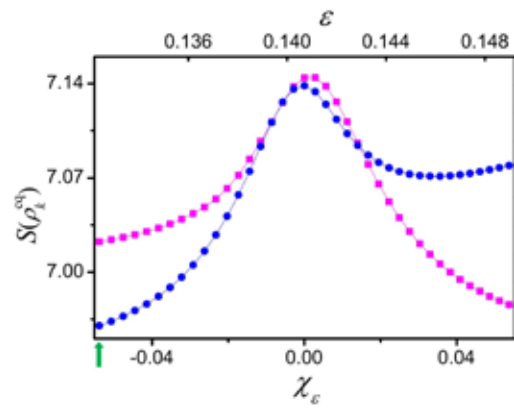


Fig4.jpg

# Plasmon enhanced generation of stimulated emission of laser dyes in pores of Al<sub>2</sub>O<sub>3</sub>

Tuesday, 2nd October @ 13:30: Poster Session (HALL & ROOM 3) - Poster - Abstract ID: 286

*Prof. Aitbek Aimukhanov*<sup>1</sup>, *Prof. Niyazbek Ibrayev*<sup>1</sup>

*1. Karaganda State University named after academician E.A. Buketov*

In this work, we present the results of a research of the properties of fluorescence and stimulated emission of the pyrometene 567 (PM 567) and 6-amino-1h-phenalen-1-one molecules in pores of aluminum oxide with Ag and Au nanoparticles. Films of porous alumina were obtained by electrochemical anodizing. Synthesis of AgNPs in the pores of Al<sub>2</sub>O<sub>3</sub> was carried out by the single-jet crystallization method. Au nanoparticles in alumina pores were obtained by reduction of HAuCl<sub>4</sub> with alkali NaOH. It is shown that the fluorescence of the PM567 dye in porous alumina depends on the concentration of AgNPs. The maximum value of the luminescence intensity is achieved at a concentration of  $C_{Ag} = 0.42 \cdot 10^{-7}$  mol, and a further increase in  $C_{Ag}$  results in quenching of the fluorescence. Enhanced emission of PM567 in the pores of Al<sub>2</sub>O<sub>3</sub> at  $C_{Ag} = 0.42 \cdot 10^{-7}$  mol was obtained in the short-wave maximum of the fluorescence band (Fig. 1). Comparison of the experimental data for the samples with and without AgNPs shows a correlation between changes in the radiation intensity and the half-width of the emission spectrum. For a film with AgNPs, the lasing threshold is reduced by a factor of 1.4. The effect of AgNPs on the efficiency of the generation of PM 567 molecules in pores showed that the efficiency of generation increased and amounted to 0.4%. For the 6-amino-1h-phenalen-1-one dye, the fluorescence spectrum overlaps well with the plasmon spectrum of AuNPs. The maximum intensity of the fluorescence of the dye was obtained with  $C_{Au} = 0.32 \cdot 10^{-6}$  mol. In figure 2 shows the appearance of stimulated emission (curve 2) of the dye in Al<sub>2</sub>O<sub>3</sub> films with AuNPs. In the absence of NPs at the same pump power, only spontaneous emission is observed (curve 1). Stimulated emission of 6-amino-1h-phenalen-1-one molecules in the pores of aluminum oxide was obtained at the maximum of the fluorescence band. The threshold of stimulated emission was 1.7 MW/cm<sup>2</sup>.

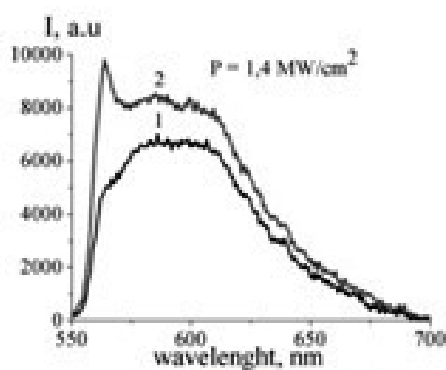


**Figure 1.**  
Fluorescence spectra (1)  
and stimulated emission  
(2) of PM 567 molecules  
in Al<sub>2</sub>O<sub>3</sub>

Figure 1.jpg

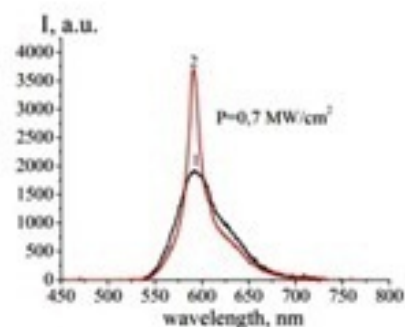


**Figure 2.**  
Fluorescence spectra (1)  
and stimulated emission (2)  
of 6-amino-1h-phenalen-1-  
one molecules in Al<sub>2</sub>O<sub>3</sub> with  
AuNPs

Figure 2.jpg



# Near-field imaging of surface-plasmon vortex-modes on a gold film with a single elliptical nanohole

Tuesday, 2nd October @ 13:30: Poster Session (HALL & ROOM 3) - Poster - Abstract ID: 289

**Dr. Claudia Triolo**<sup>1</sup>, **Prof. Salvatore Savasta**<sup>1</sup>, **Dr. Sebastiano Trusso**<sup>2</sup>, **Prof. Rosalba Saija**<sup>1</sup>, **Dr. Nisha Agarwal**<sup>3</sup>, **Prof. Salvatore Patanè**<sup>1</sup>

1. University of Messina, 2. CNR-IPCF, Istituto per i Processi Chimico-Fisici del CNR, Messina, 3. University of Ontario Institute of Technology

Nanostructured thin films that support plasmon resonances are interesting systems as they allow to investigate exotic optical phenomena related to the excitation of surface plasmon polaritons (SPPs), and to the spin-orbit interactions (SOIs). These optical features are very relevant at the subwavelength scale. SOIs phenomena allow to control the spatial degrees of freedom of light selecting the spin states of incident photons. Spatially inhomogeneous or anisotropic materials enhance the optical effects due the SOIs, leading to the observation of the photonic spin Hall effect (SHE), and of plasmonic vortex modes.

In this context, we study the SOI effects of an evanescent field around an isolated elliptical nanohole, fabricated by focused ion beam milling, in an 88nm thick Au film using a near-field scanning optical microscope (SNOM) working in transmission mode. Exploiting the rotational symmetry breaking due to the elongated shape of the nanohole, we generate a plasmonic vortex mode (Fig.1a) by illuminating the hole with an incident light beam without a spin state (linearly polarized beam). We show that a direct observation of the vortex mode is possible thanks to the ability of the SNOM technique to obtain information on both the amplitude and the phase of the near field. Interestingly, the rotation direction of the vortex (right- or left-hand rotation) depends on the angle between the polarization direction and the axis of the nanohole ( $\pm 45^\circ$ , respectively). This behaviour can be considered a photonic SHE generated in absence of the spin state of the light and caused by the rotational symmetry breaking of the nanostructure. This interpretation is supported by Finite Element Method (FEM) simulations, which reproduce the plasmonic vortex mode of the scattered field around the nanohole at 2nm from the sample surface (Fig.1b). Due to the geometrical anisotropy of the nanohole, both the number and the distribution of the phase singularities change (Fig.1c): when the linear polarization direction of incident field and the symmetry axes are tilted, phase singularity points are odd and the system acquires a topological charge, which generates a spiral-like flow of the Poynting vector around the nanohole and, hence, of the scattered field.

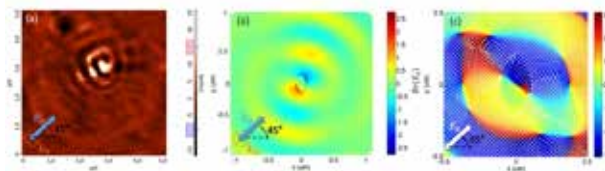


Figure.jpg

# A Parametric Analysis of Phase-gradient Meta-tips for Label-free Sensing Applications

Tuesday, 2nd October @ 13:30: Poster Session (HALL & ROOM 3) - Poster - Abstract ID: 343

**Dr. Maria Principe**<sup>1</sup>, **Prof. Marco Consales**<sup>2</sup>, **Prof. Giuseppe Castaldi**<sup>3</sup>, **Prof. Vincenzo Galdi**<sup>3</sup>, **Prof. Andrea Cusano**<sup>2</sup>

1. University of Salerno, 2. Optoelectronic Division – Eng. Dept., University of Sannio, 3. University of Sannio

Within the emerging framework of “lab-on-fiber” technologies, we demonstrated the integration of metasurfaces on the tip of an optical fiber. The resulting optical-fiber “meta-tips” represent a major breakthrough in the lab-on-fiber technology roadmap and promise to empower the typical fiber-optics application scenarios with the advanced light-manipulation capabilities endowed by metasurfaces. Here, we explore the possibility to exploit this platform in label-free biological or chemical sensing applications. Specifically, we carry out a parametric study of the surface sensitivity, and show that the phase-gradient can be effectively exploited as an additional degree of freedom in the design of high-sensitivity fiber optic devices. We considered phase-gradient optical fiber meta-tips (see Figure 1a) based on Babinet-inverted plasmonic nanoantennas, i.e., rectangular aperture antennas in a gold film, rotated by 45° in the  $x$ - $y$  plane. The geometry of the macrocell is shown in Figure 1b, where the two antennas have the same sidelengths, and are rotated by 90°. This configuration admits a simple gradient-free benchmark, which preserves the properties inherent of the single antenna geometry, but removes the phase-gradient effects (Figure 1c). We carry out a parametric study of the surface sensitivity, by varying the intensity of the phase gradient and the thickness of the gold layer,  $t$ . All numerical results are obtained by means of a free 2-D implementation of the Rigorous Coupled-Wave Analysis. For  $d=530, 700, 1000$  nm and  $t=15, 30, 50, 80$  nm, we compute numerically the MS and BC sensitivities, defined as the shift of the resonance wavelength upon the addition of a thin overlay. In Table 1, the values of the sensitivity gain of the MS with respect to the BC are shown for the different configuration analyzed. In Figure 2, the spectra computed for the MS and the BC for  $t=15$  nm and  $d=530, 700,$  and  $1000$ nm are shown.

The results from this study confirm that the phase-gradient can be effectively exploited as an additional degree of freedom in the design of high-performance sensors based on plasmonic arrays. Indeed, we show that the simple introduction of a constant phase-gradient always yields a gain with respect to the corresponding zero-gradient benchmark.

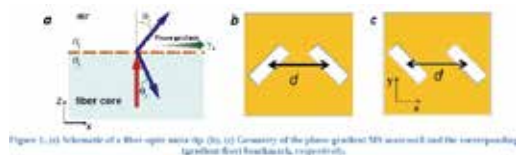


Figure1.png

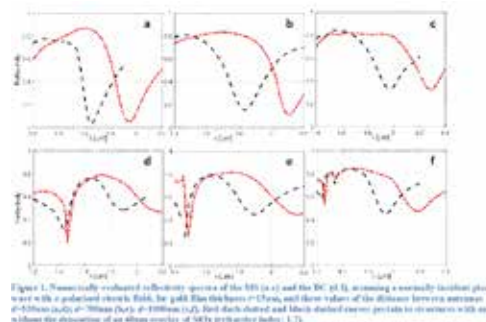


Figure 2. Numerically evaluated reflectance spectra of the MS (a-c) and the BC (d-f), assuming a normally incident plane wave in the  $z$  direction, in the gold film (Babinet-inverted) metasurface, and their values of the distance between antennas  $d=530, 700,$  and  $1000$  nm. The phase gradient values  $0, \pi/4,$  and  $\pi/2$  are indicated by the dashed lines. The solid lines represent the reflectance spectra of the MS (a-c) and the BC (d-f) with and without the deposition of an ultra-thin overlay of  $15$  nm thickness (a-f).

Figure2.png

$t$ [\(\mu\text{m}\)] \(\backslash\) $d$ [\(\mu\text{m}\)]	530	700	1000
15	1.1	1.1	1.2
30	1.2	1.2	1.3
50	1.4	1.5	1.4
80	1.7	1.8	1.4

Table 1. Numerically computed sensitivity gain of the phase gradient MS with respect to the refractive index  $n^{\text{eff}}$  for different values of the gold film thickness  $t$  and antenna distance  $d$ .

Table1.png

---

# Improved stability and sensitivity of plasmonics metal layers with MPTS adhesion layer and CVD grown graphene transfer in water

---

Tuesday, 2nd October @ 13:30: Poster Session (HALL & ROOM 3) - Poster - Abstract ID: 377

---

**Mr. Quaid Zaman**<sup>1</sup>, **Mr. André Do Nascimento Barbosa**<sup>2</sup>, **Dr. Omar Pandoli**<sup>3</sup>, **Dr. Ricardo Queiroz Aucélio**<sup>4</sup>, **Dr. Marco Cremona**<sup>1</sup>, **Dr. Fernando Lázaro Freire Júnior**<sup>1</sup>, **Dr. Tommaso Del Rosso**<sup>1</sup>

1. Department of Physics, Pontifícia Universidade Católica do Rio de Janeiro, Rua Marques de São Vicente, 22451-900, Rio de Janeiro., 2. Department of Physics, Pontifícia Universidade Católica do Rio de Janeiro, Rua Marques de São Vicente, 22451-900, Rio de Janeiro, 3. Department of Chemistry, Pontifícia Universidade Católica do Rio de Janeiro, Rua Marques de São Vicente, 22451-900, Rio de Janeiro., 4. Department of Chemistry, Pontifícia Universidade Católica do Rio de Janeiro, Rua Marques de São Vicente, 22451-900, Rio de Janeiro

## Introduction:

To date, the use of metallic adhesion layer such as Cr and Ti severely deteriorates the plasmonics features of thin metal film by damping the plasmon mode due to intermetallic diffusion and dissipative dielectric functions and thus depleted the active plasmonics properties of thin metal film for practical applications. Here we successfully demonstrated the use of a low absorption molecular adhesion layer and graphene protected metallic thin film with the aim to enhance the plasmonics properties and temporal stability of gold and silver thin film deposited on SF4 substrates functionalized with (3-mercaptopropyl) trimethoxysilane (MPTS). Graphene has been proposed as a promising material for sensitivity enhancement and for the detection of toxic mercury ( $\text{Hg}^{+2}$ ) ions due to its high surface to volume ratio and exceptional optical and chemical properties.

## Methods:

The schematic representation of our proposed structure is shown in figure 1.

## Results:

The instability of the SPR signal for different configuration was monitored in term of shift in resonance angle ( $\Delta\theta_{\text{SPR}}$ ) and change in FWHM over 24 hours in DI water as shown in the figure 2. The major result that we detected for the first time is the significant decrease in  $\Delta\text{FWHM}\%$  of about 5% up to 5 hours in the case of MPTS/Au/ $\text{H}_2\text{O}$ , which is attributed to the rearrangement of evaporated Au atoms on top of S-atoms of MPTS due to hydration of siloxane (Si-O-Si) bond and revert to silanol (Si-OH) groups and leave the surface smooth confirm by our AFM results. The graphene based SPR sensors show a higher bulk refractive index sensitivity as compared to conventional metal thin sensors as shown in figure 3(a). The SPR resonance angle shows a rapid response of about  $0.06^\circ$  upto a concentration of 0.005ppm, which reveals a greater affinity of graphene SPR sensors to  $\text{Hg}^{+2}$  ions as shown in figure 3(b).

## Conclusion

We have demonstrated the temporal stability and sensitivity of SPR sensor consists of Cr and MPTS as adhesion layer and graphene as protecting layer. Our results validated the outstanding performance of Graphene SPR sensor, suggesting that its application as a heavy metal detector in environmental monitoring.

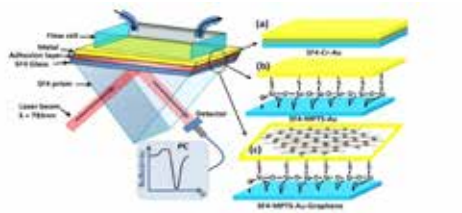


Figure 1: Left: Schematic representation of proposed SPR sensors by Kratoschek and Gopferich comprising the prism, glass substrate, adhesion layer and over layer system. Right: Edge structure of SPR edge either with (a) Cr, (b) MPTS as adhesion layer, and (c) graphene as over layer.

Fig-1.jpg

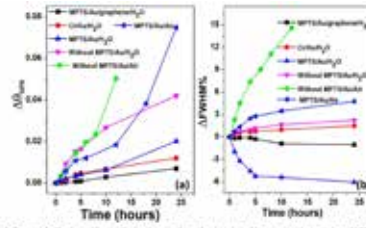


Figure 2: Influence of adhesion, without adhesion layer and graphene protected layer on (a) the variation of SPR angle and the FWHM for Au thin film as a function of time in air and 0.1 water. The SPR spectra were measured in single interrogation scheme of the laser (HeNe) Resonance (SPR) spectroscopy with TM polarization mode at excitation wavelength of 780nm.

Fig-2.jpg

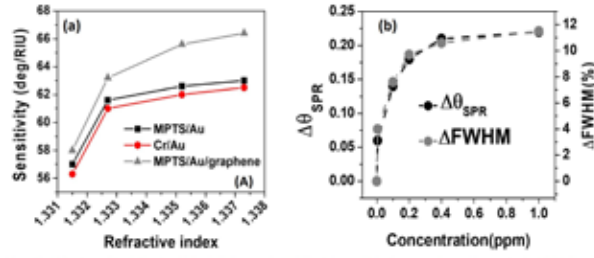


Figure 3: (a) Experimentally calculated sensitivity of SPR sensors with MPTS and Cr as adhesion layer as well as graphene protected gold thin film. The refractive index of sensing layer were changes from 1.3297 to 1.3615 by injecting different concentration of NaCl solutions. (b) SPR angular shift and change in FWHM upon the detection of different concentration of  $Hg^{2+}$  on graphene SPR sensor.

Figure 3a-b.jpg

---

# Fluorescence Magnetic Immunoassays Using Graphene Quantum Dots and Fe<sub>2</sub>O<sub>3</sub>@SiO<sub>2</sub> Composite for AFP Detection

---

Tuesday, 2nd October @ 13:30: Poster Session (HALL & ROOM 3) - Poster - Abstract ID: 399

---

*Ms. Yun TENG<sup>1</sup>, Prof. Philip W. T. Pong<sup>1</sup>*

*1. The University of Hong Kong*

## Introduction

Alpha-fetoprotein (AFP) is a single polypeptide chain glycoprotein, and high AFP levels are found in some typical cancer tumors such as the cancer tumors in ovaries, stomach, pancreas or liver<sup>1</sup>. Therefore, AFP can be used as a biomarker to detect cancer cells. However, due to the time-consuming, low sensitivity and complex operation in conventional methods for AFP detection, the effective and simple technology is still in dire need. The silica-coated iron oxide nanoparticles (NPs) hold much promise for targeted drug delivery and bio-separation. Furthermore, graphene quantum dots (GQDs) with novel photoproperties are widely used in biomedical diagnosis<sup>2</sup>. Motivated by these advantages, we report a novel strategy of fluoro-magnetic immunoassay based on GQDs and Fe<sub>2</sub>O<sub>3</sub>@SiO<sub>2</sub> for AFP detection.

## Methods

GQDs were fabricated by citric acid pyrolysis method, and AFP antibody Ab1 was covalently conjugated on GQDs with fluorescence labelling (Fig.1A). The spherical Fe<sub>2</sub>O<sub>3</sub> NPs were prepared through a modified thermal decomposition method and modified with silica and the carboxylic group, which induced the covalent connection with the capture antibody Ab2 (Fig.1B). The AFP detection was performed in two steps that the AFP antigen was initially incubated with Ab2/Fe<sub>2</sub>O<sub>3</sub>@SiO<sub>2</sub>NPs. Then the Ab1/GQD were added to form a sandwich immunocomplex separated by the magnet (Fig.1C). Finally, the obtained immunocomplex was determined with fluorescence signal.

## Results and discussion

We show that the as-prepared GQDs presented good dispersion in water solution with the size of 3±0.4 nm (Fig.2a), and these GQDs with blue fluorescence exhibited an absorption peak at 358 nm (Fig.2b). The Fe<sub>2</sub>O<sub>3</sub>@SiO<sub>2</sub> NPs were with 10 nm core diameter and 9 nm shell thickness (Fig.2c). The silica shell not only prevented particle aggregation but also avoided the possible fluorescence quenching effect by the Fe<sub>2</sub>O<sub>3</sub> cores. The concentration of AFP was quantified by the fluorescence intensity of Ab1/GQD-AFP-Ab2/Fe<sub>2</sub>O<sub>3</sub>@SiO<sub>2</sub> sandwich immunocomplex.

## Conclusion

We developed a simple and accurate immunoassays strategy based on fluorescence magnetic sandwich structure Ab1/GQD-AFP-Ab2/Fe<sub>2</sub>O<sub>3</sub>@SiO<sub>2</sub> immunocomplex for AFP detection. It can be an available platform for medical diagnosis and fluoroimmunoassay device application.

## References

1. E. Waidely. et al., *Analyst*. 141, 36-44 (2016).
2. Y. Zhang et al., *Theranostics*. 2, 631 (2012).

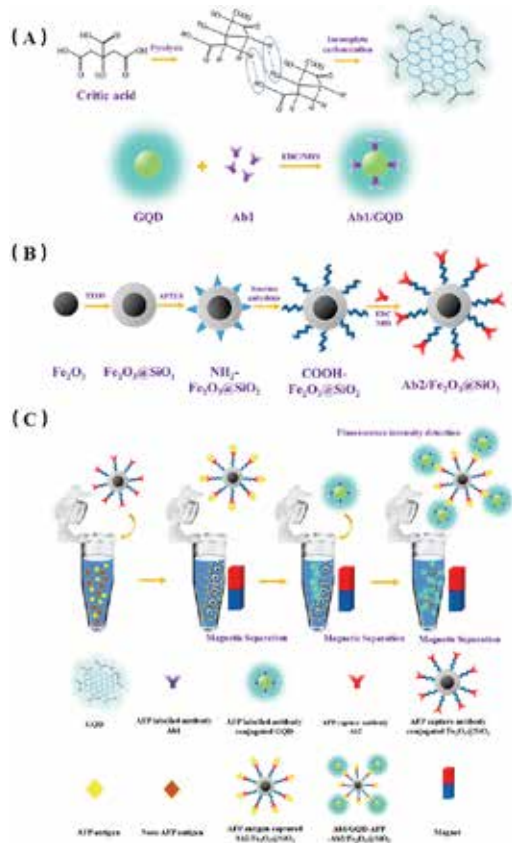


**Fig. 1** Schematic illustration of the fabrication process of (A) GQDs and conjugate with AFP antibody Ab1, (B) Fe<sub>3</sub>O<sub>4</sub>@SiO<sub>2</sub> nanoparticles and conjugate with AFP antigen, and (C) Experimental procedure of fluoro-magnetic immunoassay based on using Ab1/GQD and Ab2/Fe<sub>3</sub>O<sub>4</sub>@SiO<sub>2</sub> NPs for AFP detection.

Fig.1.png

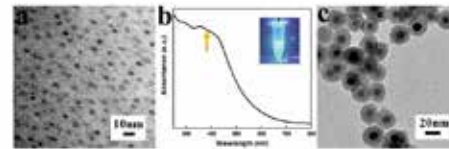


**Fig. 2** (a) TEM image and (b) UV-Vis absorption of GQDs, and (c) TEM image of Fe<sub>3</sub>O<sub>4</sub>@SiO<sub>2</sub> nanoparticles.

Fig.2.png

# Strain sensitivity of surface plasmon-polaritons excitation by attenuated total reflection in graphene

Tuesday, 2nd October @ 13:30: Poster Session (HALL & ROOM 3) - Poster - Abstract ID: 439

**Mr. Maksim Usik<sup>1</sup>, Dr. Dmitry Kuzmin<sup>1</sup>, Prof. Igor Bychkov<sup>1</sup>, Prof. Vladimir Shavrov<sup>2</sup>**

1. Chelyabinsk State University, 2. Kotelnikov Institute of Radioengineering and Electronics of RAS

In this work, we theoretically investigated the excitation of surface plasmon-polaritons (SPPs) in deformed graphene by attenuated total reflection method. We considered the Otto geometry for SPPs excitation in graphene layer under external strain. We calculated the light reflectance from the structure, which allows concluding what part of the energy of the incident wave has passed into the excitation of SPPs. During the work, we investigated plasmonics of deformed graphene lattice, as illustrated in Fig. 1. The optical conductivity tensor for this modified graphene lattice has non-zero off-diagonal components [1]  $\sigma_{xy} = \sigma_{yx} = 2\sigma_0(\omega)\beta s_x/a$  and modified diagonal components  $\sigma_{xx,yy} = \sigma_0(\omega)[1 \pm 2\beta s_x/a]$ , where  $\sigma_0(\omega)$  is graphene conductivity,  $\beta$  the electron Gruneisen parameter,  $s_x$  and  $s_y$  are the components of relative displacement of graphene sub-lattice  $s$ . A possible scenario for such deformation could occur in graphene grown on a substrate with an appropriate combination of lattice mismatch between the two crystals [2, 3].

Calculations show that elastic strain leads to significant effect in SPPs excitation (see Fig. 2). We have considered graphene lattice with the relative displacements  $s = (0.04, 0.03)$ . In the deformed graphene, excitation of SPPs may be observed for narrower frequency region than in the isotropic graphene. The frequency and the incident angle of the most effective excitation of SPPs strongly depend on the polarization of the incident light. Our results may open up new possibilities for strain-induced molding flow of light at nanoscales.

[1] M. Oliva-Leyva, G.G. Naumis, Phys. Rev. B 93, 035439 (2016).

[2] G.-X. Ni et al., Adv. Mater. 26, 1081 (2014).

[3] S.-M. Lee et al., Nano Res. 8, 2082 (2015).

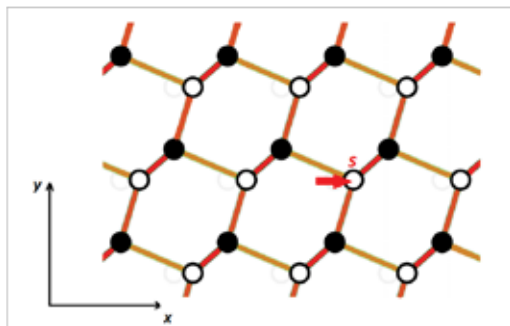


Fig1.png

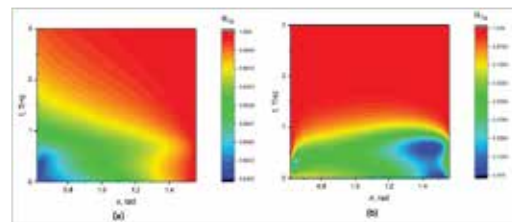


Fig2.png



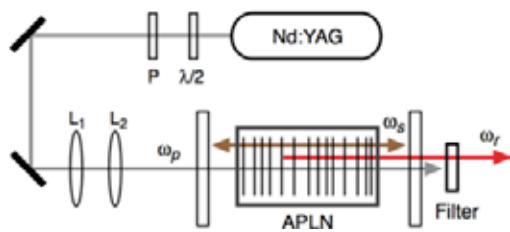
# 710 nm red light source based on cascaded nonlinear optical processes for use in biomedical application.

Tuesday, 2nd October @ 13:30: Poster Session (HALL & ROOM 3) - Poster - Abstract ID: 463

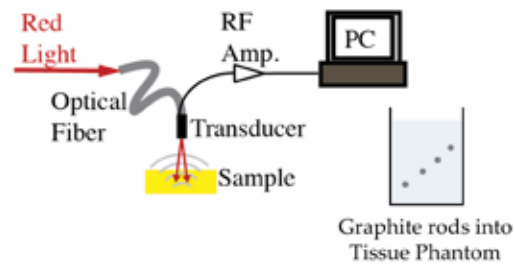
*Dr. Juan Gonzalez*<sup>1</sup>, *Dr. Liliana Martinez*<sup>1</sup>, *Dr. Roger Cudney*<sup>2</sup>, *Dr. Jose Enriquez*<sup>1</sup>, *Dr. Rurik Farias*<sup>1</sup>,  
*Mr. Eduardo Melendez*<sup>1</sup>

1. Universidad Autónoma de Ciudad Juárez, 2. CICESE

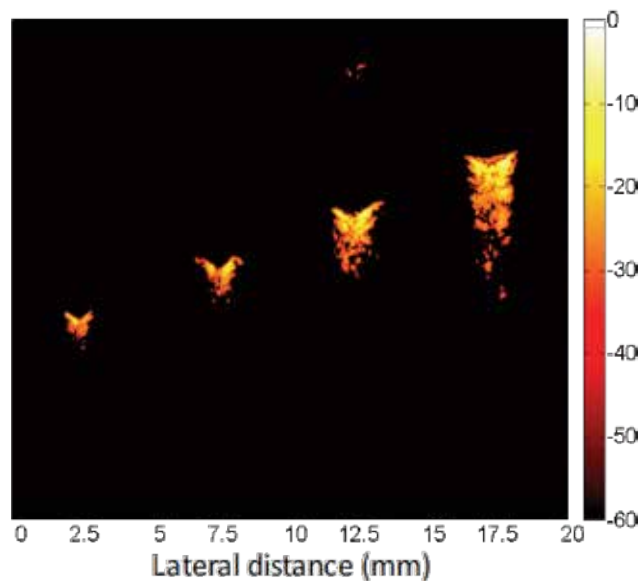
Photoacoustic imaging is a diagnostic technique which is based on the detection of acoustic waves induced in tissue by the absorption of electromagnetic radiation, usually from pulsed sources on a nanosecond timescale and with wavelengths between 600 and 900 nm. This technique can be used to detect microcalcifications in breast tissue and a wavelength between 600 and 800 nm is optimal for this particular case. In this work we present a scheme for an inexpensive and simple device that emits 9 nanosecond pulses over 1 mJ at a 710 nm wavelength which is based on an aperiodically poled ferroelectric crystal (Lithium Niobate,  $\text{LiNbO}_3$ ) pumped with a Nd:YAG pulsed laser source to obtain the red beam and is a viable source for biomedical applications like Photoacoustic imaging. The wavelength conversion from 1064 nm to 710 nm was achieved by two cascaded nonlinear optical processes within the Lithium Niobate crystal. First by optical parametric generation at degeneracy point a signal wave with 2128 nm wavelength is generated and simultaneously a sum-frequency generation process between the pump and signal waves results in the red beam.



Red source.png



Pai 1.png



Pai 2.png

---

# Identification of bacteria using surface-enhanced Raman spectroscopy

---

Tuesday, 2nd October @ 13:30: Poster Session (HALL & ROOM 3) - Poster - Abstract ID: 484

---

**Dr. Dmitry Kopitsyn**<sup>1</sup>, **Mr. Maksim Gorbachevskii**<sup>1</sup>, **Dr. Ekaterina Botchkova**<sup>1</sup>, **Ms. Maria Bychenko**<sup>1</sup>,  
**Dr. Pawel Gushchin**<sup>1</sup>, **Dr. Andrei Novikov**<sup>1</sup>

*1. Gubkin University*

## *Introduction*

Surface enhanced Raman scattering (SERS) spectroscopy can be efficiently employed for the label-free detection and discrimination of different bacteria. The fingerprint-quality bacterial spectra allow identification of bacteria at the genus, the species, and even at the intraspecies level.

## *Methods*

SERS spectra were acquired with BWS415 spectrometer (BWTEC, Germany). The specimen was put on the XYZ-stage, while position of laser focus was controlled by USB microscope Mikmed-2000R (Micromed, Russia). SERS spectra of bacteria were registered using drop-casted nanoparticle-based substrates either with or without the oxidative treatment with hydrogen peroxide.

## *Results*

SERS spectra were registered for the number of clinically relevant bacterial species. Fluorescence background subtraction, filtering, normalizing and automated peak recognition were performed by means of home-developed GNU/Octave subroutines. Recognized peaks were assembled into the matrix, and processed by principal component analysis (PCA).

## *Discussion*

Bacterial SERS spectra were significantly amplified while registering with oxidative treatment. The discriminating spectral performance was reduced, but was still high enough for the reliable identification of bacteria. This work was funded by the Russian Science Foundation (project 17-79-10489).

---

# Rough silver films for surface plasmons generation and SERS optical properties study

---

Tuesday, 2nd October @ 13:30: Poster Session (HALL & ROOM 3) - Poster - Abstract ID: 505

---

***Dr. Ilia Samusev*<sup>1</sup>, *Dr. Anna Tcibulnikova*<sup>1</sup>, *Ms. Elizaveta Konstantinova*<sup>1</sup>, *Mr. Andrey Zyubin*<sup>1</sup>, *Dr. Vasily Slezhkin*<sup>2</sup>, *Prof. Valery Bryukhanov*<sup>1</sup>, *Ms. Polina Medvedskaya*<sup>1</sup>, *Mr. Ivan Lyatun*<sup>1</sup>, *Mr. Aleksandr Vinichenko*<sup>1</sup>, *Dr. Maksim Demin*<sup>1</sup>**

*1. Immanuel Kant Baltic Federal University, 2. Kaliningrad State Technical University*

We used electron microscopy and AFM, ellipsometry, and Raman microscopy to investigate dielectric and optical properties of rough silver films fabricated by electrodeposition from a cyanide-thiocyanate electrolyte and modified by electrochemical and physicochemical treatment. We studied spectral reflectance of p-polarized light of silver films manufactured with/without anodic dissolution (AD). This work presents experimental results and simulation calculations of the dielectric functions of silver surfaces with varying roughness, manufactured with/without AD. A juxtaposition of the theoretical distribution and the experimentally measured function  $\epsilon(\omega)$  allowed to establish the bandgap width of the rough surfaces. The width ranged from 0.7 eV, which is close to the band values characteristic of  $\text{Ag}_2\text{O}$  (1.4 eV). We identified the bandgap width for AD silver surfaces, which had been modified by the silver NPs from a borohydride sol. The bandgap width amounted to 0.13 eV. It was established experimentally that the dissolution of the oxide layer of a rough silver surface with an ammonia solution translated into a significant reduction in the band gap width (to  $E_0 \approx 0.05$  eV). We studied the Raman scattering spectra (RSS) of silver films treated at different anodic dissolution rates and of AD surfaces with adsorbed nanoparticles of borohydride silver. Upon laser excitation at 532 and 632 nm, the intensity of RSS of silver films differed, since the maximum of the spectra of plasmon resonance of rough silver surfaces is at 405 nm. After the dissolution of the samples' oxide layers with an ammonia solution, the RSS intensity decreased by an order of magnitude. This has practical importance for the manufacture of plasmon resonance-based optical sensors. We calculated Purcell factors, which describe the processes of local electromagnetic field enhancement under Raman light scattering in micro- and nanocavities of different rough surfaces. The established up to  $10^4$ -fold factor of Raman scattering enhancement on rough silver surface manufactured using the above metal electrodeposition techniques can contribute to obtaining surface-enhanced Raman scattering in creating biosensors with different molecular systems.

The reported study was carried out within Russian Academic Excellence Project "5-100".

# Numerical simulation of light extraction efficiency of GaN-based blue micro-LED structures

Tuesday, 2nd October @ 13:30: Poster Session (HALL & ROOM 3) - Poster - Abstract ID: 534

*Prof. Han-Youl Ryu*<sup>1</sup>

*1. Inha University*

Recently, there are growing interest in micro-scale light-emitting diodes (LEDs) that can be utilized as light sources of deformable displays, optogenetics, and visible light communications. In this work, we perform three-dimensional (3-D) finite-difference time-domain (FDTD) simulations to investigate the light extraction efficiency (LEE) of flip-chip micro-LED structures. A whole micro-LED structure is included inside the FDTD computational domain, and the dependence of dipole source positions and polarizations on LEE is investigated.

Figure 1(a) shows a schematic cross-sectional view of the FDTD computational domain for a micro-LED structure. It is basically composed of an n-GaN layer, InGaN/GaN multiple-quantum-well active region, and a p-GaN layer on a high-reflectance Ag mirror. The micro-LED chip is assumed to have cylindrical shape with a diameter of 20  $\mu\text{m}$ , and enclosed with an epoxy encapsulant. The thickness of the n-GaN layer and the active region was set at 3000 and 50 nm, respectively. In the source spectrum, center wavelength and full-width at half maximum of the spectrum are chosen to be 460 and 20 nm, respectively.

Figure 2(a) shows simulated results of LEE as a function of the source position in the horizontal direction,  $x$ . The LEE decreases as the source position increases especially for the y-polarization. As  $x$  increases, the coupling of the dipole source with whispering gallery (WGM) modes becomes stronger. The light coupled to the WGM cannot radiate easily out of the micro-LED structure, resulting in the decrease of LEE. Fig. 2(b) shows the averaged LEE as a function of the p-GaN thickness. A strong dependence of the averaged LEE on the p-GaN thickness is observed. In this case, the p-GaN thickness of 100 nm is the best choice for achieving a high LEE of  $\sim 0.6$ .

In this work, we numerically investigated the LEE of blue micro-LED structures with 20- $\mu\text{m}$  diameter using 3-D FDTD simulations. It was found the LEE of micro-LEDs depends strongly on dipole source positions, dipole polarizations, and the p-GaN thickness. For a properly chosen p-GaN thickness, the LEE of  $\sim 60\%$  was obtained. More optimization of the micro-LED structure is expected to lead to even higher LEE.

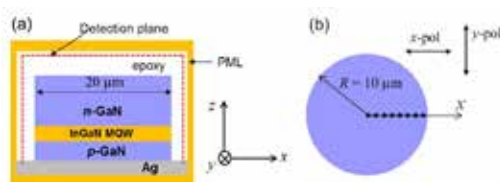


Fig1 simulation structure.jpg

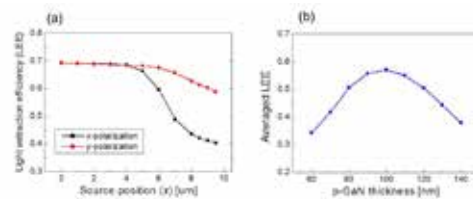


Fig2 simulation result.jpg

## Planar focusing reflectors based on high contrast gratings

---

Tuesday, 2nd October @ 13:30: Poster Session (HALL & ROOM 3) - Poster - Abstract ID: 348

---

***Dr. Paulina Komar*<sup>1</sup>, *Dr. Marcin Gębski*<sup>2</sup>, *Dr. Maciej Dems*<sup>1</sup>, *Prof. Tomasz Czyszanowski*<sup>1</sup>, *Dr. Michał Wasiak*<sup>1</sup>**

*1. Institute of Physics, Lodz University of Technology, ul. Wólczańska 219, 90-924 Łódź, Poland., 2. 1. Institute of Physics, Lodz University of Technology, ul. Wólczańska 219, 90-924 Łódź, Poland. 2. Institute of Solid State Physics, Center of Nanophotonics, Technical University of Berlin, Hardenbergstraße 36, 10632 Berlin, Germany.*

Vertical cavity surface emitting lasers (VCSELs) attract a lot of attention due to steadily growing demand for radiation emitters that are used in the short- and middle-range networks aimed at high-speed data transfer. Two Distributed Bragg Reflectors (DBRs), composed of alternating layers of materials repeated many times occupy major part of the laser volume. DBRs are located on both sides of an active region and form a resonant cavity of a VCSEL. In principle, planar reflectors based on a High Contrast Grating (HCG) may substitute at least one DBR in a VCSEL leading to simplification of the laser structure due to the fact that an HCG is around ten times thinner compared to a DBR.

We will present the simulations of GaAs-based focusing HCGs designed for 980 nm. In particular, we will compare the performance of three types of HCG-based reflectors, namely, a membrane from GaAs suspended in the air, a GaAs-based HCG embedded in oxidation, and a monolithic HCG from GaAs.

The project (Homing/2017-4/34) is carried out within the HOMING programme of the Foundation for Polish Science co-financed by the European Union under the European Regional Development Fund.

# Observation of Surface Plasmons in Subwavelength Gratings

Tuesday, 2nd October @ 13:30: Poster Session (HALL & ROOM 3) - Poster - Abstract ID: 366

**Prof. Nikolai Petrov**<sup>1</sup>, **Mr. Victor Danilov**<sup>1</sup>, **Dr. Vladimir Popov**<sup>2</sup>, **Mr. Boris Usievich**<sup>3</sup>

1. Scientific and Technological Center of Unique Instrumentation of Russian Academy of Sciences, 2. Lomonosov Moscow State University, 3. Prokhorov General Physics Institute of the Russian Academy of Sciences

The interest in subwavelength gratings is growing due to their promising applications in high performance transmission and reflection filters, optoelectronic devices using surface plasmons, spectral-selective external optical mirrors for lasers (VCSELs). Such structures for the complete absorption of radiation in the far IR region were considered in [1]. In [2] subwavelength gratings were proposed and demonstrated for combining red, green and blue light beams into a single beam.

In the present work it is shown that the effect of full absorption can be also observed in sub-wavelength metallic gratings for radiation in the visible range of the spectrum. Diffraction of light of a visible spectral range by subwavelength metal gratings (Fig. 1) is investigated theoretically and experimentally. The influence of different grating parameters (filling factor, shape and depth, material, angle of incidence, wavelength and polarization of radiation) on the diffraction efficiency is investigated. High diffraction efficiency in the -1st order is observed with increasing depth of the grating relief (more than 70% at a depth  $h = 80$  nm). It is shown that under certain conditions an effect of plasmon resonance occurs, at which a complete absorption of the incident radiation takes place. The considered optical elements can be used in systems for image processing, projection displays, in the development of a variety of sensors, etc.

In Fig. 2 the results of calculations and measurements of diffraction efficiency of the zero order of the nickel grating depending on the angle of incidence of radiation with  $p$ -polarization are presented. It is seen that the effect of plasmon resonance at the incidence angle of  $\sim 33^\circ$  takes place. With a relief depth of  $h = 80$  nm and angle of incidence  $= 31^\circ$  almost all incident energy is absorbed by the grating. This property can be used to develop various devices, in particular, in solar cells and displays.

Acknowledgement: This research was supported by the Russian Science Foundation (project No. 17-19-01461).

## References

1. Vial B., Demesy G., Zolla F., et.al. JOSA B. 2014. V.31. p. 1339-1346.
2. Petrov N.I., Nikitin V.G., Danilov V.A., Popov V.V., Usievich B.A. Applied Optics. 2014. v.53. p.5740-5744.

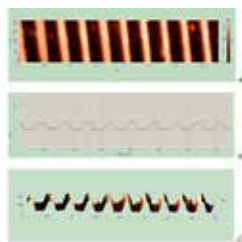


Fig. 1. Images of gratings obtained with AFM: (a) top view, (b) side view, and (c) 3D image (grating period  $\Lambda = 400$  nm).

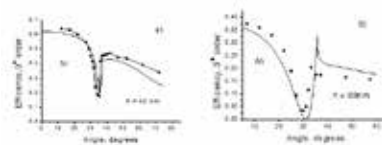


Fig. 2. Calculated (solid lines) and measured (dots) diffraction efficiencies of the zero order depending on the angle of radiation incidence for the nickel grating with a period of  $\Lambda = 400$  nm and a depth of  $h = 40$  nm (a) and  $h = 80$  nm (b) at a wavelength of radiation  $\lambda = 641$  nm with  $p$ -polarization.

Grating fig1.jpg

Plasmon res fig2.jpg

---

## Enhanced Raman spectroscopy of proteins on native cell membranes stretched on super-hydrophobic surface.

---

Tuesday, 2nd October @ 13:30: Poster Session (HALL & ROOM 3) - Poster - Abstract ID: 393

---

***Dr. Manola Moretti*<sup>1</sup>, *Dr. Marco Allione*<sup>1</sup>, *Dr. Maria Teresa De Angelis*<sup>2</sup>, *Prof. Giovanni Cuda*<sup>2</sup>, *Prof. Enzo Di Fabrizio*<sup>1</sup>**

*1. KAUST, 2. Universita Magna Graecia Catanzaro*

There is an urgency to fully overcome the limitations of known techniques (X-ray diffraction, NMR, TEM imaging) to solve the structure of roughly 70% of the cell membrane proteins. The limiting factors are the low yield in extraction and crystallization of these proteins and/or the limited resolution of the instrument, plus the need of thousands of replicas for the same protein. Enhanced spectroscopy techniques are widely used in biological applications, due to their sensitivity, versatility and often low interaction/toxicity with a delicate sample. In recent work we have demonstrated the potential of a micro-fabricated super-hydrophobic device combined with different types of analysis (Raman spectroscopy, electron microscopy), to characterize single/few biological molecules with utmost sensitivity. Here we are performing SERS analysis of a specific subunit (SCN1a) of the Voltage gated Sodium channel (Na<sub>v</sub>) on extracted cell membranes stretched over the pillars.

Basically, extracted cell membranes are stretched on top of the SHS, immuno-gold labeled for the SCN1a subunit and analyzed at the Raman spectrometer. To access the plasmonic effect on the gold nanoparticles, laser wavelength at 633 nm is used.

In Fig. 1 the experimental results are shown. The Raman mapping shows several areas of interest, including the ones identifying the membranes (Fig. 1d) and the gold nanoparticles *per se* (Fig. 1e). Moreover SERS effect is noticed nearby some of the gold nanoparticles (Fig. 1f, g). Several sharp peaks appear on the two spectra. Most of them are related to single aromatic aminoacids, like the ones at 643 cm<sup>-1</sup> (Tyr), 958, 1348, 1551 cm<sup>-1</sup> (Trp), 1049 cm<sup>-1</sup> (Phe).

These preliminary results show the potential of the method to chemically characterize single proteins by using SERS effect on a native cell membrane surface in dry, background free conditions. The signal enhancement given by the gold nanoparticle can be complemented by the topography and the plasmonic enhancement accessible with an AFM probe tip. This advancement will likely show the vibrational modes of the secondary structures of the protein thus giving access to structural information at the single molecule level.

---

# Dynamic Metasurface based optical cavity for enhanced optical phase modulation

---

Tuesday, 2nd October @ 13:30: Poster Session (HALL & ROOM 3) - Poster - Abstract ID: 404

---

***Mr. Tayyab Nouman***<sup>1</sup>, ***Prof. Jae-hyung Jang***<sup>1</sup>, ***Mr. Ji Hyun Hwang***<sup>1</sup>, ***Mr. Gyejung Lee***<sup>1</sup>

*1. Gwangju Institute of Science and technology*

Metasurfaces consist of 2-dimensional array of resonators that allow for controlling the phase of the optical wavefronts to realize lenses and deflectors.

Realizing such devices with dynamically reconfigurable optical characteristics would greatly extend the scope of their applications. Here, we experimentally demonstrate a dynamic metasurface cavity structure, operating in Terahertz (THz) frequency range. The dynamic metasurface cavity structure consists of modified split ring resonators realized on top of vanadium dioxide (VO<sub>2</sub>) thin films, shown in Fig. 1(a). By applying a bias current to the device, VO<sub>2</sub> present at the split gaps can be made to transition from insulator to metallic state. This modulates the optical response of the device. The fabricated metasurface device is characterized using a THz time domain spectroscopy (THz-TDS) setup and the measured reflectance and phase shift are shown in Fig. 1(b) & (c). Varying the applied bias current from 0 mA to 170 mA, results in various interesting changes in both reflectance and phase response of the cavity structure. A maximum reflectance modulation of 97 % and phase modulation up to 180° is observed.

The above measured results are fully reproduced (not shown in the manuscript) by modelling the metasurface cavity structure using transmission line theory and the effective surface admittance approach. In the above approach, propagation of a plane wave in a dielectric is described by an equivalent transmission line. The metasurface at the interface of two dielectric media is considered as an effective surface admittance, attached to the junction between two transmission lines, as shown in Fig. 2. The above equivalent model fully explains the dynamic resonant behavior of the metasurface cavity structure as well as the accompanied phase modulation characteristics.

The reported results demonstrate the potential of such devices for realizing tunable holograms, high efficiency modulators and tunable optical filters. The analytical approach presented here, can be applied for design and analysis of metasurface cavity structures based on other material systems at frequencies ranging from THz to mid infrared.



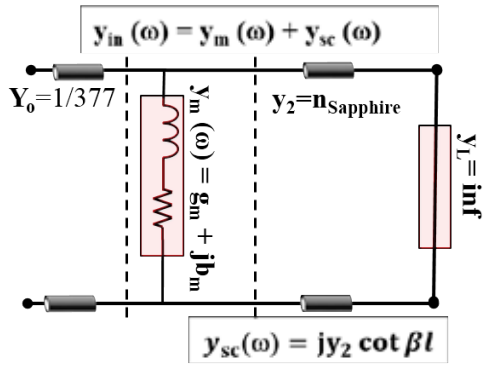


Fig 2.png

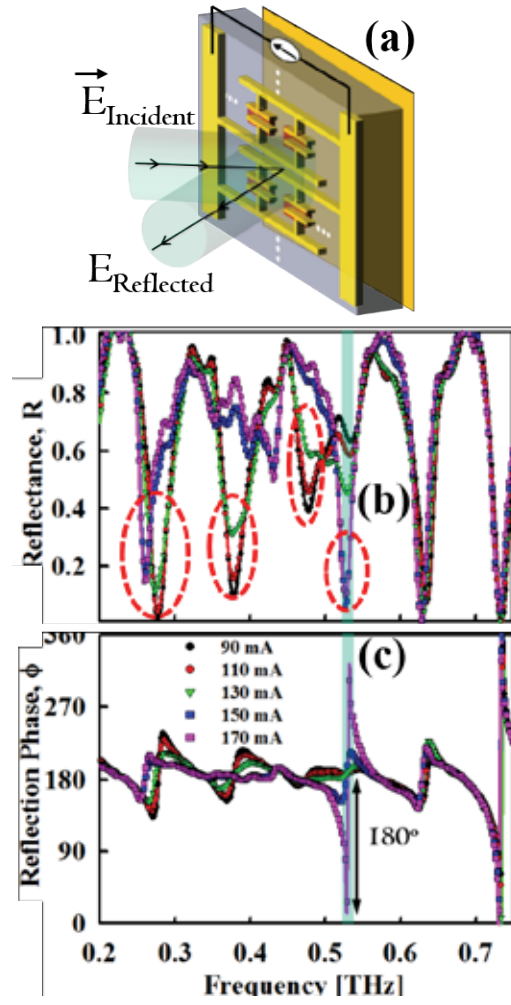


Fig 1.png

# Particle sizing and concentration through elastic light scattering at small angles

Tuesday, 2nd October @ 13:30: Poster Session (HALL & ROOM 3) - Poster - Abstract ID: 406

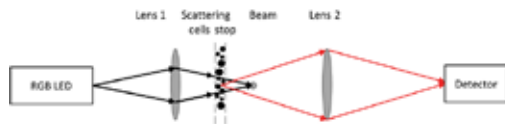
***Prof. MIGUEL CASAS-RAMOS<sup>1</sup>, Dr. Eduardo Sandoval-romero<sup>1</sup>***

*1. Centro de Ciencia Aplicadas y Desarrollo Tecnológico, UNAM*

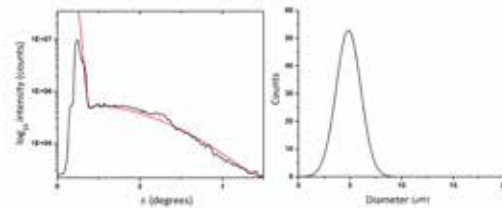
Elastic light scattering has been used for several decades as an important research tool in biomedicine. The significant interest in light scattering is due as a noninvasive and nondestructive optical tool capable of characterize parameters of biological samples. But for biological materials, most of the light is scattered in nearly the forward direction; and low angle light scattering measurements should yield quite accurately the mean cell size value and the concentration per unit area.

Because of this, the angular dependence of light scattering by the sphere-like yeast and lymphocyte cells was measured at angles up to  $7^\circ$ . By illuminating the cell with a converging beam from an inexpensive RGB LED, angularly resolved scattering patterns are imaged by a CMOS sensor and the intensity recorded by a photodetector. The analysis of these patterns with Mie theory leads to the predictions of size distribution of the particles, where we found a mean diameter of  $4.0 \pm 0.02 \mu\text{m}$  and the measurable concentration range was  $\sim 153 \#/\mu\text{m}^2$  to  $\sim 226 \#/\mu\text{m}^2$  for yeast cells, the measured concentration error was 11.38–14.37%. The measurable concentration range could be adjusted simply by changing the system configuration.

The scattering by the yeast cells was found to agree substantially with the predictions of the Mie equations for the homogeneous sphere, and how properties of the blood cells can be extracted through the light scattering at small angles.



Arreglo optico.png



Scattering analysis green.jpg

---

## Hydrogel-based plasmonic sensor system

---

Tuesday, 2nd October @ 13:30: Poster Session (HALL & ROOM 3) - Poster - Abstract ID: 194

---

***Mr. Christoph Kroh*<sup>1</sup>, *Mr. Roland Wuchrer*<sup>2</sup>, *Dr. David Ulkoski*<sup>3</sup>, *Dr. Margarita Günther*<sup>1</sup>, *Prof. Carmen Scholz*<sup>3</sup>, *Prof. Thomas Härtling*<sup>2</sup>, *Prof. Gerald Gerlach*<sup>1</sup>**

*1. Technische Universität Dresden, 2. Fraunhofer Institute for Ceramic Technologies and Systems IKTS, 3. University of Alabama in Huntsville*

Fast and reliable evaluation of liquid properties such as pH, temperature, ethanol- or carbon dioxide concentrations is of extreme importance for the in-line process monitoring in the fields of water treatment, biotechnology, food, and pharmacy industry. We undertook the challenge of the in-line measurements by integrating hydrogels on optical sensors. At the Fraunhofer Institute of Ceramic Technologies and Systems a robust optical sensor, based on a plasmonic gold nanostructure, is being developed. The nanostructure is fabricated by means of nanoimprint lithography (NIL). The use of polymer foils as a carrier material improves biocompatibility and reduces production costs of the sensor substrate as it allows roll-to-roll fabrication. The patterning of the sensor substrate allows for excitation of surface plasmons in the metal layer with light under normal incidence.

It is well known that the spectral transmission properties of the gold nanostructure depend on the refractive index of the surrounding. Hydrogels change their swelling state with varying values of the parameters listed above. Swelling and deswelling causes a change in the effective refractive index. As very thin hydrogel layers (well below 1  $\mu\text{m}$  thickness) can be applied on the gold nanostructure, the diffusion-controlled hydrogel swelling process will be fast and, hence, the sensor response will be sufficiently short (in the range of minutes). The concept of using plasmonic sensors with analytically sensitive hydrogels offers an opportunity for an inexpensive and robust system for in-line measurements.

Initial studies for this concept were carried out with both a pH- and a carbon dioxide sensitive hydrogel and results demonstrating the working principle will be presented. Furthermore, we will present the opportunities and challenges of the fabrication process for the foil-based sensor substrates.

# Thermoplasmonic maskless lithography assisted by gold nanostars

Tuesday, 2nd October @ 13:30: Poster Session (HALL & ROOM 3) - Poster - Abstract ID: 210

**Dr. Eduardo Martínez<sup>1</sup>, Prof. Ricardo Urbano<sup>1</sup>, Prof. Carlos Rettori<sup>2</sup>**

1. University of Campinas (UNICAMP), 2. University of Campinas (UNICAMP) / Federal University of ABC (UFABC)

## Introduction:

The heat dissipation upon excitation of gold nanostars' (AuNSs) plasmon resonance can produce more than 100 °C increase in the local temperature. On the other hand, polylactic acid (PLA) is a thermoplastic biodegradable polymer with a glass transition temperature around 60 °C. Here, we show that by covering the PLA films with AuNSs it is possible to locally modify them by harvesting the thermoplasmonic effect. Under a 976 nm focused laser beam, the local temperature in AuNSs surpasses the glass transition of the base polymer producing their attachment to its surface. The following dissolution of the unexposed material allows the precise control of the engraving process in the microscale. A computer numerical control system (CNC) was developed to transfer 2D patterns, opening up the thermoplasmonic lithography technique and the laser printing of nanoparticles on rigid and flexible substrates. Furthermore, by embedding Er<sup>3+</sup> doped upconversion nanoparticles (UCNPs) which can act as primary nanothermometers into the polymer layer, it is possible to optically determine the local temperature, visualize the NIR laser spot and produce luminescent patterns. The methods developed were applied to produce patterned substrates for surface enhanced Raman spectroscopy (SERS), and optical encoding for anti-counterfeiting technologies.

## Methods:

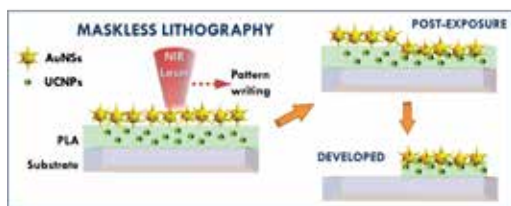
PLA films were formed by dissolving commercial 3D printing filaments in chloroform and depositing the solution by spin coating on different substrates (glass, silicon and polyimide tape). AuNSs of ca. 50 nm in diameter were synthesized by using spherical gold seed nanoparticles and by controlling the growth of the branches by stoichiometric addition of AgNO<sub>3</sub> and ascorbic acid at room temperature. Poly(styrenesulfonate) (PSS) was added to stabilize the AuNSs colloids.

## Results:

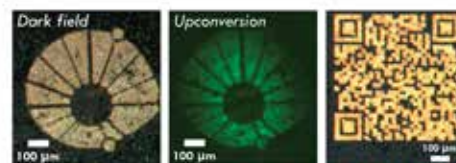
The full characterization of the surface topography and the resolution of the technique is presented. Raman spectroscopy measurements of rhodamine 6G deposited inside and outside the engraved patterns of AuNSs reveal the SERS effect. Optical encoding was demonstrated by transferring a generated QR code on a PLA-UCNPs film.

## Discussion:

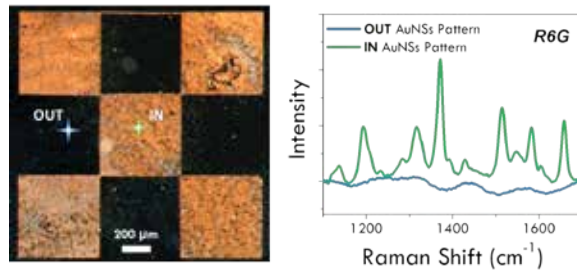
The technique and the materials presented here are relevant for the development of plasmonic-based devices and as a fabrication tool that combines bottom-up and top-down approaches in a synergic way.



Scheme thermoplasmonic lithography.png



Upconversion luminescent patterning.png



Aunss sers active pattern.png

# High efficiency gradient index GaN metasurfaces

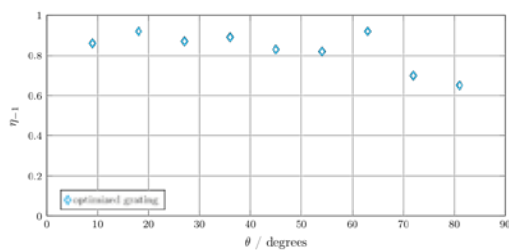
Tuesday, 2nd October @ 13:30: Poster Session (HALL & ROOM 3) - Poster - Abstract ID: 269

**Mr. Gauthier Briere<sup>1</sup>, Mr. Nikolai Schmitt<sup>2</sup>, Mr. Niklas Georg<sup>3</sup>, Mr. Dimitrios Loukrezis<sup>4</sup>, Dr. Patrice Genevet<sup>1</sup>, Dr. Stéphane Lanteri<sup>2</sup>, Prof. Ulrich Römer<sup>3</sup>, Prof. Claire Scheid<sup>5</sup>**

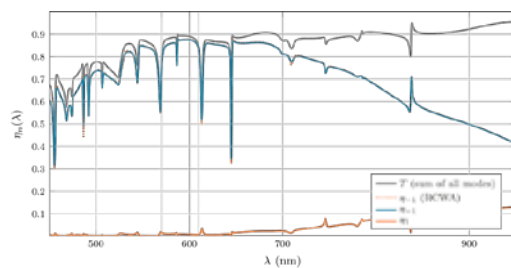
1. Université Côte d'Azur, CNRS, CRHEA, 2. Université Côte d'Azur, Inria, CNRS, LJAD, 3. Technische Universität Braunschweig, Institut für Dynamik und Schwingungen, 4. Technische Universität Darmstadt, Institut für Theorie Elektromagnetischer Felder, Germany, 5. Université Côte d'Azur, LJAD, CNRS, Inria

Metasurfaces are promising optical components for accurate phase, amplitude and polarization control of the transmitted light. Their fabrication simplicity and their extreme compactness with respect to more traditional volume-based diffraction components make them attractive for lightweight and integrated applications. In this contribution, we designed efficient metasurface beam deflectors, able to address a wide range of deflection angles from zero to almost 90 degrees. The devices are designed to work in transmission. They are optimized in order to maximize constructive interference in the first diffractive order while maintaining destructive interference for its symmetric counterpart, leading to maximal transmission into the design direction. In this study, we designed various GaN grating couplers for various deflection angles and obtained very high efficiencies up to 95 % for deflection angles of less than 63° at a wavelength of 600 nm. The performance decreases down to 70 % for a deflection angle of 81° (see Figure 1).

During the design phase, we relied on a goal-oriented optimization procedure based on Rigorous Coupled Wave Analysis (RCWA) simulations. These results have been benchmarked with the Discontinuous Galerkin Time Domain (DGTd) method. Moreover, we have studied the broadband behavior with the DGTd simulations (see Figure 2). In order to ensure the robustness of our design, we have performed Uncertainty Quantification regarding the metasurface's geometry, taking into account fabrication tolerances of the e-beam lithography. Fabrication processes of GaN-based metasurfaces and the experimentally measured performances of these structures will be reported during this presentation. The utilization of GaN material offers interesting perspectives in particular due to its negligible absorption in the entire visible range.



Abst nanop 2018-fig1.png



Abst nanop 2018-fig2.png

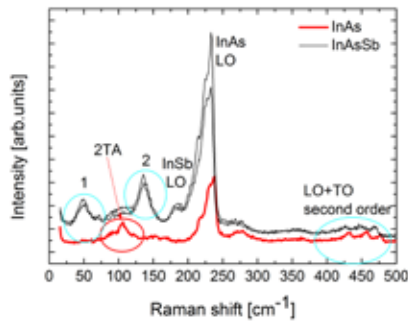
# Raman scattering for InAsSb

Tuesday, 2nd October @ 13:30: Poster Session (HALL & ROOM 3) - Poster - Abstract ID: 296

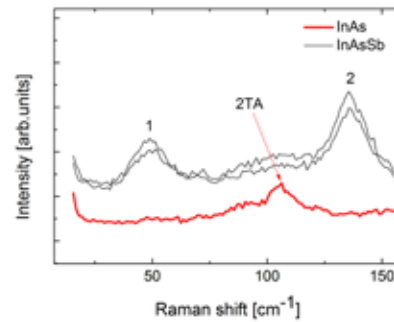
**Mr. Krzysztof Murawski<sup>1</sup>, Dr. Kacper Grodecki<sup>1</sup>, Mr. Krystian Michalczewski<sup>1</sup>, Mr. Bogusław Budner<sup>1</sup>, Prof. Piotr Martyniuk<sup>1</sup>**

*1. Military University of Technology*

The  $\text{InAs}_{1-x}\text{Sb}_x$  ternary alloy band gap nonlinearly depends on the composition, which gives the opportunity to use this material in devices operating in a wide range of infrared radiation [1–2]. We present experimental results for  $\text{InAs}_{1-x}\text{Sb}_x$  samples for Sb composition from 0.1 to 0.8. Raman spectrum of InAs and InSb in the range of 20 - 250  $\text{cm}^{-1}$  exhibits two main LO peaks and 2TA peak [4,5]. On the other hand in the range 20-250 for InAsSb in Raman spectra two additional peaks (44 $\text{cm}^{-1}$  and 140 $\text{cm}^{-1}$ ) are present, while they are not existing neither in pure InAs nor in InSb. 44 $\text{cm}^{-1}$  and 140 $\text{cm}^{-1}$  are close to phonon energy for momentum equals K for InAs. In this case in Raman scattering not only gamma point is active, but also K point.



Graph1.jpg



Graph4.jpg

# Numerical investigation on metamaterial side of epoxy resins at visible light

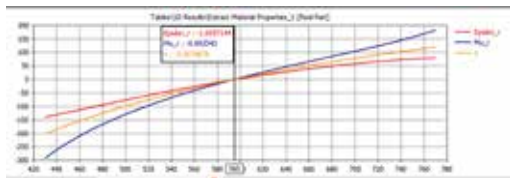
Tuesday, 2nd October @ 13:30: Poster Session (HALL & ROOM 3) - Poster - Abstract ID: 27

***Ms. HANAN ALI***<sup>1</sup>

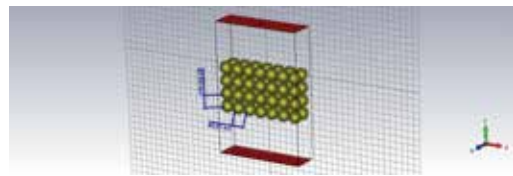
*1. Central China Normal University*

Metamaterials are composite materials whose material properties (acoustic, electrical, magnetic, optical, etc.) are determined by their geometrical structure, especially the unit cells. The development of metamaterials continues to redefine the boundaries of materials science. These materials offer excellent design flexibility with their customized properties and their tunability.

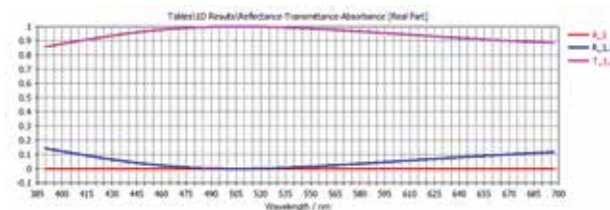
The proposed structure in this paper is made from epoxy resins nanospheres. Each nanosphere has a radius of 20nm. The structure was modeled in CST suite studio along the frequency range 430-700THz. The results showed that this structure has both negative refractive index and extremely high refractive index. It also showed that all of the parameters permittivity, permeability and refractive index have negative values along the frequency range 430-597THz which cover the colors red, orange, yellow and green. In addition it has almost unitary transmission for those colors which make the structure useful in the lens industry. The frequency 597THz would be considered as a frequency shift between very low refractive index and very high refractive index. The structure showed an excellent transmission of the light with zero absorption and weak reflection. After that the effect of the radius were studied. The results showed that increasing the radius of the spheres make the refractive index move towards positive values, with the same result applied on epsilon and mu, in addition to a small value of imaginary part for that wavelength.



Material properties at 20nm.v2.png



Geometrical design at raduis 20nm.v3.png



T r and a for 20nm.v2.png



---

## Indirect nanoplasmonic sensing.

---

Tuesday, 2nd October @ 13:30: Poster Session (HALL & ROOM 3) - Poster - Abstract ID: 56

---

***Dr. Benjamin Demirdjian*<sup>1</sup>, *Dr. Igor Ozerov*<sup>1</sup>, *Mr. Alain Ranguis*<sup>1</sup>, *Mr. Frédéric Bedu*<sup>1</sup>, *Dr. Claude R. Henry*<sup>1</sup>**

*1. Aix-Marseille Univ., CNRS, CINaM UMR 7325*

Indirect nanoplasmonic sensing (INPS) allows following the adsorption of gases on chemically active nanoparticles deposited onto a regular array of gold disks fabricated by electron-beam lithography. We measure UV-VIS absorption spectra corresponding to localized surface plasmon resonance (LSPR) signals coming from gold disks. The gas molecules adsorbed onto nanoparticle surfaces change their dielectric properties and this induces a spectral shift of the LSPR signal of the underlying gold disk sensor [1].

We illustrate this work by results obtained on water molecules adsorbed on both hydrophobic and hydrophilic soot nanoparticles [2] and give some perspectives concerning catalytic heterogeneous reactions. Indeed by coupling INPS with mass spectrometry it becomes possible to follow quantitatively and with a high sensitivity the reactivity of gases (CO, NO<sub>x</sub>, ...) with metallic nanoparticles (Pt, Pd, ...) involved in catalysis.

### **References**

[1] E. M. Larsson, C. Langhammer, I. Zoric, B. Kasemo, *Science* **326**, 1091-1094 (2009).

[2] B. Demirdjian, F. Bedu, A. Ranguis, I. Ozerov, A. Karapetyan and C. R. Henry, *The Journal of Physical Chemistry Letters* **6**, 4148-4152 (2015).

# Numerical modelling of green and red emitting quantum dot based optical films by Monte Carlo ray tracing method for smartphone display applications

Tuesday, 2nd October @ 13:30: Poster Session (HALL & ROOM 3) - Poster - Abstract ID: 273

Mr. S. Efdal Mutcu<sup>1</sup>, Dr. Güneş Aydınoğan<sup>1</sup>, Mr. Sezer Caynak<sup>1</sup>, Mr. Sadra Sadeghi<sup>2</sup>, Mr. Kıvanç Karslı<sup>1</sup>, Prof. Sedat Nizamoğlu<sup>2</sup>

1. Vestel Electronics Corp., 2. Koç University

Among several components that affect the performance of display devices, i.e. LED, optical films, or liquid crystal (LC) cell; quantum dot (QD) based optical films are newly employed constituents of display technologies that aim to replace conventional solid state lighting techniques, e.g. blue-LED-chip-plus-yellow-phosphor combination. Despite their main advantages such as high efficiency, narrow emission band, and spectral tunability, quantum dots suffer from the optical losses due to reabsorption at different concentrations.

In this study, we focus on the computational modelling of green-emitting CdSe/ZnS- and red-emitting CdSe/CdS-based optical films as color convertors to reveal the effects of QD concentrations on the output spectrum. The evaluation of the numerical results is compared in terms of color gamut, luminance and chromaticity coordinates. A Monte Carlo ray-tracing algorithm in MATLAB is developed to simulate the QD based optical sheets (QDs) for smartphone usage at different green and red QD concentration levels, and the output that yields the highest luminous efficiency, the highest color gamut, and chromaticity coordinates best fit to display standards ( $C_x = 0.285$ ,  $C_y = 0.293$  in CIE 1931 color space) are presented. The results are also confirmed with that of the commercial optical-simulation software LightTools.

We use at least 100000 incident photons onto the QDs to obtain reproducible results. Before the incident photons reach the nanoparticles, they first interact with the boundary of the optical host material of PDMS. The algorithm mainly tracks the movement of every single photon from their first entry to the QD boundaries until their withdrawal. The simulations yield satisfactory results, i.e., 80% DCI Color Gamut in CIE 1976 standards, or chromaticity coordinates (0.288, 0.293), and the spectra of the corresponding QD concentration levels are plotted. It must be noted that these simulations contain only QDs among the optical components that constitutes the backlight unit of a smartphone. Considering the lack of additional films, i.e. diffuser sheet, prism sheet, and reflective polarizer, a Color Gamut value of 80% corresponds to a value close to 100% with the addition of the mentioned optical components.

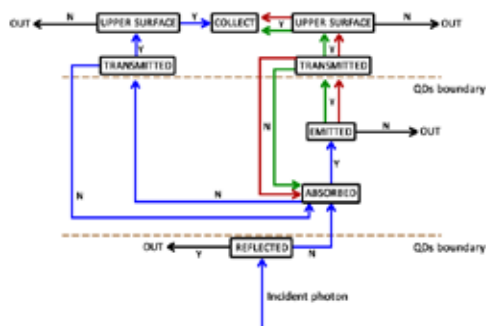


Figure 1 - algorithm.jpg

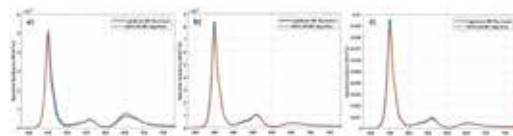


Figure 2 - simulation results.jpg

#	<i>Green QD Conc. (mMol/L)</i>	<i>Red QD Conc. (mMol/L)</i>	<i>C<sub>x</sub></i>	<i>C<sub>y</sub></i>	<i>Lum. (nit)</i>	<i>Color Gamut</i>
1	140	260	0.319	0.300	1.37	80.29%
2	220	100	0.294	0.318	2.23	72.61%
3	180	120	0.288	0.293	2.08	72.14%

Table 1 - parameters.jpg

---

# Inkjet printing of anisotropic structures by cellulose nanocrystals

---

Tuesday, 2nd October @ 13:30: Poster Session (HALL & ROOM 3) - Poster - Abstract ID: 536

---

*Ms. Elena Eremeeva*<sup>1</sup>, *Prof. Alexandr Vinogradov*<sup>1</sup>, *Prof. Vladimir Vinogradov*<sup>1</sup>

*1. ITMO University*

Cellulose is one of the most promising biopolymer material. According to its high mechanical properties, sensing for electric and magnetic fields, and unique optical properties could be usable for many purposes. For now, a water suspension of cellulose and its derivatives are suitable to manufacture flexible electronics, paper production, food, and additives in optical and pharmaceutical industries. This work reports about a new way of application CNC dispersion as a transparent ink for hidden patterns printing.

The cellulose microcrystal suspension was prepared according to the method described by Marchessault et al, which is commonly used for preparing nonflocculating cellulose suspensions.

CNC dispersion form anisotropic structure in a bulk, because of assembling of rod-like shape particles in the hydrodynamic process of CNC colloid drying. Reflected polarized light interference in the dry CNC layer. Difference thickness facilitates changes of the imposition of minimums and maximums of slow and fast rays, that showed an iridescent of CNC layers which is visible only in polarized light.

Rheological properties of CNC dispersion allow to use it as inks for material printer Fujifilm Dimatix 2831. The final substance which was used to print consist of 1% mass fraction of CNC without any additives to control the rheological properties (viscosity – 2.4 cP, surface tension – 69.8 N/m). Low quantity of solid phase in dispersion dictates used patterns with high dpi because of only with terms of coalescence of drops we can obtain enough thickness of printed layer with strong optical anisotropy. Changing the number of printed layers let us have different colors.

The work was supported by the grant of Russian Science Foundation 16-19-10394.

# Numerical computation of plasmonic resonances in dispersive media: Application to metallic gratings

Tuesday, 2nd October @ 13:30: Poster Session (HALL & ROOM 3) - Poster - Abstract ID: 114

*Dr. Guillaume Demesy*<sup>1</sup>, *Dr. Boris Gralak*<sup>2</sup>, *Prof. André Nicolet*<sup>2</sup>

1. CNRS Institut Fresnel, 2. Institut Fresnel

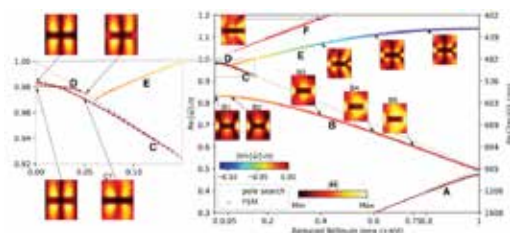
We present several methods for the direct computation of the resonances associated with electromagnetic structures involving highly frequency dispersive permittivities, such as metals and/or semi-conductors in the visible or infrared range of frequencies - this is a fundamental problem for plasmonic applications.

Computing the eigenfrequencies corresponding to source free solutions of an electromagnetic problem (e.g. the harmonic wave equation for the electric field  $E$ ) is a spectral problem. In presence of materials with flat dispersion, the discretization of such problems using the Finite Element Method (FEM) in the harmonic case classically leads to linear (matrix) eigenvalue problems giving pairs of resonant frequencies (eigenvalues) together with associated eigen-fields (modes).

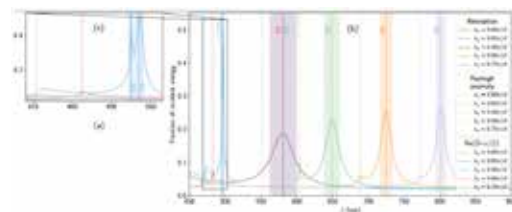
Now, we consider relative permittivity functions heavily dependent on the very frequency that we are trying to determine: We are facing a non-linear eigenvalue problem. We are also interested in the case where several dispersive media are present in the structure as it often occurs in practice. We benchmark various FEM formulations of this non-linear eigenvalue problem, from auxiliary fields to brute numerical linearization, and we compare their performances. Very recent advances in linear algebra algorithms have provided efficient libraries able to directly tackle

such problems, such as the SLEPc library [cite{slepc-users-manual}]. Direct calls to this library have been implemented in the open source FEM software GetDP.

The method is extended to open problems using Perfectly Matched Layers (PMLs) to determine the Quasi Normal Modes (QNMs). Note that the eigenfrequencies are then necessarily complex valued for the twofold reason that the dispersive media are dissipative and that the geometry is unbounded. As an example, we present the modal analysis of a gold diffraction grating in the visible range. The structure is both open and periodic. The Floquet-Bloch theory is applied to tackle the periodicity combined with PMLs to obtain the QNMs. A complex dispersion relation of the structure is obtained. It is shown that the physical behavior of this system can be efficiently described using a small number of QNMs - that can even be reduced to a single one.



Screen shot 2018-04-09 at 5.50.17 pm.png



Screen shot 2018-04-09 at 5.50.37 pm.png

---

# Multipole analysis of metasurfaces composed of nanoparticles supporting electric and magnetic optical resonances

---

Tuesday, 2nd October @ 14:30: Metamaterials (ROOM 1) - Oral - Abstract ID: 69

---

***Dr. Andrey B. Evlyukhin***<sup>1</sup>

*1. Laser Zentrum Hannover e.V.*

Theoretical approach to the multipole analysis of the extinction and scattering spectra of arbitrary shaped particles and the reflection and transmission spectra of metasurfaces composed from them is demonstrated and discussed. The main attention is given to the first multipoles including magnetic quadrupole and electric octupole moments. The method is applied to high refractive-index nonspherical nanoparticles with resonant multipole responses in the optical range. Firstly, we show that the role of multipoles in the optical theorem (light extinction) and scattering by arbitrarily shaped nanoparticles can be different [1]. This can result in seemingly paradoxical conclusions with respect to the appearance of multipole contributions in the scattering and extinction cross sections. This fact is especially important for absorptionless nanoparticles, for which the scattering cross section can be calculated using the optical theorem, because in this case extinction is solely determined by scattering. Secondly, spectral multipole resonances of single parallelepiped-, pyramid-, and cone-like shaped silicon nanoparticles excited by linearly polarized light waves are investigated. It is demonstrated how specially configured scattering diagrams are connected with overlapping of different multipole modes resonantly excited in the nanoparticles [2]. At last, the multipole expansions of the reflection and transmission coefficients of 2D arrays of nanoparticles (metasurfaces) are developed and applied for investigation of the metasurface optical properties. Suppressions of light reflection or transmission in metasurfaces composed of nonspherical silicon nanoparticles are explained as interference between waves generated by several multipole moments resonantly excited in these nanoparticles by incident light waves. The developed approach can be extremely useful for designing and optimization of metasurfaces with predetermined optical properties.

[1] A.B. Evlyukhin, T. Fischer, C. Reinhardt, and B. N. Chichkov, *Phys Rev B* **94**, 205434 (2016).

[2] P.D. Terekhov, K. V. Baryshnikova, Y. A. Artemyev, A. Karabchevsky, A. S. Shalin, and A. B. Evlyukhin, *Phys. Rev. B* **96**, 035443 (2017).

# Pixel-level Microsecond Electrical Switching of Infrared Transparent Phase Change Materials

Tuesday, 2nd October @ 14:47: Metamaterials (ROOM 1) - Oral - Abstract ID: 217

*Dr. Vladimir Liberman*<sup>1</sup>, *Mr. Yifei Zhang*<sup>2</sup>, *Dr. Mikhail Shalaginov*<sup>2</sup>, *Mr. Paul Robinson*<sup>1</sup>, *Dr. Christopher Roberts*<sup>1</sup>, *Dr. Myungkoo Kang*<sup>3</sup>, *Dr. Yadav Anupama*<sup>3</sup>, *Prof. Kathleen Richardson*<sup>3</sup>, *Prof. Juejun Hu*<sup>2</sup>, *Dr. Jeffrey Chou*<sup>1</sup>

*1. MIT Lincoln Lab, 2. massachusetts institute of technology, 3. University of Central Florida*

## Introduction

Previously, we have reported on a novel class of chalcogenide phase change materials, based on Ge-Sb-Se-Te (GSST) alloys, with excellent infrared transparency from 1.5 to > 10 micron wavelengths. As shown in Fig. 1(a), increasing Se substitution leads to a progressive lowering of extinction coefficient.

A material in this family with a particular useful stoichiometry,  $\text{Ge}_2\text{Sb}_2\text{Se}_4\text{Te}_1$  (GSS4T1), possesses broadband transparency through the infrared range while maintaining a large index contrast between amorphous and crystalline phases (Fig. 1(b)).

## Methods

Here, for the first time, we report reversible electrical switching of GSS4T1 pixelated devices. The devices are fabricated in a CMOS-compatible clean room on 8 inch wafers utilizing a full Si-based fabrication capabilities. Devices of pixel sizes from 1 to 30 micron were fabricated (Fig. 2(a)). Additionally, fabrication of more complicated sub-pixel metasurfaces was demonstrated (Fig. 2(a)). The pixel cross-section includes a 50-nm thick tungsten heater layer, 50-nm thick GSS4T1 layer, and a thin capping layer (Fig. 2b). Electrical switching measurement is obtained by applying electrical pulse trains through a programmable voltage generator into the gate of a high powered transistor (as shown in Fig. 2(b)), while measuring the reflection of a 1550-nm laser off the surface using an InGaAs imager.

## Results and Discussion

Microsecond switching of 30-micron and 1-micron pixels in a wafer-scale device has been demonstrated. Figure 3 shows 1550-nm laser reflectivity as the 30-micron pixel is cycled between amorphous (high reflectance) and crystalline (low reflectance) phases. Amorphization with a single 1-microsecond pulse with 50% duty cycle at 25 Volts is demonstrated. Crystallization requires a train of 15 V pulses with a period of 1 ms, 50% duty cycle, with a total pulse train duration of 50 ms. The results represent the first embodiment of a pixelated electrical switched display for applications from short wave to longwave infrared. With further optimization, we expect sub-microsecond switching times for both crystallization and amorphization times, enabling realization of megahertz switching speeds.

We anticipate that these devices will enable a variety of applications in the infrared photonics such as ultrafast spatial light modulators, holographic devices, beam steering and neuromorphic networks for reservoir computing

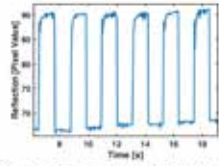


Figure 3. Reflection rate vs. time of an electrically-switched 30-nm-thick PCM pixel (area: Figure 2, left). The data was captured at 1300 nm.

Fig3 switching performance.jpg

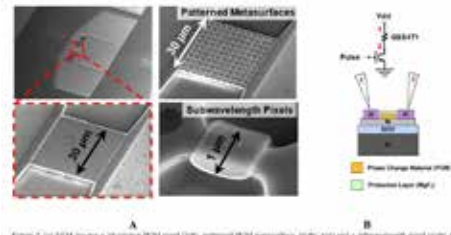


Figure 2. (a) SEM images of 30-nm-thick PCM pixel (left), patterned 30-nm metasurface (right, top) and a subwavelength pixel (right, bottom). (b) Pixel Region and the cross-section of a single pixel of the switching device.

Fig 2 pixelated sem pcm structures.jpg

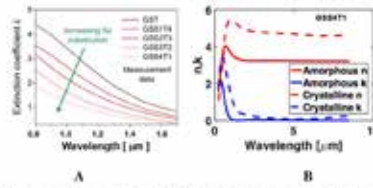


Figure 1. (a) Effect of Se substitution on absorption reduction in the Ge-Sb-Te alloy system. (b) Optical properties of amorphous (dashed lines) and crystalline (solid lines) Ge-Sb-Te from the visible range to 1.5  $\mu\text{m}$ .

Fig1 spectral data.jpg



---

# Transitions between States in Topological Waveguide Systems by Time-Periodic Driving

---

Tuesday, 2nd October @ 15:04: Metamaterials (ROOM 1) - Oral - Abstract ID: 19

---

*Ms. Christina Jörg<sup>1</sup>, Mr. Christoph Dauer<sup>1</sup>, Mr. Fabian Letscher<sup>1</sup>, Prof. Sebastian Eggert<sup>1</sup>, Prof. Michael Fleischhauer<sup>1</sup>, Prof. Georg Von Freymann<sup>1</sup>*

*1. TU Kaiserslautern*

We study the transition between bulk states and an edge state in the topologically nontrivial Su-Schrieffer-Heeger (SSH) system, in which the edge state is driven by a local AC-field. Theory is verified by experiments in evanescently coupled dielectric waveguide systems.

Introduction:

The SSH model consists of a linear chain of sites, where each two sites are connected via a strong bond and a weak bond alternately. We introduce an “edge” by putting a defect with two weak bonds at either side into the chain (at site 0). That creates an edge state that is exponentially localized around site 0, as the topological invariant in the left side of the chain differs from that in the right side.

Now we drive site 0 periodically by modulating its position in the y-direction sinusoidally with frequency  $\omega$ . This makes the coupling from site 0 to its neighbors time-dependent. Also, the on-site potential at site 0 differs from that of the other sites due to the curvature. If we solve the time-dependent Schrödinger equation with the system’s Hamiltonian, we see that Floquet replicas [1] of the edge state appear, spaced with  $\omega$  around zero energy.

Whenever the driving frequency  $\omega$  is such that the replicas hit the bulk bands the edge state couples to the bulk states, i.e. the light delocalizes from site 0. For the cases where the replicas lie outside the bands no Floquet replica can couple to bulk states and the light stays localized around site 0.

Methods:

Experiments were conducted in arrays of 3D printed dielectric evanescently coupled waveguides [2].

Results and Discussion:

The experiments confirm the effect predicted by theory. Light is localized around the defect except for frequencies resonant with the bulk bands. By selecting the frequency we can also control the angle under which the light spreads into the bulk.

Our setup serves to control the localization and steering of light via an external parameter. It also gives insight into Floquet mechanisms.

[1] S. A. Reyes *et al.*, New J. Phys. **19**, 043029 (2017).

[2] C. Jörg *et al.*, New J. Phys. **19**, 083003 (2017).

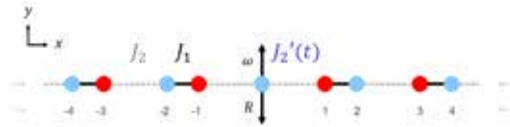


Figure 1: Sketch of the SSH model with defect at site 0, modulated with frequency  $\omega$  and amplitude  $R$ .  $J_1, J_2$  is the coupling of the strong (weak) bond AND  $J_2'(t)$  the time-dependent coupling from site 0 to its neighbors.

Fig1 sshchain model withcaption.png

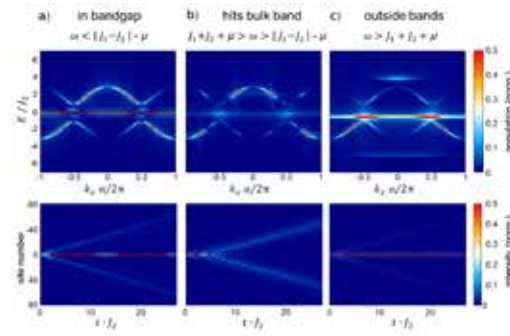


Figure 2: Numerically calculated band structures (top) and propagation (bottom) for the three frequency regimes. When the driving frequency  $\omega$  is resonant with the bulk bands the edge state couples to the bulk states and the light delocalizes from site 0 (b). For the cases where the replica lies outside the bulk bands the light stays localized around site 0 (a and c).

Fig2 the three frequency regimes withcaption.png

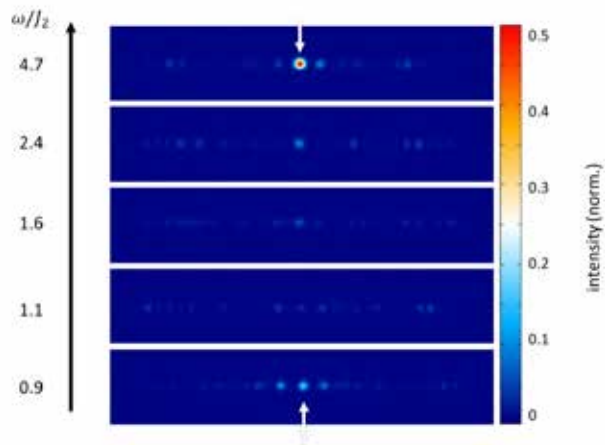


Figure 3: Measurements in arrays of evanescently coupled waveguides with defects of different frequencies  $\omega$ . For small frequencies ( $\omega = 0.9 J_2$ ) light is localized around site 0 (indicated by the arrow), while for intermediate frequencies it spreads into the bulk. For  $\omega > 4.7 J_2$  the light localizes again.

Fig3 measurement withcaption.png

---

# Metamaterials for manipulating light polarization

---

Tuesday, 2nd October @ 15:21: Metamaterials (ROOM 1) - Oral - Abstract ID: 150

---

***Dr. Jakub Haberko*<sup>1</sup>, *Dr. Michal Nawrot*<sup>2</sup>, *Dr. Lukasz Zinkiewicz*<sup>2</sup>, *Dr. Piotr Wasylczyk*<sup>2</sup>**

*1. AGH University of Science and Technology, Faculty of Physics and Applied Computer Science, 2. University of Warsaw, Faculty of Physics, Institute of Experimental Physics, Photonic Nanostructure Facility*

## **Introduction**

Controlling the polarization state of light is of utmost importance in many scientific and industrial applications, such as stereoscopic vision, polarization microscopy or non-linear light frequency conversion. Typically, to achieve this goal dichroism, birefringence or optical activity are utilized. However, new ideas are also investigated, involving plasmonic metasurfaces or designer metamaterials. On one hand novel nano/microfabrication techniques, such as two-photon laser nanolithography, have recently allowed these ideas to become reality. On the other hand computer simulation techniques facilitate the search for innovative metamaterial designs. I will present two different concepts: i) a successfully designed and fabricated array of twisted bands [1] and ii) a metasurface consisting of quasi-random metallic pixels, designed with a stochastic search algorithm, acting as a waveplate in the near- to mid-infrared range [2].

## **Methods**

The twisted band array (i) was first manufactured by two-photon laser nanolithography in a polymer photoresist and was consecutively sputter-coated with a 50 nm layer of gold. The polarization of light reflected off the array was measured with a Fourier transform infrared spectrometer. Polarization properties of the structure were simulated using the Finite Difference Time Domain technique (FDTD). The optimal geometry of the metasurface (ii) was determined using the FDTD method combined with a custom-designed stochastic search algorithm.

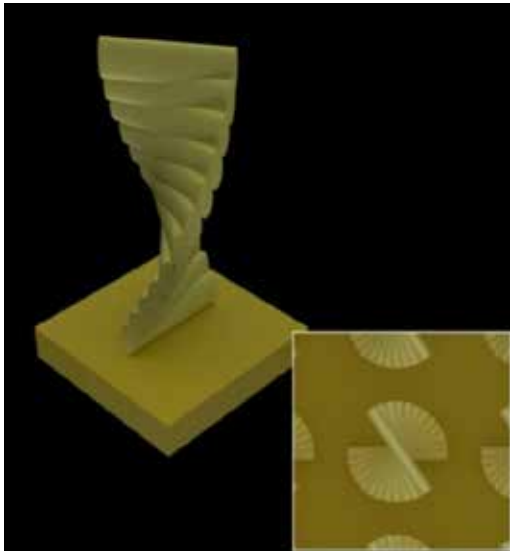
## **Results and discussion**

We have been able to design and manufacture a twisted band array transforming linearly-polarized light into circularly-polarized wave for a specific wavelength and into elliptically polarized light with ellipticity above 0.9 in a considerable frequency range. Computer simulations are in good qualitative agreement with experimental results, but also show sensitivity of the design to geometric parameters. We have also proposed a simple stochastic search algorithm which, provided a suitable fitness function, successfully optimizes a metallic metasurface geometry to act as a broadband quarter- or half-waveplate, working in reflection in a wavenumber range of 3000-4500 cm<sup>-1</sup>. Similar methodology can be utilized to design other classes of optical devices, such as polarization rotators. Both designs presented here are scalable and can be tuned to a different frequency range.

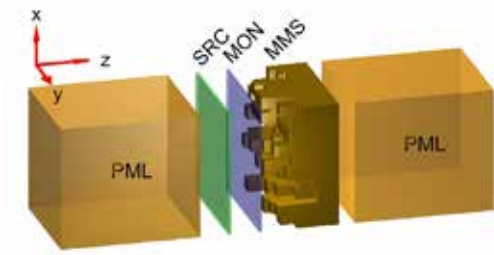
## **Literature**

[1] Appl. Phys. B (2017) 123:285

[2] Opt. Comm. 410 (2018) 740-743



Metallic twisted band cgi and sem.jpg



Metallic metasurface simulation setup.jpg

# Switchable Holographic Device Using Electrochemical Method

Tuesday, 2nd October @ 15:38: Metamaterials (ROOM 1) - Oral - Abstract ID: 283

*Dr. Seong M. Cho*<sup>1</sup>, *Ms. Sujung Kim*<sup>1</sup>, *Dr. Yong-Hae Kim*<sup>1</sup>, *Dr. Tae-Youb Kim*<sup>1</sup>, *Dr. Sang Hoon Cheon*<sup>1</sup>,  
*Dr. Joo Yeon Kim*<sup>1</sup>, *Dr. Chil Seong Ah*<sup>1</sup>, *Ms. Juhee Song*<sup>1</sup>, *Dr. Hojun Ryu*<sup>1</sup>, *Dr. Chi-Sun Hwang*<sup>1</sup>, *Dr.*  
*Jeong-Ik Lee*<sup>1</sup>

1. Electronics and Telecommunications Research Institute

The holographic display based on digital technology has attracted much attention as a next generation realistic display. Spatial light modulator (SLM) is considered as a key element to enable such digital holography technology. However, pitch scale down for securing wide viewing angle has become a big technical issue in the development of SLM. In this study, we propose a novel device using reversible electrodeposition to overcome the limitation of the pitch scale down which has been recognized as the limit of the voltage driving device such as liquid crystal display.

The reversible electrodeposition technology is a technology that reversibly deposits or removes Ag on the electrode surface by application of an electric field. We propose a new device structure that can make hologram image using reversible electrodeposition technology.

Figure 1 shows the structure of the proposed device. The device consists of a lower mirror, a lower ITO electrode, an electrolyte, a WO<sub>3</sub> counter electrode, and an upper ITO electrode. Ag can be deposited or erased on the surface of the lower ITO electrode by application of an electric field. The left picture shows the state where Ag is erased, and the right picture shows the state where Ag is deposited. In these two cases, the reflective layer of the incident light changes. When Ag is not deposited, the primary reflection occurs in the lower mirror layer, but when Ag is deposited, a reflection occurs in the deposited Ag layer. Therefore, the light reflected from these two cases has a phase difference due to the thickness of the ITO layer and the thickness of the deposited Ag.

Figure 2 shows the simulation result of the complex reflectance of the reflected light, which is characterized by phase modulation. Figure 3 shows the hologram-driven image of the device with 1 $\mu$ m pixel pitch. The device is capable of on / off driving and it is possible to realize excellent hologram image.

## Acknowledgment

This work was supported by Institute for Information & communications Technology Promotion(IITP) grant funded by the Korea government(MSIT) (No.2017-0-00065, The core technology development of high performance materials and devices for volumetric display)

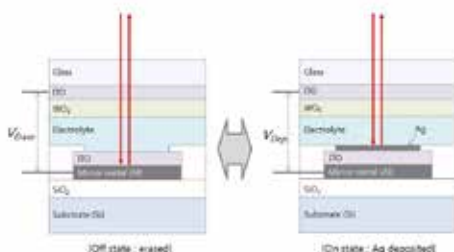


Fig. 1 Schematic diagram showing the structure and operating principle of the device

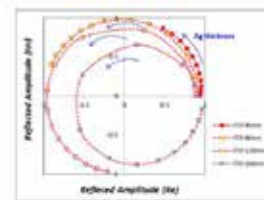


Fig. 2 simulation results on the complex reflectance change of the device with deposited Ag thickness. The blue arrow shows the increasing direction of Ag deposition. The Ag deposition amount was in the range of 0 to 60 nm. A significant difference was observed with ITO thickness.

Fig 1 schematic diagram showing the structure and operating principle of the device.jpg

Fig 2 simulation results on the complex reflectance of the device.jpg

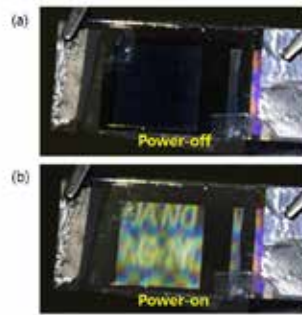


Fig. 3 Photographs of the switchable holographic device; (a) erased state, (b) Ag deposited state. The device was illuminated with a white LED light.

Fig 3 photographs of the switchable holographic device.jpg

# Nanoparticles obtained via solid state dewetting of silver thin film

Tuesday, 2nd October @ 15:55: Metamaterials (ROOM 1) - Oral - Abstract ID: 349

**Dr. Iryna Gozhyk<sup>1</sup>, Dr. Paul Jacquet<sup>2</sup>, Ms. Barbara Bouteille<sup>1</sup>, Dr. Renaud Podor<sup>3</sup>, Mr. Johann Ravaux<sup>3</sup>, Mr. Joseph Lautru<sup>3</sup>, Dr. Morten Kildemo<sup>4</sup>, Dr. Romain Dezert<sup>5</sup>, Dr. Alexandre Baron<sup>5</sup>, Dr. Jacques Jupille<sup>6</sup>, Dr. Rémi Lazzari<sup>6</sup>, Dr. Jeremie Teisseire<sup>2</sup>**

1. Surface du Verre et Interfaces, UMR 125 CNRS/Saint-Gobain Recherche, 2. Saint-Gobain Recherche, 3. Institut de Chimie Séparative de Marcoule, UMR 5257 CEA-CNRS-UM-ENSCM, 4. Norwegian University of Science and Technology, 5. CRPP Université de Bordeaux, 6. Institut des NanoSciences de Paris, Sorbonne Universités, UMR 7588

## Introduction

Ordered metallic nano-particles can exhibit unique properties of light scattering, confinement and absorption, prominent for a vast number of applications (energy harvesting, bio-sensing, surface enhanced Raman spectroscopy etc). However, deposition of such arrays over macroscopic surfaces remains challenging.

Among various methods known for the fabrication of metal nano-particles, we chose the solid-state dewetting of very thin metallic films. This technique alone results in randomly distributed islands with an important size distribution. But if the metal layer is deposited on a patterned surface, the dewetting results in the arrays of metallic nano-particles.

## Methods

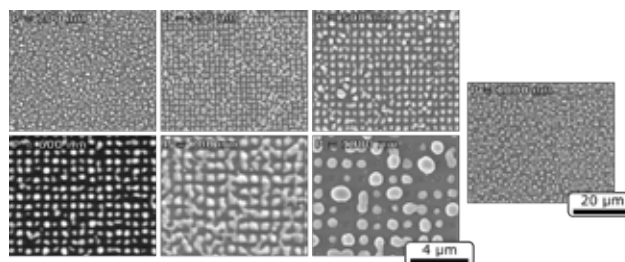
The morphology and optical properties of our samples are examined both post-mortem and through the combination of in situ and real-time techniques (environmental scanning electron microscopy and spectroscopic ellipsometry).

## Results

In this contribution, we demonstrate how nano-imprint process combined to silver dewetting leads to an innovative, simple and scalable approach for fabrication of silver nano-particles arrays (Fig.1). It allows us to drastically increase the fabrication scalability and obtain the  $8 \times 8 \text{ cm}^2$  sample. Moreover, this new technique is not limited to wafer-based substrates and can be applied on transparent substrates such as glass, which paves a way for optical characterization in transmission.

Figure 1. SEM images treated of arrays of nanoparticles obtained through the dewetting of silver layer deposited on patterned silica surface (square array, lattice constant varied in range from 200 to 1000 nm)

Discussion We prove the excellent organization of our silver nano-particles array showing both order and uniform size distribution. We control the size and organization of particles with the initial thickness and graininess of the silver film and the period of patterns. Finally we investigate both experimentally and through numerical simulations the optical properties of these surfaces containing the arrangement of nano-particles and in particular the position of the surface lattice resonance with respect to lattice constant of the array.



Mebtext.png

---

# Superradiant properties of Collective plasmon modes in ultra-dense film of silver nanoparticles

---

Tuesday, 2nd October @ 14:30: Optics and transport on 2D materials (ROOM 2) - Oral - Abstract ID: 53

---

**Dr. Julien Laverdant**<sup>1</sup>, **Mr. Gérard Colas Des Francs**<sup>2</sup>, **Mr. Hugo Varguet**<sup>2</sup>, **Dr. Jean-michel Benoit**<sup>1</sup>,  
**Mr. Ruben Mascart**<sup>1</sup>, **Dr. Jeremie Margueritat**<sup>3</sup>, **Dr. Alice Berthelot**<sup>1</sup>

1. Université Claude Bernard Lyon 1, 2. LICB, CNRS UMR 6303, Université de Bourgogne, 3. Université

Random metallic films, before the percolation threshold, present a concentration of electromagnetic field at the nm scale, below the diffraction limit [1], These generated hot spots, induce huge enhancement of light-matter coupling and these substrates thus constitute performing systems for enhanced spectroscopies. However, the nature of the plasmon modes is still unclear at the percolation threshold and this manuscript presents experimental and theoretical investigations of these plasmon modes. Films are synthesized by evaporation of silver glass. By varying the effective thickness, one goes from isolated metallic structure to continuous thin film. Then, the nature of the plasmon mode, evolving from Localized Surface Plasmon Resonance (LSPR) to Surface Plasmon Polariton (SPP), is probed by Attenuated Total Reflection measurements (ATR). Our ATR study shows that before the transition to conductive state, in TM excitation, two drastically different behaviors are present at the same wavelength but for different angles of incidence. For supercritical angles, the specular reflection is totally extinguished while at critical angle, the specular reflection is maintained for a large part of the visible spectrum due to the presence of bright plasmon modes. These latter modes present unexpected spectral broadening and an angular squeezing close to the percolation threshold. At this level of deposition, film can be seen as a ultra dense array of plasmonic nanosystems. The actual model of the hybridization for coupled plasmon modes is not sufficient to explain our experimental results. We explain this behavior by considering that transverse Localized Surface Plasmon Resonances of each nanoparticle, interact in a collective and coherent way via a common confined light mode: the evanescent wave. Using Dyadic Green formalism [2], our model confirms the existence of these collective modes for a dense array of plasmon systems and explains the observed spectral broadening and angular squeezing. This superradiance phenomenon, increasing with the numbers of involved particles, is maximum before the percolation threshold where the density of large nanoparticles is maximum and disappears after where nanoparticles coalesce.

[1] M. I. Stockman et al PRL, **87**, 167401 (2001).

[2] J.J. Choquette et al PRA , **82**, 1 (2010).



# Fundamental Limits in the Coupling between Light and 2D Polaritons

Tuesday, 2nd October @ 14:47: Optics and transport on 2D materials (ROOM 2) - Oral - Abstract ID: 329

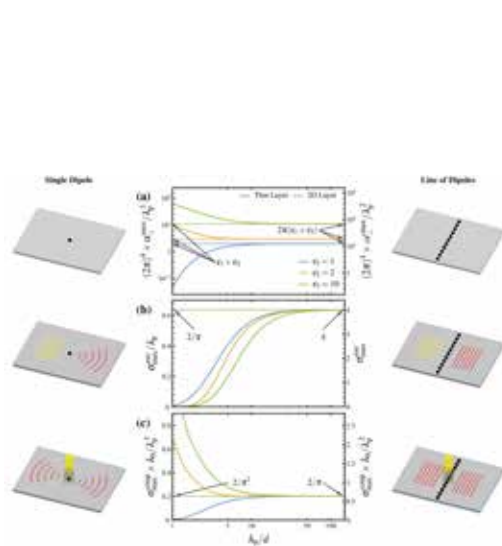
*Mr. Eduardo Brioso Dias<sup>1</sup>, Prof. Javier García de Abajo<sup>1</sup>*

*1. ICFO - The Institute of Photonic Sciences*

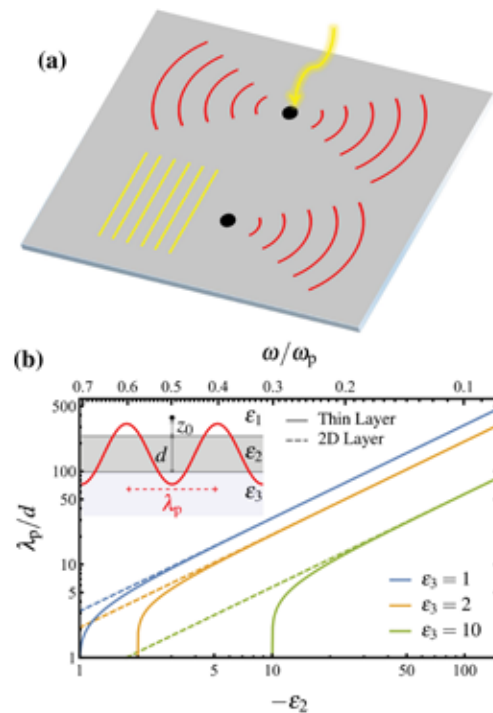
Polaritons in 2D materials have been extensively studied over the past decade due to their fundamental interest and as a platform for applications in telecommunications and sensing. The wavelength of these polaritons is generally small compared to that of a photon of the same frequency, and thus these excitations evolve in the electrostatic regime. This property makes them attractive to manipulate light at deep-subwavelength distances, although it simultaneously implies that their in/out-coupling to propagating light is intrinsically weak.

In this work, we address some fundamental limits in the coupling of radiation to 2D polaritons. We study the scattering properties of 0D and 1D scatterers over a 2D or finite-thickness layer and find a generalization of the optical theorem to 2D polaritons, which we express as a maximum possible value of their effective polarizability. Remarkably, this value is independent of material and we write the result as a universal curve that is applicable to any layer thickness in the electrostatic approximation. Additionally, this result leads to a maximum light-polariton coupling cross-section. We formulate our results for both 0D and 1D scatterers, including material edges, and present them in simple closed-form expressions.

This work has been supported in part by the Spanish MINECO (MAT2017-88492-R and SEV2015-0522) and the European Commission (Graphene Flagship 696656, Marie Skłodowska-Curie 713673). Eduardo Brioso Dias acknowledges support from a “la Caixa” INPhINIT Fellowship Grant.



Max polarizability extinction coupling.png



Plasmons dispersion relation.png

# Characterization of Airy Surface Plasmon Polaritons by Photoemission Electron Microscopy

Tuesday, 2nd October @ 15:04: Optics and transport on 2D materials (ROOM 2) - Oral - Abstract ID: 304

*Mr. Matthias Falkner*<sup>1</sup>, *Mr. Amit V. Singh*<sup>1</sup>, *Dr. Goran Isic*<sup>2</sup>, *Prof. Thomas Pertsch*<sup>1</sup>

*1. Institute of Applied Physics, Abbe Center of Photonics, Friedrich-Schiller-Universität Jena, 2. Institute of Physics Belgrade*

## Introduction

Airy surface plasmon polaritons (SPPs) are propagating surface plasmon excitations that are confined to the metal-dielectric interface, containing the properties of Airy beams. The generation of such non-diffracting beams that are suitable for flat land photonics has always been of interest. It opens up new capabilities in prominent device application, e.g., optical traps and tweezers, biosensors, selective on-chip manipulation of nanoparticles.

Here, we report a versatile method of the investigation of Airy SPPs on a metallic surface by PhotoEmission Electron Microscopy (PEEM). It can provide a spatial resolution of the order of 20nm. PEEM allows for direct visualization of the plasmon field through photoemission, where the photo-emitted electrons provide a map of electromagnetic fields at the surface.

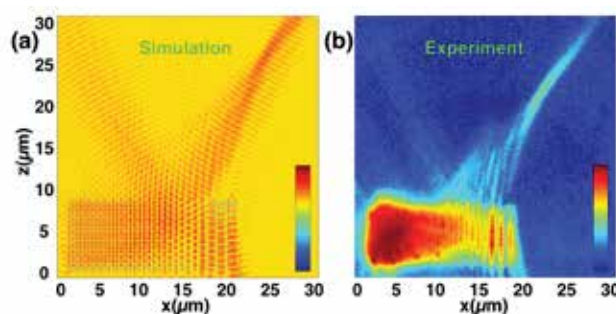
## Methods

Our sample design is inspired by Minovich et al. and was realized by focused ion beam milling into a 200 nm thick gold film. This specially designed diffraction grating can generate the Airy beam profile and simultaneously can couple free space propagating waves to SPPs. For the illumination, we used a home-built tunable optical parametric chirped pulse amplifier. The central wavelength was varied between 690 and 840 nm. The emitted photoelectrons were imaged by a PEEM from Focus GmbH. Large-scale 3D finite difference time domain simulations were performed to optimize and theoretically verify the design.

## Results

Both theory and experiment show an excellent agreement. On the air-gold interface, the Airy SPP is launched at the grating edge and simultaneously interferes with the incident laser pulse. The photo-emitted electrons provide the direct visualization of the total field. The area of constructive and destructive interference leads to higher and lower nonlinear photoemission yield. This result clearly shows SPP generation containing all the properties of Airy beams. The main lobe of the Airy SPP propagates along a curved trajectory for more than 25 $\mu$ m.

In conclusion, we have experimentally investigated the Airy plasmons with high spatial resolution, and their propagation along the curved trajectory has been visualized. The experimental results not only match with theoretical results but also contain deeper insight into the structure.



Airy spp.png

# Nonlinear semiconductor superlattices for the Gigahertz to the Mid Infrared ranges

Tuesday, 2nd October @ 15:21: Optics and transport on 2D materials (ROOM 2) - Oral - Abstract ID: 82

**Prof. Mauro Fernandes Pereira**<sup>1</sup>, **Dr. Apostolos Apostolakis**<sup>1</sup>, **Mr. Vladimir Anfertev**<sup>2</sup>, **Prof. Vladimir Vaks**<sup>2</sup>

1. Department of Condensed Matter Theory, Institute of Physics of the Czech Academy of Sciences, 2. Institute for Physics of Microstructures, Russian Academy of Sciences

The generation of high power coherent radiation in the GHz to THz ranges is a very important topic of recent research, notably after recent findings that synchronization between superlattices leads to a dramatic increase in output power [1]. Nonlinear optical effects in semiconductor materials have been strongly investigated in the near infrared and visible spectra, but the GHz-THz-Mid Infrared (MIR) ranges are wide open for investigation. This talk starts with a fully predictive microscopic approach combining Nonequilibrium Green's Functions and relaxation-rate approximations for the Boltzmann equation describing the nonlinear polarization in semiconductor superlattices (SSLs) at arbitrary orders in very good agreement with experiments [2,3]. Next we investigate the ultimate efficiency of SSLs as devices [4] for room temperature THz emission based on harmonic on multiplication of GHz inputs including limitations imposed by the buildup of electric field domains [5].

These results open the possibility of extending the whole field of nonlinear optics to the GHz-THz range and the possibility of designing materials and devices for a large number of applications, including spectroscopy of biomolecules, which typically have strong GHz-THz resonances.

References:

- [1] B. Gaifullin et al, Phys. Rev. Applied 7, 044024 (2017).
- [2] M.F. Pereira et al, Phys. Rev. B 96, 045306 (2017).
- [3] M.F. Pereira et al, Nanophoton 11 (4), 046022 (2017).
- [4] Karl F. Renk et al, Advances in Optoelectronics, 54042 (2007).
- [5] K. N. Alekseev, et al, EPL (Europhysics Letters), 73(6):934, 2006.

Figure Captions:

Fig.1. Normalized Harmonic Power of the 1<sup>th</sup> harmonic to the 3<sup>rd</sup> harmonic nonlinearly generated by input fields oscillating. The corresponding solid lines have been calculated using our theory.

Fig. 2. Calculated efficiency for a ( $3 \times \omega_1=300$  GHz) parametric oscillator as a function of the pump amplitude  $U_1$ . The amplitude of the third harmonic is fixed at  $U_3=0.1U_c$ . The dark grey region indicates the response of efficiency if one assumes that electric instability (domains) at large pump amplitudes does not prevent the field in the resonator from growing.

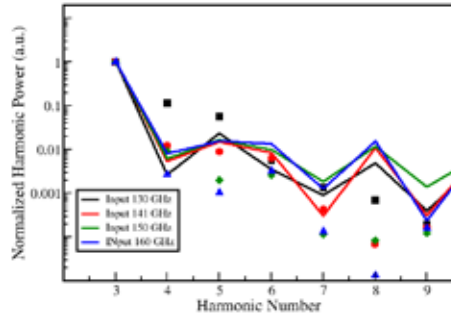


Fig.1.png

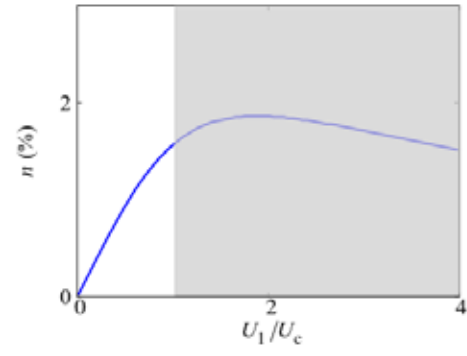


Fig.2.png

# Clusters of nanoparticles as isotropic Huygens sources for metasurfaces applications

Tuesday, 2nd October @ 15:38: Optics and transport on 2D materials (ROOM 2) - Oral - Abstract ID: 338

**Mr. Romain Dezert <sup>1</sup>, Dr. Philippe Richetti <sup>1</sup>, Prof. Alexandre Baron <sup>1</sup>**

<sup>1</sup>. University of Bordeaux

We present spherical clusters, composed of spherical dielectric or metallic inclusions, as a new kind of efficient and isotropic Huygens sources. The clusters considered act as nanoantennas in the visible or near infrared domain, and exhibit highly asymmetrical scattering resulting from interferences between their optically induced modes. We demonstrate overlapped electric and magnetic resonances in our structure, giving rise to high forward scattering on resonance. We propose designs of broadband Huygens sources. In contrast to the path commonly followed in the literature [1], our approach to obtain such sources relies on the engineering of the refractive index of the effective particle rather than its geometrical shape [2]. Figure 1(a-c) are examples of several cluster realizations of different nature that show overlapped electric and magnetic multipolar behaviors and the corresponding portion of forward-scattered energy under plane wave illumination (d-f).

We show that clusters may also serve as building blocks for metasurfaces applications. We investigate their possible uses in high transmittance phase-control devices, and in thin absorber metalattices. Full wave numerical simulations show that arrays of silicon clusters can be used to shape the wavefront of a transmitted wave in the near infrared (see Fig. 2(a)). By tuning the size of the clusters or on the surface fill-fraction of the metasurface, the phase of the transmitted wave can be tuned from 0 to  $2\pi$  while maintaining high transmission. By exploiting the generalized Kerker conditions involving quadrupolar resonances, we also show that our Huygens sources can be exploited to build perfect absorbers. These devices are angle-independent resonant systems that absorb close to 100% of incoming light (see Fig. 2(b)).

From an experimental point of view, clusters are particularly well-suited to bottom-up fabrication and self-assembly. They can be synthesized by making emulsions of two immiscible phases, one of which contains the nanoparticle inclusions. Therefore, they offer an alternative to the classical lithographically fabricated Huygens meta-atoms and can be made in large volumes. Examples of such synthesized particles will be shown.

[1] Decker, M., et al. (2015), *Advanced Optical Materials*, 3(6), 813-820.

[2] Dezert, R., et al. (2017), *Physical Review B*, 96(18), 180201.

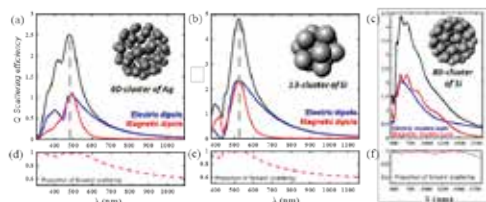


Fig1 abaron huygens.png

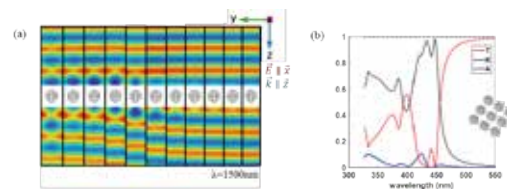


Fig2 abaron huygens.png

---

# Plasmonic Luneburg lens characterization with phase detection

---

Tuesday, 2nd October @ 15:55: Optics and transport on 2D materials (ROOM 2) - Oral - Abstract ID: 322

---

***Dr. César E. García-Ortiz*<sup>1</sup>, *Dr. Rodolfo Cortés-Martínez*<sup>1</sup>, *Dr. Jesus Gomez-Correa*<sup>2</sup>, *Dr. Eduardo Pisano*<sup>3</sup>, *Dr. Jacek Fiutowski*<sup>4</sup>, *Dr. Victor Ruiz-cortes*<sup>5</sup>, *Dr. Víctor M. Coello-Cárdenas*<sup>1</sup>**

*1. CICESE, Unidad Monterrey, 2. UANL, 3. CICESE Unidad Monterrey, 4. SDU, 5. CICESE*

Luneburg lenses are optical elements with a gradient refractive index that focus plane waves at the outer surface of the lens without aberration. In this work, we designed, fabricated and characterized a plasmonic Luneburg lens which focuses a surface-plasmon polariton (SPP) beam at the boundary of the structure [Fig. 1]. The gradient in the effective refractive index was produced by a periodic array of holes with different radii in a nano-patterned PMMA structure, and a grating is used to couple the incident light into SPPs. An almost plane SPP beam is incident onto the two-dimensional (2D) Luneburg lens and it focuses at the close vicinity of its surface. The characterization was performed using leakage radiation microscopy (LRM), for usual intensity distribution imaging [Fig. 2], and phase detection was achieved using a slight modification of the illumination properties, which allowed to directly observe the SPP wavefront distribution as the beam propagates through the lens and focuses [Fig. 3]. Phase detection is obtained by imaging the interference pattern produced by the incident light and the leakage radiation of the SPPs, which are out of phase. The results are in good agreement with the 2D numerical simulations. The proposed design is efficient to focus SPPs at the surface of the structure, and opens the possibility to be operated inversely, i.e., to generate a plane SPP beam if excited with a point SPP source positioned at the outer surface. Moreover, Fourier imaging, available in most LRM setups, provides a new analysis approach for plasmonic Luneburg lenses, as it is possible to obtain the effective index of the SPP mode as it propagates through the lens. Such Fourier analysis can help verify the values of the designed gradient-index lens.

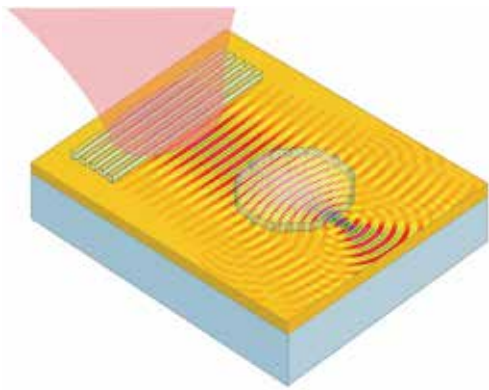


Fig1.jpg

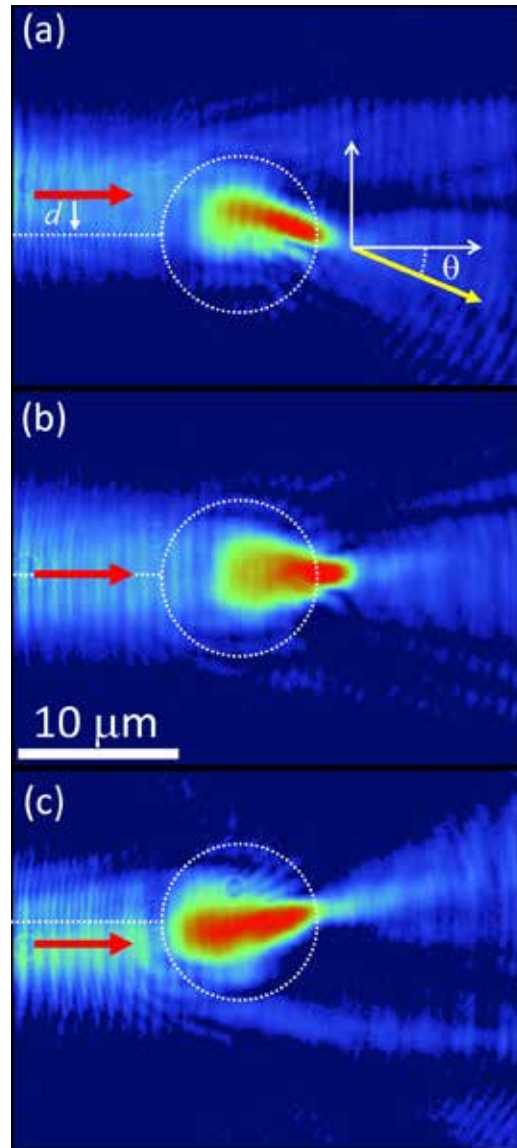


Fig2.jpg

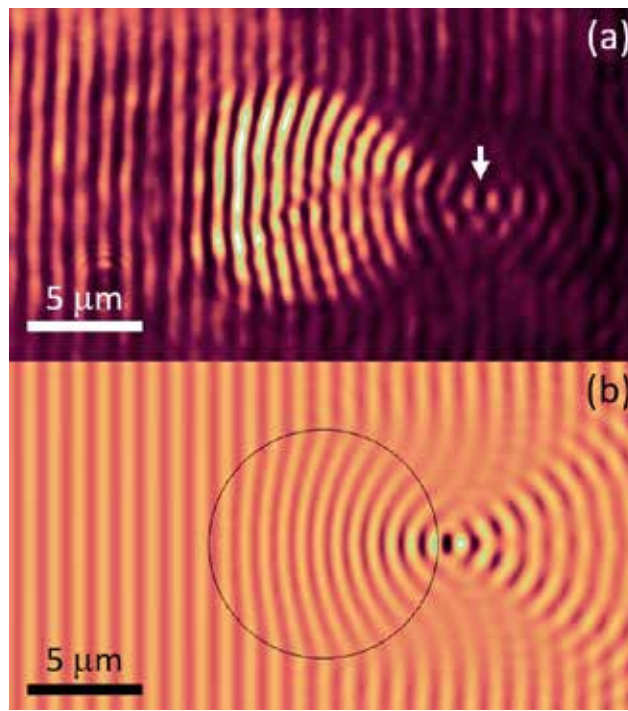


Fig3.jpg



---

# Polymer distributed Bragg reflectors: an old structure with unexpected sensing capabilities

---

Tuesday, 2nd October @ 14:30: Enhanced spectroscopy and sensing (AUDITORIUM) - Oral - Abstract ID: 50

---

***Dr. Paola Lova***<sup>1</sup>, ***Prof. Alberto Servida***<sup>1</sup>, ***Prof. Davide Comoretto***<sup>1</sup>

*1. University of Genova*

## Introduction

Polymer distributed Bragg reflectors (DBRs) are gaining attention thanks to mass fabrication technologies, lightweight, and flexibility, which are unconceivable with other photonic structures.<sup>1</sup> Indeed, they are increasingly studied for lasing,<sup>2</sup> fluorescence enhancement,<sup>3-5</sup> and optical switching.<sup>6</sup> Moreover, their easy assimilation with packaging fabrication technologies<sup>7</sup> makes them interesting integrated transducers for barrier polymers employed in the encapsulation of moisture-sensitive devices. Notwithstanding the low permeability of barrier polymers, small molecules like water and oxygen can permeate through the polymers affecting the device. We demonstrate that when the barrier films are structured to form a DBR, such intercalation allows to evaluate *in-situ* the molecular diffusion parameters, which are currently assessed *ex-situ* with complex gravimetric methods. Indeed, when a small molecule intercalates into a DBR the interaction between the polymer and the molecules allows a shift of the photonic band-gap with kinetics and magnitude that depends on the chemico-physical interactions between the two players.<sup>8-9</sup> Such effects, which are unconceivable with inorganic systems, consent to esteem diffusivity and allows simple colorimetric selective label-free transducers for a variety of pollutants.

## Methods

DBRs were fabricated by spin-coating of alternated layer of polystyrene (PS) and cellulose acetate (CA) solutions. More details on preparation and optical characterization are reported in Ref.<sup>8-9</sup>

## Results

Figure 1a shows the reflectance of a PS:CA DBR before and after exposure to methanol vapors. Before the exposure the structure displays a maximum assigned to the stop-band at 840 nm (purple), which shift to ~940 nm after 90 min in methanol rich environment (red). From the dynamics of the stop-band shift, it is possible to retrieve the *optical* sorption-curves reported in Figure 1b for methanol and other alcohols. There, the stop-band reaches a plateau within 90 min for methanol, while heavier alcohols display longer kinetics.

## Discussion

The data of Figure 1b deliver information on the analyte diffusivity within the polymers, which depends on free-volume, polarity, weak-bonding, and molecular size.<sup>8-9</sup> Then, we can retrieve, for instance, diffusivity values of  $\sim 10^{-8} \text{ cm}^2/\text{min}$  for methanol, in full agreement with gravimetric data.<sup>10-11</sup> Moreover, the DBR response allows label-free selectivity, which nowadays requires long time sampling, separation processes and analyses.

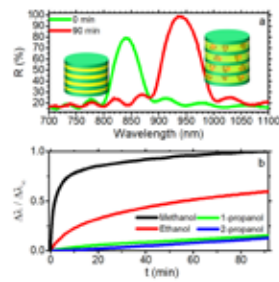


**Figure 1.** a) Reflectance spectra of a PS:CA DBR before and after 90 minutes of exposure to Methanol. b) Optical sorption-curves retrieved for methanol, ethanol, 1-propanol and 2-propanol.

Figure 1.jpg

#### References

- (1) Cavallo, D.; Goossens, H.; Meijer, H. E. H., *Organic and Hybrid Photonic Crystals*, 1st ed.; Springer International Publishing: Cham, Switzerland, 2015; Vol. 1, pp 493.
- (2) Cusazza, G.; Scotognella, F.; Lanzani, G.; De Silvestri, S.; Zavelani-Rossi, M.; Comoretto, D. Lasing from all-polymer microcavities, *Laser Phys. Lett.* **2014**, *11*, 035804
- (3) Lova, P.; Cortecchia, D.; S. Krishnamoorthy, H. N.; Giusto, P.; Bastianini, C.; Bruno, A.; Comoretto, D.; Soci, C. Engineering the Emission of Broadband 2D Perovskites by Polymer Distributed Bragg Reflectors, *ACS Photonics* **2018**, DOI:10.1021/acsp Photonics.7b01077.
- (4) Manfredi, G.; Lova, P.; Di Stasio, F.; Kralac, R.; Comoretto, D. Directional fluorescence spectral narrowing in all-polymer microcavities doped with CdSe-CdS dot-in-rod nanocrystals, *ACS Photonics* **2017**, *4*, 1761–1769.
- (5) Lova, P.; Grande, V.; Manfredi, G.; Patrini, M.; Herbst, S.; Würflner, F.; Comoretto, D. All-polymer photonic microcavities doped with perylene bisimide J-aggregates, *Adv. Opt. Mater.* **2017**, *5*, 1700523.
- (6) Knurr III, R. J.; Manfredi, G.; Martinelli, E.; Pannocchia, M.; Repetto, D.; Mennucci, C.; Solano, I.; Canepa, M.; Bustier de Mongeot, F.; Galli, G.; Comoretto, D. In-plane anisotropic photoresponse in all-polymer planar microcavities, *Polymer* **2016**, *84*, 383-390.
- (7) Song, H.; Singer, K.; Lott, J.; Wu, Y.; Zhou, J.; Andrews, J.; Baer, E.; Hiltner, A.; Weder, C. Continuous melt processing of all-polymer distributed feedback lasers, *J. Mater. Chem.* **2009**, *19*, 7520-7524.
- (8) Lova, P.; Bastianini, C.; Giusto, P.; Patrini, M.; Rizzo, P.; Guerra, G.; Iodice, M.; Soci, C.; Comoretto, D. Label-free vapor selectivity in poly(p-phenylene oxide) photonic crystal sensors, *ACS Appl. Mater. Interfaces* **2016**, *8*, 31941–31950.
- (9) Lova, P.; Manfredi, G.; Boirino, L.; Comite, A.; Laus, M.; Patrini, M.; Marabelli, F.; Soci, C.; Comoretto, D. Polymer distributed bragg reflectors for vapor sensing, *ACS Photonics* **2015**, *2*, 537-543.
- (10) Perrin, L.; Nguyen, Q. T.; Sacco, D.; Lochou, P. Experimental Studies and Modelling of Sorption and Diffusion of Water and Alcohols in Cellulose Acetate, *Polym. Int.* **1997**, *42*, 9-16.
- (11) Bernardo, G. Diffusivity of alcohols in amorphous polystyrene, *J. Appl. Polym. Sci.* **2013**, *127*, 1803-1811.

References.png

---

# Imaging-based molecular barcoding with pixelated dielectric metasurfaces

---

Tuesday, 2nd October @ 14:47: Enhanced spectroscopy and sensing (AUDITORIUM) - Oral - Abstract ID: 290

---

***Dr. Andreas Tittl*<sup>1</sup>, *Mr. Aleksandrs Leitis*<sup>1</sup>, *Dr. Mingkai Liu*<sup>2</sup>, *Dr. Filiz Yesilkoy*<sup>1</sup>, *Prof. Duk-Yong Choi*<sup>2</sup>, *Prof. Dragomir Neshev*<sup>2</sup>, *Prof. Yuri Kivshar*<sup>2</sup>, *Prof. Hatice Altug*<sup>1</sup>**

*1. École polytechnique fédérale de Lausanne, 2. Australian National University*

Mid-infrared spectroscopy allows for the direct characterization of molecular structures with chemical specificity unique to this spectral range. Nanophotonics has extended this approach to nanometer-scale samples and low numbers of surface-bound molecules by exploiting the strong near-field enhancement of subwavelength resonators.

Such surface-enhanced infrared absorption spectroscopy techniques have traditionally relied on plasmonic platforms based on metallic antennas, which are limited by low quality factor (Q-factor) resonances imposed by resistive loss [1]. Nanostructured resonators based on high-index low-loss dielectric materials can overcome this limitation. However, so far, the prospects of combining high-Q dielectric resonators with molecular spectroscopy have not been realized.

Here, we introduce an imaging-based nanophotonic method for detecting mid-infrared molecular fingerprints, and implement it for the chemical identification and compositional analysis of surface-adsorbed analytes. In contrast to previous approaches where high-Q resonances in metasurfaces are generated via the interference of super-radiant and sub-radiant modes, our design exploits the collective behavior of Mie resonances to provide strong near-field enhancements and spectrally clean high-Q resonances, which enables the highly selective enhancement of molecular fingerprint information [2].

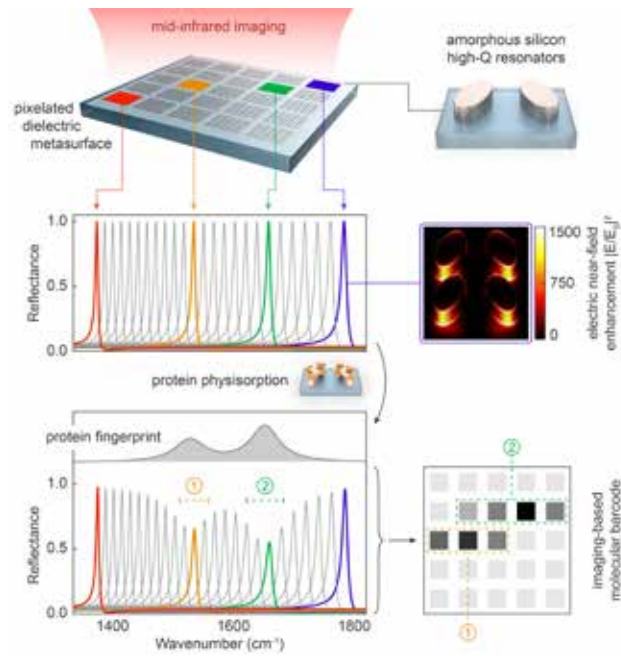
We experimentally realize a two dimensional array of high-Q metasurface pixels, where the resonance positions of individual metapixels are tuned to discrete frequencies. This configuration allows us to assign each resonance position to a specific pixel of the metasurface, enabling us to detect molecular absorption signatures at multiple spectral points simultaneously. By comparing the imaging-based readout of this spatially encoded vibrational information before and after the coating of target analyte molecules, we retrieve chemically specific molecular barcodes suitable for chemical identification and compositional analysis.

Specifically, we will present additional results and analysis on how our method can detect the characteristic signatures for biological, polymer, and pesticide molecules, covering application areas such as biosensing, materials science, and environmental monitoring.

Crucially, our method can be combined with broadband light sources and detectors to resolve molecular absorption fingerprints without the need for spectrometry, frequency scanning, or moving mechanical parts, paving the way towards sensitive and versatile miniaturized mid-infrared spectroscopy devices.

[1] Neubrech et al., *Chem. Rev.* 117, 5110–5145 (2017)

[2] Tittl et al., *Science* 360, 1105–1109 (2018)



Molecular barcoding 1.png

---

# Silver Nanoparticle Films with Highly Tunable Plasmon Properties: Tuning the Plasmon Resonance Band for X-Ray Detection

---

Tuesday, 2nd October @ 15:04: Enhanced spectroscopy and sensing (AUDITORIUM) - Oral - Abstract ID: 436

---

***Dr. Eder Guidelli*<sup>1</sup>, *Prof. David Clarke*<sup>2</sup>, *Prof. Oswaldo Baffa*<sup>1</sup>**

*1. Universidade de São Paulo, 2. Harvard University*

- Plasmon-enhanced luminescence is a powerful approach for enhancing many sensing technologies but appropriate tuning of the plasmon band with the excitation and/or emission band of the luminescent species remains a challenge[1–3]. We developed a simple and fast microwave-assisted method to grow silver nanoparticle films with tunable plasmon resonance band. The plasmonic properties can be easily tuned by controlling the microwaving time and the number of deposition cycles. Films can be grown with microwaving times as short as 20 s. Microwaving time of 30 s leads for films with a single well-defined plasmon resonance band (400 nm), whereas films produced with times longer than 40 s presented higher wavelength resonances modes, with at least two distinguishable plasmon resonance bands at 400 nm and 500 nm. The films were employed to enhance the sensitivity of x-ray detectors, which was assessed by the luminescence emitted from irradiated KCl crystals by Optically Stimulated Luminescence (OSL). By tuning the plasmon resonance band to overlap with the OSL stimulation (530 nm), luminescence enhancements of greater than 100-fold were obtained, demonstrating the importance of tuning the plasmon resonance band to maximize the OSL intensity and detector sensitivity. These findings reveal the versatility of the method developed here to produce silver nanoparticles films with tunable plasmonic properties, standing as promising platform for developing more sensitive, and miniaturized, radiation detectors as well as advanced sensing technologies involving plasmon enhanced luminescence and SERS.

## References

- [1] K. a Willets, R.P. Van Duyne, Localized surface plasmon resonance spectroscopy and sensing., *Annu. Rev. Phys. Chem.* 58 (2007) 267–97. doi:10.1146/annurev.physchem.58.032806.104607.
- [2] E.J. Guidelli, A.P. Ramos, O. Baffa, Optically Stimulated Luminescence Under Plasmon Resonance Conditions Enhances X-Ray Detection, *Plasmonics*. 9 (2014). doi:10.1007/s11468-014-9713-4.
- [3] E.J. Guidelli, A.P. Ramos, O. Baffa, Silver nanoparticle films for metal enhanced luminescence: Toward development of plasmonic radiation detectors for medical applications, *Sensors Actuators, B Chem.* 224 (2016). doi:10.1016/j.snb.2015.10.024.

---

# Flexible SERS Membrane: a Universal Platform for Quantitative SERS Analysis

---

Tuesday, 2nd October @ 15:21: Enhanced spectroscopy and sensing (AUDITORIUM) - Oral - Abstract ID: 291

---

*Dr. Qi Hao<sup>1</sup>, Dr. Libo Ma<sup>1</sup>, Prof. Oliver G. Schmidt<sup>1</sup>*

*1. IFW Dresden*

Surface enhanced Raman scattering (SERS) has been demonstrated as an efficient tool for highly sensitive molecular sensing. However, the lack of reproducibility in Raman signals limits this technique in quantitative analyses. Herein, we propose a straightforward approach to perform quantitative SERS analyses in homogeneous aqueous environment by using a flexible SERS membrane to eliminate the limitations in solid state measurement. The flexible SERS chip is composed of a transparent polymer membrane and well-patterned plasmonic nanodimers on its undersurface (figure 1). The chip spreads and floats on aqueous solution, working as a real-time interface sensor to monitor the absorption and reaction dynamics in solution. In our experiment, a quantitative SERS agreement with excellent relative standard deviation (< 10%) for Rhodamine 6G molecule is established with a detection limit down to  $10^{-13}$  M. This robust and feasible approach significantly simplifies sample pretreatment procedures confronting practical applications, providing a universal platform for in-situ and real time monitoring of chemical reactions and elucidating reaction mechanisms.

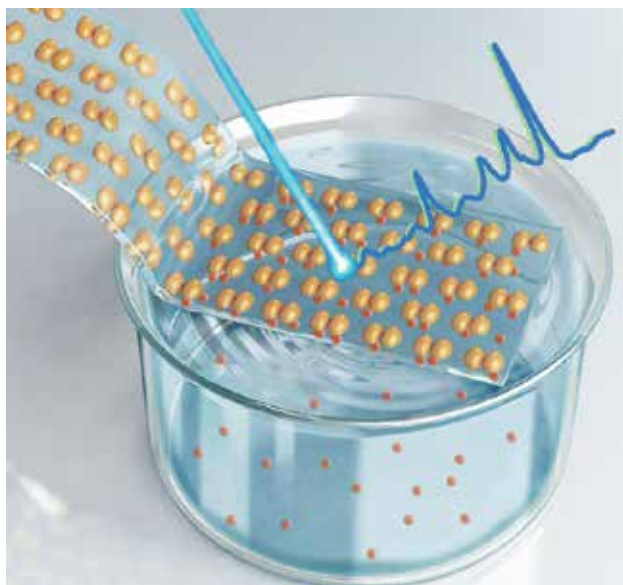


Figure 1.jpg

# LAB ON FIBER SERS OPTRODES BY NANOSPHERE LITHOGRAPHY

Tuesday, 2nd October @ 15:38: Enhanced spectroscopy and sensing (AUDITORIUM) - Oral - Abstract ID: 277

**Dr. Giuseppe Quero**<sup>1</sup>, **Dr. Gianluigi Zito**<sup>2</sup>, **Dr. Stefano Managò**<sup>2</sup>, **Dr. Francesco Galeotti**<sup>3</sup>,  
**Dr. Marco Pisco**<sup>1</sup>, **Dr. Anna Chiara De Luca**<sup>2</sup>, **Prof. Andrea Cusano**<sup>1</sup>

1. Optoelectronic Division – Eng. Dept., University of Sannio, 2. Institute of Protein Biochemistry, National Research Council, 3. Institute for Macromolecular Studies, National Research Council

We report on the engineering of repeatable surface enhanced Raman scattering (SERS) optrodes realized through nanosphere lithography on optical fiber (Figure 1). In particular, the Lab-on-Fiber SERS optrode consists of polystyrene nanospheres in close-packed arrays (CPA) configuration covered by a thin film of gold onto the optical fiber tip. The SERS surfaces were fabricated by using a nanosphere lithography approach that already demonstrated to be able to produce highly repeatable patterns on the fiber tip [1]. Starting from the promising pristine results, in order to engineer and optimize the SERS probes, we first evaluated and compared the SERS performances in terms of Enhancement Factor (EF) pertaining to different patterns with different nanospheres diameters and gold thicknesses. To this aim, the EF of SERS surfaces with a pitch of 500, 750 and 1000 nm, and gold films of 20, 30 and 40 nm have been retrieved, adopting the SERS signal of a monolayer of biphenyl-4-thiol (BPT) as a reliable benchmark (Figure 2). The analysis allowed us the identification of the most promising SERS platform: for the samples with nanospheres diameter of 500 nm and gold thickness of 30 nm, we measured values of EF of  $4 \times 10^5$ , which is comparable with state-of-the-art SERS EF achievable with highly performing colloidal gold nanoparticles [2]. The reproducibility of the SERS enhancement was thoroughly evaluated. Finally, in order to determine the most suitable optical fiber probe, in terms of excitation/collection efficiency and Raman background, we selected several commercially available optical fibers and tested them towards a BPT solution used as benchmark. A fiber probe with pure silica core of 200  $\mu\text{m}$  diameter and high numerical aperture (i.e. 0.5) was found to be the most promising fiber platform providing the best trade-off between high excitation/collection efficiency and low background (Figure 3). Ongoing activities are devoted to use our Lab-on-Fibre SERS optrodes for cancer cell identification with the ambitious aim to achieve a highly advanced in-vivo sensor.

1 M. Pisco, et al., Light: Science & Applications, 2017, 6, e16229.

2 G. Quero, et al., Sensors, 2018, 18, 8, 680.

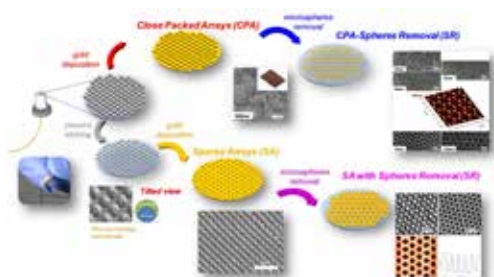


Figure 1. Schematic illustration of the fabrication steps used to realize different periodic structures on the optical fiber. CPA: Close packed array; SA: Sphere array; SR: Spheres removal. The insets show scanning electron microscope (SEM) images of the fiber facet for the corresponding fabricated structures.

Figure 1.jpg

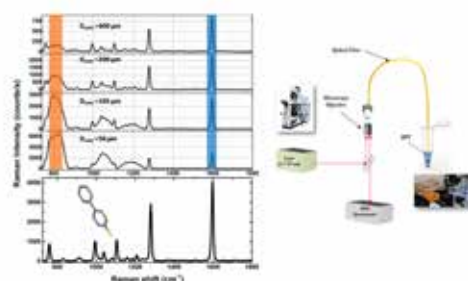


Figure 3. SERS spectra from BPT monolayer by illuminating OFT with different core diameter and schematic of the experimental setup for the optical fiber type selection.

Figure 3.jpg

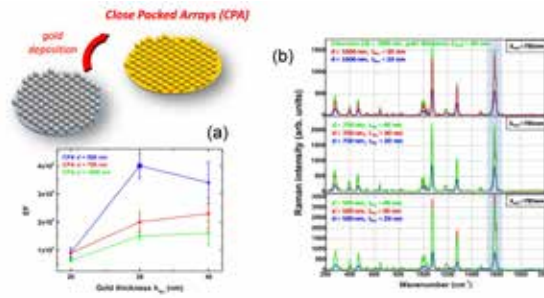


Figure 2: (a) Average BPT SERS (laser at 785 nm) spectra, on 49 acquisitions, for the considered substrates: CPA with different diameter ( $d=500, 750, 1000$  nm) and different gold films ( $t_{Au}=20, 30, 40$  nm). (b) Measured enhancement factor for the different analyzed geometry as a function of gold layer thickness.

Figure 2.jpg



---

## Hot carriers on organic semiconductors: relating mechanics and electronic properties.

---

Tuesday, 2nd October @ 15:55: Enhanced spectroscopy and sensing (AUDITORIUM) - Oral - Abstract ID: 410

---

***Dr. Bruno Torre*<sup>1</sup>, *Dr. Andrea Giugni*<sup>1</sup>, *Dr. Marco Allione*<sup>1</sup>, *Ms. Xinyu Zhang*<sup>1</sup>, *Prof. Enzo Di Fabrizio*<sup>2</sup>**

*1. King Abdullah University of Science and Technology (KAUST), 23955-6900, Thuwal KSA, 2. KAUST*

Hot Electron Nanoscopy and spectroscopy (HENs) is a recently developed technique relying on the unbiased emission of energetic electrons at a Schottky junction after plasmon decay, once excited by an impinging laser excitation. Recently we employed this technique with an AFM based architecture to exploit the nanometric spatial resolution and controlled interaction on several inorganic semiconductor and 2D materials, proofing an extremely high efficiency in hot carriers generation and high spatial resolution. Here we show the first application to p-doped organic semiconductor, broadening the range of applicability to a new class of materials where conductance is dominated by holes. At the same time this studies pave the way to the possibility to study hot carriers conduction under controlled strain and deformation, and the influence of morphology on conductance. For this reason we have coupled a Raman detection channel to the plasmon photonic decay channel at the tip to provide structural information aside of the conductive/ spectroscopic one.

# Chiral coupling of atoms near plasmonic and photonic interfaces

Tuesday, 2nd October @ 16:50: Quantum nano-optics (ROOM 1) - Oral - Abstract ID: 409

*Dr. Mihail Petrov*<sup>1</sup>, *Mr. Danil Kornovan*<sup>1</sup>, *Dr. Ivan Iorsh*<sup>1</sup>

<sup>1</sup>. ITMO University

Nanophotonic systems offer unique opportunities for controlling and stimulating light-matter coupling. One of the important topics which draws the interest of the researchers is artificial chirality in quantum sources interaction with surface photonic or plasmonic modes. The presence of the transverse optical spin component of guided modes opens the possibility to control their direction of propagation by means of the so called spin-locking effect. The atom transition with nonzero spin moment (chiral atoms) can excite surface modes in preferable direction, or, on the contrary, the scattering of surface mode is very sensitive to chirality of atomic transitions.

In this work we present a brief overview of the current progress in the field of quantum chiral optics. We will discuss our theoretical results on coupling of chiral atoms with surface guiding modes. In particular, we consider the scattering of a nanofiber guided mode (Fig. 1) on ensemble of atoms with chiral transitions, and show how the spin of nanofiber modes governs the scattering spectrum [1]. Moreover, we propose a model of atomic ensemble of chiral atoms with perfect unidirectional coupling, and suggest a rigorous solution in such system [2], which demonstrates the main features of unidirectional coupling (Fig. 2). Such a system can be implemented with a simple metal nanowire, where the spin-locking effect is extremely strong. Finally, we will discuss the effect of quantum anisotropy, which allows coupling of orthogonal quantum states close to a nanophotonics systems. We show by using anisotropic metasurfaces (Fig 3 a) that one can couple two atomic levels with chiral transition, which may result in non-inverse Rabi oscillation between two quantum states in a single atom (Fig 3 b).

[1] D. F. Kornovan, A. S. Sheremet, and M. I. Petrov, "Collective polaritonic modes in an array of two-level quantum emitters coupled to optical nanofiber," *Phys. Rev. B*, vol. 94, p. 245416, 2016.

[2] D. Kornovan, M. Petrov, and I. Iorsh, "Transport and collective radiance in a basic quantum chiral optical model," *Phys. Rev. B*, vol. 96, p. 115162, 2017.

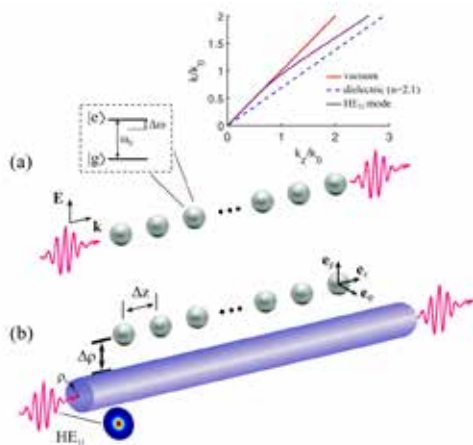


Fig1.png

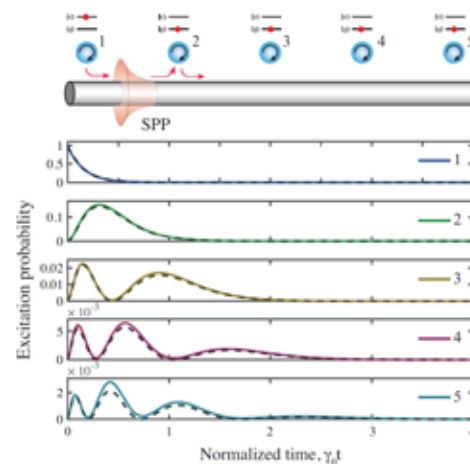


Fig2.png

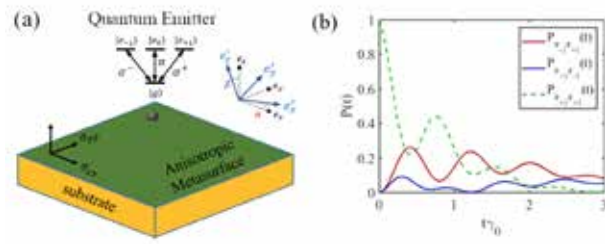


Fig3.png

# Nonlinear atom-plasmon interactions enabled by nanostructured graphene

Tuesday, 2nd October @ 17:07: Quantum nano-optics (ROOM 1) - Oral - Abstract ID: 449

**Dr. Joel Cox<sup>1</sup>, Prof. Javier García De Abajo<sup>1</sup>**

*1. ICFO - The Institute of Photonic Sciences*

The extreme spatial light confinement associated with electrically-tunable plasmons in doped graphene is anticipated to yield strong light-matter coupling with resonant quantum emitters. However, plasmon resonance frequencies in graphene typically lie in the infrared and terahertz regimes, away from optically-active electronic transitions in many robust quantum light sources and biologically-interesting molecules. Here we propose to utilize the near-field generated by the plasmon-enhanced nonlinear optical response of nanostructured graphene to resonantly couple the 2D layer with proximal quantum emitters operating in the near-infrared. As a proof-of-concept, we predict that the nonlinear plasmonic third-harmonic near-field produced by a moderately-doped graphene nanodisk can strongly excite a two-level emitter and drive electromagnetically-induced transparency or coherent population control in three-level atoms, and that these processes can be actively controlled when the third-harmonic of a graphene plasmon resonance is tuned to the relevant atomic transition. In the present scheme, emitter and plasmon resonances are non-degenerated, circumventing strong plasmonic enhancement of spontaneous decay in the emitter. We envision potential applications for the proposed nonlinear plasmonic coupling scheme in nonlinear sensing and in actively-controllable elements for quantum information networks.

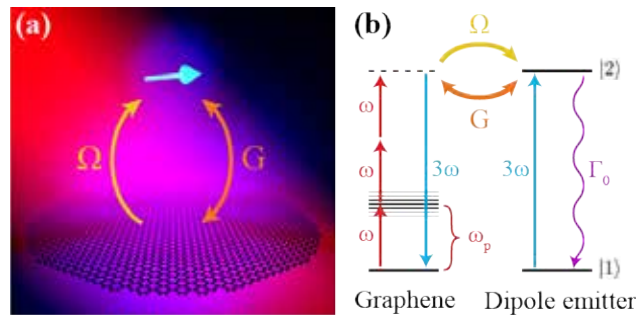


Fig1 og.png

---

# Bright and Stable Single-Photon Emission from Single Molecules in Organic Nanocrystals

---

Tuesday, 2nd October @ 17:24: Quantum nano-optics (ROOM 1) - Oral - Abstract ID: 77

---

Mrs. Sofia Pazzagli<sup>1</sup>

1. LENS

Introduction: Quantum technologies could largely benefit from the development of single quantum emitters in sub-micrometric size crystals providing single photons on demand. They can be deterministically integrated in complex nanostructures, such as photonic crystal devices, nano-guides and optical antennas.

Methods, Results, and Discussion

In this work we report on the fabrication and the morphological analysis and an extensive optical characterization of the single-photon emission unprecedented performances of single-photon emission from organic nanocrystals (average size of hundreds nanometers) made of anthracene (Ac) and doped with dibenzoterrylene (DBT) molecules.

The growth procedure is based on reprecipitation, an easy and inexpensive method that we here adapted for a precise tuning of DBT concentration. Investigations on single molecules' photophysics demonstrate a single-photon emission with an uncorrected purity,  $g^2(0)$ , as low as 0.05 and a well-defined dipole orientation parallel to the crystal plane and the substrate. Single-photon emission around 785 nm from individual molecules is bright (with 1.5 MHz detected photon-rate at saturation) and photostable at room temperature. At cryogenic temperatures, 00-zero phonon lines show linewidths close to the lifetime-limited value (about 50 MHz) which are spectrally stable over time scale of hours. Such optical properties in a nanocrystalline environment make the proposed organic nanocrystals a unique single-photon source for integrated photonic quantum technologies. Preliminary results on the manipulation and integration of the nanocrystals in different polymeric materials are discussed as possible writable system for applications in integrated quantum optics and nanophotonics.

---

# Fine structure splitting energy correction for single quantum dot via quadrupole potential

---

Tuesday, 2nd October @ 17:41: Quantum nano-optics (ROOM 1) - Oral - Abstract ID: 146

---

***Mr. Mohd Zeeshan***<sup>1</sup>, ***Mr. Nachiket Sherlekar***<sup>1</sup>, ***Mr. Arash Ahmadi***<sup>1</sup>, ***Dr. Sandra Gibson***<sup>1</sup>, ***Prof. Michael Reimer***<sup>1</sup>

*1. Institute for Quantum Computing, University of Waterloo*

Entangled photon sources are crucial for quantum optics, quantum sensing and quantum communication. Semiconductor quantum dots in nanowires have recently emerged as leading candidates to generate entangled photons due to their high brightness and directional Gaussian emission profile for near-unity fiber coupling. However, the structural asymmetry of the quantum dot leads to a fine-structure splitting (FSS) and severely limits the use of quantum dots as a source of entangled photon pairs with high fidelity. Here, we propose a novel approach for generating a pair of entangled photons from the quantum dot with high fidelity by correcting the spatial asymmetry of the excitonic wave function via application of a quadrupole electrostatic potential. The proposed device architecture and the far field emission profile is presented in Figure 1: Proposed device. We have performed numerical simulations for the proposed device by Nextnano3 in 2D, which solves the Schrödinger-poisson equation self-consistently. In Figure 2, FSS and electron-hole (e-h) overlap is plotted as a function of quadrupole potential,  $V$  applied on the proposed device. Our results demonstrate that the spatial asymmetry of the excitonic wave function can be tuned without compromising the spatial overlap between electron and holes. Importantly, the FSS can be tuned to zero, meaning that the excitonic wavefunction is symmetric, even when the electrical gates are misaligned with respect to the quantum dot asymmetry. Finally, we will present the nanofabrication of the first generation of devices and initial results (Figure 3: fabricated device). This work paves the way toward a deterministic source of entangled photons with high fidelity and unprecedented collection efficiency.

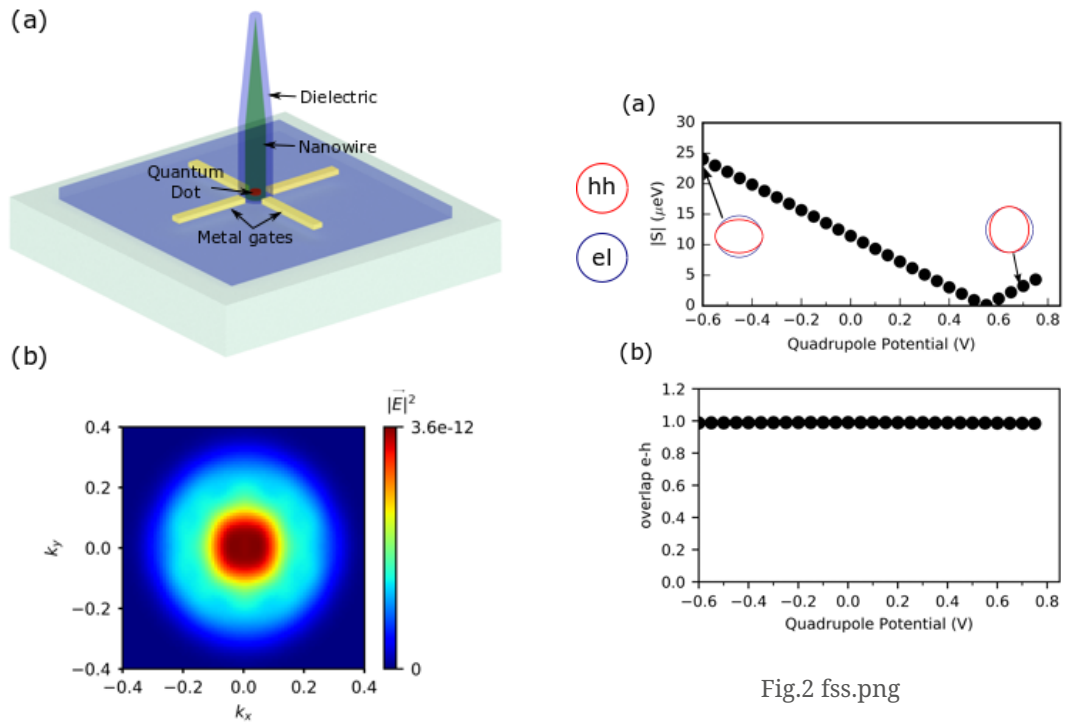


Fig.1 proposed device.png

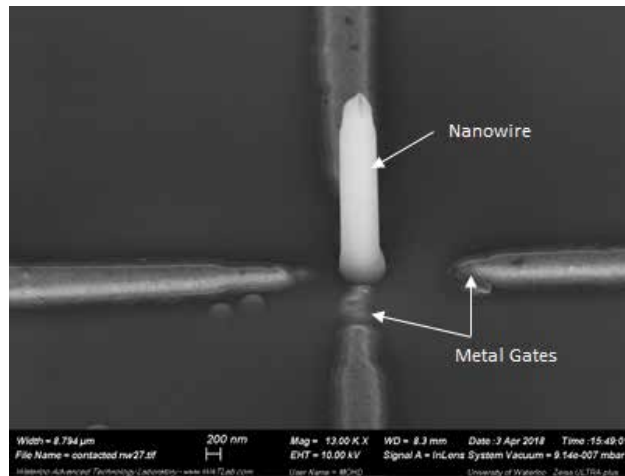


Fig.3 fabricated device.png

# Quantum Nonlinear Optics in Nanoscale Waveguides

Tuesday, 2nd October @ 17:58: Quantum nano-optics (ROOM 1) - Oral - Abstract ID: 130

***Dr. Hashem Zoubi***<sup>1</sup>

*1. Holon Institute of Technology*

We develop a systematic method for deriving quantum optical multi-mode Hamiltonian for the interaction of photons and phonons in nanophotonic dielectric materials by applying perturbation theory to the electromagnetic Hamiltonian [1]. The Hamiltonian covers radiation pressure and electrostrictive interactions on equal footing. As a paradigmatic example, we apply our method to a cylindrical nanoscale waveguide, and derive a Hamiltonian description of Brillouin quantum optomechanics. We show analytically that in nanoscale waveguides radiation pressure dominates over electrostriction, in agreement with recent experiments [2, 3]. We explore the possibility of achieving a significant nonlinear phase shift among photons propagating in nanoscale waveguides exploiting interactions among photons that are mediated by vibrational modes and induced through Stimulated Brillouin Scattering (SBS) [4]. We introduce a configuration that allows slowing down the photons by several orders of magnitude via SBS involving sound waves and two pump fields. We extract the conditions for maintaining vanishing amplitude gain or loss for slowly propagating photons while keeping the influence of thermal phonons to the minimum. The nonlinear phase among two counter-propagating photons can be used to realize a deterministic phase gate.

[1] H. Zoubi, K. Hammerer, Phys. Rev. A 94, 053827 (2016).

[2] R. Van Laer, et al., Nature Phot. 9, 199 (2015).

[3] E. K. Kittlaus, et al., Nature Phot. 10, 463 (2016).

[4] H. Zoubi, K. Hammerer, Phys. Rev. Lett. 119, 123602 (2017).

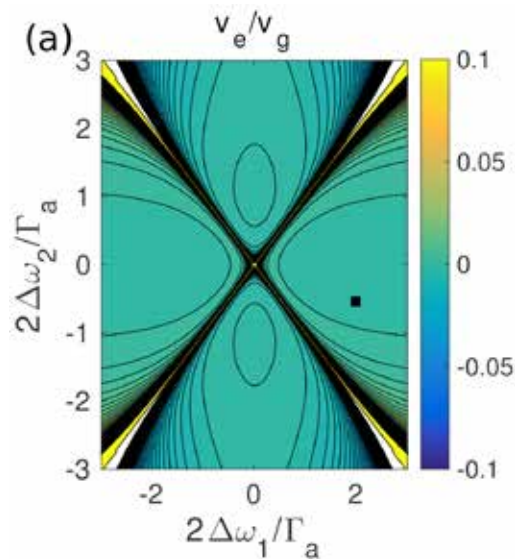


Fig3a.jpg

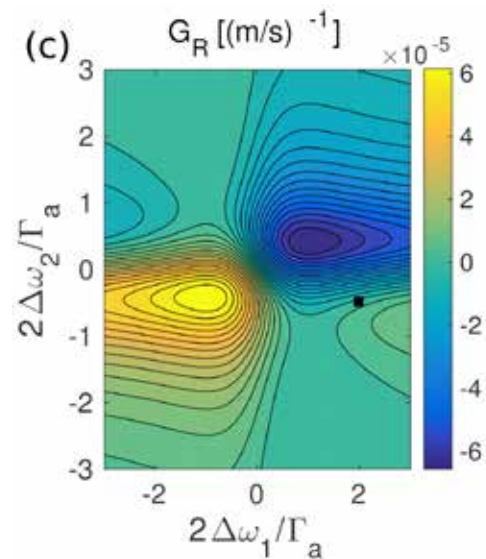


Fig3c.jpg



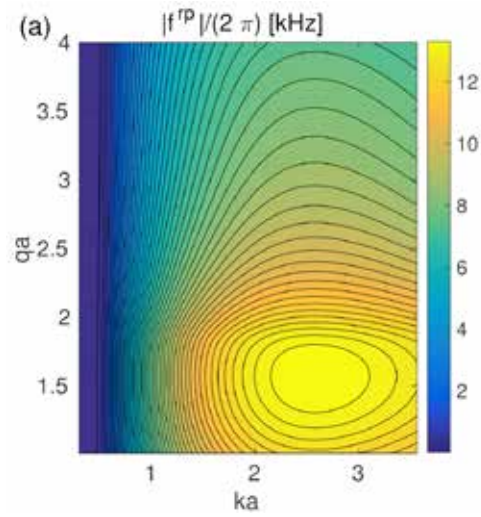


Fig6a.jpg

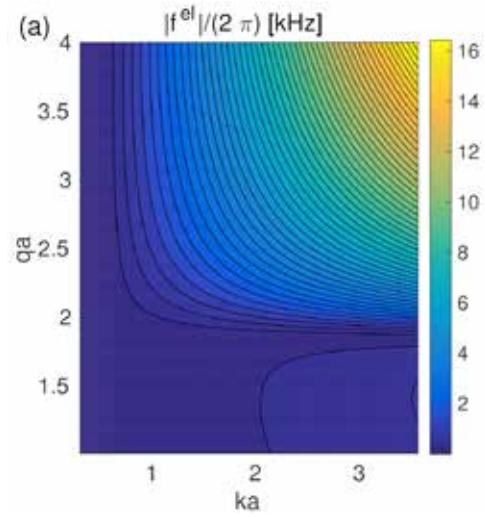


Fig7a.jpg

---

# Weak Measurement of the Dipolar Emitter Polarization State via its Far-Field Polarization Singularities

---

Tuesday, 2nd October @ 18:15: Quantum nano-optics (ROOM 1) - Oral - Abstract ID: 207

---

***Dr. Sergey Nechayev*<sup>1</sup>, *Dr. Martin Neugebauer*<sup>1</sup>, *Mr. Martin Vorndran*<sup>1</sup>, *Prof. Gerd Leuchs*<sup>1</sup>, *Dr. Peter Banzer*<sup>1</sup>**

*1. Max Planck Institute for the Science of Light*

We investigate polarization singularities [Proc. R. Soc. A **389**, 279 (1983)] in the far-field of an elliptically polarized dipole, exhibiting in general four points of purely circular polarization (C points). We reveal that the helicities of the C points and their angle of observation in the far-field bare full information on the polarization state of the dipolar emitter [arXiv:180403890]. For a highly eccentric (almost linear) dipole moment, four singularities occur along directions almost aligned with the major axis of the dipole polarization ellipse. The low overall power emitted by the dipole into the far-field in this direction prevents a direct experimental observation of the C points.

We experimentally realize a weak-measurement technique [Phys. Rev. Lett. **60**, 1351 (1988)] in a vectorial vortex polarization basis (radial and azimuthal) to create a strongly directive far-field intensity pattern [Nano Lett. **14**, 2546 (2014)]. This pattern is obtained by projecting the far-field emitted light on a complex spatially varying polarization state. The extrema of the intensity distribution of the projected far-field pattern reveal the properties of the polarization singularities and, eventually, the polarization state of the dipolar emitter. The developed experimental technique also allows for precise sensing of orientation of a linear dipole moment [arXiv:180403890].

The sensitivity of our experimental scheme to tiny changes of the polarization state of a dipolar emitter suggests far-reaching applications for localization and position sensing. An experimentally induced dipole moment in a polarizable dipole-like scatterer is proportional to the local strength and orientation of the electric field. Therefore, the variation of the intensity and polarization profile in the focal volume of a tightly focused beam relate the induced dipole moment to the position of the scatterer within the focal volume. We experimentally confirm our theoretical findings utilizing a tightly focused radially polarized beam, which features a spatially varying axially symmetric distribution of transversely spinning electric fields within its focal volume. Weak measurement of the position dependent dipole moment, excited by a focused radially polarized beam in a spherical gold nanoparticle, allows us to localize the nanoparticle with deep sub-nanometer precision [M. Neugebauer, S. Nechayev et al., *in preparation* (2018)].

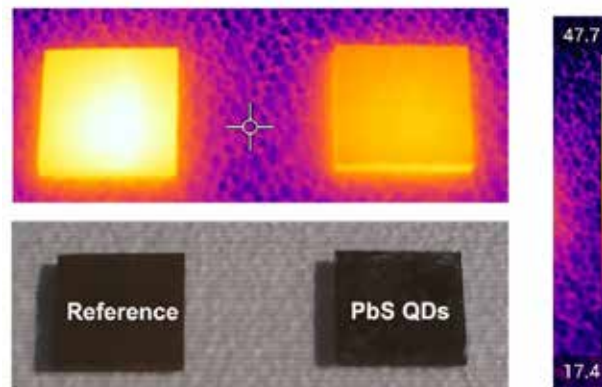
# Urban Heat Island Mitigation with PbS quantum dots

Tuesday, 2nd October @ 18:32: Quantum nano-optics (ROOM 1) - Oral - Abstract ID: 407

***Ms. Samira Garshabi<sup>1</sup>, Prof. Mat Santamouris<sup>1</sup>, Prof. Shujuan Huang<sup>1</sup>***

*1. University of New South Wales*

Urban overheating is a serious problem with high impact on the environmental quality, energy consumption and health. Since high absorbing materials such as asphalt are one of the main contributors to urban overheating, one of the effective methods to overcome the urban overheating phenomena is the use of materials with less heat generating effect. Urban surfaces with lower surface temperature can be obtained by utilizing the photoluminescence/fluorescence phenomena. Based on the literature, application of conventional fluorescent materials shows 6.5°C lower surface temperature than conventional materials. This paper explores the possibility of utilizing quantum dots as nano-scale fluorescent materials to tackle urban overheating. One of the main advantages of quantum dots over conventional fluorescent materials is the possibility to manipulate their optical properties to achieve the highest mitigation potential. In this paper, PbS quantum dots with emission in the infrared range have been synthesized. Afterwards, QDs coated sample was exposed to sunlight from 8 a.m to 4 p.m and its mitigation potential was compared against reference sample. Based on results, QDs coated sample shows up to 10°C lower surface temperature than the reference sample.



1.jpg

---

# Revealing local material properties with high resolution optical microscopy

---

Tuesday, 2nd October @ 16:50: Enhanced spectroscopy and sensing (ROOM 2) - Oral - Abstract ID: 372

---

**Dr. Marius Van Den Berg<sup>1</sup>, Mr. Tobias Koeninger<sup>1</sup>, Mr. Yu-ting Chen<sup>1</sup>, Dr. Anke Horneber<sup>1</sup>, Prof. Alfred Meixner<sup>1</sup>, Dr. Dai Zhang<sup>2</sup>**

*1. University of Tübingen, 2. Eberhard Karls University of Tübingen*

The high resolution optical technique combining scanning probe microscopy and optical microscopy has shown its distinct capability in characterizing materials with high sensitivity and topography information [1]. We actively contributes to the development of high resolution optical technique in a variety of aspects [2-4].

In this talk, two topics of our recent research will be presented:

1) **Phase-segregation induced bandgap instability in mixed-halide perovskite** [4]. We demonstrate that photo-induced phase-segregation preferentially occurs at grain boundaries rather than within the grain centers by using shear-force scanning probe microscopy in combination with confocal optical spectroscopy.

2) **Morphology and optical properties of Si and Au nanostructures processed by helium-ion microscopy**. Different helium-ion doses are used to produce Si and Au nanostructures. The mechanisms of nanostructure-formation are discussed. The potential morphology and optical property changes due to the interaction with helium ions are investigated.

[1] A. Kern, D. Zhang, M. Brecht, et al., Chem. Soc. Rev., 42 (2014) 965.

[2] a) X. Wang, A. J. Meixner, D. Zhang\*, et. al., Adv. Func. Mater., 20 (2010) 492; b) D. Zhang\*, U. Heinemeyer, C. Stanciu, et al., Phys. Rev. Lett., 104 (2010) 056601; c) X. Wang, A. J. Meixner, D. Zhang\* et al., Small, 7 (2011) 2793. d) P. Anger, A. Feltz, T. Berghaus, et al., J. Microscopy, 209 (2003) 162. e) A. Horneber, K. Braun, A. J. Meixner, D. Zhang\* et al., Phys. Chem. Chem. Phys., 17 (2015) 21288 ; f) X. Wang, K. Braun, D. Zhang, A. J. Meixner\*, et al., ACS Nano, 9 (2015) 8176.

[3] a) J. Y. Wang, J. Butet, A.-L. Baudrion, A. Horrer, G. Lévêque, O. J. F. Martin, A. J. Meixner, M. Fleischer, P.-M. Adam,\* A. Horneber, D. Zhang,\* J. Phys. Chem. C, 120 (2016), 17699; b) J. Y. Wang, E. Gürdal, A. Horneber, S. Dickreuter, S. Kostcheev, A. J. Meixner, M. Fleischer, P. M. Adam,\* D. Zhang,\* Nanoscale, 10 (2018) 8240.

[4] X. F. Tang, M. van den Berg, E. N. Gu, A. Horneber, G. J. Matt, A. Osvet, A. J. Meixner, D. Zhang,\* C. J. Brabec\*, Nano Lett., 8 (2018) 2172.

---

# Enhanced multimodal biosensing using plasmonic paper-based nanoplatfoms

---

Tuesday, 2nd October @ 17:07: Enhanced spectroscopy and sensing (ROOM 2) - Oral - Abstract ID: 364

---

**Ms. Andreea Campu<sup>1</sup>, Mr. Filip Orzan<sup>2</sup>, Dr. Frederic Lerouge<sup>3</sup>, Prof. Stephane Parola<sup>3</sup>, Prof. Simion Astilean<sup>1</sup>, Dr. Monica Focsan<sup>1</sup>**

*1. Babes-Bolyai University, Nanobiophotonics and Laser Microspectroscopy Center, Interdisciplinary Research Institute on Bio-Nano-Sciences and Biomolecular Physics Department, 2. Babes-Bolyai University, 3. Ecole Normale Supérieure de Lyon, CNRS, Université Lyon 1, Laboratoire de Chimie*

The study of biosensing devices proving portability, high efficiency and sensitivity, ease of use and low-cost increases in research interest continuously. Such promising point-of-care tools are plasmonic paper-based nanoplatfoms due to their advantages such as facile fabrication, high specific surface area, flexibility, or excellent wicking ability due to capillary forces. The robustness of this nanosensor design enables the use of multiple techniques proving a decreased analysis time, improved molecule differentiation and ultra-low concentration detection.

In this work, we present a new plasmonic paper-based nanoplatfom with enhanced multimodal Localized Surface Plasmon Resonance (LSPR) – Surface Enhanced Raman Spectroscopy (SERS) – Metal Enhanced Fluorescence (MEF) biodetection capabilities in terms of sensitivity, efficiency and reproducibility. Therefore, we took advantage of the unique optical properties of gold nanobipyramids (AuBPs) by synthesizing colloidal solutions with different aspect ratios. After the deposition onto cellulose fibers, confirmed by HRTEM, SEM and dark-field microscopic images, the bulk sensitivity of the platform was determined by changing the refractive index of the medium with water-glycerol mixtures of various concentrations. The previously chemically formed p-aminothiophenol@biotin linker is attached to the immobilized AuBPs ensuring thus: (i) the active binding spot for the target streptavidin molecule; (ii) the indirect SERS detection through the well-known p-ATP Raman reporter and (iii) the optimal distance between the gold surface and the proximal streptavidin-linked Alexa680 molecule for MEF to occur as a result of the target molecule capture. The multimodal streptavidin detection capabilities of the plasmonic paper-based nanoplatfoms have been successfully demonstrated using three complementary analysis techniques. Subsequent to the biotin-streptavidin binding event, the change of the refractive index induces a LSPR red-shift, the presence of the p-ATP molecule fingerprint in the SERS spectrum provides indirectly information about the antigen-antibody interaction, while the evaluation of the emission behavior of Alexa680 proves the recognition interaction via MEF detection.

**Acknowledgments** Funding by the CNCS-UEFISCDI Romania, under the project number PN-III-P1-1.1-TE-2016-2095, and by the Babes-Bolyai University research funds – doctoral grants are gratefully acknowledged.

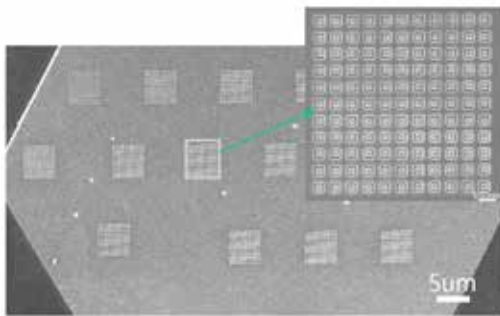
# The SERS performance optimization with coupled modes and low-loss metals

Tuesday, 2nd October @ 17:24: Enhanced spectroscopy and sensing (ROOM 2) - Oral - Abstract ID: 38

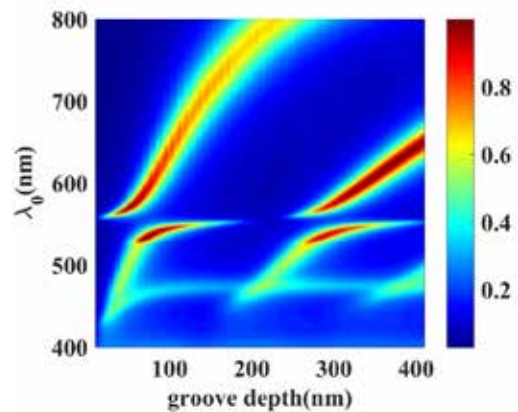
*Mr. Kang Qin<sup>1</sup>, Prof. Yongyuan Zhu<sup>1</sup>, Prof. Yanqing Lu<sup>1</sup>, Prof. Xuejin Zhang<sup>1</sup>*

*1. Nanjing University*

The signal enhancement and repeatability affect the practical applications for surface-enhanced Raman scattering (SERS). The physical mechanism of SERS is dominated by localized surface plasmon resonances (LSPRs). However, the LSPRs belong to localized modes and render rather large losses, compared to propagating modes. Here we attempt to obtain high reproducible SERS substrates with enormous enhancement by means of physical mechanism of propagating modes and their coupling modes, high-quality metallic materials from bottom-up approach, and advanced technologies. Moreover, we pay more attention to the structural parameter optimization of the metasurface structure, which underlies the SERS performance. We perform theoretical calculations including finite-difference time-domain simulation and rigorous coupled-wave analysis. Experimental investigations are fulfilled by confocal microscopy measurements,  $k$ -space spectroscopy, etc.



Single crystalline ag.jpg



Coupling effect.jpg

# Surface-enhanced Raman spectra and higher order scattering in Bi<sub>2</sub>O<sub>3</sub>-Ag nanoplasmonic eutectic composite

Tuesday, 2nd October @ 17:41: Enhanced spectroscopy and sensing (ROOM 2) - Oral - Abstract ID: 428

**Dr. Piotr Piotrowski**<sup>1</sup>, **Mr. Kamil Szlachetko**<sup>1</sup>, **Mr. Paweł Osewski**<sup>2</sup>, **Dr. Katarzyna Sadecka**<sup>2</sup>, **Dr. Dobrosława Kasprowicz**<sup>3</sup>, **Prof. Dorota A. Pawlak**<sup>4</sup>

1. Faculty of Chemistry, University of Warsaw, Pasteura 1, 02-093 Warsaw, 2. Institute of Electronic Materials Technology, ul. Wólczyńska 133, 01-919, Warsaw, 3. Faculty of Technical Physics, Poznan University of Technology, Piotrowo 3, 61-138, Poznań, 4. Centre of New Technologies, University of Warsaw, Banacha 2C, 02-097, Warsaw, Poland

Generation of high electromagnetic field near metallic nanostructures upon excitation of localized surface plasmon resonance (LSPR) leads to an enhanced signal, i.e. Raman scattering, of adjacent nanosystems. Surface-enhanced Raman scattering (SERS) is a powerful tool in system characterization with sensitivity reaching down to a single molecule. As there are examples of application of Raman scattering in optical devices, e.g. amplifiers/lasers, SERS is a promising technique to be utilized in that field due to its tunability. However, most of the SERS-based studies involve either nanoparticle-modified solid surfaces or molecules attached to metallic nanostructures, which are challenging to incorporate in optical instruments. Therefore, there is an interest in development of novel volumetric SERS-active materials.

In this work, the first example of the SERS effect in a bulk plasmonic material is presented. Bi<sub>2</sub>O<sub>3</sub>-Ag nanocomposite is obtained by micro-pulling-down from a eutectic mixture. In the structure, Bi<sub>2</sub>O<sub>3</sub> grains with metallic microprecipitates in-between are observed. Raman microscopy confirms that two different phases of Bi<sub>2</sub>O<sub>3</sub> occur in the composite: the grains consist of  $\alpha$ -Bi<sub>2</sub>O<sub>3</sub>, while  $\gamma$ -Bi<sub>2</sub>O<sub>3</sub> is incorporated in the precipitates.

Spectra of  $\gamma$ -Bi<sub>2</sub>O<sub>3</sub> from the nanocomposite exhibit different features than for the bulk  $\gamma$ -Bi<sub>2</sub>O<sub>3</sub>. Not only there is a huge intensity increase of the bands, but also their positions shift (**Figure 1**). The most prominent change is visible for the band of the symmetric stretching vibrations of BiO<sub>4</sub> tetrahedra (825 cm<sup>-1</sup>). Additionally, overtones of the bands appear. Intensity of the 825 cm<sup>-1</sup> band displays resonant dependence on the excitation wavelength (not seen in bulk), which overlaps with the LSPR peak originating from silver nanoparticles (Ag-NPs; **Figure 2**). Control of the SERS effect efficiency in the composite is achieved through preparation conditions.

**Acknowledgements:** This project was supported financially by the TEAM programme of the Foundation for Polish Science (No. TEAM/2016-3/29), co-financed by the European Union under the European Regional Development Fund.

**Figure 1.** a: Raman spectrum, bulk  $\gamma$ -Bi<sub>2</sub>O<sub>3</sub>, b: SERS spectrum,  $\gamma$ -Bi<sub>2</sub>O<sub>3</sub> in Bi<sub>2</sub>O<sub>3</sub>-Ag. Differences are due to plasmonic AgNPs in the nanocomposite ( $\lambda_{exc}=532$  nm).

**Figure 2.** Extinction spectrum of Bi<sub>2</sub>O<sub>3</sub>-Ag (blue) and intensities of the band at 825 cm<sup>-1</sup> (red) exhibiting resonant behaviour.

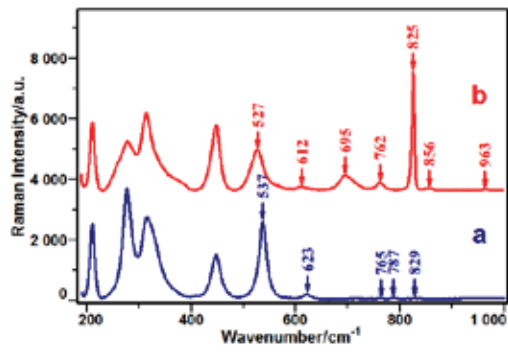


Figure 1.png

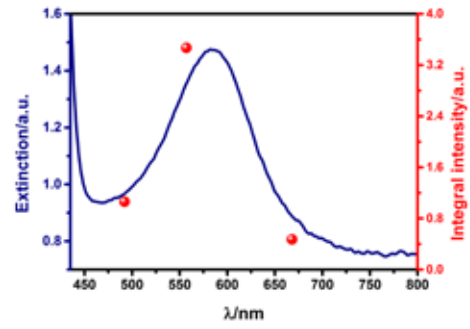


Figure 2.png



# Probing out of-equilibrium optical excitations with fast electrons

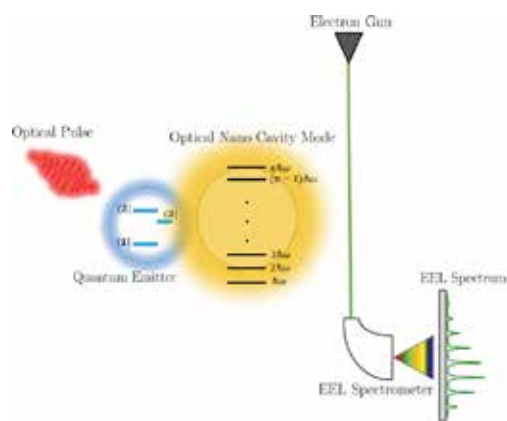
Tuesday, 2nd October @ 17:58: Enhanced spectroscopy and sensing (ROOM 2) - Oral - Abstract ID: 452

**Mr. Valerio Di Giulio**<sup>1</sup>, **Dr. Vahagn Mkhitarian**<sup>1</sup>, **Prof. Javier García de Abajo**<sup>2</sup>

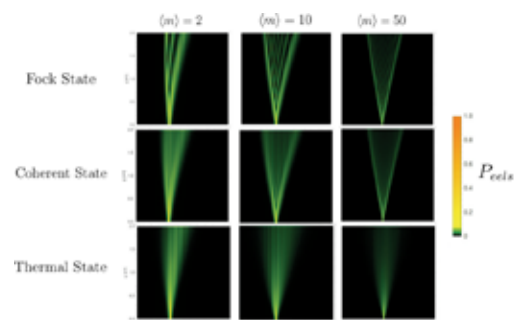
1. ICFO, Institut de Ciències Fotòniques, The Barcelona Institute of Science and Technology, 2. ICFO - The Institute of Photonic Sciences

Probing optical excitations with nanometer resolution is important for understanding their dynamics and interactions down to the atomic scale. Currently, electron energy-loss spectroscopy (EELS) performed in state-of-the-art electron microscopes offers the unparalleled ability of rendering spatially-resolved spectra with combined meV and sub-nm resolution. Additionally, for typical energetic electron beams in the few-to-many keV kinetic energy range, the probability of interaction between a beam electron and an optical excitation is very small, thus preventing modification of the optical response of the sample, unlike other popular techniques based on the used of sharp tips (near-field scanning optical microscopy). A new frontier has recently emerged in this context with the availability of femtosecond electron pulses, which can be synchronized with femtosecond light pulses illuminating the sample. This technique, known as ultrafast electron microscopy, offers the possibility of studying the interaction of beam electrons with highly populated optical modes, which results in multiple energy losses and gains by the electrons, visualized through the recorded electron spectra.

In this theoretical work, we study fundamental aspects of the interaction of fast electrons with localized optical modes. Specifically, we unveil a universal scaling in the interaction strength, depending on the electron energy, the spatial extension of the optical mode, and the optical frequency. We support these findings with extensive numerical simulations for a wide range of morphologies and energies. As an example of potential application, we investigate the differences observed in the electron spectra depending on the statistics of the optical mode (bosons vs fermions) and its population (coherent bosonic states, Fock states, and thermal populations). Based on these results, we propose a new range of experiments intended to probe the quantum characteristics of the sample excitations and their populations.



Fock eels setup.png



Quantum different populations eels.png

---

## Upgraded nanoparticle-based SERS substrates: superhydrophobicity and oxidative treatment

---

Tuesday, 2nd October @ 18:15: Enhanced spectroscopy and sensing (ROOM 2) - Oral - Abstract ID: 483

---

*Dr. Andrei Novikov*<sup>1</sup>, *Mr. Maksim Gorbachevskii*<sup>1</sup>, *Dr. Dmitry Kopitsyn*<sup>1</sup>, *Dr. Mikhail Kotelev*<sup>1</sup>, *Ms. Alexandra Kuchierskaya*<sup>1</sup>, *Dr. Evgenii Ivanov*<sup>1</sup>, *Prof. Vladimir Vinokurov*<sup>1</sup>

*1. Gubkin University*

### *Introduction*

Gold nanoparticles can be easily assembled to potent substrates for surface-enhanced Raman spectroscopy (SERS). We studied additional amplification of SERS signal by the oxidative treatment [1], and by providing the superhydrophobic properties of the substrates.

### *Methods*

We have synthesized nearly spherical citrate-capped gold nanoparticles of different size from 20 to 120 nm by known method with modifications [2]. The maximum enhancement (above  $10^6$ ) in SERS experiments with 785-nm excitation (BWTEK BWS415) was provided by structures fabricated from 50-nm nanoparticles. Superhydrophobic substrates were produced by drop-casting of C18-silanized halloysite nanotubes dispersion.

### *Results*

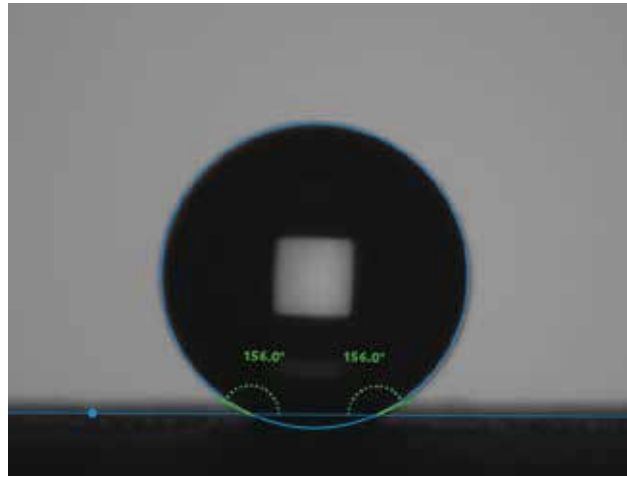
These nanoparticles demonstrated catalytic activity in oxidation of dyes with hydrogen peroxide, following the pseudo-first-order kinetics. In SERS-controlled catalytic experiments we observed additional enhancement, and the maximal one was observed with 3%(v/v) hydrogen peroxide. Exploiting this phenomenon, we detected model analytes at concentration of  $5 \times 10^{-9}$  M, while it was impossible without the hydrogen peroxide addition. Further improvement in the SERS substrates sensitivity was achieved by aggregation of gold nanoparticles on the superhydrophobic surface.

### *Discussion*

The nanoparticle-based SERS substrates can be upgraded by making the hot spots available for adsorption of analyte, and by concentrating the analyte on the superhydrophobic surface. The substrates upgraded this way have the sensitivity more than an order higher in comparison with simple drop-casted substrates.

**Acknowledgements:** This work was supported by the Ministry of Education and Science of the Russian Federation (Grant No 14.Z50.31.0035).

1. M.V. Gorbachevskiy, D.S. Kopitsyn, M.S. Kotelev, E.V. Ivanov, V.A. Vinokurov, A.A. Novikov. *RSC Advances*, 2018, 8, 19051-19057.
2. N.G. Bastus, J. Comenge, V. Puntes. *Langmuir*, 2011, 27, 11098.



2016-06-22 ca sers substrate.jpg

---

# Two-Color Fluorescent Cross-Correlation Spectroscopy as a valuable tool to evaluate the loading efficiency of DNA liposome complexes to improve cell reprogramming

---

Tuesday, 2nd October @ 18:32: Enhanced spectroscopy and sensing (ROOM 2) - Oral - Abstract ID: 250

---

*Dr. Aline Marie Fernandes*<sup>1</sup>, *Mr. Matej Siketanc*<sup>1</sup>, *Dr. Ana Isabel Gómez Varela*<sup>1</sup>, *Dr. Juliane Assis*<sup>2</sup>, *Dr. Adelaide Miranda*<sup>1</sup>, *Prof. Rafael Valverde*<sup>2</sup>, *Prof. Marcelo Einicker Lamas*<sup>2</sup>, *Dr. Pieter De Beule*<sup>1</sup>

1. INL, 2. Federal University of Rio de Janeiro

Nanophotonics technology heralds advances for applications in nanomedicine, where the generation of induced Pluripotent Stem cells (iPS) represents a promising key enabling technology. Current preferred technology to achieve the latter consists of viral based solutions introducing the so called pluripotency genes. However, their application is well-known to present increased mutagenesis risks. Liposomes on the other hand are considered as a promising carrier to drug and gene delivery, but currently don't achieve viral vector reprogramming efficiencies. Here, we present the application of Two-Color Fluorescent Cross-Correlation Spectroscopy (2c-FCCS) as a remarkable tool to analyze and potentially optimize the load-efficiency of DNA-liposome complexes for the reprogramming of human fibroblasts into iPS (Figure 1).

Knowing that the composition of liposomes can directly affect cell toxicity and uptake, we initially tested different lipid combination of DOPC, DOTAP and C18-ceramide (Cer). These liposomes not only exhibit better cell uptake in comparison to the commercial transfection reagent Lipofectamine but also exhibited low toxicity (Figure 2). Aided by 2c-FCCS we can propose Cer-based lipoplexes as good choice for iPS generation since they obtain higher load-efficiency for some of the plasmids (Figure 3). Based on our work we suggest the use of 2c-FCCS as a direct method to monitor and potentially optimize the formation of new lipoplex formulations.

Figure 1. Overview of lipoplex formation optimization through 2c-FCCS: only if both biomolecules co-diffuse there will exist a correlation between them (right). A low or zero cross-correlation amplitude means that liposomes and plasmids diffuse separately through the confocal volume (left).

Figure 2. Cell uptake and death analysis of human fibroblast treated with DiI-liposomes (red): a – e) cell uptake of DOPC/Cer (a), DOTAP/Cer (b), DOPC/DOTAP/Cer (c), Lipofectamine (d) and DOTAP (e). Nucleus labeled with DAPI (blue). (f) Cell death quantification through PrestoBlue assay using H<sub>2</sub>O<sub>2</sub> as positive control. Graph bars represents mean ± SEM, where \*p < 0.0001.

Figure 3. Two-Color Fluorescent Cross-Correlation Spectroscopy analysis: a–d) Auto- and cross-correlation FCCS curves using DOPC/Cer for lipoplex formation assessment; f) Graph representation of the loading-efficiency of the different combinations of lipoplex using pluripotent genes.

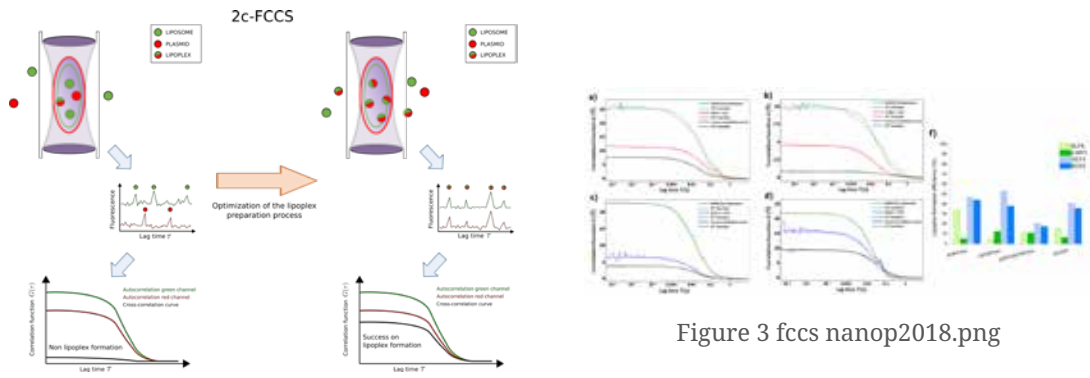


Figure1.png

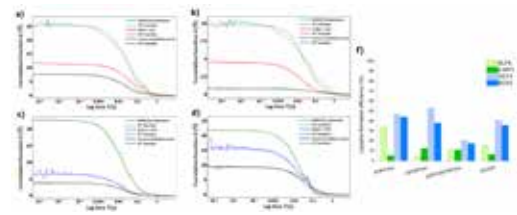


Figure 3 fccs nanop2018.png

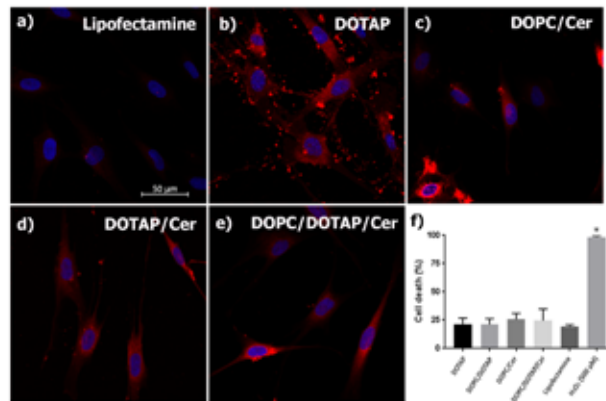


Figure 2 imuno nanop2018.png

---

## Thermoplasmonics of Platinum nanoparticles

---

Tuesday, 2nd October @ 16:50: Optical properties of nanostructures (ROOM 3) - Oral - Abstract ID: 222

---

***Dr. Akbar Samadi*<sup>1</sup>, *Dr. Henrik Klingberg*<sup>1</sup>, *Dr. Liselotte Jauffred*<sup>1</sup>, *Prof. Andreas Kjaer*<sup>2</sup>, *Dr. Poul Martin Bendix*<sup>1</sup>, *Prof. Lene B. Oddershede*<sup>1</sup>**

*1. University of Copenhagen/Niels Bohr Institute, 2. University of Copenhagen/Dept. of Clinical Physiology*

Plasmonic nanoparticles can absorb part of incident laser energy and liberate it into the local environment in the form of heat. This effect can be used in an advantageous manner, for thermoplasmonic applications in the life sciences, nano-medicine, and bio-medical engineering. Current efforts focus on the development of NIR resonant plasmonic nanoparticles with, sizes optimized for delivery into tumors (d=50-100 nm), higher light-to-heat conversion efficiency and less toxicity for bio-applications.

Here, we quantify the extraordinary thermoplasmonic properties of Platinum Nanoparticles, PtNPs (d=50-70 nm), via both experiment and simulation, and their efficiency in photothermal cancer therapy demonstrated in vitro.

Using a novel bio-compatible assay, we directly quantified the temperature profile of individual irradiated PtNP and results are backed-up by Finite Element Modeling (FEM). Toxicity and photothermal cancer therapy of PtNPs for human SK-OV-3 ovarian cancer cells assessed in vitro.<sup>5</sup>

We find that PtNPs (d=50-70 nm), are capable of reaching temperatures as high as 700 °C while maintaining structural integrity (Figure 1), under NIR irradiation which can penetrate deeper into the bio-material, e.g., tumor tissue. Thus, the plasmonic properties of PtNPs and their low toxicity, in connection with the commercial availability of high quality PtNPs, makes the future bright for utilizing these exceptional particles for hot bio-engineering purposes.

### **Caption:**

(a) Illustration (not to scale) of temperature measurements. A tightly focused 1064 nm laser (red cone) irradiates a PtNP immobilized onto a coverslip coated with a lipid-bilayer (dark green) incorporating phase-sensitive fluorophores which partition into the melted area (light green).  $r_m$  denotes the radius of the melted area around the heated NP and  $T_m$  is the phase transition temperature. (b) Confocal images showing the partitioning of phase-sensitive fluorophores into the melted area around an irradiated 70 nm PtNP. The laser powers used are 85 mW, 195 mW and 315 mW, respectively, from left to right. Scale bar is 10  $\mu$ m. (c) Temperature profile around a 70 nm PtNP irradiated by a 1064 nm laser with 195 mW. The white symbols are experimentally determined temperature profile (n = 7 experiments) and the red solid line shows the temperature profile predicted via FEM.

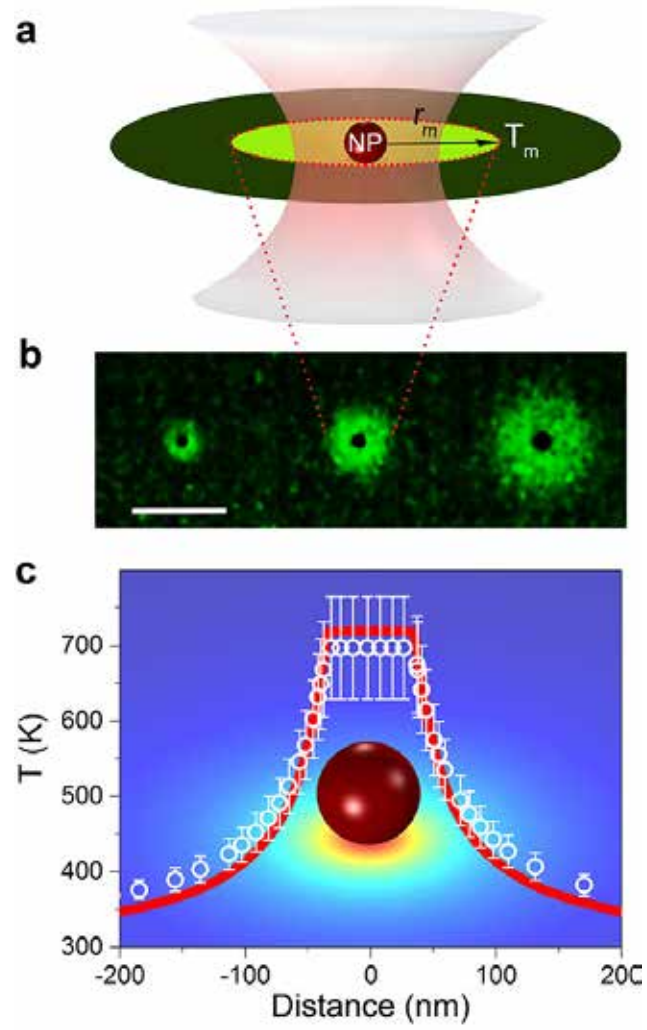


Fig1-abstract.jpg

# Detecting plasmonic heating via liquid crystals thermometry

Tuesday, 2nd October @ 17:07: Optical properties of nanostructures (ROOM 3) - Oral - Abstract ID: 327

**Dr. Luciano De Sio**<sup>1</sup>, **Dr. Ugo Cataldi**<sup>2</sup>, **Dr. Alexa Guglielmelli**<sup>3</sup>, **Prof. Thomas Bürgi**<sup>2</sup>, **Dr. Nelson Tabiryan**<sup>4</sup>, **Dr. Timothy J. Bunning**<sup>5</sup>

1. Sapienza University of Rome, 2. University of Geneva, 3. University of Calabria, 4. BEAMCo, 5. Air Force Research Laboratory

Plasmonic nanoparticles (NPs) when pumped sufficiently with resonant radiation have the unique capability to concentrate an incredible amount of heat at the nanoscale, thanks to a phenomenon called localized plasmonic resonance (LPR) [1, 2]. Thermotropic liquid crystals (LCs) are an excellent candidate medium as they are extremely responsive to external perturbations such as electric fields, optical fields and temperature [3, 4]. LCs have been exploited as active media for controlling the LPR frequency or for detecting photo-induced temperature variations in several plasmonic architectures. The work here [5] shows the possibility of combining a large area (1 inch<sup>2</sup>) of randomly distributed gold NPs (GNPs) immobilized on a glass substrate and covered with a cholesteric LC (CLC) as an active overlayer for controlling simultaneously both the photonic and plasmonic properties of the hybrid system. Upon exposure to resonant radiation, local heating of the NPs induces changes to the optical properties of the CLC in terms of selective reflection. As a consequence, the refractive index change of the CLC induces a blue shift of the LPR frequency of about 20nm. The system demonstrates that suitable optical radiation be utilized to affect both the plasmonic and photonic properties of the system.

## References

1. Liz-Marzán, L.M., *Nanometals: Formation and color*. Materials Today, 2004. 7(2): p. 26-31.
2. O'Neal, D.P., et al., *Photo-thermal tumor ablation in mice using near infrared-absorbing nanoparticles*. Cancer Letters, 2004. 209(2): p. 171-176.
3. De Sio, L., et al., *Nano-Localized Heating Source for Photonics and Plasmonics*. Advanced Optical Materials, 2013. 1(12): p. 899-904.
4. De Sio, L., et al., *Next-generation thermo-plasmonic technologies and plasmonic nanoparticles in optoelectronics*. Progress in Quantum Electronics, 2015. 41: p. 23-70.
5. De Sio, L., et al., *Dynamic optical properties of gold nanoparticles/cholesteric liquid crystal arrays*. MRS Communications, 2018: p. 1-6.

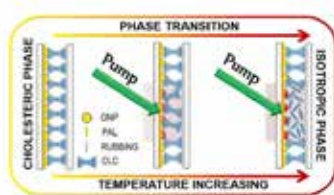


Figure 1: Schematic of the sample with the pump beam turned off (left) and on (middle and right) at different power level.

Nanofinal.jpg



# Light-Emitting Halide Perovskite Nanoantennas

Tuesday, 2nd October @ 17:24: Optical properties of nanostructures (ROOM 3) - Oral - Abstract ID: 385

**Ms. Ekaterina Tiguntseva**<sup>1</sup>, **Mr. George Zograf**<sup>1</sup>, **Prof. Anvar Zakhidov**<sup>2</sup>, **Dr. Sergey Makarov**<sup>1</sup>, **Prof. Yuri Kivshar**<sup>3</sup>

1. Department of Nanophotonics and Metamaterials, ITMO University, 2. University of Texas at Dallas, 3. Australian National University

Halide perovskites are known like a very attractive material for all-dielectric resonant nanophotonics due to their properties. Here we employ halide perovskites to create light-emitting nanoantennas with enhanced photoluminescence due to the coupling of their excitons to dipolar and multipolar Mie resonances and demonstrate that the halide perovskite nanoantennas can emit light in the range of 530–770 nm depending on their composition.

Organic-inorganic (hybrid) perovskites of the  $\text{MAPbX}_3$  family represent a class of dielectric materials with excitonic states at room temperature, refractive indices ( $n=2-3$ ) high enough for the efficient excitation of Mie resonances, low losses at the exciton wavelength, chemically tunable band gap over the entire visible range (400–800 nm) by simple replacing or mixing the anion compound (I, Br or Cl), high defect tolerance, and high quantum yield (more than 30%) of photoluminescence (PL). These properties make them perfect candidates for effective nanoscale light sources.

In this work, we fabricate by laser printing method perovskite nanoparticles (NPs) supporting electric and magnetic dipolar and multipolar Mie resonances.

Fig.1 (a) Red curve corresponds to experimental DF scattering spectrum for single perovskite NP with diameter 415 nm. Green and blue lines stand for analytical mode decomposition for single spherical perovskite NP of 440 nm in homogeneous air media. (b) PL spectra (marked by the corresponding colors of the frames of SEM image) normalized to the volume for perovskite NPs as well as for 0.5  $\mu\text{m}$  perovskite film. Scale bar in the SEM image is 400 nm.

Fig.2 Resonant properties of perovskite nanoparticles with different composition. (a,c,e) Blue curve corresponds to experimental dark-field scattering spectra for single perovskite nanoparticles of different composition on a glass substrate. Filled color areas correspond to experimentally measured PL spectra of perovskite nanoparticles. (b,d,f) Red solid line shows analytical scattering spectrum in dark-field configuration for  $\text{MAPbBr}_3$ ,  $\text{MAPbBr}_{1.5}\text{I}_{1.5}$ ,  $\text{MAPbI}_3$  perovskite nanoparticles with diameters of 280, 240, and 260 nm, respectively. Green and blue lines stand for the mode decomposition in air (green dashed, MQ; blue dashed, EQ; green solid, MD, blue solid, ED).

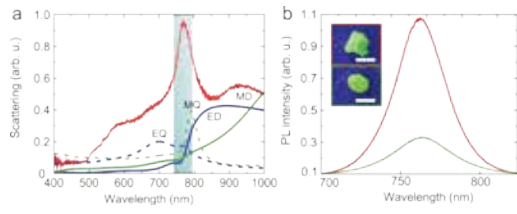


Fig.1.png

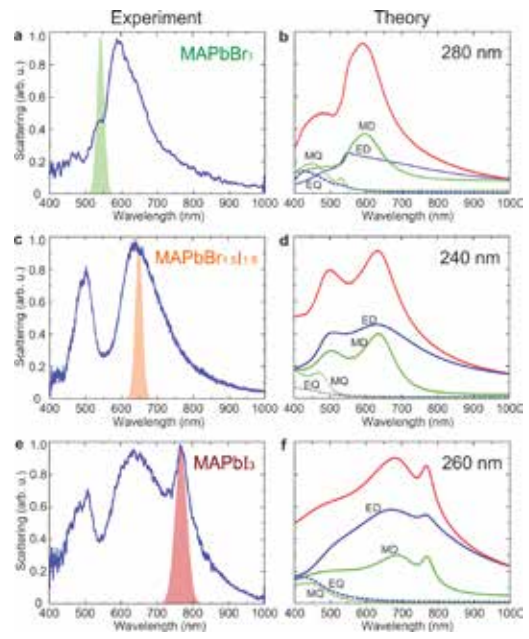


Fig.2.png

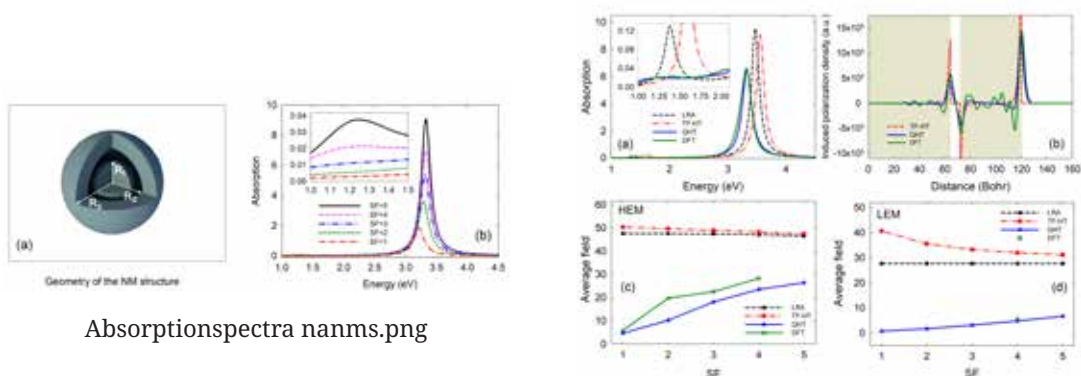
# Plasmonic behavior of spherical core-shell structures in the tunneling regime

Tuesday, 2nd October @ 17:41: Optical properties of nanostructures (ROOM 3) - Oral - Abstract ID: 388

*Dr. Muhammad Khalid*<sup>1</sup>, *Dr. Fabio Della Sala*<sup>1</sup>, *Dr. Cristian Ciraci*<sup>1</sup>

*1. Italian Institute of Technology*

Many experimental studies have revealed that plasmonic behavior of metallic nanostructures with subnanometer gap distances cannot be predicted by conventional local response models due to nonlocal or quantum effects. Optical interactions in these systems can be in principle correctly described by *ab initio*-based approaches, such as time-dependent density function theory (TD-DFT). However, TD-DFT methods can only handle very small systems due to its high computational costs. Quantum hydrodynamic theory (QHT), on the other hand, is a promising tool which is computationally much cheaper and can be applied to fairly large plasmonic particles to study both microscopic as well as macroscopic optical properties. QHT has proven its potential in efficiently and correctly describing the plasmon resonances, electron spill-out and retardation effects. In the present study, we apply state-of-the-art QHT to investigate the effect of electron tunneling on the optical properties of plasmonic nanostructures. In particular, we consider spherical core-shell structures, also known as nanomatryoshkas (NMs), with sub-nanometer core-shell gap distances, both for Au and Na metals. We compare the results obtained by using QHT with the reference TD-DFT computations, performed using an in-house developed code and we find an excellent agreement between the two theories. We also study optical properties of quite big systems, both for Au and Na, whose sizes make them inaccessible for DFT calculations and we examine the impact of core-shell spacing on near-field and far-field optical behavior of these systems. We find that the QHT method efficiently predicts the nonlocal and quantum behavior of plasmonic systems with different length scales. A systematic comparison between the local response approximation (LRA), Thomas-Fermi hydrodynamic theory (TF-HT) and QHT method has also been presented. The results show that as the core-shell distance decreases the nonlocal or quantum effects strongly influence the plasmonic properties of these systems which can be nicely described by the QHT. For numerical implementation of these structures, we fully exploit the symmetry of the geometry and use a 2.5D simulation technique which reduces the computational efforts to a great extent.



Absorptionspectra nanms.png

Dft vs qht nanms.png

# Hybrid Longitudinal-Transverse Modes in Surface Phonon Polariton Systems

Tuesday, 2nd October @ 17:58: Optical properties of nanostructures (ROOM 3) - Oral - Abstract ID: 279

*Dr. Christopher Gubbin<sup>1</sup>, Dr. Simone De Liberato<sup>1</sup>*

*1. University of Southampton*

Surface phonon polaritons (SPhPs) are formed by hybridisation of photons with the coherent oscillations of a polar dielectric crystal. Like plasmons these modes allow for confinement of light on the nanoscale. Unlike plasmons, SPhPs typically have narrow linewidths and corresponding long lifetimes [1]. SPhPs are supported in the mid-infrared spectral region, specifically in the Reststrahlen region between the supporting polar dielectric's transverse and longitudinal optical phonon frequencies. Their large intrinsic nonlinearities [2,3] and ease of fabrication make SPhP systems an excellent platform for mid-infrared nonlinear optics.

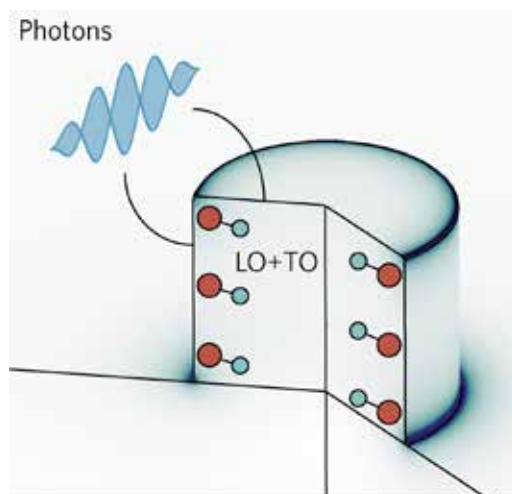
Although the phonon branches of a polar dielectric crystal are dispersive the optical properties of the SPhP systems studied thusfar are dependent solely on the zone-centre phonon frequencies of the lattice. This is because the lengthscale of a typical SPhP nanoresonator is 100nm, many orders of magnitude larger than the supporting polar dielectric's lattice constant.

This talk will discuss a system where this zone-centre treatment of the lattice fails leading to hybridisation of longitudinal and transverse SPhPs as shown in the first figure. Exploiting the polymorphism of silicon carbide, whose polytypes unit cells are identical in two dimensions but extended to varying degree in the third, it is possible to fold the dispersive longitudinal optical phonon of the lattice back to zone-centre as illustrated in the second figure. We will discuss the implications of this folding for the optical response of SPhP nanoresonators, demonstrating theoretically and experimentally that this hybridisation can lead to strong-coupling, or formation of a mixed longitudinal-transverse mode. In addition we will discuss the possibility of exploiting these hybridised modes to create electrically pumped SPhP devices powered by the Fröhlich interaction.

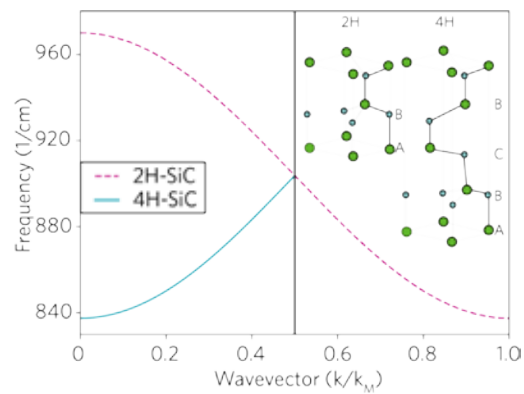
[1] J. D. Caldwell et. al., Nano Letters 13, 3690 (2013).

[2] C. R. Gubbin and S. De Liberato, ACS Photonics 4, 1381 (2017).

[3] C. R. Gubbin and S. De Liberato, ACS Photonics 5, 284 (2017).



Locouplinga.png



Locouplingb.png

# Plasmonic magneto-optical 1D nanostructure: Wood's anomaly and the Faraday rotation for biosensing

Tuesday, 2nd October @ 18:15: Optical properties of nanostructures (ROOM 3) - Oral - Abstract ID: 159

*Mr. Alexey Shaymanov*<sup>1</sup>, *Dr. Nikolay Orlikovsky*<sup>1</sup>, *Mr. Eldar Khabushev*<sup>1</sup>, *Mr. Alexander Zverev*<sup>1</sup>, *Ms. Anastasiya Pishimova*<sup>1</sup>, *Dr. Georg Sharonov*<sup>1</sup>, *Dr. Georgii Yankovskii*<sup>1</sup>, *Dr. Ilya Rodionov*<sup>1</sup>,  
*Dr. Alexander Baryshev*<sup>1</sup>

*1. Dukhov All-Russia Research Institute of Automatics*

Plasmonic nanostructures are actively investigated in order to make sensors portable and more sensitive [1]. In particular, the way to improve sensitivity is utilization of the magneto-optical multilayer in structure to measure a magneto-optical (MO) response instead of the amplitude of transmitted or reflected wave [2].

In the present work, we demonstrate 500-nm-sized slabs of plasmonic 1D nanostructures for detecting low density lipoproteins (LDL): sample **A**—dielectric nanoridges coated with 40-nm-thick Au and sample **B** is a similar one based on bismuth-substituted yttrium iron garnet (Bi:YIG). We experimentally and theoretically studied their optical spectra, gave an explanation on resonant light coupling and optimized designs of the structures. For these designs, we measured and numerically analyzed optical and magneto-optical (MO) responses in the transmission geometries when modeling biomolecular binding for LDL detection with a low concentration. Numerical models of sample **A** and **B** were set up for one unit cell of the 1D grating; experiment and calculations were carried out for the  $E_x$ -polarized light (see Fig.1).

We have found that, by introducing Bi:YIG layer, the sensitivity can be significantly enhanced when measuring the MO response in the vicinity of the Fano peak. Indeed, a change in the angle of Faraday rotation  $\Delta\theta = 1^\circ$  was demonstrated for sample **B** with optimized parameters. The sensitivity of sample **B** was  $1.56 \cdot 10^{-7}$  RIU when analyzing the direction of polarization plane. Note that the sensitivity of sample **A** was  $2 \cdot 10^{-6}$  RIU when measuring the amplitude of transmitted wave.

Fig. 1. A sketch of the unit cells of experimental sample **A** ( $D = 650$  nm,  $h_{\text{HSQ}} = 100$  nm,  $d_{\text{Au}} = 40$  nm,  $d_{\text{Ti}} = 5$  nm,  $d_{\text{HSQ}} = 65$  nm,  $h_{\text{HSQ}} = 80$  nm) and the model of sample **B** ( $D = 500$  nm,  $d_{\text{BiYIG}} = 140$  nm,  $d_{\text{Au}} = 30$  nm,  $h_{\text{R}} = 110$  nm,  $d_{\text{R}} = 60$  nm). Structural parameters for optimized samples are given in parentheses.

[1] B. Špačková, P. Wrobel, M. Bocková, J. Homola, Proceedings of the IEEE. 104 (2016) 2380 - 2408.

[2] A. V. Baryshev, K. Kawasaki, M. Inoue, Proc. BioPhotonics 2011, 12123238.

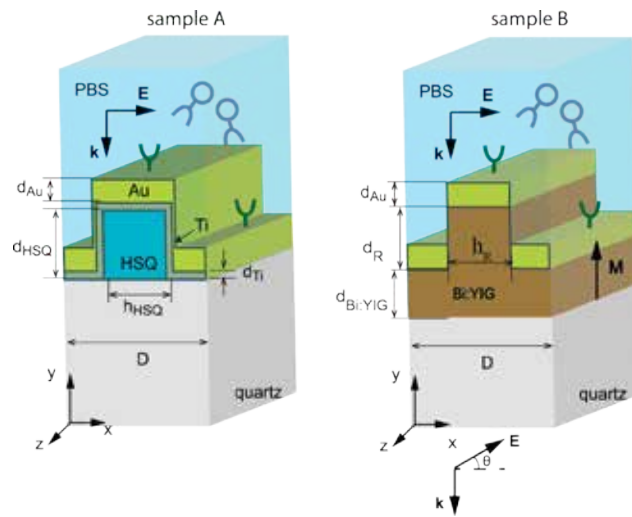


Fig1 1.png

# One-dimensional spherical photonic crystal

Tuesday, 2nd October @ 18:32: Optical properties of nanostructures (ROOM 3) - Oral - Abstract ID: 253

**Mr. Lewis Asilevi<sup>1</sup>, Mrs. Ségolène Pélisset<sup>1</sup>, Ms. Myriam Bailly<sup>1</sup>, Mrs. Leila Ahmadi<sup>1</sup>, Prof. Emiliano Descrovi<sup>2</sup>, Prof. Matthieu Roussey<sup>1</sup>**

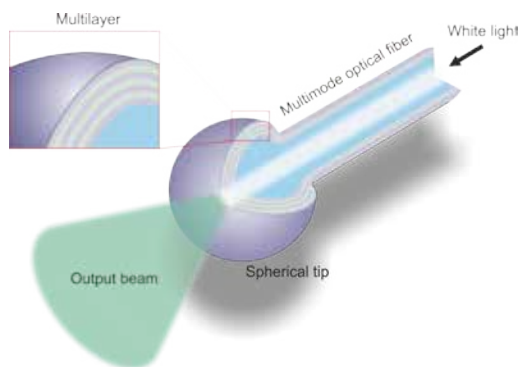
1. Institute of Photonics, University of Eastern Finland, 2. Politecnico di Torino

We report on an experimental demonstration of a one-dimensional photonic crystal with a spherical geometry. The photonic crystal is fabricated by atomic layer deposition of bi-layers of aluminum oxide and titanium dioxide at the end of a multimode fiber shaped as a ball by fusion (see figure “Concept”). In addition to the simulations providing an optimized design and a theoretical explanation of the behavior of light in such a device, we present an experimental characterization of the structure optical features.

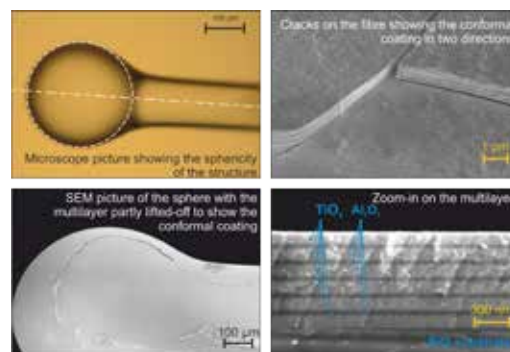
The fabrication of the sphere is done using a fiber splicer. By adapting current and time of the electric arc generated by the device, it is possible to shape the end of a multimode fiber into a ball with desired controllable diameter and position with respect to the fibers axis. The fiber is coated with a multilayered structure. The multilayer, designed by transfer matrix method and finite difference time domain method is fabricated by atomic layer deposition (ALD). This technique allows a high control of the thickness and a conformal coating all around the fiber. The multilayer is optically interrogated at different angles, by using with a supercontinuum as a light source and an optical spectrum analyzer as a detector, in a goniometric arrangement.

The multilayers is designed to open a photonic band gap in the visible region of light. Scanning electron micrograph (SEM) pictures (see figure “SEM pictures”) show that the sphere is conformally coated. The thickness of the high refractive index layers is 80 nm and the thickness of the low refractive index layers is 55 nm. When a white light source is injected in the fiber, transmitted light shows a photonic band gap spectrally centered at 650 nm, as expected from simulations.

The development of such a structure fabricated at the end of a fiber opens a way to the high integration of sources together with filters, with applications in the field of lab-on-fiber, laser, specialty fibers, and other fiber integrated components.



Concept.png



Sem pictures.png

---

# Plasmonic nanoparticle doping of the active layer for enhancing efficiency and stability in organic photovoltaic devices

---

Tuesday, 2nd October @ 16:50: Photonic & plasmonic nanomaterials (AUDITORIUM) - Oral - Abstract ID: 2

---

**Dr. Barbara Paci**<sup>1</sup>, **Dr. Amanda Generosi**<sup>1</sup>, **Dr. Emmanuel Stratakis**<sup>2</sup>, **Dr. Emmanuel Kymakis**<sup>3</sup>

1. *Istituto di Struttura della Materia/CNR, Via del Fosso del Cavaliere 100, 00133 Roma*, 2. *Institute of Electronic Structure and Laser (IESL) Foundation for Research and Technology-Hellas (FORTH), Heraklion, GR-711 10, Crete.*, 3. *Center of Materials Technology and Photonics, TEI, Heraklion, GR-710 04, Crete,*

## Introduction

Major goal of this research is the study of new materials and architectures for the enhancement of the photovoltaic properties and the improvement of the stability in organic photovoltaics (OPVs). A factor limiting OPVs efficiency is the relatively low absorption in the near-IR range of the organic active layer - constituted by an interpenetrated bulk heterojunction (BHJ) of donor (polymer) and acceptor (fullerene) materials. An advanced approach to elude this problem is the use of plasmonic metallic nanoparticles (NPs), exploiting Localized Surface Plasmon Resonance (LSPR) effects. Consequently, the doped BHJ structural/morphological and interfacial properties must be assessed.

## Methods

In-situ Energy Dispersive X-ray Reflectivity and Diffraction are applied jointly with atomic force microscopy to uncover degradation/stabilization effects in plasmonic OPV devices.

## Results and Discussion

The characteristics of high efficiency plasmonic OPV devices are investigated. Plasmonic metallic nanoparticles, produced by ultrafast laser ablation in liquids and embedded in the BHJ of the photovoltaic devices result in an increase in the PV efficiency, attributed to improved absorption of the photoactive layer caused by LSPR effects. Moreover a significant enhancement in lifetime is obtained due to the twofold beneficial effect of NPs incorporation: first the NPs act as stabilizer of the polymer conformational properties, preserving the BHJ donor-acceptor network nanoscale morphology; additionally using gold NPs the cathode buried interface is preserved from photo-oxidation effects. The unconventional structural/morphological cross-monitoring method we used is demonstrated to be a very efficient approach in studying the various aspects that concur in improving the device performances, opening the way to enhanced efficiency and stability OPVs.

## References:

- [1] B. Paci, G. Kakavelakis, A. Generosi, J. Wright, C. Ferrero, E. Stratakis, E. Kymakis, *Solar Energy Materials & Solar Cells*, **159**, 617–624, 2017.
- [2] B. Paci, D. Bailo, V. Rossi Albertini, J. Wright, C. Ferrero, G. D. Spyropoulos, E. Stratakis, E. Kymakis, *Adv. Mater.*, **25**, 4760-4765, 2013.
- [3] B. Paci, A. Generosi, V. Rossi Albertini, G. Spyropoulos, E. Stratakis, E.; Kymakis, *Nanoscale*, **4** (23), 7452 – 7459, 2012.
- [4] B. Paci, A. Generosi, D. Bailo, V. Rossi Albertini, G. Spyropoulos, E. Stratakis, E. Kymakis, *Adv. Funct. Mater.*, **21**, 3578-3582, 2011.



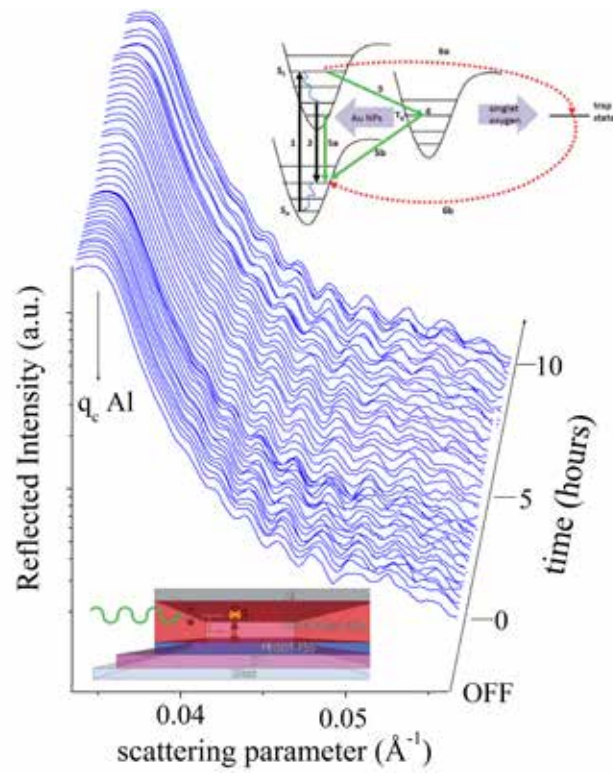


Figure1.jpg

## Diode-like asymmetric transmission in hyperbolic epsilon-near-zero media

---

Tuesday, 2nd October @ 17:07: Photonic & plasmonic nanomaterials (AUDITORIUM) - Oral - Abstract ID: 108

---

***Dr. Carlo Rizza*<sup>1</sup>, *Dr. Xin Li*<sup>2</sup>, *Dr. Andrea Di Falco*<sup>2</sup>, *Prof. Elia Palange*<sup>3</sup>, *Dr. Andrea Marini*<sup>3</sup>, *Dr. Alessandro Ciattoni*<sup>1</sup>**

*1. CNR - SPIN L'Aquila, 2. University of St Andrews, 3. University of L'Aquila*

Epsilon-near-zero (ENZ) media have attracted a great deal of interest since ENZ regime is able to trigger secondary light-matter interactions such as nonlinear and nonlocal effects. Here, we show the boosting of asymmetric transmission for forward and backward propagation of tilted circular polarized optical waves in ultrathin epsilon-near-zero hyperbolic slabs. Remarkably, this effect is solely triggered by anisotropy without resorting to any breaking of reciprocity and chiral symmetries or spatial nonlocal effects. The ENZ enhancement is due to the fact that the hyperbolic dispersion activates etalon resonances where extraordinary waves accumulate propagation phase even though the slab is ultrathin. The proposed strategy holds promise for realizing ultra-compact and efficient polarization devices at different frequency bands.

# Hybrid photonic-plasmonic devices for enhanced sensitivity biosensors

Tuesday, 2nd October @ 17:24: Photonic & plasmonic nanomaterials (AUDITORIUM) - Oral - Abstract ID: 65

**Dr. Lucia Fornasari**<sup>1</sup>, **Dr. Paola Pellacani**<sup>2</sup>, **Dr. Miguel Manso**<sup>3</sup>, **Dr. Chloe Rodriguez**<sup>3</sup>, **Dr. Vicente Torres-costa**<sup>3</sup>, **Prof. Franco Marabelli**<sup>4</sup>

1. University of Pavia, Plasmore S.r.l., 2. Plasmore S.r.l., 3. Universidad Autonoma de Madrid, 4. University of Pavia

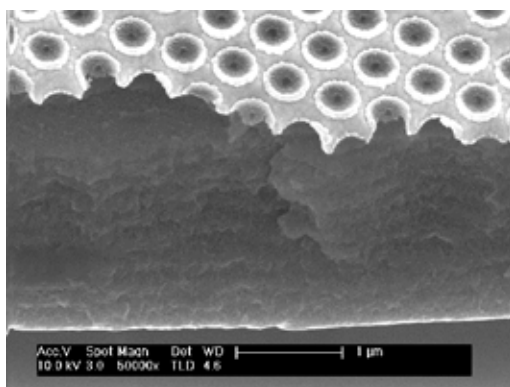
**Introduction.** Hybrid plasmonic-photonic systems attract the attention of the scientific community due to their ability in modifying the light behaviour and the electric field distribution. The study of this type of system could have significant fall-out in fields such as biosensing and optoelectronics. In this work, multilayer porous silicon (PSi) interference structures have been used as a support for arrays of Au nanocavities to combine the photonic properties of the former with the plasmonic properties of the latter and to develop an hybrid photonic-plasmonic device. Finite Difference Time Domain (FDTD) simulation have been implemented in order to interpret the experimental results.

**Methods.** PSi multilayer stacks were produced by electrochemical etching of p-type monocrystalline silicon wafers to produce contrasting porosity strata and thus achieve a predetermined interference response [1]. On top of this structure, a large area nanostructured plasmonic structure was created by colloidal lithography [2]. These hybrid structures have been characterized by scanning electron microscopy, which has allowed to infer the main characteristics of the system, and by variable-angle spectral-resolved reflectance measurements at each fabrication step that allowed evaluating the individualized optical contribution of each structure and their coupling (Figure 1). FDTD simulations of the plasmonic, photonic and hybrid structures have been performed in order to interpret the results. The sensitivity of the hybrid structure to refractive index changes has been evaluated through the deposition of nanometric polyelectrolyte layers.

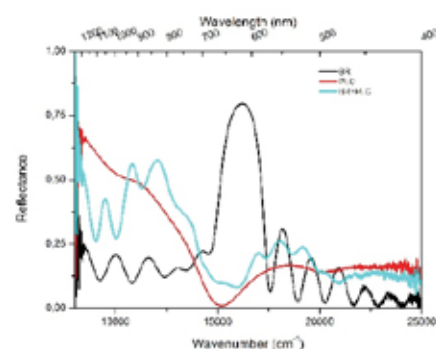
**Results and Discussion.** Results suggest that the optical response of these type of hybrid structures is dominated by the plasmonic features, modulated by the interference fringes of the photonic structure (Figure 2). The analysis of the dispersion mode highlights the presence of the Tamm mode and of a complex interplay between the plasmonic and photonic components (see Figure 3). The estimate of the sensitivity shows that the hybrid structure is most sensitive to refractive index changes in the visible region around 650 nm.

[1] C. Pacholski. Photonic Crystal Sensors Based on Porous Silicon. *Sensors* 2013, 13, 4694-4713.

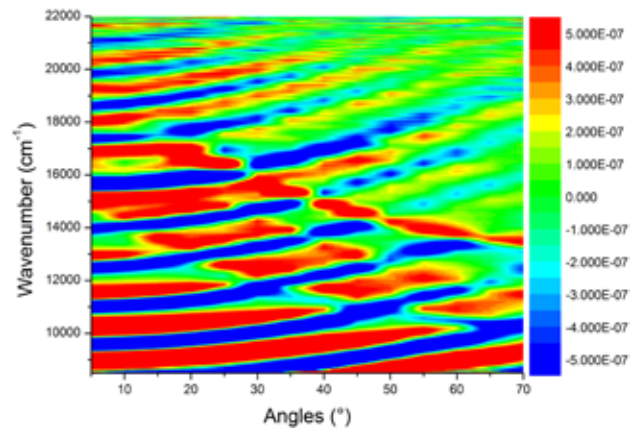
[2] B. Bottazzi, et al. Multiplexed label-free optical biosensor for medical diagnostics. *Journal of Biomedical Optics* 2014, 19 (1), 017006.



Sem hybrid system.png



Spectra of the plasmonic photonic and hybrid structure.png



Map of the second derivative of the light intensity as a function of wavenumber and angles.png

# Plasmonic Photodetector Incorporating SrTiO<sub>3</sub> Interfacial Layer

Tuesday, 2nd October @ 17:41: Photonic & plasmonic nanomaterials (AUDITORIUM) - Oral - Abstract ID: 335

**Dr. Takayuki Matsui**<sup>1</sup>, **Dr. Yi Li**<sup>2</sup>, **Prof. Rupert F Oulton**<sup>2</sup>, **Prof. Lesley F Cohen**<sup>2</sup>, **Prof. Stefan A Maier**<sup>3</sup>

1. Imperial College London, Toyota Central R&D Labs., Inc., 2. Imperial College London, 3. Imperial College London, Ludwig-Maximilians-Universität München

Hot carrier injection over Schottky barrier between metal and semiconductor is one of the promising ways to effectively use Ohmic losses of plasmonic structure. Regarding plasmon induced photo-detection, much effort was putted in exploring high absorption structure with enough thin metal. Besides simple metal/semiconductor structure, inserting a functional interfacial layer expands research fields and applications.

In this study, we propose and demonstrate stable and bias-dependent photocurrents upon resonant plasmonic excitation with ultrathin SrTiO<sub>3</sub> interfaces [Adv. Funct. Mater. 2018, 1705829]. The structure is gold gratings on p-type silicon substrate; lattice matched epitaxially grown SrTiO<sub>3</sub> layer is inserted between them. After the cyclic voltage scanning, the device shows p-type Schottky-like rectified response. Opto-electric properties of the device, after soft-electric breakdown, are evaluated using custom built microscope system with super continuum white laser. We verified wavelength and polarization dependent photocurrent, whose resonance wavelength and polarization agree well with numerical calculations. Because the SrTiO<sub>3</sub> layer is epitaxially grown with perfect lattice matching, our device has shown stable electric response under reverse bias as high as 100 V, allowing tunability of the Schottky photodetector. Although we examined the photocurrent response on different SrTiO<sub>3</sub> thicknesses (5, 10, and 40 nm), the device with 10 and 40 nm of SrTiO<sub>3</sub> shows no detectable photo-induced currents. Because it is known that thicker SrTiO<sub>3</sub> become more conductive; leaky path in thicker SrTiO<sub>3</sub> hinder the photo-induced current over the barrier. There should be the optimal thickness of the interfacial layer for plasmonic photo-detection scheme.

These observations remarkably expand contemporary knowledge on the hot carrier behaviors surpassing the interfaces, and are beyond conventional considerations for designing a functional Schottky photodetectors. We believe that the investigation paves the way toward plasmon-induced photodetection for practical applications. [Attached Figures; (Fig. 1) Schematic of the device. (Fig. 2) current-voltage plots before and after soft-electric breakdown. (Fig. 3) Measured r photo-induced current of the device. ]

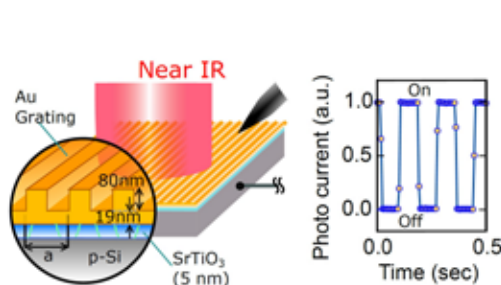


Fig1.jpg

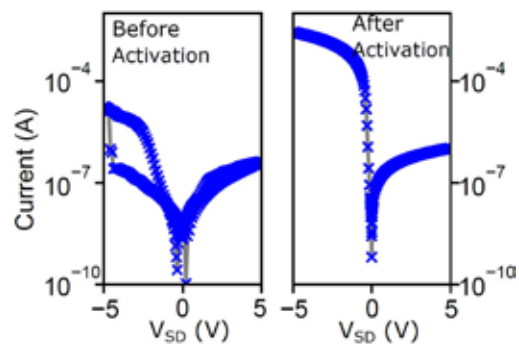


Fig2.jpg

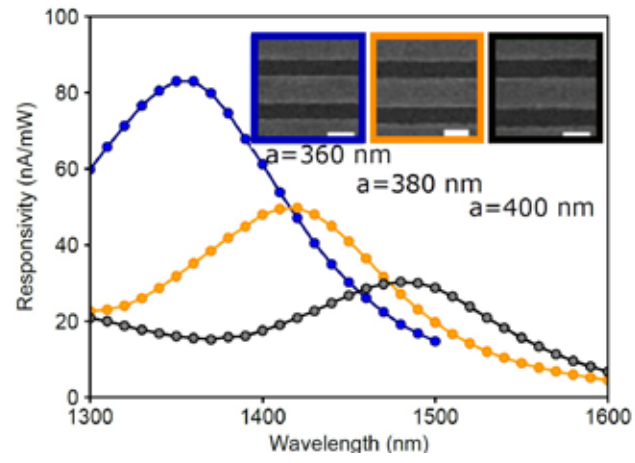


Fig3.jpg

# Preparation of plasmonic HfN nanoparticle arrays for hot-electron photochemistry

Tuesday, 2nd October @ 17:58: Photonic & plasmonic nanomaterials (AUDITORIUM) - Oral - Abstract ID: 350

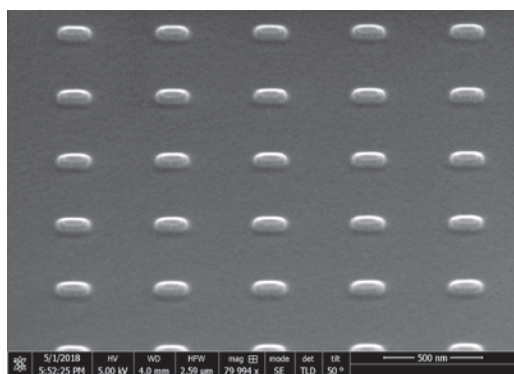
*Dr. Sven Askes*<sup>1</sup>, *Prof. Erik Garnett*<sup>1</sup>, *Ms. Evgenia Kontoleta*<sup>1</sup>

*1. Center for Nanophotonics, AMOLF*

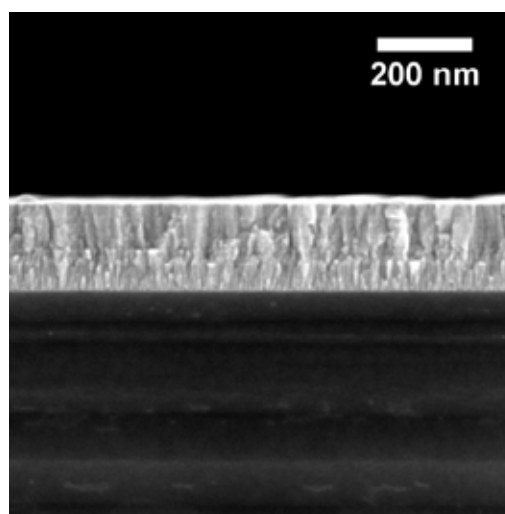
Plasmonic nanostructures feature extraordinary absorption cross sections, highly tunable optical responses, and capability of concentrating the energy of the light in subwavelength volumes. Upon excitation of such structures, all the plasmon energy is dumped in a single electron, which becomes “hot” for a brief period of time. Recent advances have demonstrated the vast potential of these hot electrons to drive chemical reduction reactions, such as hydrogen generation or organic molecule transformations.

However, although our understanding of the electron transfer mechanisms, electron energy distributions, time scale of mechanisms, and chemical substrate specificity is steadily progressing, the overall reaction efficiencies remain well below that of application requirements (<1 %). One major factor contributing to these low efficiencies is the extremely short lifetime of the hot electron: traditional plasmonic materials such as gold and silver feature hot electron lifetimes of only 1 - 2 ps, which results in ultrafast recombination of hot electrons and holes and loss of the energy as heat.

Will tuning of the hot electron lifetime offer us control over photochemical reaction yield and/or chemical specificity? To answer this question, we focus on the development of nanostructured materials that feature higher hot electron lifetimes. Especially interesting materials are zirconium nitride and hafnium nitride, which feature bulk hot electron lifetimes up to three orders of magnitude longer than that in gold due to a large phonon bandgap. Furthermore, favorable material properties such as high melting point, hardness, chemical inertness, and high free electron density make these materials excellent candidates to be used in photochemical applications. However, neither the nanostructuring of these materials, nor the plasmonic properties of such devices have been investigated thus far. Here we report for the first time on hafnium nitride nanoparticle arrays that were prepared by an electron-beam lithography synthesis. These results pave the way towards development of real-world hot-electron photochemical devices with plasmonic hafnium nitride in which hot electrons are efficiently used.



Hfn nanorod array - tilted view.png



Hfn thin film cross section.png

## Random lasers for spectroscopy applications

Tuesday, 2nd October @ 18:15: Photonic & plasmonic nanomaterials (AUDITORIUM) - Oral - Abstract ID: 391

***Mrs. Alice Boschetti<sup>1</sup>, Dr. Andrea Taschin<sup>1</sup>, Dr. Paolo Bartolini<sup>1</sup>, Dr. Lorenzo Pattelli<sup>1</sup>, Prof. Renato Torre<sup>1</sup>, Prof. Diederik Wiersma<sup>1</sup>***

### 1. LENS

Well-established examples of super-resolved microscopy, as STORM, PALM and FPALM, allow to reconstruct images with higher resolution than that imposed by the diffraction limit. These methods are based on the sequential activation and time-resolved localization of fluorophores. During imaging, only an optically resolvable subset of fluorophores is activated, and the position of each fluorophore can be determined with high precision by finding its centroid. Subsequent iterations allow the localization of large numbers of fluorophores, creating a super-resolved image of the sample. The aim of this work is to export this concept to the spectral domain, that is, to obtain a highly resolved spectrum of a given sample, whose spectral features are well below the spectral resolution of the measuring spectrometer.

Ideally, to perform this analysis, a tunable laser can be used as a source. In this case, the target spectrum can be retrieved simply by combining the transmission amplitude at each input frequency, with the final spectral resolution being limited only by the spectral width of the illumination source. Here, we demonstrate that the tunable laser input source can be conveniently replaced by a much more cost-effective random laser.

Random lasers are laser sources using a highly disordered gain medium. It has no optical cavity, but the principles of operation are the same of a laser. An optically pumped random laser can easily be obtained suspending scattering nano-particles such as titanium dioxide or zinc oxide in a dye solution. At each pump laser shot, only few modes rise above the lasing threshold as determined by mode competition and gain depletion. Due to the intrinsic, dynamic disorder of the suspension, such single-shot spectra are entirely uncorrelated, with narrow peaks appearing at independent frequencies.

We simulate a measurement of the transmitted frequency response of a Fabry-Perot (F-P) filter and a Fibonacci-1D crystal (Fig.1) with fine spectral features below the finite resolution of the spectrometer. The statistical reconstruction of their transmittance curves relies on the stochastic intensity fluctuations of the random laser modes, which allows only few of them to be excited at each pump pulse.

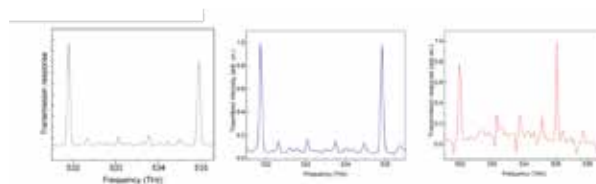


Fig1.png



---

# Efficient Generalized Mie Theory Analysis of Nano Silver Dimers for Optical Field Enhancement in the Plasmonic Photoconductive THz Antenna

---

Tuesday, 2nd October @ 18:32: Photonic & plasmonic nanomaterials (AUDITORIUM) - Oral - Abstract ID: 390

---

*Ms. Faezeh zarrinkhat*<sup>1</sup>, *Prof. Jordi Romeu*<sup>1</sup>, *Prof. Juan Rius*<sup>1</sup>, *Prof. Lluís Jofre*<sup>1</sup>

*1. Commsenslab, Universitat Politècnica de Catalunya - BarcelonaTECH*

Generalized Mie theory (GMT) is a rigorous analytical method to investigate the optical properties of a cluster of nano-spheres, providing useful optical information [1]. We propose a nano-dimer configuration, for which a GMT matrix equation with size of  $S=4n(n+2)$  should be solved, where  $n$  indicates the number of modes. To simplify this method for symmetrical nano-spheres, we can remove half the mode coefficients due to the symmetry of configuration. If we investigate each optical mode participation to generate the final field coefficients precisely, it will reveal that by eliminating weak mode coefficients the matrix equation size will reduce. It should be noted that decreasing the distance between the nano-spheres and increasing the size of them leads to a larger number of significant modes. Also, in the polarization parallel to the symmetry axis the number of the effective modes are larger than for the perpendicular polarization. Figure 1 shows how this approach matches with the GMT.

Photoconductive antennas exhibit significant application such as high-efficiency THz generation, THz detection, THz time-domain spectroscopy, and THz imaging. The main problem in this area is optical to THz wave conversion efficiency [2]. The idea is to design a symmetrical nano-dimer to resonate at the  $\lambda=800\text{nm}$ , which is a commercial laser wavelength. By applying a cluster of silver nano-dimers between the electrodes of a PC antenna, plasmons will be stimulated at such configuration and intensify the local electrical field of the laser pump beam. This approach enhances the ratio of the generated THz photocurrent power to the optical power in the PC material, which is the optical-to-electrical efficiency. The accuracy and efficiency of the GMT allows us to design improved configurations, optimizing the size of the nano-spheres, inter-particles distance, material, the angle of the incident plane wave, and the permittivity of surrounding medium. Figure 2 depicts the electrical field distribution for a silver nano-dimer configuration that resonates at  $\lambda=800\text{nm}$ . The physical properties presented in table 1.

1. D.W Mackowski, Proc. R. Soc. A 443, 599–614 (1991)
2. C.W. Berry, et al. Nat. Commun. 4, 1622 (2013)
3. P. B. Johnson, et al. Physical Review 6 (12), 4370-4379 (1972)

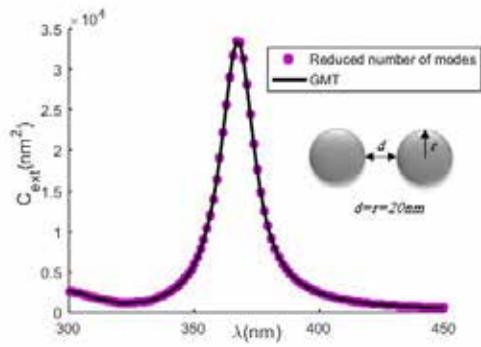


Figure 1 comparison of the optical extinction cross-section of a plasmonic nanodimer by reduced number of modes method and the gmt in the parallel polarization.jpg

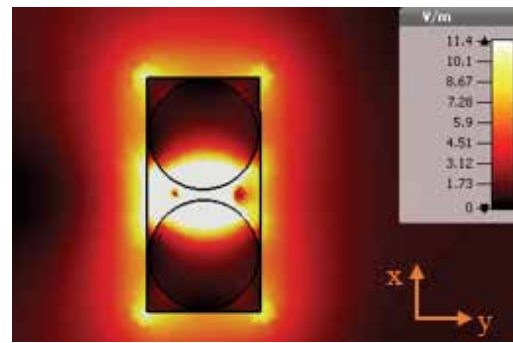


Figure 2 the electrical field distribution of designed configuration at lambda 800nm.png

<b>r</b>	<b>25 nm</b>
<b>d</b>	<b>5 nm</b>
<b>x</b>	<b>102 nm</b>
<b>y</b>	<b>52 nm</b>
<b>z</b>	<b>52 nm</b>
$\epsilon_{medium}$	<b>12.96</b>
$\epsilon_{sphere}$	<b>[3]</b>
<b>Polarization</b>	<b>Parallel</b>

Table 1 the physical properties of designed nanodimer.jpg

## Controlling Light at the Atomic Scale

---

Wednesday, 3rd October @ 09:00: Plenary Speeches (AUDITORIUM) - Oral - Abstract ID: 537

---

***Prof. Javier García de Abajo***<sup>1</sup>

*1. ICFO - The Institute of Photonic Sciences*

Plasmons in atomic-scale structures exhibit intrinsic quantum phenomena related to both the finite confinement that they undergo and the small number of electrons on which they are supported. Their interaction with two-level emitters is also evidencing strong quantum effects. In this talk I will discuss several salient features of plasmons in graphene and other atomic-scale materials, and in particular their ability to mediate ultrafast heat transfer, the generation of high harmonics, their interaction with molecules and quantum emitters, and their extreme nonlinearity down to the single-photon level.

# Charge transfer in nanoplasmonics as an avenue for control of chemical SERS enhancement and molecular self-assembly

Wednesday, 3rd October @ 09:00: Plenary Speeches (AUDITORIUM) - Oral - Abstract ID: 1

***Prof. Stefan A Maier***<sup>1</sup>

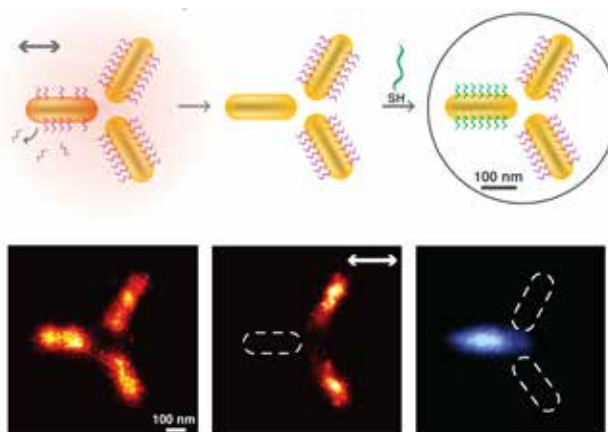
*1. Imperial College London*

The decay of localized surface plasmons in metallic nanostructures via Landau damping creates short-lived energetic electron/hole pairs, which can be used to drive nano-localized chemistry. After a brief discussion of the fundamentals of this process, I will demonstrate applications of plasmonic charge transfer for control over chemical enhancement in SERS, and to locally induce chemical reactions in reactivity hot spots of plasmonic nanoantennas. Hot electron dynamics in complex metallic nanostructures further facilitates designer molecular self-assembly in multi-element plasmonic nanoantennas.

Plasmonic nanoantennas allow the localization of electromagnetic radiation from the far field to sub-diffraction near-field hot spots of enhanced field energy. The driving principle behind surface enhanced Raman scattering (SERS), electromagnetic field hot spots have thus far dominated research efforts in making surface enhanced spectroscopies efficient and reliable. Here I will focus on a different aspect of localized surface plasmons, namely the understanding and exploitation of charge transfer and hot electron generation upon plasmon decay for applications in spectroscopy, sensing, and molecular self-assembly.

Chemical enhancement of SERS via charge transfer can be optically controlled in hybrid nanoassemblies of Au or Ag colloids on a UV-activated TiO<sub>2</sub> substrate. I will present a model of the underlying physics of this phenomenon, and present applications in the detection of plastic explosives. The talk will then focus on the fundamentals of hot electron generation via Landau damping of surface plasmons, with a view on how to exploit the energetic electrons for nanoscale surface chemistry.

In addition to the well-known electromagnetic hot spots, I will demonstrate how we can map hot spots in reactivity around plasmonic nanoantennas, due to controlled modification of molecular overlayers of plasmonic nanoantennas in regions of enhanced hot electron emission. This leads to the notion of well-defined reactivity hot spots around plasmonic nanoantennas, and I will argue that their control will be instrumental for the further optimization of plasmon-based surface-enhanced spectroscopies. Lastly, I will show how we can utilize the dynamics of plasmon decay and hot electron generation for gaining control over molecular self-assembly on multi-element plasmonic nanoantennas. This allows us to functionalize individually different regions of multi-element metallic nanoclusters.



Refunctionalization headline.png

## Plasmonics for high quality light sources

---

Wednesday, 3rd October @ 10:45: Plenary Speeches (AUDITORIUM) - Oral - Abstract ID: 230

---

***Prof. Femius Koenderink***<sup>1</sup>

*1. Center for Nanophotonics, AMOLF*

Already 15 years ago it was envisioned that plasmon antennas can control how fast fluorophores emit light, into which spatial mode they do so, and with what polarization. Turning this promise into quantitative net benefits for light sources, however, has been a difficult road, requiring breakthroughs in plasmonic resonator design, as well as in nanoscopy for characterization of single nano-objects. I will present two strands of work from our group. The first strand deals with nanoscopy: I will review our efforts to realize quantitative mapping of the radiation patterns of single nanosources in terms of amplitude, polarization and phase that gives unprecedented insight into plasmonics and metamaterials, in terms of multipole moments, building-block coupling and spin-orbit coupling effects. The second strand deals with experiments aiming to achieve plasmonic mode volumes at microcavity Qs in hybrid plasmonic-photonic resonators. I will demonstrate how plasmon antennas coupled to cavities without detrimental loss of Q, giving tangible emission enhancement advantages in experiments with quantum dot emitters.

---

# Polariton quantum fluids

---

Wednesday, 3rd October @ 11:25: Plenary Speeches (AUDITORIUM) - Oral - Abstract ID: 549

---

***Prof. Daniele Sanvitto***<sup>1</sup>

*1. Institute of Nanotechnology – CNR*

There is a growing interest in the study of polaritonic systems, mixed states of photons and excitons, for both, the observation of quantum macroscopic phenomena, and the realisation of all-optical devices that could offer limitless advantages in terms of energy consumption, dissipation-less operation and high clock frequencies<sup>1</sup>. More recently, entangling one photon with one polariton, it has even been shown that these particles can also be ideal carriers of quantum information<sup>2</sup>.

Here we show several macroscopic quantum phenomena that can be observed in polariton condensates, both at low temperature, in inorganic semiconductor microcavities—for which the very long lifetime allows the formation of the BKT phase<sup>3</sup>, typical of equilibrium systems—and in organic based polaritons, where phenomena like superfluidity can be observed up to room temperature<sup>4</sup>. We also speculate on the possibility of using hybrid semiconductors with reduced dimensionality to achieve the regime of highly interacting polaritons. These materials include monocrystalline two-dimensional perovskites and transition metal dichalcogenides that have demonstrated nonlinear responses similar to those of low temperature inorganic semiconductors. Such results move in the direction of using polaritons as ultrafast and efficient electro-optical converters, optical switches and transistors.

## **References**

1. Sanvitto, D. & Kena-Cohen, S. The road towards polaritonic devices. *Nat. Mater.* **15**, 1061–1073 (2016).
2. Cuevas, Á. *et al.* First observation of the quantized exciton-polariton field and effect of interactions on a single polariton. *Sci. Adv.* **4**, eaao6814 (2018).
3. Caputo, D. *et al.* Topological order and thermal equilibrium in polariton condensates. *Nat. Mater.* **17**, 145–151 (2018).
4. Lerario, G. *et al.* Room-temperature superfluidity in a polariton condensate. *Nat Phys* **13**, 837 (2017).

# Polarization state transfer and photon routing with discrete high-index dielectric nanowaveguides

Wednesday, 3rd October @ 13:30: Poster Session (HALL & ROOM 3) - Poster - Abstract ID: 378

*Mr. Roman Savelev*<sup>1</sup>, *Mr. Vitaly Yaroshenko*<sup>1</sup>, *Mr. Danil Kornovan*<sup>1</sup>, *Dr. Mihail Petrov*<sup>1</sup>

1. ITMO University

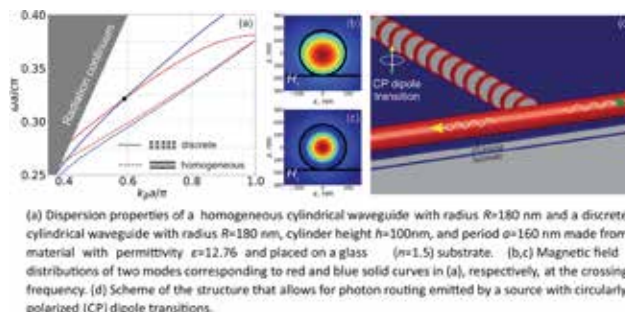
The topic of chiral light-matter interaction attracts a lot of interest during several last years due to the promising applications in nanophotonics and quantum optics [1]. Non-zero transverse component of the spin momentum density, inherent for the fields with complex spatial profiles, leads, for instance, to the so-called spin-momentum locking, when the direction of light propagation becomes coupled to the spin orientation of the source emitter and, therefore, to the associated photon polarization state [2,3]. Many types of quantum emitters, e.g. quantum dots or 2D materials, in practical schemes exhibit dipole transitions polarized in the plane of substrate. Efficient integration of such emitters with planar photonic circuits requires coupling of these transitions to the planar optical nanowaveguides. As compared with conventional homogeneous dielectric nanowaveguides, discrete waveguides provide one with additional freedom in their dispersion engineering due to the mutual coupling of the resonances of their constituent elements.

Here we theoretically address the subject of coupling of a quantum emitter to a discrete nanophotonic waveguide. Numerical calculations presented in Fig.1(a-c) show that specially designed waveguide can possess two orthogonal modes polarized in the plane of the substrate that cross at a certain frequency and wavenumber. From these calculations we expect that electric dipole transitions orthogonally polarized in the plane of substrate and placed below or above such a waveguide couple to both these modes. Therefore, at the crossing frequency out-of-plane spin state of an emitter can be mapped onto two orthogonal modes of the discrete waveguide and transferred over relatively large distances. We also demonstrate the possibility of routing of the emitted circularly polarized photons in the substrate plane by a specially designed hybrid planar system shown in Fig.1(d). The phase difference between two modes of the discrete waveguide determined by the polarization of emitter transition allows for unidirectional coupling to a homogeneous waveguide by changing the handedness of the transition.

[1] P. Lodahl et.al. Nature, v.541, pp. 473–480, 2017.

[2] K. Y. Bliokh, F. Nori, Phys. Rep., v.592, pp. 1-38, 2015.

[3] J. Petersen et.al., Science, v.346, pp. 67-71, 2014.



Dispersion of a discrete waveguide.jpg

# Switching of surface plasmon-polariton transmittance through the graphene stub nanoresonator with quantum dot

Wednesday, 3rd October @ 13:30: Poster Session (HALL & ROOM 3) - Poster - Abstract ID: 380

*Dr. Alexei Prokhorov*<sup>1</sup>, *Dr. Mikhail Gubin*<sup>1</sup>

*1. Vladimir State University named after A. G. and N. G. Stoletovs*

In this work we study a switching effect for surface plasmon-polariton (SPP) transmittance through a graphene waveguide integrated with the stub nanoresonator and loaded with a core-shell quantum dot (QD). For this aim, the geometry of the nanoresonator is optimized for realization of effective interaction of SPP modes with the QD. For obtaining of the switching effect we suggest to use two SPP waves, one of them is the signal SPP wave, propagation through the system, and another is a SPP wave that manages excited states of the QD. We show that in the regime of strong nonlinear interaction the effective control the phase shift of the signal SPP via variation of the power of the manage SPP wave can be obtained. With increasing of the phase shifts of signal SPP the transmission ability of the nanoresonator can significantly change. In particular, we demonstrate that it is possible to get dramatic increase in transmittance of the signal SPP from 0 to 90% applying the managing SPP. From the practical point of view, we consider the switching of SPP at a wavelength of 1.55  $\mu\text{m}$  in a system with 5 nm InN/GaN core-shell QD, loaded in few nm width graphene stub. Using FDTD simulation of the time evolution of the signal and managing SPP waves in graphene nanostructure, the complete agreement of numerical results with our analytical solutions is demonstrated.

The proposed model can be used for development of all-plasmonic transistors and new processors architecture for the near-infrared spectral rang. In addition the achievement of high-temperature superconductivity of graphene can provide conditions for realization of the lossless plane circuits based on the SPP propagation.

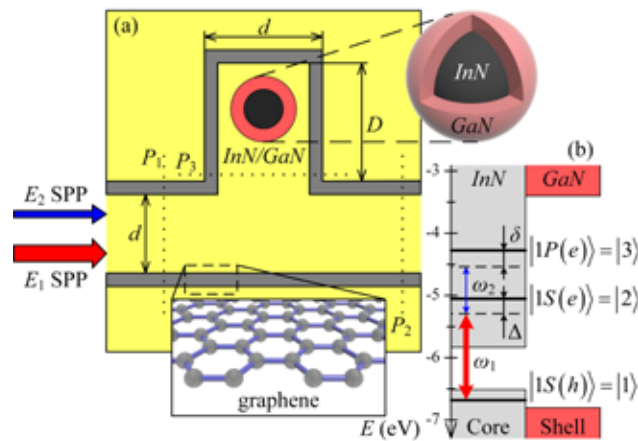


Fig1.jpg



---

# Stabilization of quantum dots on modified natural aluminosilicate nanotubes for biological application

---

Wednesday, 3rd October @ 13:30: Poster Session (HALL & ROOM 3) - Poster - Abstract ID: 497

---

**Dr. Anna Stavitskaya**<sup>1</sup>, **Dr. Andrei Novikov**<sup>1</sup>, **Dr. Elvira Rozhina**<sup>2</sup>, **Mrs. Fereshtech Pouresmaeil**<sup>1</sup>, **Mr. Danila Logvinenko**<sup>1</sup>, **Dr. Pawel Gushchin**<sup>1</sup>, **Prof. Rawil Fakhrullin**<sup>2</sup>, **Prof. Yuri Lvov**<sup>3</sup>, **Prof. Vladimir Vinokurov**<sup>1</sup>

1. Gubkin University, 2. Kazan Federal University, 3. Louisiana Tech University

## Introduction

Metal chalcogenides quantum dots (MChQDs) are of great interest due to tunable optical properties depending on the size and chemical composition. MChQDs for bioimaging are often synthesized using the complicated stabilization techniques to make them less cytotoxic and soluble in water. One of the methods to decrease toxicity and enhance stability of QDs is adsorption on carriers. Here we propose natural aluminosilicate nanotubes as carriers for MChQDs [2, 3].

## Methods

We synthesized metal sulfide QDs of various composition stabilized on natural halloysite nanotubes using in-situ synthesis of nanoparticles from nanotube-ligand-metal complexes. First, the clay nanotubes were modified with different ligands such as silanes, azines. Then the metal complexes were formed using nanotubes-ligands and Cd, Cu, Zn salts as metal precursors. Finally, sulfur precursor solutions were added to the system. The materials were characterized using TEM, XRD, and TGA analysis. Fluorescence spectra and diffusion reflectance spectra were obtained. Cytotoxicity was measured.

## Results

The formed nanosystems are well structured materials with nanoparticles adsorbed on 0.5-1.0  $\mu\text{m}$  long clay nanotubes with internal diameter from 10 nm to 30 nm. Approximately 50 to 200 nanoparticles were formed on the surface of each nanotube. The particles size distribution was rather monodisperse about 6-9 nm. The systems showed good fluorescent properties as well as good oxidation and photostability, low cytotoxicity. The confocal and enhanced dark-field microscopy images showed the potential of these materials for human cancer cells labeling.

## Discussion

The method proposed helps obtaining more than 50 stabilized quantum dots on one single nanotube. Synthesized systems are quiet stable in time and might be use for biological applications due to enhanced stability and decreased cytotoxicity. Good water dispersability of MChQDs stabilized on natural nanotubes important for bioimaging was achieved. The quantum dots may be synthesized at the outer tube's surface or encapsulated inside the clay nanotubes allowing their safe delivery into biocells.

**Acknowledgements:** This work was supported by the Ministry of Education and Science of the Russian Federation (Grant No 14.Z50.31.0035).

1. Stavitskaya A., et al. *Nanomaterials*, 2018, 8, 391-402
2. Lazzara G., et al. *Current Opinion Coll. Interface Science*, 2018, 35, 42-50

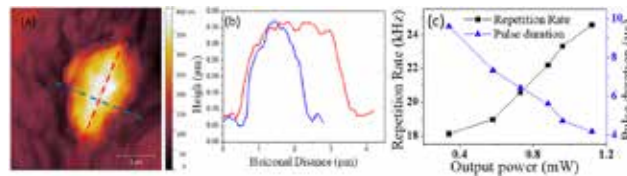
# Passively Q-switched fiber laser using PtS<sub>2</sub> microflakes saturable absorber

Wednesday, 3rd October @ 13:30: Poster Session (HALL & ROOM 3) - Poster - Abstract ID: 153

**Mr. Xinyu Wang<sup>1</sup>, Mr. Ping Kwong Cheng<sup>1</sup>, Mr. Chun Yin Tang<sup>1</sup>, Mr. Wayesh Qarony<sup>1</sup>, Dr. Yuen Hong Tsang<sup>1</sup>**

*1. The Hong Kong Polytechnic University*

The passive Q-switching technique with saturable absorber (SA) offers a simple, low-cost, compact, and reliable way to produce Q-switching pulses. Novel two-dimensional (2D) layered nanomaterials have recently gained significant attention on pulsed laser applications due to their excellent optoelectronic properties. Nevertheless, fabrication of nanoscale materials always requires huge energy consumption, complicated preparation techniques, and high expertise. Substituting low-cost bulk- or micro-sized counterparts with similar performance for nanoscale materials provides an alternative solution. A recent developed group-10 2D layered material, Platinum disulfide (PtS<sub>2</sub>), exhibits encouraging prospects for the laser photonic applications owing to its good stability, great carrier mobility, and broad tunable bandgap energy. In this work, the passively Q-switched Erbium-doped fiber laser with PtS<sub>2</sub> microflakes SA is firstly introduced with an operational wavelength of 1568.8 nm. The SA is fabricated by exfoliating PtS<sub>2</sub> bulk powder in N-Methyl-2-pyrrolidone (NMP) solvent then incorporated it into polyvinyl alcohol (PVA) polymer thin film. The stable Q-switched signals corresponding to 1.1 mW of the maximum average output power, 24.6 kHz of repetition rate, 4.2 μs of pulse duration, and 45.6 nJ of single pulse energy, comparable to MoS<sub>2</sub> and WS<sub>2</sub>, are successfully obtained in a fiber laser ring cavity with this PtS<sub>2</sub>-SA. These promising results may contribute to further development of optical applications of this novel PtS<sub>2</sub> or other group-10 2D materials.



Passively q-switched fiber laser using pts2 microflakes saturable absorber.png

# Strong coupling between excitons in transition metal dichalcogenides and optical bound states in the continuum

Wednesday, 3rd October @ 13:30: Poster Session (HALL & ROOM 3) - Poster - Abstract ID: 72

*Ms. Zarina Sadrieva*<sup>1</sup>

*1. Department of Nanophotonics and Metamaterials, ITMO University*

TMDC are direct-gap semiconductors, exhibiting strong light-matter coupling. These structures support excitons characterized by both large binding energies and large oscillator strength. While the former leads to the existence of strong excitonic response at room temperature, the latter provides substantial exciton-photon interaction. These properties allow the observation of the strong coupling regime in structures comprising TMDC monolayer and an optical cavity.

The design of structure is shown in Fig.1 - a WSe<sub>2</sub> flake is placed on top of an one-dimensional Ta<sub>2</sub>O<sub>5</sub> grating. The strong light-matter coupling demands high-Q photonic structures. We address this problem by tuning the PCS shape and material parameters to the regime of bound states in the continuum(BIC) providing a giant Q-factor of resonator which is limited by surface roughness and finite size of the sample only.

We begin with analysis of the eigenmode spectrum (Fig.2) of the PCS applying the guided-mode expansion (GME) method. The spectrum of energies and inverse lifetimes of upper(UP) and lower(LP) exciton-polariton branches calculated using GME is shown in Fig. 3(a,b). Figure 3(a) demonstrates strong coupling between the exciton and the off-Gamma BIC which manifests itself as an avoided resonance crossing with Rabi splitting of the order of 3 meV. The radiation losses of both exciton-polariton branches are shown in Fig. 3(b) in comparison with the losses of photonic and exciton modes. The lifetime of polariton modes can exceed the bare exciton lifetime by almost three orders of magnitude and reaches 0.66 ns. Such giant enhancement is the special effect intrinsic to BIC. The most important, Fig. 3(b) shows the maximal lifetime can be realized not at the center or the edge of the Brillouin zone, but at the point of phase space, where the group velocity of the mode is finite. For the LP branch, this practically means that polaritons can condense to a long-living state with nonzero energy flow at low temperatures, resulting in moving condensate. Our findings open new route for the realization of the moving exciton-polariton condensates with non-resonant pump and without the Bragg mirrors which is of paramount importance for polaritonic devices.

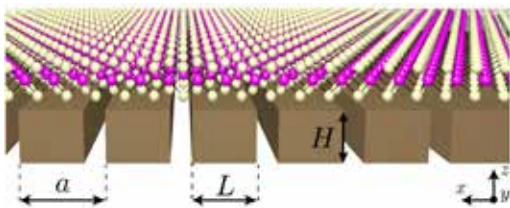


Fig1.jpeg

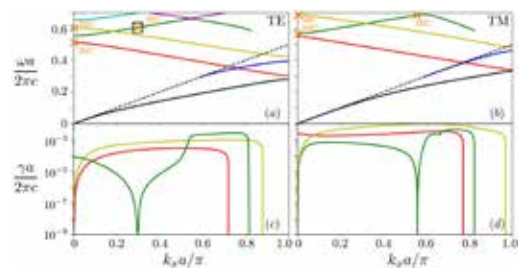


Fig2.jpeg

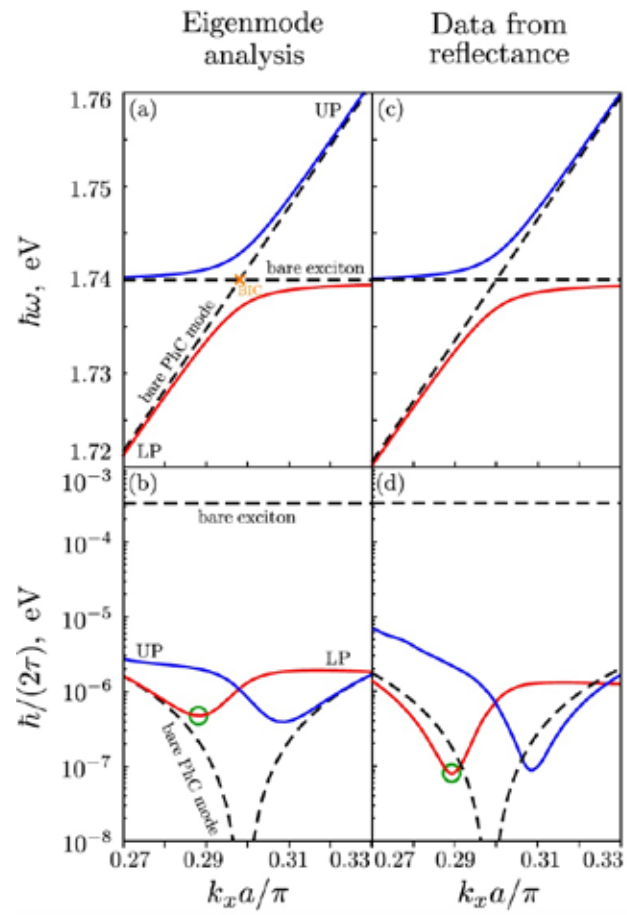


Fig3.jpeg

# Self-trapping of optical solitons in double Josephson junctions formed by spatially coupled soliton and surface-plasmons

Wednesday, 3rd October @ 13:30: Poster Session (HALL & ROOM 3) - Poster - Abstract ID: 294

*Dr. Güneş Aydınođan*<sup>1</sup>, *Prof. Kaan Güven*<sup>2</sup>

1. Vestel Electronics Corp., 2. Koç University

Transfer of population between a surface plasmon excitation on a metal surface and a spatially coupled optical soliton in a nonlinear dielectric waveguide bears similarities to the transition dynamics of a Josephson junction in three-level Bose-Einstein condensates, which demonstrates that a photonic Josephson junction, in which a Kerr-type nonlinearity is sandwiched between cascaded dielectric and metal layers on both sides, can be obtained through a surface plasmon-soliton-surface plasmon coupled optical system. The nonlinear coupling that inherently depends on the population imbalance of the levels is the driving parameter of this type of transition. The physics behind the transition dynamics in both numerical and analytical investigative basis reveals a well-known quantum mechanical phenomenon: macroscopic self-trapping of soliton state. This phenomenon is based on a quantum theory of light propagation in a system of two optical waveguides in which tunneling is enabled by a common continuum of modes coupled to both optical channels. For classical light waves, the emergence of a trapped state placed in the continuum is caused by Fano interference between different light leakage channels. This paper claims that plasmonic structures originally designed to mimic the quantum mechanical phenomena, may exhibit themselves as proper analogues of macroscopic quantum self-trapping. Transfer of population between three states results periodic behavior caused by the dissipationless characteristics of the system. However, the system can be configured into a particular state, in which the soliton amplitude oscillations can be suppressed into stationary soliton propagation, so that the soliton channel becomes a dark state between two surface plasmons, which otherwise couldn't affect one another. This phenomenon can be obtained for a large combination of system parameters, as well as the initial surface plasmon and the soliton amplitudes within the physical limitations. The conditions that yield the self-trapping are discussed along with the realistic parameters for experimental realization.

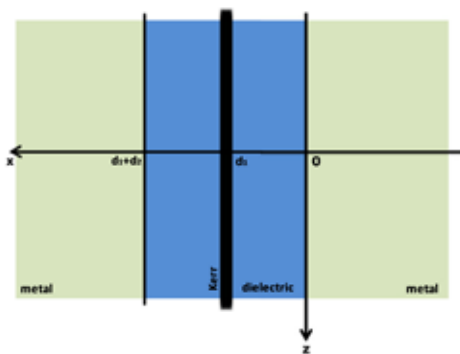


Figure 1 - schematics.jpg

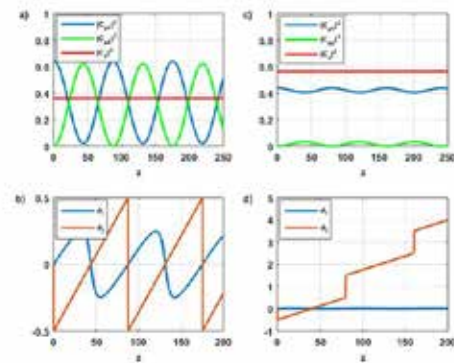


Figure 2 - transition dynamics.jpg

---

# Fabrication of Fluorescence Graphene Quantum Dots/CoFe<sub>2</sub>O<sub>4</sub>@SiO<sub>2</sub> Nanoparticles and Potential Application for Targeted Drug Delivery and Fluorescence Imaging of Cancer Cells

---

Wednesday, 3rd October @ 13:30: Poster Session (HALL & ROOM 3) - Poster - Abstract ID: 401

---

*Ms. Yun TENG<sup>1</sup>, Prof. Philip W. T. Pong<sup>1</sup>*

*1. The University of Hong Kong*

## **Introduction**

Researchers are placing much efforts on the nanocomposites with physiochemical properties. Graphene quantum dots (GQDs) have attracted remarkable interest in drug delivery and biosensing attributed to their tunable photoluminescence and great biocompatibility<sup>1</sup>. Moreover, inverse spinel cobalt ferrite (CoFe<sub>2</sub>O<sub>4</sub>) is gaining significant attention due to its moderate saturation magnetization and great chemical-stability<sup>2</sup>. The CoFe<sub>2</sub>O<sub>4</sub> nanoparticles present promising potential in biomedical application, especially in targeted drug delivery that can alleviate the side effects of conventional chemotherapy by reducing the systemic distribution of drugs. However, there are no reports of GQDs/CoFe<sub>2</sub>O<sub>4</sub> based nanocomposites for targeted drug delivery and fluorescence imaging of cancer cells.

## **Methods**

In this work, we fabricated the novel GQD/CoFe<sub>2</sub>O<sub>4</sub>@SiO<sub>2</sub>-FA nanoparticles and investigated their potential application as the fluorescence nanoprobe for the tumor-targeted drug delivery. GQDs were synthesized by the carbonization of citric acid (CA). The CoFe<sub>2</sub>O<sub>4</sub> were synthesized via thermodecomposition. The surface modification of CoFe<sub>2</sub>O<sub>4</sub> nanoparticles with silica and amine group enabled the covalent bonding with GQDs. Then the attached FA led to the tumor-targeted delivery and intracellular release of anticancer drug DOX in Hela cells (Fig.1).

## **Results and discussion**

We show that the resulting CoFe<sub>2</sub>O<sub>4</sub> nanoparticles possessed an average size of 15.3±1.7 nm (Fig.2a). The spherical GQDs with the average size of 3 nm exhibited blue fluorescence under 365nm UV light and no fluorescence in bright field compared with blank solvent (Fig.2b-2d), indicating the rendered blue fluorescence property of the fabricated GQDs. The drug loading capacity onto GQD/CoFe<sub>2</sub>O<sub>4</sub>@SiO<sub>2</sub>-FA was explored. The qualitative and quantitative analyses of cellular drug release in vitro and the fluorescence imaging of living Hela cells were performed. The biocompatibility of fabricated GQD/CoFe<sub>2</sub>O<sub>4</sub>@SiO<sub>2</sub> nanoparticles was confirmed with cytotoxicity assessment.

## **Conclusion**

We fabricated the fluorescence GQD/CoFe<sub>2</sub>O<sub>4</sub>@SiO<sub>2</sub>-FA nanoparticles and explored the potential application for targeted drug delivery and fluorescence imaging of cancer cells. These GQD@CoFe<sub>2</sub>O<sub>4</sub> based nanocomposite could be a promising platform for cancer therapy, leading to further developments of intelligent anticancer drug carrier.

## **Reference**

1. Y. Li et. al, Adv. Mater. 23, 776-780 (2011).
2. Urs. Häfeli et. al, Springer, (2013).

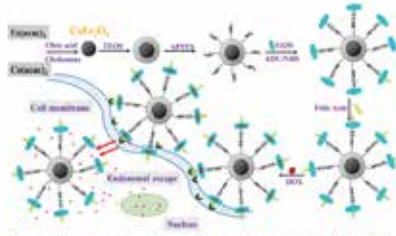


**Fig. 1** Schematic illustration for the synthesis of GQD/CoFe<sub>2</sub>O<sub>4</sub>@SiO<sub>2</sub> nanoparticles and working protocol for targeted drug delivery.

Fig.1.png



**Fig. 2** (a) TEM image of CoFe<sub>2</sub>O<sub>4</sub> nanoparticles, (b) TEM image of GQDs, (c) Bright field optical image and (d) 365nm UV light optical image of GQDs (right) and blank solvent (left).

Fig.2.png

# Experimental Demonstration of the Purcell Effect in Silicon Mie-resonators with Embedded Ge(Si) Quantum Dots

Wednesday, 3rd October @ 13:30: Poster Session (HALL & ROOM 3) - Poster - Abstract ID: 545

**Ms. Viktoriia Rutckaia<sup>1</sup>, Dr. Mihail Petrov<sup>2</sup>, Dr. Frank Heyroth<sup>1</sup>, Dr. Alexey Novikov<sup>3</sup>, Dr. Vadim Talalaev<sup>1</sup>, Prof. Joerg Schilling<sup>1</sup>**

1. Martin-Luther University, 2. ITMO University, 3. IPAM Nizhny Novgorod

CMOS-compatible light emitters are intensely investigated for integrated active silicon photonic circuits. One of the approaches to achieve on-chip light emitters is the epitaxial growth of Ge(Si) QDs on silicon. Their broad emission in 1.3-1.5  $\mu\text{m}$  range is attractive for the telecomm applications.

We investigate optical properties of Ge(Si) QD multilayers, that are grown in a thin Si slab on a SOI wafer, by steady-state and time-resolved micro-photoluminescence. We identify Auger recombination as the governing mechanism of carrier dynamics in such heterostructures.

Then we demonstrate the possibility of light manipulation at the nanoscale by resonant nanostructures investigating Si nanodisks with embedded Ge(Si) QDs. The nanodisks were fabricated using either focused ion beam milling or by the combination of electron-beam lithography with reactive ion etching (Figure 1). We show that the Mie resonances of the disks govern the enhancement of the photoluminescent signal from the embedded QDs due to a good spatial overlap of the emitter position with the electric field of Mie modes (Figure 2). Furthermore, we engineer collective Mie-resonances in a nanodisk trimer resulting in an increased Q-factor and an up to 10-fold enhancement of the luminescent signal due to the excitation of anti-symmetric magnetic and electric dipole modes (Figure 3).

Using time-resolved measurements we show that the minima of the effective lifetime coincide with the positions of the Mie resonances for a large variation of disk sizes confirming the impact of the Purcell effect on QD emission rate (Figure 4). Purcell factors at the different Mie-resonances are determined and agree well with the modelled ones.

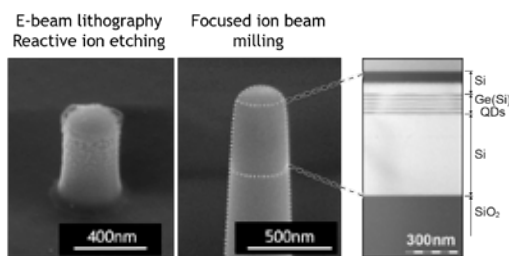


Figure 1.png

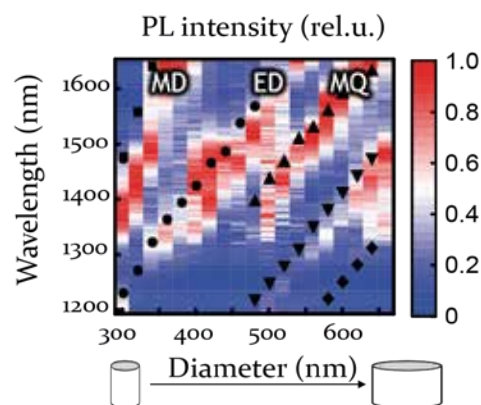


Figure 2.png



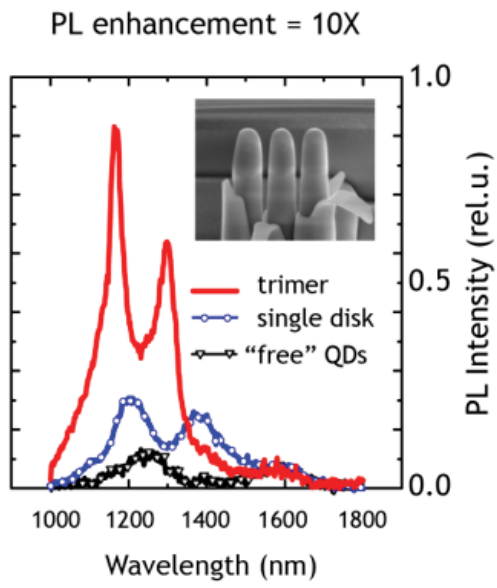


Figure 3.png

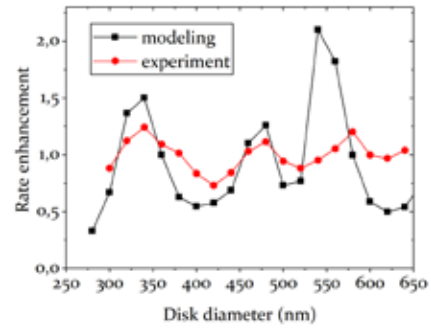


Figure 4.png

---

# Cellulose based photonic architectures

---

Wednesday, 3rd October @ 13:30: Poster Session (HALL & ROOM 3) - Poster - Abstract ID: 91

---

*Ms. Camilla Dore*<sup>1</sup>, *Dr. André Espinha*<sup>1</sup>, *Mr. Cristiano Matricardi*<sup>1</sup>, *Dr. Maria Isabel Alonso*<sup>1</sup>, *Dr. Alejandro Goni*<sup>2</sup>, *Dr. Johann Osmond*<sup>3</sup>, *Dr. Agustin Mihi*<sup>1</sup>

1. ICMAB-CSIC, 2. ICMAB-CSIC, ICREA, 3. ICFO

## Introduction

Cellulose is the most abundant polymer on Earth and for centuries has had a wide technological impact in areas such as textile, packaging or knowledge storage. It is biodegradable, biocompatible and possesses excellent mechanical characteristics that have raised the interest of many engineering fields [1]. The versatility of cellulose has opened new venues in advanced materials in electronics, energy or biological applications [2]. Here we introduce a cellulose derivative as an eco-friendly and water developable resist. Furthermore, we revolutionize the field of transient photonics by directly moulding the cellulose itself into flexible photonic and plasmonic architectures.

## Methods

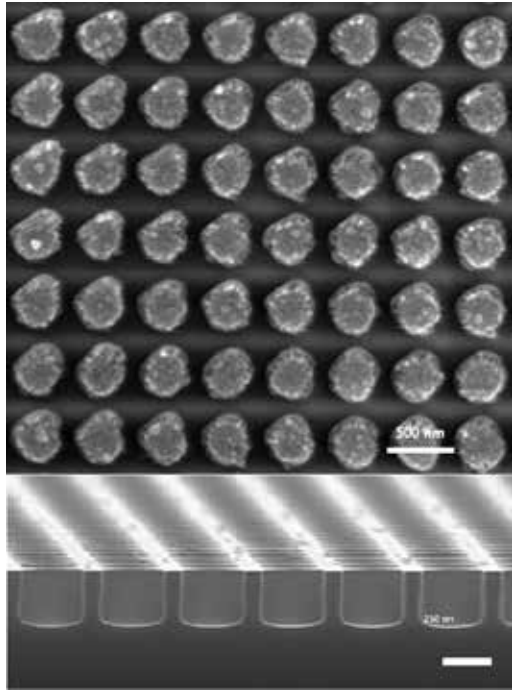
We combine cellulose with nanoimprinting lithography (NIL), the most promising method for mass-produced inexpensive nanostructures over large areas and with a very low density of defects [3].

## Results and discussion

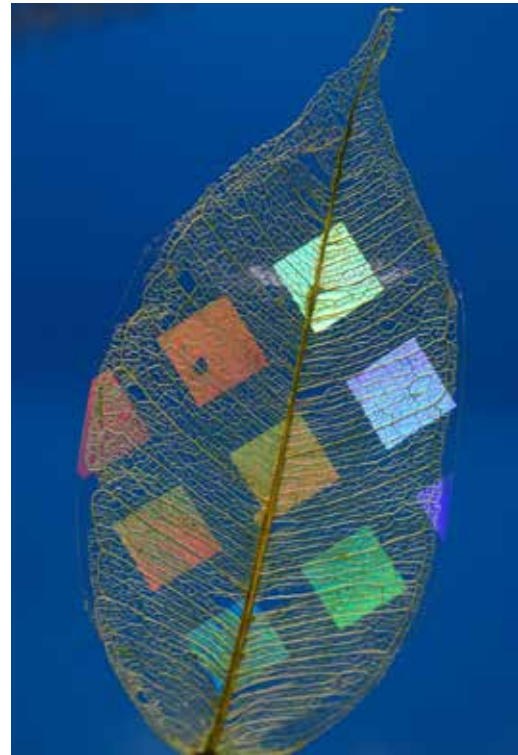
We fabricated free standing cellulose photonic and plasmonic membranes, illustrating their outstanding performance in several applications such as structural colours, photoluminescence enhancement and as disposable Surface Enhanced Raman Scattering substrates [4]. Furthermore using cellulose as a resist and NIL, we are able to pattern silicon wafers or fabricate metallic nanoparticle arrays using water as the only solvent [5]. Finally we demonstrate herein the fabrication of PMMA and HPC stacks in which one of the two materials can be selectively developed.

## References

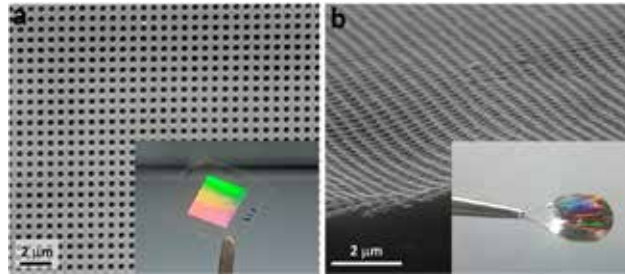
- [1] Hoeng, F. et al. *Nanoscale* 8, (2016)13131-13154.
- [2] Polavarapu, L. et al. *Phys. Chem. Chem. Phys.* 15 (2013) 5288-5300 .
- [3] J. A. Rogers, H. H. Lee, Wiley-Blackwell, Oxford (2009).
- [4] A. Espinha et al. *Nature Photonics*, 12, 343–348 (2018) .
- [5] C. Dore, J. Osmond, A. Mihi, *Nanoscale* (2018) on press.



Nanofabrication using cellulose based resist.jpg



Photonic leaf skeleton.jpg



Cellulose free standing membranes.jpg

# Ultrahigh Purcell factor achieved in a single sphere-gap-cone hybrid nanoantenna

Wednesday, 3rd October @ 13:30: Poster Session (HALL & ROOM 3) - Poster - Abstract ID: 34

*Ms. Yali Sun<sup>1</sup>, Dr. Sergey Makarov<sup>1</sup>, Dr. Dmitry Zuev<sup>1</sup>*

*1. ITMO University*

Hybrid nanostructures exhibit extraordinary optical properties combining near field enhancement and inherent magnetic and electric response induced by metal and dielectric components, respectively. Here, we study theoretically optical properties of a novel type of hybrid sphere-gap-cone nanostructure. We demonstrate, this type of nanostructure provides strong magnetic and electric response in the visible range. Especially, looking into single resonant wavelength indicates unidirectional scattering of this nanostructure. Besides, ultrahigh Purcell factor is achieved by placing a discrete dipole in the gap in different orientations.

A schematic of sphere-gap-cone nanostructure is presented in Fig. 1a. As can be seen, the gold sphere is located on the truncated crystalline silicon cone with a 10 nm gap in the middle. The bottom base's diameter as well as the height of the cone is 190 nm. The diameter of the cone upper base is half of the bottom base, i.e., 95 nm. Fig.1b indicates the scattering cross section of the novel sphere-gap-cone, in which points A, B, C are the resonances, respectively. Fig. 1c are the electric field distributions corresponding to points A, B, C. Obviously, resonances A, B covers dipole resonances. Moreover, the inset in Fig. 1b shows high directivity in one direction. Consequently, this nanostructure supports strong magnetic and electric response as well as unidirectional scattering in the visible range.

Fig. 2 represents the ultrahigh Purcell factor achieved in the sphere-gap-cone nanostructure. As usual, when dipole orientates along the z axis, we can obtain much higher Purcell factor (over 10000). If we change the dipole orientation to the x axis, the corresponding Purcell factor will reduce 40 times. Besides, this Purcell factor spectrum has a wide bandwidth resonance, which is promising for emission enhancements. In summary, we propose a novel hybrid sphere-gap-cone nanostructure, corresponding scattering cross section and near field distribution indicate this nanostructure provide strong magnetic and electric response as well as unidirectional scattering in the visible range. Besides, ultrahigh Purcell factor is achieved by placing a discrete dipole in the gap in various orientations. Thus this proposed type of hybrid nanostructure can be applied for sensing as well as optical modulators.

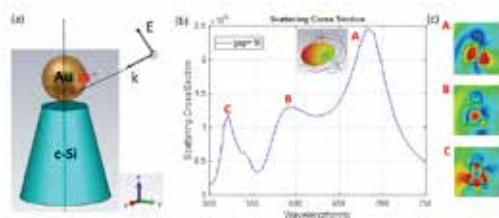


Fig. 1.png

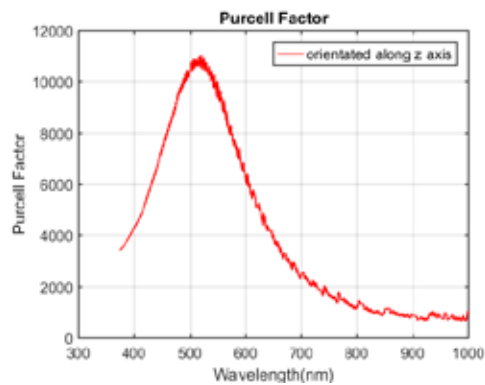


Fig. 2.png

---

# Dynamic plasmonic metasurface holograms

---

Wednesday, 3rd October @ 13:30: Poster Session (HALL & ROOM 3) - Poster - Abstract ID: 39

---

***Dr. Jianxiong Li*<sup>1</sup>, *Prof. Na Liu*<sup>1</sup>**

*1. Max Planck Institute for Intelligent Systems*

Plasmonic metasurfaces represent a new class of quasi two-dimensional metamaterials that provide fascinating capabilities for manipulating light with an ultrathin platform. Such metasurfaces allow for generating a wide range of position-dependent discontinuous interfacial phase profiles. By simply engineering the metasurface-induced phase profile, a nearly arbitrary wavefront can be achieved. This unique approach promises interesting device applications beyond the scope of conventional components that rely on gradual phase accumulation for wavefront shaping. Several exotic phenomena have been demonstrated using metasurfaces including anomalous reflection and refraction,[1] the spin Hall effect of light, plasmonic metalens, optical polarization conversion, among others. Recently, metasurfaces have been also used to achieve computer-generated holograms (CGH) with high efficiency and high image quality in the visible and near-infrared regions.[2] The dispersionless nature of metasurfaces enables broadband operation without sacrificing the image quality. Thus, metasurface holograms feature a great advantage over other conventional methods such as CGH with spatial light modulators or diffraction optical elements.

In this work, we demonstrate dynamic plasmonic holography based on catalytic magnesium (Mg) metasurfaces in the visible range. Through the unique hydrogenation and dehydrogenation between Mg and magnesium hydride (MgH<sub>2</sub>), different information components on the plasmonic holograms become fully addressable in space and can be individually switched on/off. These results in dynamic plasmonic holograms with designated multiple states, giving rise to high-level information control with unprecedented dynamic performance. Our work outlines the inevitable transformation from metasurfaces to metadevices, opening the door to a futuristic research horizon. Such dynamic plasmonic holograms will allow for a wealth of applications for high-resolution displays,[3] advanced security labels, high-density data storage and information processing.

## References

- [1] Yu, N. *et al.* Light Propagation with phase discontinuities: generalized laws of reflection and refraction. *Science* **334**, 333–337 (2011).
- [2] Zheng, G. *et al.* Metasurface holograms reaching 80% efficiency. *Nat. Nano.* **10**, 308–312 (2015).
- [3] Duan, X. *et al.* Dynamic plasmonic colour display. *Nat. Commun.* **8**, 14606 (2017).

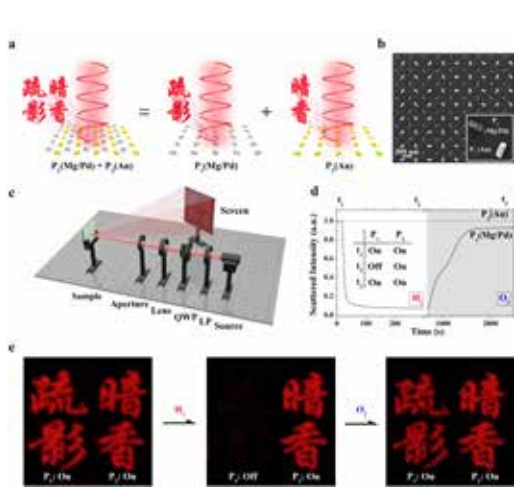


Figure1.jpg

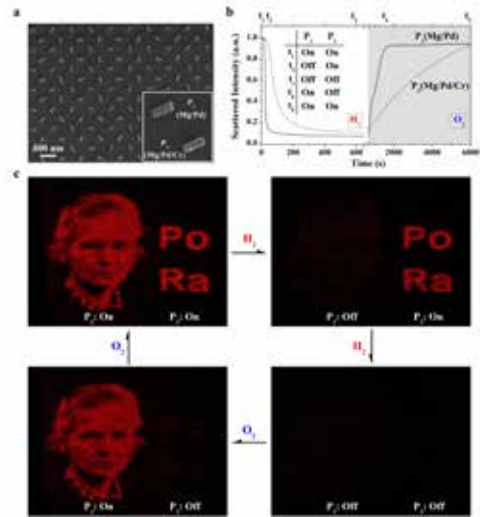


Figure2.jpg

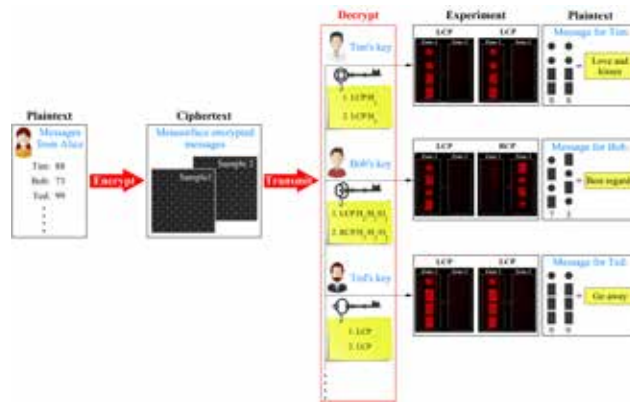


Figure3.jpg

---

# Temperature-dependent optical properties of plasmonic nanosystems

---

Wednesday, 3rd October @ 13:30: Poster Session (HALL & ROOM 3) - Poster - Abstract ID: 51

---

***Mr. Michele Magnozzi*<sup>1</sup>, *Ms. Marzia Ferrera*<sup>1</sup>, *Dr. Francesco Bisio*<sup>2</sup>, *Prof. Maurizio Canepa*<sup>1</sup>**

*1. Università di Genova, 2. CNR-SPIN*

The variation of optical properties of metals with temperature is becoming an increasingly relevant issue in fields like thermoplasmonics, particle-mediated hyperthermia or heat transfer at the nanoscale. Indeed, when light-induced heating of metallic nanoparticles is performed, the systems' properties are modified, dramatically altering the heating process itself.

Whereas temperature dependencies of bulk materials are relatively well investigated, much less is known about the same phenomenon for metallic nanoparticles, where surface effects and finite-size constraints may contribute to strongly affect the temperature-dependent system response. For example, it is known that for thin Au films there is an increase of more than 100% of the imaginary part of the Au permittivity going from room temperature to 500 °C [1]. For particles, it could be in principle significantly different.

In typical laser-heating experiments on nanoparticle systems, the actual system temperature at the nanoscale is often determined *ex-post* by means of simulations that, at their best, employ the temperature-dependent permittivity of the corresponding bulk systems. Here we attempt to reverse this paradigm by measuring the optical response of a system of nanoparticles heated at a well-defined temperature, and retrieving the actual temperature-dependent system response.

We present a spectroscopic-ellipsometry study of 2D arrays of gold nanoparticles [2] at variable temperatures in the 245-1700 nm spectral range and in the 25 °C to 350 °C temperature interval. The ellipsometric spectra were acquired in-situ, under high-vacuum conditions, employing a custom-built roll-on/roll-off mini-vacuum chamber fitted to a J.A. Woollam M-2000 ellipsometer [3]. Using a dedicated effective medium approximation developed for this kind of systems [2], we are able to reproduce the SE spectra at different temperatures, noticing that contributions from surface softening or melting may play a key role as the temperature is increased.

## References

- [1] H. Reddy, U. Guler, A.V. Kildishev, A. Boltasseva, V.M. Shalaev. *Optical Materials Express*, **6**, 2776-2802 (2016)
- [2] L. Anghinolfi, R. Moroni, L. Mattera, M. Canepa, F. Bisio. *Journal of Physical Chemistry C*, **115**, 14036-14043 (2011).
- [3] M. Magnozzi, F. Bisio, M. Canepa, *Applied Surface Science*, **421**, 651-655 (2017).

# Tunable MIM plasmonic near-infrared transmissive metasurface

Wednesday, 3rd October @ 13:30: Poster Session (HALL & ROOM 3) - Poster - Abstract ID: 293

**Mr. Arash Nemati<sup>1</sup>, Prof. Minghui Hong<sup>1</sup>, Dr. Jinghua Teng<sup>2</sup>**

1. National University of Singapore, 2. IMRE (A\*STAR)

Metasurfaces are engineered surfaces consisting of deep subwavelength artificial structures that enables full control of the electromagnetic waves. Metasurfaces are not only being used in many applications from microwave to optics but also paving the way to many new exciting applications such as programmable on-demand optics and photonics in the near future. Active control of light absorption in the near-infrared spectrum has very practical and fundamental significance. Although different mechanisms and materials including graphene [1] and ITO [2] has been used to design such tunable metasurfaces, they have mostly been reflection type, at longer wavelength up to middle-infrared, and very sensitive to light polarization. Here, we demonstrate an MIM plasmonic transmissive light modulator metasurface in the near-infrared spectrum.

Each unit cell includes circular MIM structure (radius=530 nm) with 70 nm thick Aluminum on top and bottom and 60 nm thick SiO<sub>2</sub> as an insulator and 6 nm thick ITO as the tunable material between top Al and SiO<sub>2</sub> insulator (Figure 1). Each unit cell is 800 nm square with 30 nm thick beam (DC connection) attached to both sides of each circular resonator. ITO, a transparent conductive oxide, is modeled using Drude model with the plasma frequency  $\omega_{p0}=8.24\times 10^{14}$  rad/s [3]. The refractive index has the highest change in the wavelength range of 1500-2000 nm when the plasma frequency is increased to  $\omega_{p1}=2.55\times 10^{15}$  rad/s [3] after applying DC voltage (Figure 2), while the extinction coefficient is increased as a result. The transmission coefficient is increased from 0% to 20% at the wavelength of 1650 nm while the reflection coefficient is dropped from 66% to 48% (Figure 3). The transmission coefficient drops 50% from 65% to 15% at 1820 nm while the reflection coefficient increases from 0% to 22%.

Here we demonstrate a tunable transmissive metasurface using ITO films in the MIM resonators. The performance of the metasurface is shown using FDTD simulations. The operational frequency of the metasurface could be easily altered by changing the radius of resonators and ITO film properties during the fabrication process.

[1] 10.1021/ph5003279

[2] 10.1021/acs.nanolett.6b00555

[3] 10.1364/OL.42.000005

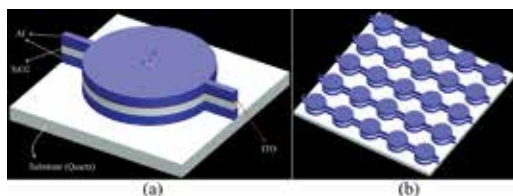


Figure 1. 3d schematic view of the a unit cell and b 5 5 array metasurface.jpg

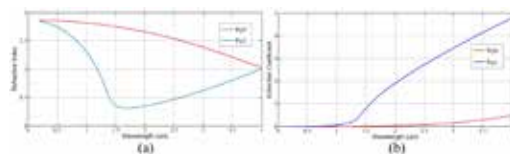


Figure 2. a refractive index and b extinction coefficient of the ito film.jpg



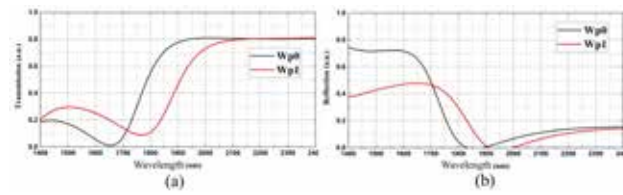


Figure 3. simulated a transmission and b reflection coefficients of metasurface at different plasma frequencies.jpg

# Development of a rapid measurement method of bacterial concentration by light-induced assembly based on photothermal effect

Wednesday, 3rd October @ 13:30: Poster Session (HALL & ROOM 3) - Poster - Abstract ID: 326

Mr. Yasuyuki Yamamoto<sup>1</sup>, Prof. Shiho Tokonami<sup>1</sup>, Prof. Takuya Iida<sup>1</sup>

1. Osaka Prefecture University

Photothermal effect at the solid-liquid interface under laser illumination can generate a bubble and fluid flow<sup>1,2</sup> to assemble dispersoids within a few minutes. Such a phenomenon enables us to colloidal lithography<sup>3</sup> and concentration measurement of small objects (microparticles, bacteria, *etc.*)<sup>4</sup>. In this method, it is required to assemble various dispersoids (constituent material, size, *etc.*) at an arbitrary place with high efficiency and good reproducibility. However, there is little knowledge on physicochemical mechanism for the highly efficient assembly and the control of assembly dynamics. Here, focusing on the surface modulation of the bubble with a nonionic surfactant, we have clarified that this process greatly affects on assembly dynamics of polystyrene microparticles (PS) (Figure 1a) and improves assembly efficiency (= the number of assembled PS / total number of PS in liquid), 10-20 times in comparison with the case of no surfactant (Figure 1b)<sup>5</sup>. The number of assembled PS was obtained by dividing the volume of the assembled region by the volume of a PS. This result can extend the limit of measurable concentration by one order. Furthermore, we revealed the influence of concentration and constituent material of dispersoids (PS and bacteria, SA) on assembly efficiency (Figure 1c) and led to improvement of measurement precision. These results are significant for the laser-induced assembly leading to rapid concentration measurement of dispersoids available for the hygiene inspection, microfabrication, and so on.

References:

1. Baffou G.; Monneret S. *et al.*; *J. Phys. Chem. C* **2014**, *118*, 4890-4898.
2. Lin L.; Zheng Y.; *Nano Lett.* **2016**, *16*, 701-708.
3. Fujii S.; Haga M. *et al.*; *Langmuir* **2011**, *27*, 8605-8610.
4. Yamamoto Y.; Iida T.; Tokonami S. *et al.*; *Opt. Mater. Exp.* **2016**, *6*, 1280-1285.
5. Yamamoto Y.; Tokonami S.; Iida T.; *in preparation.*

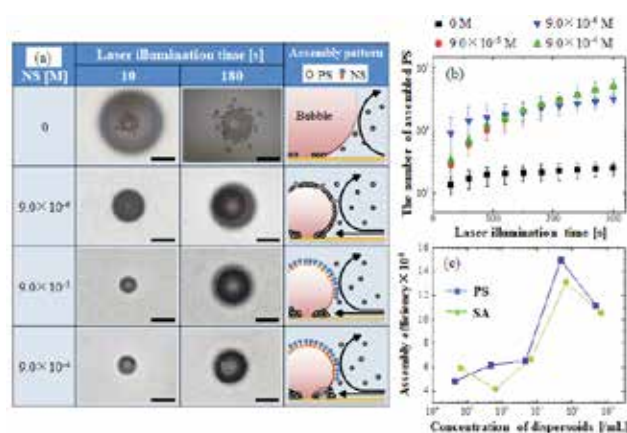


Figure 1. (a) Transmission images at 10, 180 s after laser illumination and schematic illustrations of assembly pattern in each concentration of the surfactant. The length of scale bar is 50  $\mu\text{m}$ . (b) The number of assembled PS as a function of laser illumination time in each concentration of the surfactant. (c) Assembly efficiency as a function of concentration of dispersoids (PS, SA).

Figure1.png

## Generation of shear waves in a soft medium by 2.1 $\mu\text{m}$ light source based on periodically poled ferroelectric crystal

---

Wednesday, 3rd October @ 13:30: Poster Session (HALL & ROOM 3) - Poster - Abstract ID: 464

---

***Dr. Liliana Martinez*<sup>1</sup>, *Dr. Juan Gonzalez*<sup>1</sup>, *Mr. Amaury Garcia*<sup>1</sup>, *Dr. Luis Rios*<sup>2</sup>, *Dr. Rurik Farias*<sup>1</sup>,  
*Dr. Jose Enriquez*<sup>1</sup>**

*1. Universidad Autónoma de Ciudad Juárez, 2. CICESE*

Optical coherence tomography (OCT) is a noninvasive technique capable of imaging tissue microstructure at high spatial resolution. PhS-OCT is an OCT based technique which can be used to detect surface acoustic waves propagating on skin and cornea surfaces, leading to quantification of the elasticity of underlying tissues. For generating shear waves propagating within a soft medium a piezoelectric actuator is used. Because tissue presents high absorption for electromagnetic waves at  $\sim 2 \mu\text{m}$  wavelength, in this work we propose a simple device that emits nanosecond pulses at a wavelength of 2.1  $\mu\text{m}$  as an alternative for shear waves generation. This device is based on a periodically poled ferroelectric crystal pumped with a Nd:YAG pulsed laser source to obtain the emission. The conversion from 1.06 to 2.1  $\mu\text{m}$  was achieved by optical parametric generation (OPG) at degeneracy point where signal wave with 2128 nm wavelength was generated.

---

# Combined effect of Etched diameter and thickness of Reduced Graphene Oxide coating on the sensitivity of Fiber Bragg Grating sensors for DNA application

---

Wednesday, 3rd October @ 13:30: Poster Session (HALL & ROOM 3) - Poster - Abstract ID: 488

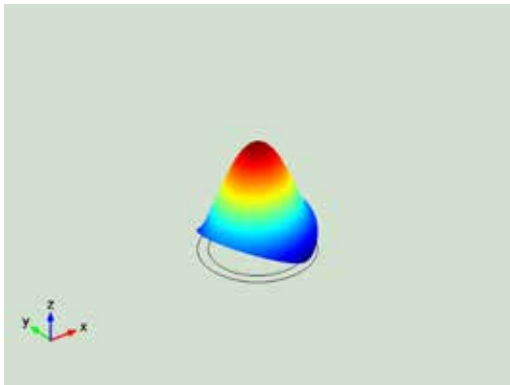
---

***Mrs. Kavitha Srinivasan<sup>1</sup>, Prof. Asokan Sundarrajan<sup>1</sup>, Ms. Radhika Nambannor<sup>1</sup>***

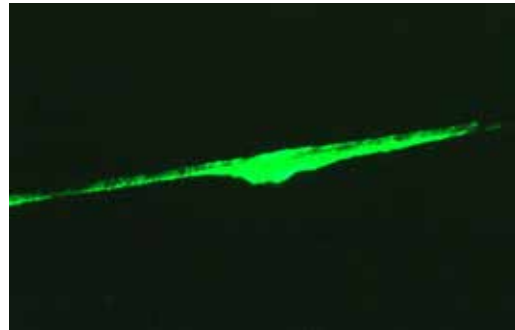
*1. Indian Institute Of Science, Bengaluru*

Etched Fiber Bragg Grating (eFBG) sensors find applications in various fields. Etching of sensors and coating of nano materials over them is a widely researched field. Etching of sensors to improve their sensitivity to the surrounding environmental conditions by the interaction of evanescent waves have been studied extensively and many theoretical proofs have also been published. The electrical, mechanical, optical properties, etc. of the optical fibers have also been research topics from many years.

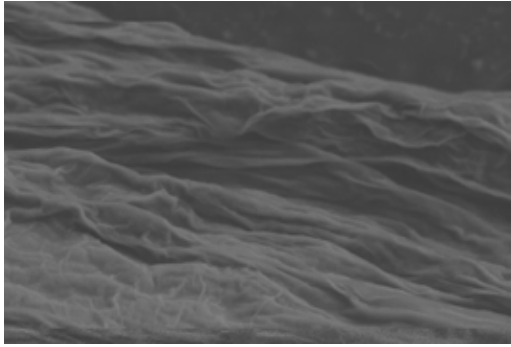
In this paper the combined effect of both the etching diameter of the Fiber Bragg Grating sensors and the thickness of reduced Graphene Oxide (rGO) coating have been studied with respect to one application of sensing i.e. DNA attachment. This is an important observation as it gives an insight into the requirement of the sensor; higher or lower etched diameters, thin or thick coating; these can be decided upon as per the application requirement. Optimization of the initial steps during sensor preparation can be reduced to a large extent with this data. The experimental results are also backed with simulation results using COMSOL Multi physics 5.2<sup>®</sup> and characterized using Optical fluoroscope and Scanning Electron Microscope.



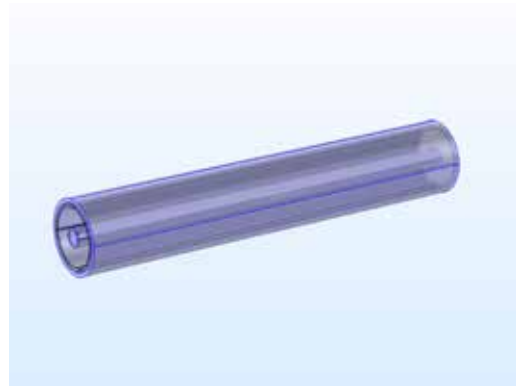
Electric field lp01 in the core of the sensor using  
comsol multiphysics 5.2.png



Dna coating on etched fbg sensor.png



Rgo coating on etched fbg sensor.png



Fiber bragg grating sensor model in comsol  
multiphysics 5.2.png

---

## A new fluorescent 1,8-naphthalimide based chemosensor for detection of dinitrobenzene

---

Wednesday, 3rd October @ 13:30: Poster Session (HALL & ROOM 3) - Poster - Abstract ID: 52

---

**Dr. Jiri Zednik<sup>1</sup>, Prof. Vladimir Sedlarik<sup>2</sup>, Dr. Diana Harea<sup>2</sup>**

*1. Department of Physical and Macromolecular Chemistry, Faculty of Science, Charles University in Prague., 2. Center of Polymer Systems, Tomas Bata University in Zlín*

The development of chemosensors for the detection of specific ions in solution is a current topic of research, which elegantly combines preparative organic chemistry and spectroscopic studies, with the ultimate goal of applying such sensors for biological and environmental purposes. Fluorescent probes are frequently used as the detection unit of chemosensors, combined with a recognition unit, nonetheless, some fluorescent probes may act as a single detection/recognition system.

Therefore, a novel highly water-soluble fluorescence sensing 1,8-naphthalimide unit has been designed, synthesized and investigated as a fluorescent probe. The obtained probe exhibited bright green photoluminescence under UV irradiation. The fluorescence properties of this probe toward various ions of aromatic elements have been investigated by UV-Vis and fluorescence spectra in water solution. According to the ion titration experiments, 1,8-naphthalimide unit showed high sensitivity and selectivity for detection of dinitrobenzene over other ions of aromatic nitro compounds. Upon progressive addition of dinitrobenzene, a gradual quenching process in fluorescence intensity of 1,8-naphthalimide based sensor was observed, due to inhibition of the PET process. The fluorescent detection limits of 1,8-naphthalimide was calculated to be 0.15  $\mu\text{M}$  and the Stern-Volmer quenching constant was found to be  $K_{sv} = 3.32 \times 10^5 \text{ M}^{-1}$ . The higher sensitivity of synthesized 1,8-naphthalimide unit towards aromatic ions can be attributed to a combination of fluorescent, steric and electronic factors. These results indicate a greater sensitivity of the fluorescent probe towards dinitrobenzene ions, that the fluorescent 1,8-naphthalimide based chemosensor can be used as a potential probe for dinitrobenzene detection.

## Nanostructured Si- and Al for advanced microLED imaging

---

Wednesday, 3rd October @ 13:30: Poster Session (HALL & ROOM 3) - Poster - Abstract ID: 131

---

***Prof. Aliaksandr Smirnov<sup>1</sup>, Dr. Andrey Stepanov<sup>1</sup>, Mr. Yauhen Mukha<sup>1</sup>, Mr. Boris Kazarkin<sup>1</sup>, Mr. Ilya Zacharchenya<sup>1</sup>***

*1. Belarusian State University of Informatics and Radioelectronics*

The usage of nanostructured Si- and Al in high efficient CMOS compatible microLED imaging system will be the main issue of this presentation.

These systems can be incorporated in low cost high performance augmented- or virtual-reality products. They can be a real alternative to well known LCOS, QLED or OLED-on-Silicon approach.

In general, this microLED imaging system includes a matrix of a very fast electroluminescent nanoporous Si / nanostructured Al Schottki structures fabricated onto a Si wafer using standard CMOS technology. The light emission in visible spectral range is evident.

The resolution of a microLED imaging system can be very high due to small pixel size (in the range of 1,0  $\mu\text{m}$ ). Moreover, the electro optic response (switch on – switch off times) of a light emitting pixel is fast enough to address a large number of pixels in an independent manner using passive addressing technique.

In this presentation we will concentrate on the usage of novel technologies to fabricate nanostructured materials with unique features for high efficient EL- and conductive transparent layers.

Possible areas of application in low cost high performance augmented- or virtual-reality optical devices will be also discussed.

# Plasmon-enhanced Förster resonance energy transfer in Langmuir-Blodgett films based on organic dyes

Wednesday, 3rd October @ 13:30: Poster Session (HALL & ROOM 3) - Poster - Abstract ID: 317

**Prof. Niyazbek Ibrayev<sup>1</sup>, Dr. Evgeniya Selivertsova<sup>1</sup>, Ms. Nazerke Zhumabay<sup>1</sup>**

*1. Institute of Molecular Nanophotonics, Buketov Karaganda State University*

Nanoparticles and island films of metals are of particular interest for nanotechnology. The intermolecular electronic excitation energy transfer underlies in many important physical and photochemical processes. Despite the available studies, the mechanism of intermolecular energy transfer in the presence of plasmon nanoparticles remains poorly understood.

Here the results of studying of the interlayer energy transfer (FRET) between organic dyes on the surface of silver island films are presented.

The amphiphilic derivatives of Rhodamine B (HERB) and Nile red (NR) were chosen as an energy donor and acceptor. Island silver films (SIF) were deposited onto glass substrates by the method of thermal vacuum deposition. Then films of donor or acceptor were deposited onto SIF by Langmuir-Blodgett (LB) method on the KSV Nima trough. The distance from the dye film to the SIF was varied by monolayers of stearic acid (SA, molecule length  $\sim 0.2$  nm). The absorption and fluorescence spectra of the films were measured on the Cary and Eclipse (Agilent) spectrometers, correspondingly. The fluorescence lifetimes of the donor and acceptor were recorded by using of TCSPC system (Becker&Hickl) at  $\lambda_{\text{ex}}=488$  nm. The energy transfer efficiency was estimated by the Förster formula.

Studying of plasmon effect on pure donor and acceptor films have shown that increase in the fluorescence intensity of both HEBR and NR is approximately 25% was registered at a distance from the dye to the SIF of  $\sim 6$  nm (Figures 1 and 2).

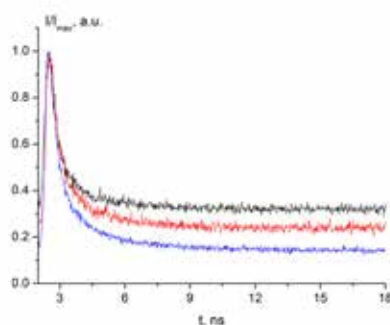
In FRET studies the fluorescence quenching of the donor and the appearance of sensitized fluorescence of the acceptor molecules were registered. Spectral-kinetic measurements of donor-acceptor films without SIF and in their presence have shown that the efficiency of energy transfer in the presence of silver nanoparticles was increased. At the same time, when the donor-acceptor film is separated from the SIF, the energy transfer efficiency was decreased (Table).

Thus, it was shown that, in the presence of an SIF, the efficiency of the FRET can be increased. In this case, the increase in  $E_{\text{ET}}$  can be associated with an increase in the fluorescence quantum yield of the energy donor upon direct contact with the SIF.

Table. Life times of fluorescence of energy donor in the presence of acceptor and SIF

Sample	$\tau_{\text{don}}$ , ns	$E_{\text{ET}}$
Donor	1.8	-
Donor +SIF	1.0	-
Donor +SA+ SIF	1.0	-
Donor +acceptor	1.10	0.38
Donor + acceptor +SIF	0.82	0.50
Donor + acceptor +SA+ SIF	0.80	0.2

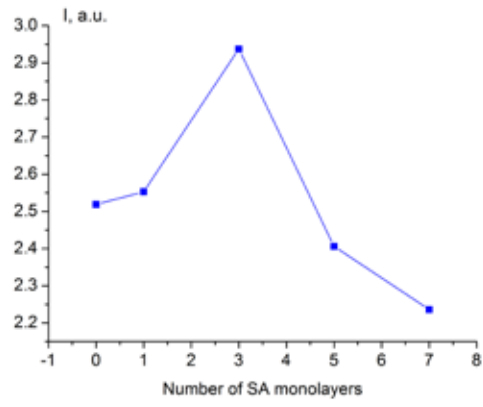
Table.jpg



Fluorescence decay kinetics of herb at various distance to the sif monolayers of sa 1 - pure dye 2

- 0 3 - 3.jpg





Distance dependence of fluorescence intensity of herb at various distance to the sif.jpg

## Improvement of the photoinduced birefringence in azopolymer PAZO doped with TiO<sub>2</sub> via thermal annealing

---

Wednesday, 3rd October @ 13:30: Poster Session (HALL & ROOM 3) - Poster - Abstract ID: 93

---

***Mr. Georgi Mateev*<sup>1</sup>, *Prof. Lian Nedelchev*<sup>1</sup>, *Prof. Dimana Nazarova*<sup>1</sup>, *Dr. Anton Georgiev*<sup>2</sup>**

*1. Institute of Optical Materials and Technology – Bulgarian Academy of Sciences, 2. University of Chemical Technology and Metallurg*

We present a study of the photoinduced birefringence in nanocomposite films of an azopolymer (PAZO) doped with nanoparticles (NP) with different concentrations before and after thermal treatment. The NP are spheres of TiO<sub>2</sub> with radius of 21nm. The concentrations of the NP were varied from 0% (non-doped azopolymer film) to 10 wt %. The thermal procedure includes 1 h at 200°C. Our previous studies of PAZO have indicated that the polymer is stable up to 270°C. We observe the dependance of the maximal birefringence induced with He-Cd laser ( $\lambda = 442$  nm) on the concentration of the TiO<sub>2</sub>NP. The birefringence increases for the samples after the thermal procedure and also the optimal concentration after heating is different than the optimal concentration before heating.

Authors are grateful for the financial support provided by National Science Fund of Bulgaria under the project ДФНП 17-57.

# Nonlinear optical behavior of metallic nanoparticle suspensions at high laser fluences

---

Wednesday, 3rd October @ 13:30: Poster Session (HALL & ROOM 3) - Poster - Abstract ID: 254

---

*Ms. Stefanie Dengler*<sup>1</sup>, *Dr. Bernd Eberle*<sup>1</sup>

*1. Fraunhofer IOSB*

A large number of nanomaterials as well as several organic molecular systems were found to possess strong nonlinear optical (NLO) response under intense illumination with laser light. These nonlinear (NL) materials are of special interest for a multitude of applications in optoelectronics, like optical switching and limiting, as well as in optical computing, optical memory and nonlinear spectroscopy. (1)-(3)

This work presents a detailed study on the NLO response of suspended metallic nanoparticles from low up to very high laser fluences. The different NL phenomena, like NL transmittance and NL scattering were investigated using nanosecond laser pulses at 532 nm. The nanoparticles were characterized regarding their linear optical properties by spectral transmission measurements and regarding their structure by electron microscopy. We discuss our results in terms of the suitability of metallic nanoparticle suspensions for optical limiting applications.

(1) R. S. Marder, Chem. Commun., 2006, 131–134

(2) P. C. Ray, Chem. Rev., 2010, 110, 9, 5332–5365

(3) N. Venkatram, R. S. S. Kumar, R. D. Narayana, S. K. Medda, S. De, G. De, J. Nanosci. Nanotechnol., 6, 2006, 1990-1994

# Assessment of the optical properties of two cover materials of greenhouse on the heat transfer

---

Wednesday, 3rd October @ 13:30: Poster Session (HALL & ROOM 3) - Poster - Abstract ID: 522

---

**Dr. LALMI Djemoui**<sup>1</sup>

*1. Unité de Recherche Appliquée en Energies Renouvelables, URAER, Centre de Développement des Energies Renouvelables, CDER, 47133, Ghardaïa, Algeria*

*In the present work, we interested to describe numerically the effects of the optical proprieties of the polyethylene and polycarbonate used as a cover of a greenhouse in a semi-arid region Ghardaïa from Algeria case study. In order to evaluate the importance of this proprieties like as the absorption coefficient and reflective index the ansys fluent computational fluid dynamic code [CFD] was used for 3D and 2D simulation for the radiation heat transfer and transport phenomena inside a tunnel greenhouse.*

# Fundamental study of the size-dependent optical properties of periodic arrays of nanoscale semiconducting fin structures

Wednesday, 3rd October @ 13:30: Poster Session (HALL & ROOM 3) - Poster - Abstract ID: 423

*Mr. Andrzej Gawlik*<sup>1</sup>, *Dr. Janusz Bogdanowicz*<sup>1</sup>, *Dr. Andreas Schulze*<sup>1</sup>, *Prof. Jan Misiewicz*<sup>2</sup>, *Prof. Wilfried Vandervorst*<sup>1</sup>

1. imec, 2. Wrocław University of Science and Technology

Understanding the interaction of light with semiconducting nanostructures is of increasing importance for nanoelectronic, photonic and photovoltaic applications. However, the physical mechanisms responsible for the size-dependent optical properties of such structures are not fully understood, as typically studied with purely numerical tools. In this work, we develop an analytical model for the size-dependent optical properties, such as reflectance, of periodic arrays of nm-scale semiconducting fins. Using a mode matching technique, we show that size-dependent optical properties of such structures are due to coupling between diffraction modes existing outside the arrays and waveguide modes inside the arrays. The model is validated with scatterometry spectra collected on Si fin arrays of varying geometry (Fig.1), as well as finite-element simulations. A good agreement for sub-400 nm part of the spectra is achieved, while a red-shift of the supra-400 nm part w.r.t. the model is attributed to the tilt of the fin sidewalls. We prove that the tilt is not impacting the near-UV spectra due to high absorption and low refractive index of Si in this range. Finally, we show that for sub-40 nm fins only 2 waveguide modes are sufficient to explain the complex spectra. The generated insight is crucial for the understanding of optical properties of nm-scale structures and will mitigate manufacturing, metrology and design of nanoelectronic, photonic and photovoltaic devices.

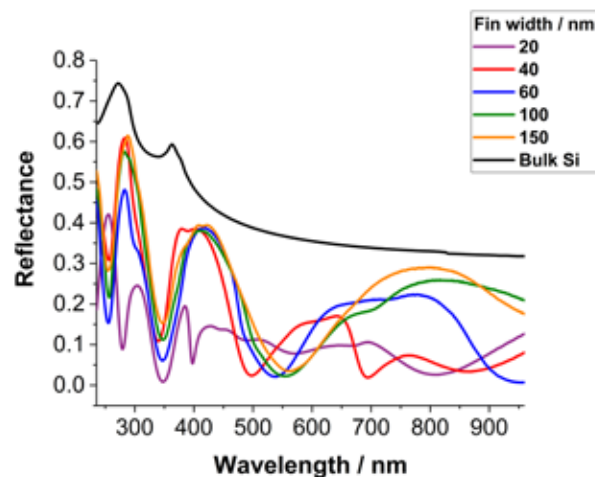


Fig.1.png

---

# Coherent reflectance of light from confined nanocolloid films: Modeling, experiment and applications

---

Wednesday, 3rd October @ 13:30: Poster Session (HALL & ROOM 3) - Poster - Abstract ID: 49

---

***Mr. Gesuri Morales-Luna<sup>1</sup>, Dr. Augusto García-Valenzuela<sup>1</sup>***

*1. Instituto de Ciencias Aplicadas y Tecnología, UNAM*

We analyze simple theoretical tools to calculate the optical reflectivity of a confined colloidal film. We extend a previously reported multiple-scattering model for the coherent reflectance of a colloidal half-space for the reflectance of a confined colloidal film. We refer to this model as the Coherent Scattering Model (CSM). We compare its predictions with experiments and effective medium models (EMM); namely the Maxwell Garnett and the so-called van de Hulst EMMs. We find an excellent agreement of the CSM with experimental measurements with gold, latex and metal-oxide nanocolloidal films. We show that the reflectivity of a confined colloidal film provides more information than the reflectivity of a semi-infinite space of the same colloid. Also, working with confined films, usually require only very small amounts of the sample. In this work, to test the theoretical models, we use an internal reflection configuration to measure the coherent reflectance of light from a colloidal thin film. The experimental setup consists of an optical cylindrical prism in contact with a nanocolloid layer of the sample and backed with a cover slide. The amount of sample used in each experiments is in the order of microliters. In this configuration there are two critical angles for light incident from the prism side, one between the prim's glass and the air outside, and another one between the prism and the nanocolloid sample. The theoretical models and the experiments show a high sensitivity of the reflectance to the optical properties of the nanocolloid between the two critical angles and specially just before the second critical angle. The method used in this work is suitable for developing a variety of compact sensors for characterizing and monitoring processes in nanocolloids. We will illustrate some sensing capabilities of the coherent reflectance of light at specific angles of incidence to monitor processes in thin colloidal films.

# Optical and electrical properties of coupled silver nanocrystal based flexible transparent nano-mesh film

---

Wednesday, 3rd October @ 13:30: Poster Session (HALL & ROOM 3) - Poster - Abstract ID: 429

---

***Ms. Mihyun KIM*<sup>1</sup>, *Mr. Hyungmok Joh*<sup>2</sup>, *Mr. Sunghoon Hong*<sup>3</sup>, *Prof. Soong Ju Oh*<sup>2</sup>**

*1. ETRI, 2. Korea University, 3. ETRI*

In this study, we present the flexible transparent conductive mesh pattern fabrication for flexible transparent EMI shielding film. The dilute silver nano ink are used as for mesh pattern on flexible PET substrate [1]. Using bar coater printing process, dilute silver nano ink was coated on flexible PET substrate and the transparent mesh pattern was formed by self-assembly process of drying step. Using nanocrystal coupling process, the transparent conductive mesh pattern was successfully fabricated on flexible PET substrate over large areas of up to a 10cm×10cm centimeters. For coupling between nanocrystals, the long ligand of the original nanocrystal was exchanged to -SCN, short conducting ligand by chemical process with low temperature[2]. The optical and electric property of the coupled silver nanocrystal based mesh film were studied by the measurement of sheet resistance, transmittance, and EM shielding effectiveness.

---

# Application of portable nanogenerator using friction charging

---

Wednesday, 3rd October @ 13:30: Poster Session (HALL & ROOM 3) - Poster - Abstract ID: 547

---

***Dr. Dongseob Kim***<sup>1</sup>

*1. KITECH*

To overcome the limitation of the battery life for portable electronics, the triboelectric nanogenerator (TENG), a new energy harvesting technology in the spotlight, has been demonstrated as a self-charging solution. However, it is difficult to combine TENGs with existing portable devices because of shape differences between the TENG based charging system and electronic devices. In this study, we successfully developed an elastic spiral triboelectric nanogenerator (ES-TENG) with cylindrical shape connected to a plate. With the flat plate substrate, devices can be attached easily to the plate and ES-TENG can work as a self-powered case accessory. The elastic sheet inside ES-TENG can generate multiple alternating current outputs during both extraction and self-retraction processes. As the elastic sheet is the key to ES-TENG, it is analyzed through dynamic motion of the elastic sheet. Furthermore, we propose fabrication guidelines for ES-TENG, depending on the size of portable electronics and based on the properties of the sheet. We demonstrate the possibility of ES-TENG as a self-charging case accessory that can light 120 white LEDs and power an engineering calculator and a rechargeable Ni-MH battery. Thus, our study is a potential energy harvesting package system for conventional portable electronics.



# Hydrogenated amorphous silicon for nano-photonic devices from visible to mid-infrared

Wednesday, 3rd October @ 14:30: Metamaterials (ROOM 1) - Oral - Abstract ID: 140

*Prof. Duk-Yong Choi*<sup>1</sup>

1. Australian National University

Silicon photonics has become the dominant technology for integrated photonic devices. It supports low power consumption, dense integration with CMOS electronics, low cost and is, therefore, promising for high-performance communication and computing. Crystalline silicon (c-Si) has been the main platform; however, high-quality c-Si is impossible to grow on a foreign substrate, implying that it cannot be used for advanced multilayer photonic integration. Hydrogenated amorphous silicon (a-Si:H) is emerging as an alternative in this perspective. A distinct advantage of a-Si:H comes from the fact that it can be deposited easily at low temperature on almost any substrates, facilitating back-end integration of a-Si:H photonic components on top of pre-processed CMOS electronic chips without any damage to the underlying metal wires. Despite of the recent progress in fabricating high quality devices, however there have been few studies of a-Si:H for 3-dimensional integrated photonic chips. In this work we have developed high quality hydrogenated amorphous silicon (a-Si:H) for various nano-photonic applications, and successfully demonstrated a vertically-stacked, amorphous silicon micro-ring resonators on c-Si photonic nanowire using SU-8 polymer interlayer. In addition the developed a-Si:H has comparable refractive index ( $\sim 3.6$  at 1550 nm), and wider transmission window from 700 nm up to 10 microns compared to c-Si. This leads to the demonstration of various nano-photonic devices in wide spectral range, including (1) angle tolerant colour filters, and a-Si:H metasurface for subtractive colouring; (2) ultrafast all-optical switch using two photon absorption of nano-resonators, micro-lens array in near-infrared (IR) band utilising conformal deposition of a-Si:H films, and an integration platform for 2D materials, for instance MoSe<sub>2</sub> for enhanced second-harmonic generation; (3) a-Si:H meta-lens at mid-infrared, and chemical sensors for proteins.

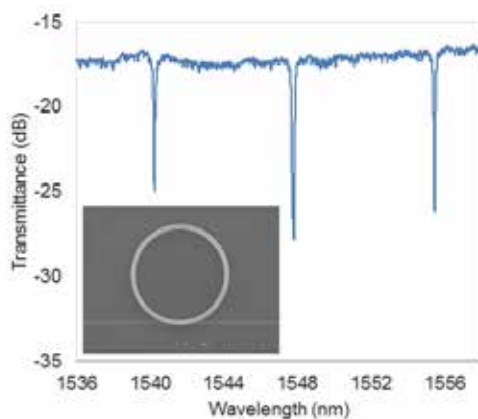


Fig1asi vcmrr.png

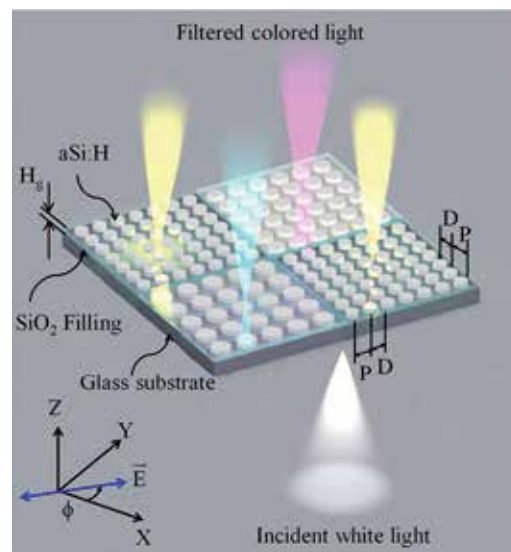


Fig2 asi-color filter.png

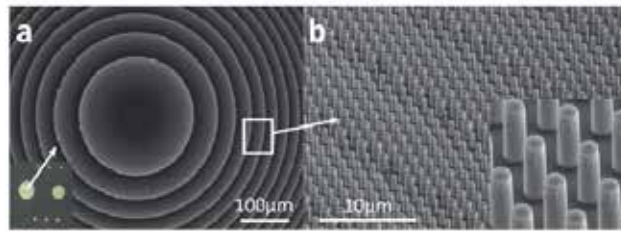


Fig3 asi mir metalens.png

---

# Large Area Optics with Silver Nanoparticles

---

Wednesday, 3rd October @ 14:47: Metamaterials (ROOM 1) - Oral - Abstract ID: 358

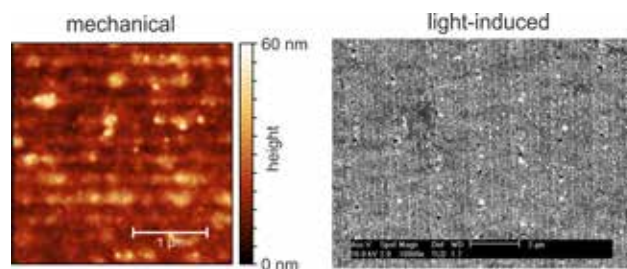
---

**Mr. Ivan Shutsko <sup>1</sup>, Mr. Maik Meudt <sup>1</sup>, Mr. Andreas Polywka <sup>1</sup>, Mr. Christian Tückmantel <sup>1</sup>,  
Prof. Patrick Görrn <sup>1</sup>**

*1. University of Wuppertal, Chair of Large Area Optoelectronics*

Due to the excitation of localized plasmons silver nanoparticles (AgNPs) strongly interact with optical radiation, and can be combined to layers with sophisticated optical properties. In order to exhaust the possibilities of AgNPs, it is desired to control both their shapes and positions with nanoscale precision. Here, we discuss novel approaches towards cost-efficient large area fabrication of AgNPs layers with recent theoretical and experimental results at hand. First, we demonstrate a mechanical method to build a metasurface with efficient optical broadband absorption. Further on, concepts based on the light-induced growth of AgNPs from liquid phase are presented. As recently shown, the interaction between AgNPs and light leads to a self-alignment process manipulating the morphology of the AgNPs in a way that the resulting structure shows an optimized interaction with the incoming light. This effect occurs due to the interference between the incident radiation and the light scattered by the nanoparticles, which modifies their growth behavior on the substrate<sup>[1]</sup>. These findings strongly hint at the possibility to utilize light-induced self-alignment of AgNPs to amplify the interaction of light with a given optical system.

[1] A. Polywka, C. Tückmantel, P. Görrn, *Sci. Rep.* **2017**, 7, 45144.



Mechanical and light induced particle alignment.png

# Second harmonic generation from zero-diffraction-order AlGaAs metasurfaces

Wednesday, 3rd October @ 15:04: Metamaterials (ROOM 1) - Oral - Abstract ID: 352

**Dr. Giuseppe Marino**<sup>1</sup>, **Mr. Carlo Gigli**<sup>1</sup>, **Dr. Ivan Favero**<sup>1</sup>, **Mr. Stéphan Suffit**<sup>1</sup>, **Dr. Arnaud Garnache**<sup>2</sup>, **Dr. Isabelle Sagnes**<sup>3</sup>, **Prof. Giuseppe Leo**<sup>1</sup>

1. Université Paris Diderot, 2. IES, CNRS-UMR 5214, Université Montpellier, 3. Centre de Nanosciences et de Nanotechnologies, CNRS-UMR9001

Dielectric metasurfaces lend themselves to intracavity mode shaping in external-cavity semiconductor lasers thanks to their ability of creating distributions of high-contrast membranes on the same epitaxial growth [1]. In this context, an intriguing option is represented by using the metasurface to generate harmonic frequencies inside the laser cavity. While  $\chi^{(3)}$  effects were reported in silicon-on-insulator nanoantennas [2], the AlGaAs-on-insulator platform has recently enabled the demonstration of second harmonic generation (SHG) in  $\chi^{(2)}$  nanoantennas [3]. Their excitation at normal incidence results in efficient SHG driven by Mie-type magnetic dipole resonance at the pump frequency in the near infrared and a polarisation behaviour dominated by a high-order multipole resonance at the second harmonic (SH) [4].

Here we focus on SHG from MOCVD-grown monolithic metasurfaces of  $\text{Al}_{0.18}\text{Ga}_{0.82}\text{As}$ -on- $\text{AlO}_x$  nanoantennas, where  $\text{AlO}_x$  is obtained from selective wet oxidation of  $\mu\text{m}$ -thick aluminium-rich AlGaAs layer. As a prototype example, we report the case of a set of coupled nanocylinders with height  $h = 400$  nm, radius  $r = 122$  nm and 300 to 900 nm periodicity, which we excite with a pump beam at  $\lambda = 1064$  nm linearly polarized along the [100] AlGaAs axis. The related SHG efficiency is low for periodicities smaller than the array diffraction limit, where SH modes stay confined in the metasurface plane. Conversely, for greater periodicities the SH modes are coupled into the zero-diffraction order. In this case, the SH fields generated from neighbouring nanoantennas constructively interfere, with a strong enhancement with respect to the case of the SHG from an isolated nanoantenna. This result paves the way to dielectric intracavity metasurfaces for SHG with an arbitrary wavefront.

## REFERENCES

- [1] M. S. Seghilani et al., *Opt. Expr.* 22, 5962 (2014).
- [2] M. R. Shcherbakov et al., *Nano Lett.* 14, 6488 (2014).
- [3] V. F. Gili et al., *Opt. Expr.* 24, 15965 (2016).
- [4] L. Ghirardini et al., *Opt. Lett.* 42, 559 (2017).

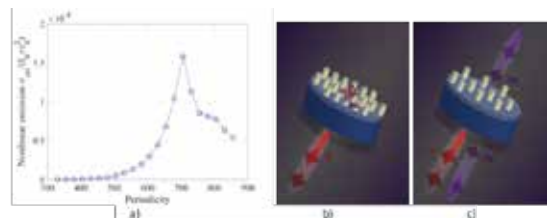


Figure. a) Calculated SHG efficiency vs periodicity. b) Schematic of SH waveguided modes for a periodicity of 300 nm. c) SH modes emitted at the zero order for a periodicity of 700 nm.

Picture1.png

---

# Intersubband plasmons induced negative refraction at mid-IR frequency in heterostructured semiconductor metamaterials

---

Wednesday, 3rd October @ 15:21: Metamaterials (ROOM 1) - Oral - Abstract ID: 248

---

**Mr. Mario Ferraro**<sup>1</sup>, **Dr. Miguel Montes Bajo**<sup>2</sup>, **Mr. Julen Tamayo-Arriola**<sup>2</sup>, **Prof. Massimo Giudici**<sup>3</sup>,  
**Dr. Angela Vasanelli**<sup>4</sup>, **Dr. Jean Michel Cheuveau**<sup>1</sup>, **Dr. Adrian Hierro**<sup>2</sup>, **Dr. Patrice Genevet**<sup>1</sup>

1. Université Cote d'Azur, CNRS, CRHEA, rue Bernard Gregory, Sophia Antipolis 06560 Valbonne, France, 2. ISOM and Dpto. Ing. Electrónica, Universidad Politécnica de Madrid, Avda. Complutense 30, 28040 Madrid, Spain, 3. Université Cote d'Azur, CNRS, InPhyni, Route des Lucioles, Sophia Antipolis 06560 Valbonne, France, 4. Laboratoire Matériaux et Phénomènes Quantiques, Université Paris Diderot, Sorbonne Paris Cité, CNRS-UMR 7162, 75013 Paris, France

## Introduction

In this paper we report theoretical and experimental results on negative refraction in highly doped layered semiconductor materials. We reveal that intersubband (ISBT) transitions induce a hyperbolic metamaterial behaviour in the quantum wells (QW).

## Methods

The proposed system consists of a stack of alternated layer of doped ZnO and undoped MgZnO forming an array of quantum wells grown on native ZnO substrate. The choice of ZnO is mainly related to the possibility of reaching very high doping level. Moreover, for non-polar growth conditions, i.e. c-axis along the plane, we avoid detrimental quantum confined Stark effect which would otherwise increase the complexity of the QW design. A scheme of the system is reported in Fig.1.

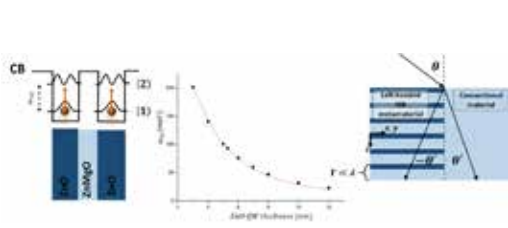
To obtain realistic material permittivity, the photonic response of the entire stack was calculated using Maxwell-Garnett theory, in the presence of QW, the barrier and the phononic response of the semiconductor. Details on the model accounting for phonon contribution, and anisotropic ISBT response will be presented.

## Results

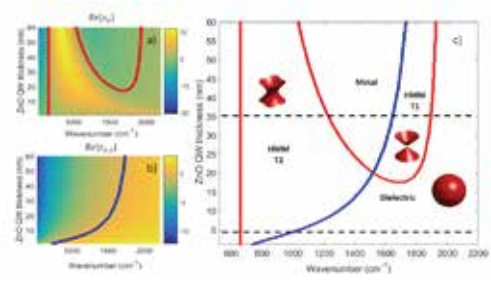
The main results are summarized in Fig.2, showing both in- and out-of-plane components of the real part of the effective medium permittivity. The optical properties range from pure metal to pure dielectric passing through HMM type 1 and 2. We show that T1 HMM originates from the intersubband plasmon response of the material. The theoretical prediction were tested experimentally with two samples of 4 and 35 nm thickness ZnO quantum wells that, according to the model, should exhibits positive and respectively negative refractions as presented in Fig.3. In presence of negative refraction a maximum (minimum) in transmission is expected for  $\theta < 0$  ( $\theta > 0$ ). These results are confirmed by experimental spectra.

## Discussion

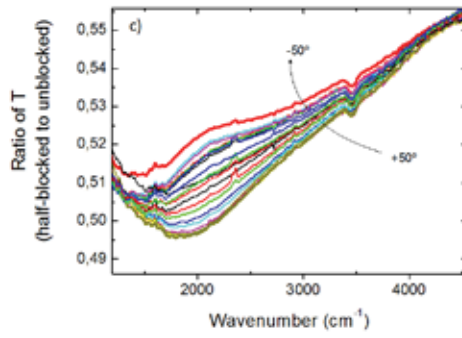
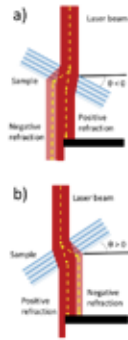
Experimental demonstration of negative refraction due to intersubband transition are in agreement with the theoretical model. Intersubband response is essentially due to both electronic confinement in subwavelength semiconductor layers and electronic doping, but as we show in this work, these materials generally exhibit -as well- inherent hyperbolic metamaterials response. Highlighting this connection between the more conventional concepts of intersubband plasmons in doped multiple quantum wells and its hyperbolic photonic response, opens avenues for designing new sources and emitters.



1.png



2.png



3.png

---

# Plasmonic Metasurface Absorber by Transfer Printing

---

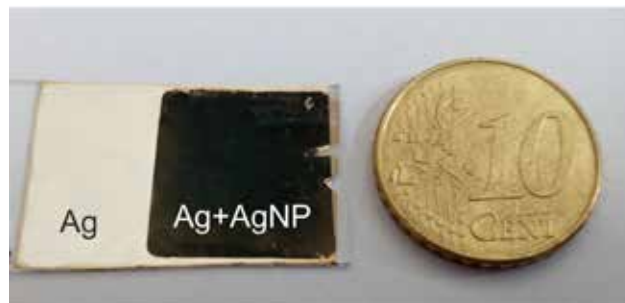
Wednesday, 3rd October @ 15:38: Metamaterials (ROOM 1) - Oral - Abstract ID: 360

---

***Mr. Maik Meudt*<sup>1</sup>, *Mr. Timo Jakob*<sup>1</sup>, *Mr. Andreas Polywka*<sup>1</sup>, *Mr. Luca Stegers*<sup>1</sup>, *Mr. Stefan Kropp*<sup>1</sup>,  
*Mr. Simon Runke*<sup>2</sup>, *Mr. Martin Zang*<sup>2</sup>, *Prof. Markus Clemens*<sup>2</sup>, *Prof. Patrick Görrn*<sup>1</sup>**

*1. University of Wuppertal, Chair of Large Area Optoelectronics, 2. University of Wuppertal, Chair of Electromagnetic Theory*

Metasurfaces are capable of manipulating photons at subwavelength scale, introducing the field of flat optics. Combined with metals, outstanding properties such as high optical absorption and thermal and electrical conductivity can be achieved at the same time. However, the fabrication of metasurfaces often relies on rather complicated and expensive production methods. Here, we present a versatile and cost-efficient fabrication method for a highly conductive black plasmonic metasurface. It consists of silver nanoparticles (AgNPs) transfer printed onto a silver film using a polydimethylsiloxane (PDMS) stamp. According to numerical simulations, gap plasmon modes between the AgNPs and the silver film are the origin of increased absorption. Further on, it is revealed that the size of the AgNPs has to be varied on subwavelength scale to further increase the spectral width and efficiency of the absorption. We achieve this control of AgNP size by modifying the surface curvature of the PDMS stamp with a commercially available sinusoidal grating relief. An absorption of up to 97% for p-polarized light and above 70% for unpolarized light in the spectral range from near-UV to near-IR is observed for a broad range of incidence angles. These results show that our approach combines the advantages of metasurfaces with cost-efficient large area fabrication methods for upcoming generations of optical systems, sensors, nonlinear optics, heat management systems and solar energy harvesting devices.



Photograph of metasurface absorber.png

---

## Gain-loss hyperbolic plasmonic metasurfaces

---

Wednesday, 3rd October @ 15:55: Metamaterials (ROOM 1) - Oral - Abstract ID: 450

---

**Dr. Dmitry Kuzmin**<sup>1</sup>, **Prof. Igor Bychkov**<sup>1</sup>, **Prof. Vladimir Shavrov**<sup>2</sup>, **Dr. Vasily Temnov**<sup>3</sup>

**1.** Chelyabinsk State University, **2.** Kotelnikov Institute of Radioengineering and Electronics of RAS, **3.** Université du Maine

Nowadays, hyperbolic plasmonics attracts researchers' attention by its exciting optical properties [1-4]. Hyperbolic metasurfaces (HMTs) support highly localized low-loss surface plasmon-polaritons (SPPs), providing drastic increase of the light-matter interactions near the surface. Moreover, HMTs allow the very effective manipulation by SPPs varying from routing them towards specific directions within the sheet, dispersion-free propagation (canalization), and to the negative refraction.

The usual realization of HMTs is constructing the surface which behaves as a dielectric in one direction and as a metal in the orthogonal one. Here, we show analytically the possibility of propagation of surface plasmon-polaritons, which have a hyperbolic isofrequency contour, along an anisotropic metasurface with gain in one direction and loss in the orthogonal one. We also propose the new class of HMTs based on the gain-loss metasurface consisting of array of lossy slabs in gain matrix.

We discuss a possible practical realization of such a metasurface operating at IR and visible light frequencies. We show that desired regime may be observed for some range of the geometrical parameters for metasurface consisting of cobalt slabs placed into quantum dots-based gain matrix. We also analyze the field structure of these SPPs, which drastically differs from that of conventional SPPs supported by uniform metallic surface.

The effects proposed here may be useful for numerous plasmonic applications ranging from plasmon manipulation for flatland optics to directive spaser design, while quite non-trivial polarization may lead to some fundamentally new effects for non-linear optical harmonic generation.

[1] J. S. Gomez-Diaz, et al., *Phys. Rev. Lett.* 114: 233901, 2015.

[2] J. S. Gomez-Diaz, et al., *Optical Materials Express* 5: 2313-2329, 2015.

[3] J. S. Gomez-Diaz, et al., *ACS Photonics* 3: 2211-2224, 2016.

[4] A. Nemilentsau, et al., *Phys. Rev. Lett.* 116: 066804, 2016.



---

# Optical properties and reliability studies of gradient alloyed green and red emitting quantum dots for white light-emitting diodes

---

Wednesday, 3rd October @ 14:30: Quantum dots and colour centres (ROOM 2) - Oral - Abstract ID: 76

---

**Dr. Rachod Boonsin<sup>1</sup>, Dr. Florian Donat<sup>2</sup>, Dr. Damien Boyer<sup>1</sup>, Prof. Raphael Schneider<sup>2</sup>, Prof. Philippe Boutinaud<sup>1</sup>, Dr. Rachid Mahiou<sup>1</sup>, Prof. Geneviève Chadeyron<sup>1</sup>**

**1.** Université Clermont Auvergne, CNRS, SIGMA Clermont, Institut de Chimie de Clermont-Ferrand (ICCF) – 63000-Clermont-Ferrand, **2.** Laboratoire Réactions et Génie des Procédés (LRGP), UMR 7274, Université de Lorraine, CNRS, 54001 Nancy -Cedex

Luminescent materials become one of interesting issues for white LED-based lighting devices (WLEDs) due to their high performances for converting the monochromatic light from UV/blue LED chips into white light. The most common current commercial devices incorporate blue-emitting InGaN diodes around 450 nm, combined to lanthanide-based phosphors (mainly cerium-doped YAG ( $Y_3Al_5O_{12}$ :  $Ce^{3+}$ ) most often associated with a red emitting phosphor) which partly converts the incident blue emission into a relatively broad emission in the yellow-red, thus generating white lighting with high luminous efficiencies and suitable colorimetric qualities in terms of color correlated temperature (CCT) and color rendering index (CRI). These phosphors contain rare-earth (RE) elements. China, which already holds 37% of rare earths world reserves, also has a near-monopoly of production (97%) and reduces export quotas each year. But global demand is growing every year by 6%, putting the market under pressure. In this context, it is now crucial to identify new cheap and REE-free phosphors capable of delivering cost-effective light energy conversion, especially in commercial white light generation. In this talk, we will report the development of rare-earth-free luminescent nanocomposites combined with UV/blue LED chips in order to provide white light. Cadmium selenide/zinc sulfide  $(CdSe)_x(ZnS)_{1-x}$  and copper indium sulfide/zinc sulfide  $(CuInS_2)_x(ZnS)_{1-x}$  quantum dots have been used to achieve the luminescent nanocomposite films in silicone as polymer matrix. The photoluminescence properties of QDs composite films obtained by incorporating gradient alloyed  $(CdSe)_x(ZnS)_{1-x}$  and  $(CuInS_2)_x(ZnS)_{1-x}$  QDs were investigated. The photometric parameters of systems consisting of luminescent nanocomposites and LEDs including color rendering index (CRI), correlated color temperature (CCT), chromaticity coordinates, and luminous efficacy which can be tuned by controlling the compositions and thickness of nanocomposite films, will be presented. Moreover, the reliability of QDs composite films was evaluated by collecting the photoluminescence (PL) intensity upon LED excitation at 375 nm or 450 nm, for different irradiation powers and different temperatures. The obtained behaviors will be discussed.

---

# Plasmon-induced in-plane band gap engineering in hydrogenated dilute nitrides

---

Wednesday, 3rd October @ 14:47: Quantum dots and colour centres (ROOM 2) - Oral - Abstract ID: 47

---

***Dr. Giorgio Pettinari*<sup>1</sup>, *Mr. Loris Angelo Labbate*<sup>1</sup>, *Dr. Silvia Rubini*<sup>2</sup>, *Prof. Antonio Polimeni*<sup>3</sup>, *Dr. Marco Felici*<sup>3</sup>**

*1. CNR IFN, 2. CNR IOM, 3. Sapienza University of Rome*

Dilute nitrides (such as GaAsN, GaPN, and InGaAsN) are III-V semiconductors alloying small, yet macroscopic ( $\leq 5\%$ ) percentages of nitrogen atoms. One of the most striking property of this class of materials is the possibility of tuning post-growth the alloy properties, as for example the band gap energy, by a controlled incorporation of hydrogen atoms. The formation of N-H complexes, indeed, neutralizes all the effects N has on the host matrix, among which the strong narrowing of band gap energy [1]. In the past years, we have demonstrated the possibility to get an in-plane band gap engineering in dilute nitrides by making use of lithographic [2] or laser-assisted [3,4] approaches to spatially control, respectively, the incorporation or removal of hydrogen atoms.

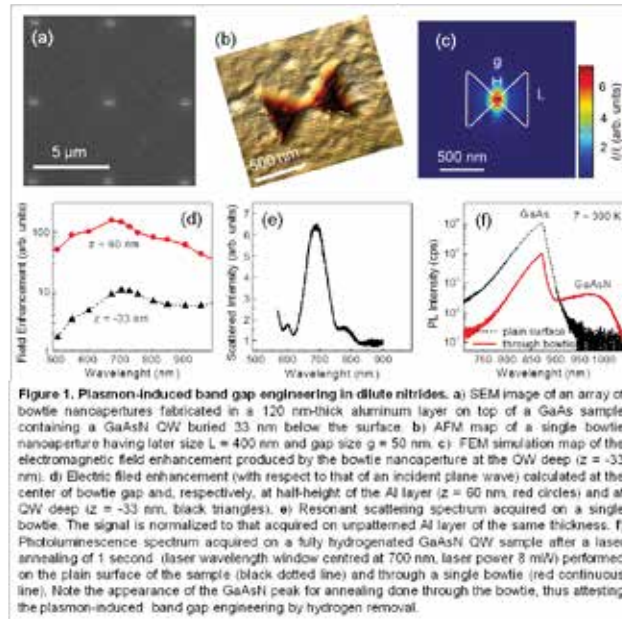
Here, we extend our studies to plasmonic structures in order to use their inherent ability to localize light at length scale well below the diffraction limit, with the aim of controlling the H removal in dilute nitrides at the nanometer scale and realize spatially controlled quantum emitters. In particular, we present a comprehensive investigation of the structural and optical properties of single bowtie-shaped plasmonic nanoapertures (NAs) in Al thin film. Different bowtie NAs have been realized by lithographic approach and investigated by scanning probe microscopy (SEM, AFM; Figs. 1a,b), FEM simulations (Figs. 1c,d), and resonant scattering spectroscopy (Fig. 1e). The condition to get the maximum field enhancement below the metal/semiconductor interface, namely at the dilute nitride quantum well (QW) position, has been identified. NAs have then been successfully employed to perform a spatially selective hydrogen removal in a fully hydrogenated GaAsN QW (Fig. 1f). The hydrogen removal results to be up to five times more efficient through the bowtie NAs than on the plain sample surface; thus demonstrating the potentiality of the plasmon-induced in-plane band gap engineering for future realization of site-controlled single-photon emitters.

[1] G. Pettinari *et al.*, JAP **115**, 012011 (2014); Photonics **5**, 10 (2018).

[2] R. Trotta *et al.*, Adv. Mater. **23**, 2706 (2011).

[3] N. Balakrishnan *et al.*, PRB **86**, 155307 (2012).

[4] F. Biccari *et al.*, Adv. Mater. **30**, 1705450 (2018).



Plasmon-induced bandgap engineering.png

---

# Control of light emission by diamond nanoantennas

---

Wednesday, 3rd October @ 15:04: Quantum dots and colour centres (ROOM 2) - Oral - Abstract ID: 191

---

***Ms. Anastasia Zalogina*<sup>1</sup>, *Mr. Dmitry Zuev*<sup>1</sup>, *Mr. Roman Savelev*<sup>1</sup>, *Prof. Ilya Shadrivov*<sup>2</sup>**

*1. ITMO University, 2. Australian National University*

One of the main motivations for the development of dielectric nanophotonics is the ability to control light on nanoscale through excitation of both electric and magnetic Mie-type resonances. In particular, control of optical emission from active centers can be achieved by modifying the environment of emitters. This can be achieved, for example, by placing them in a vicinity of a nanoantenna. Passive dielectric nanoantennas, in the form of nanoparticles of various shapes, are able to increase emission intensity, accelerate spontaneous emission rate and control the radiative pattern. It is however more efficient to place the emitter inside a dielectric nanoantenna itself, since the emitter inside a dielectric antenna can couple to the optical modes more effectively. Such coupling modifies electromagnetic emission and influences the spontaneous emission rate of emitters. One of the actively studied emitters is a nitrogen-vacancy (NV) center, which is a defect in a diamond. Diamond itself is an excellent optical material with a refractive index close to 2.4. This suggests that we can modify the emission of an NV-center by shaping the host diamond itself in the form of a dielectric nanoantenna.

Here we study nanodiamonds of sizes from (0.3x0.3)  $\mu\text{m}$  to (1.5x2)  $\mu\text{m}$ , fabricated by milling diamond films, which are grown by plasma-enhanced chemical vapor deposition. NV centers are incorporated during PECVD film growing. Nanoparticles are characterized using scanning electron microscopy, Raman spectroscopy, dark-field scattering and time correlated single photon counting methods.

We show experimentally that Mie-type resonances in nanodiamonds with NV centers lead to the twofold decrease of emission lifetime. In particular, the resonances of large diamond nanoantennas affect photoluminescence properties of NV centers providing acceleration of the emission. In contrast, subwavelength nanoparticles provide fivefold decrease of spontaneous emission rate. We show that the observed phenomena are in a good agreement with theoretical calculations based on Mie theory. We predict that further enhancement of the emission rate can be achieved by precise control of the NV center position within the nanoantennas.

Demonstrated results pave the road for further developments of active nanophotonics towards creation of single photon sources controlled by dielectric nanoantennas.

# Nanoplasmonic Sensing by Silver Nanoplates Generated by Pulsed Laser Ablation and Reirradiation in Liquids

Wednesday, 3rd October @ 15:21: Quantum dots and colour centres (ROOM 2) - Oral - Abstract ID: 381

*Dr. vittorio scardaci*<sup>1</sup>, *Mr. Marcello Condorelli*<sup>1</sup>, *Dr. Luisa D'urso*<sup>1</sup>, *Prof. Orazio Puglisi*<sup>1</sup>, *Prof. Giuseppe Compagnini*<sup>1</sup>

1. University of Catania

## Introduction

One of the most common methods to generate and modify noble metal colloids in liquid phase consists in the formation of metallic seeds by salt reduction and subsequent growth of nanostructures by specific light exposure. However, these methods use a number of chemicals, such as aggressive reducing agents, beside metallic salts.

An alternative and greener way to generate silver and gold colloids is the use of pulsed laser ablation of a metallic target in the liquid phase. This technique has so far been reported for the formation of spherical nanoparticles in the colloidal form with sizes ranging from 5 to 20 nm.

Here, we demonstrate a green, chemical-free synthesis of silver nanoplates by pulsed laser ablation in liquids and their application in nanoplasmonic sensing.

## Methods

Silver seeds have been produced by the ablation of a metallic target in water using the second harmonics of a nanosecond pulsed Nd:YAG laser (532 nm). To obtain silver nanoplates, H<sub>2</sub>O<sub>2</sub> is added to the obtained silver colloidal solutions under continuous irradiation by a narrow band LED lamp at 600 nm in a suitable reactor. Electron and Atomic Force microscopies have been performed to characterize the size and shape of the produced nanoparticles.

For nanoplasmonic sensing, the refractive index of the medium is tuned in a range between 1.33 and 1.46 by adding a sucrose solution to existing nanoplates solutions, while PR is measured by UV-Vis-NIR spectroscopy.

## Results and discussion

Spectroscopic and microscopic characterizations reveal that the final colloid consists of triangular and hexagonal silver nanoplates with in-plane size of about 150 nm and thickness around 20 nm. Under LED illumination the in-plane plasmon resonance position changes from 400 nm to 700 nm as shown in figure 1. Figure 2 shows a range of absorption spectra of a specific colloidal sample in a glucose solution as the refractive index increases. The inset shows the results of nanoplasmonic sensing experiments with a sensitivity of up to 450 nm/RIU.

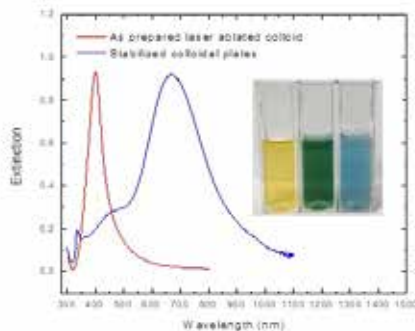


Fig1.jpg

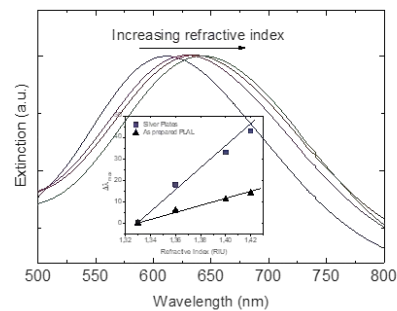


Fig2.png

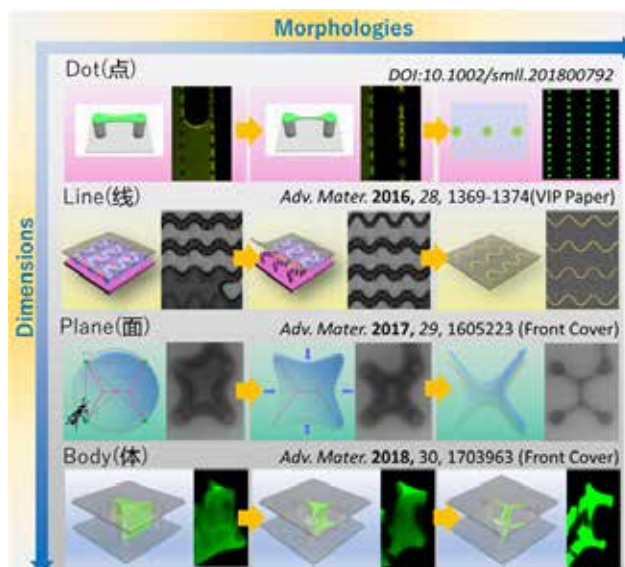
# Self-assembling of nanomaterials via droplet manipulation for multifunctional optoelectronics

Wednesday, 3rd October @ 15:38: Quantum dots and colour centres (ROOM 2) - Oral - Abstract ID: 508

**Dr. Meng Su**<sup>1</sup>

*1. Institute of Chemistry, Chinese Academy of Sciences*

The ability to rapidly and precisely construct multifunctional electronic and optic devices would enable myriad applications, including displays, solid-state lighting, wearable electronics and biomedical devices with embedded circuitry. Here, the droplet manipulation strategy is demonstrated for rapidly patterning materials over a broad range of compositions and accurately achieving the correct position at the micro- and nanoscale. Firstly, 0D microdots are connected by 1D microwires through regulating the Rayleigh-Taylor instability of materials solution or suspension, which display bright dichromatic photoluminescence. Secondly, a 3D liquid self-shaping strategy is developed for rapidly patterning materials over a series of compositions and accurately achieving micro- and nanoscale structures. The 3D architectures achieved by two different quantum dots show non-interfering optical properties with feature resolution below 3  $\mu\text{m}$ . Thirdly, three-primary-color fluorescent nanoparticles can also be integrated by successively printed with retention of their individual photoluminescence efficiency (5% variances). Yellow, magenta, cyan and white colors with clearly defined interfaces are achieved to reduce the optical cross-talk effect. Finally, nanoparticle-based curves are assembled through pillar-patterned silicon template-induced printing, and integrated as flexible sensors to perform complex recognition of human facial expression. Optimal interconnect are spontaneously patterned between certain nodes on diverse substrates, as natural systems spontaneously figuring out the shortest path. The optimal interconnect leads to a 65.9 percent decrease in the electromagnetic interference. Therefore, self-assembling of nanomaterials via droplet manipulation is achieved in all dimensions for multifunctional optoelectronics.



Meng su.jpg

---

# Color centers in diamond: from single-photons to nanoscale sensing

---

Wednesday, 3rd October @ 15:55: Quantum dots and colour centres (ROOM 2) - Oral - Abstract ID: 501

---

***Dr. Paolo Traina*<sup>1</sup>, *Dr. Ekaterina Moreva*<sup>1</sup>, *Dr. Jacopo Forneris*<sup>2</sup>, *Dr. Sviatoslav Ditalia Tchernij*<sup>3</sup>, *Dr. Federico Picollo*<sup>3</sup>, *Dr. Ivo Degiovanni*<sup>1</sup>, *Prof. Valentina Carabelli*<sup>3</sup>, *Dr. Paolo Olivero*<sup>3</sup>, *Dr. Marco Genovese*<sup>1</sup>**

*1. Istituto Nazionale di Ricerca Metrologica, 2. INFN, 3. University of Turin*

Color centres in diamond represent a very promising system for realizing bright, stable, on demand single-photon sources (SPS) but not only: they are attracting an ever-growing interest in quantum optics, quantum information and quantum sensing, due to their appealing photo-physical properties combined with ease of access and manipulation in a solid state system characterized by high transparency and structural stability. The remarkable results obtained at the state of the art on the exploitation of the unique properties of the negatively-charged nitrogen-vacancy complex (NV<sup>-</sup>), are pushing the discovery and characterization of new and appealing color centers. On the same time, techniques to exploit the optical readout of individual spins of NV centers for nanoscale, record performance sensing even at room temperature are being developed. Here we review the most recent results obtained by a collaboration among the Italian National Institutes of Metrologic Research (INRiM), the University of Torino and the Italian National Institutes of Nuclear Physics (INFN):

- introducing He- and Sn-related emitters in diamond as novel SPS [1, 2];
- electrical control NV centers in bulk single-crystal diamond by means of integrated graphitic electrodes [3];
- quantum-sensing and high-resolution mapping of local electrical fields in diamond-based devices via ensembles of NV centers [4];
- Beyond-diffraction-limit mapping of diamond color centers exploiting non-classical photon statistics [5];
- towards NV-powered optically detected magnetometry in biological samples [6].

## References

- [1] G. Prestopino et al., *Applied Physics Letters* 111, 111105 (2017);  
[2] S. Ditalia Tchernij et al., *ACS Photonics* 4 (10), 2580 (2017);  
[3] J. Forneris et al., *Scientific Reports* 5, 15901 (2015);  
[4] J. Forneris et al., *arXiv: 1706.07935* (2017);  
[5] D. Gatto Monticone et al., *Physical Review Letters* 113, 143602 (2014);  
[6] L. Guarina et al., *Scientific Reports* 8, 2221 (2018).

---

# Designing plasmonic eigenstates for optical signal transmission and logic gates nanodevices.

---

Wednesday, 3rd October @ 14:30: Nonlinear nano-optics (AUDITORIUM) - Oral - Abstract ID: 59

---

**Mr. Upkar Kumar**<sup>1</sup>, **Mrs. Sviatlana Viarbitskaya**<sup>2</sup>, **Mr. Aurélien Cuche**<sup>1</sup>, **Mr. Alexandre Bouhelier**<sup>2</sup>,  
**Mr. Gérard Colas Des Francs**<sup>2</sup>, **Mr. Christian Girard**<sup>1</sup>, **Mr. Erik Dujardin**<sup>1</sup>

1. CEMES CNRS UPR 8011, 2. LICB, CNRS UMR 6303, Université de Bourgogne

Two dimensional colloidal plasmonic cavities spatially and spectrally shape the near-field. By designing these two degrees of freedom, transduction function can be implemented in single cavities that perform Boolean logic functions. The wealth of available plasmonic modes allow to implement complex logic functions without the need of concatenating building blocks but rather by redesigning the transfer function.

Indeed, 2D plasmonic systems with mesoscopic sizes sustain higher order plasmonic modes and combine the properties of surface plasmon polaritons (SPP) and localized surface plasmon (LSP). Such multimodal plasmonic systems open a new realm in which the modal behavior is better described by the Surface Plasmon local density of states (SP-LDOS), which is solely governed by the material properties and the boundary conditions set by the structure shape, but is independent of the illumination parameters. SP-LDOS can be rationally designed to tailor the local spatial and spectral characteristics of the SP modes, while allowing information transfer over micrometer-sized distances.

The next level of information processing consists in performing Boolean logic from the incoming signal. Here again, the tailoring of the modal properties of confined plasmonic cavities can be exploited to designing reconfigurable universal logic gates that can be converted into one another, this opens the way to the integration of complex functions at the nanoscale.

## References

- [1] S. Viarbitskaya, A. Teulle, R. Marty, J. Sharma, C. Girard, A. Arbouet and E. Dujardin. *Nature Materials* 12, 426, (2013).
- [2] A. Cuche, S. Viarbitskaya, J. Sharma, A. Arbouet, C. Girard, E. Dujardin. *Sci. Rep.*, 5, 16635, (2015).
- [3] A. Cuche, S. Viarbitskaya, U. Kumar, J. Sharma, A. Arbouet, C. Girard, E. Dujardin. *Opt. Comm.*, 387, 48-54 (2017).
- [4] A. Cuche, M. Berthel, U. Kumar, G. Colas des Francs, S. Huant, E. Dujardin, C. Girard, A. Drezet. *Phys. Rev. B.*, 95, 121402R (2017).
- [5] U. Kumar, S. Viarbitskaya, A. Cuche, C. Girard, S. Bolisetty, R. Mezzenga, G. Colas des Francs, A. Bouhelier, E. Dujardin. *ArXiv* 1711.05585 (2018)



# Phase-matching-free micron-sized parametric oscillators by two-dimensional media

Wednesday, 3rd October @ 14:47: Nonlinear nano-optics (AUDITORIUM) - Oral - Abstract ID: 45

**Dr. Andrea Marini**<sup>1</sup>, **Dr. Alessandro Ciattoni**<sup>2</sup>, **Dr. Carlo Rizza**<sup>2</sup>, **Prof. Claudio Conti**<sup>3</sup>

1. University of L'Aquila, 2. CNR - SPIN L'Aquila, 3. CNR - ISC The Institute for Complex Systems, Rome

Parametric down-conversion (PDC) furnishes tunable sources of coherent radiation and generators of entangled photons and squeezed states of light. In traditional configurations, a nonlinear crystal with broken centrosymmetry and second-order nonlinearity sustains PDC. Since three-wave parametric coupling is intrinsically weak, one can achieve low oscillation thresholds only by doubly or triply resonant optical cavities. In addition, parametric effects are severely hampered by the destructive interference among the three waves propagating with different wavenumbers in the dispersive nonlinear medium because the momentum mismatch does not generally vanish. To avoid this highly detrimental effect, the use of phase-matching (PM) strategies is imperative. Here, we show that emerging two-dimensional (2D) materials with high quadratic nonlinearity open unprecedented possibilities for tunable parametric micro-sources. Very remarkably, when illuminated with different visible and infrared waves, these novel 2D materials provide a negligible dispersive dephasing owing to their atomic-scale thickness. Due to the lack of destructive interference, 2D materials support PDC without any need of satisfying a PM condition. The most famous 2D material, graphene, is not the best candidate for PDC owing to the centrosymmetric structure. Recent years have witnessed the rise of transition metal dichalcogenides (TMDs) as promising photonic 2D materials. Bulk TMDs are semiconductors with an indirect bandgap, but the optical properties of their monolayer (ML) counterpart are characterized by a direct bandgap ranging from 1.55 eV to 1.9 eV. In addition, ML-TMDs have broken centrosymmetry and thus undergo second-order nonlinear processes. We investigate PDC in microcavities embedding ML-TMDs; we find that the cavity design is extremely flexible if compared to standard parametric oscillators thanks to their phase-matching-free operation. We demonstrate that, at conventional infrared pump intensity, parametric oscillation occurs in wavelength-sized micro-cavities with ML-TMDs. We show that the output signal and idler frequencies can be engineered, tuned by the pump incidence angle, and modulated electrically by an external gate voltage.

Our results pave the way for new ultrafast tunable micron-sized sources of entangled photons, a key device underpinning any quantum protocol. Highly-miniaturized optical parametric oscillators may also be employed in lab-on-chip technologies for biophysics, environmental pollution detection and security.

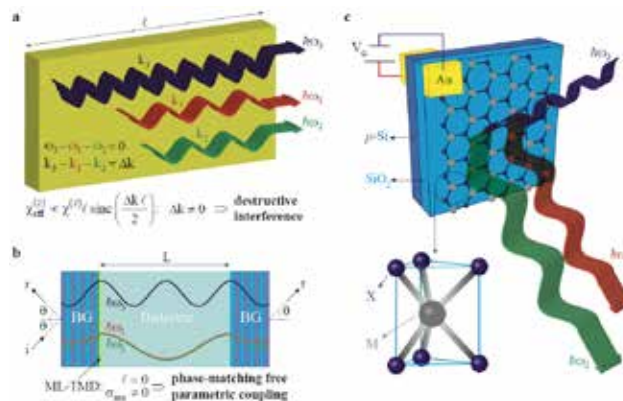


Immagine.png

---

# Active dielectric nanoantennas for directional lasing

---

Wednesday, 3rd October @ 15:04: Nonlinear nano-optics (AUDITORIUM) - Oral - Abstract ID: 164

---

**Dr. Son Tung Ha<sup>1</sup>, Dr. Yuan Hsing Fu<sup>1</sup>, Dr. Naresh K. Emami<sup>2</sup>, Dr. Zhenying Pan<sup>1</sup>, Dr. Reuben M. Bakker<sup>1</sup>, Dr. Ramon Paniagua-Dominguez<sup>1</sup>, Dr. Arseniy I. Kuznetsov<sup>1</sup>**

*1. Data Storage Institute (Agency for Science, Technology and Research, A\*STAR), 2. Indian Institute of Technology Hyderabad*

## Introduction

Dielectric nanoantennas offer an attractive alternative platform to plasmonics to control light in the nanoscale. Apart from their lower absorption losses, due to the absence of free electrons, the wealth of optical modes supported in this kind of structures enables interference effects that may be used to obtain high directionality. At the same time, some of the materials suitable for this platform, such as III-V semiconductors, have interesting electronic properties that may be used to design advanced opto-electronic and active devices. Among those, photoluminescence can be used to generate LEDs and, potentially, lasers in the nanoscale. However, the low quality factor (Q) of the optical resonances supported by this class of nanoantennas has prevented, so far, the realization of the latter. In this work we demonstrate, for the first time, that it is possible to obtain lasing in active dielectric nanoantenna arrays through a combination of individual resonances and collective generation of so called bound-states-in-the-continuum (BIC).

## Methods and Results

We demonstrate, theoretically and experimentally, directional lasing action in arrays of dielectric nanoantennas made of GaAs. By theoretical analysis we show that the studied arrays support a symmetry-protected BIC associated to the resonant excitation of an electric dipole resonance in the individual antennas. A quasi-BIC with high-Q is observed experimentally for finite sized arrays, which serves as the feedback mechanism for the laser. Lasing is obtained in a range of temperatures from 77K to 200K, with lasing thresholds as low as 10  $\mu\text{J}/\text{cm}^2$ . The laser shows a strong directionality that can be controlled by tuning the array geometry and temperature, without significantly sacrificing the high-Q of the quasi-BIC, via radiation out-coupling through designed diffraction orders. Experimentally, we show tuning of the laser emission from 3° up to 20° with respect to the normal.

## Discussion

The results presented in this work represent a significant step towards new functionalities in which the interesting properties of dielectric nanoantennas are combined with gain dielectric materials to obtain active devices. Next steps towards further miniaturization and prospects for electrical addressing will be also discussed.

---

## Mixed Frequency Generation in a Gold Antenna enables Double Blind Ultrafast Pulse Characterization

---

Wednesday, 3rd October @ 15:21: Nonlinear nano-optics (AUDITORIUM) - Oral - Abstract ID: 308

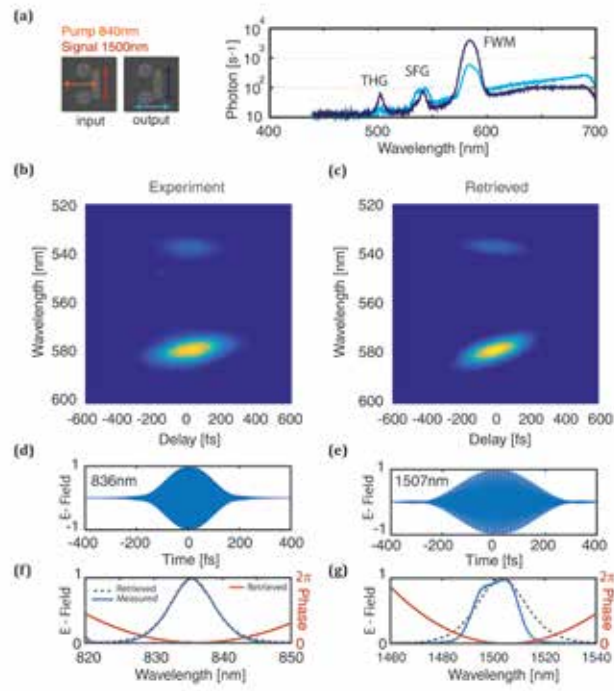
---

*Dr. Sylvain Gennaro*<sup>1</sup>, *Dr. Yi Li*<sup>1</sup>, *Prof. Stefan A Maier*<sup>2</sup>, *Prof. Rupert F Oulton*<sup>1</sup>

*1. Imperial College London, 2. Imperi*

Ultrafast pulse characterization requires the analysis of correlation functions generated by frequency mixing of optical pulses in a nonlinear medium. A two-dimensional time versus wavelength spectrogram is compiled based on either third order or second order correlation signals and analysed by an algorithm that reconstructs pulse shapes in time. In these techniques, the number of nonlinear processes involved dictates how many ultra-short pulses can be simultaneously retrieved. However, phase matching in a single nonlinear crystal will limit the types of nonlinear processes achievable and the spectral range where they can be efficient. Plasmonic optical antennas offer a promising route toward ultrathin nonlinear devices with little limitation on phase matching. These metallic nanostructures sustain strong resonant electromagnetic fields via electronic charge oscillations at their surfaces, which can simultaneously generate second (SHG) and third harmonic generation (THG), Sum Frequency Generation (SFG), and Four Wave Mixing (FWM), with interaction lengths shorter than the optical wavelength.

In this work, we exploit degenerate Four Wave Mixing (FWM) and Sum Frequency Generation (SFG) signals from an individual gold antenna to characterize two near IR ultrafast optical pulses from a Coherent Ti: Sapphire and Optical Parametric Oscillator (OPO) without the need of a known reference pulse. The multiresonant antenna consists of a gold bar and two gold disks with dipolar resonances detuned by about an octave, in this case near 1500 and 750 nm for the bar and disks respectively. Due to narrow gaps between the disks and bar, a resonant near field coupling or “Fano” interference effect arises between the dipolar mode of the disks and a less-radiative second order mode of the bar. This coupling facilitates the various nonlinear mixing processes. By temporally-scanning the pump and signal laser pulses and recording spectra at each scan delay, we can produce a spectral intensity map of relative delay versus wavelength (i.e. a spectrogram) of the various frequency mixing processes. We can then characterize the chirp and spectra of our two optical pulses assuming secant square pulses demonstrating the viability of the technique. The nonlinear mixing is efficient enough to retrieve pulses with energies in the picojoule range.



Ultrashort pulse characterisation with a single antenna.jpg

---

# Superfluid Brillouin Laser

---

Wednesday, 3rd October @ 15:38: Nonlinear nano-optics (AUDITORIUM) - Oral - Abstract ID: 225

---

***Dr. Andreas Sawadsky*<sup>1</sup>, *Dr. Christopher Baker*<sup>1</sup>, *Mr. He Xin*<sup>1</sup>, *Prof. Warwick Bowen*<sup>1</sup>**

*1. Quantum Optics Lab @ University of Queensland*

Enabled by superfluid helium's ultra low viscosity, we propose and experimentally demonstrate a superfluid Brillouin laser with ultra-high gain. Our experimental setup consists of an evanescently coupled silica microresonator (see Fig. (a)) covered by a nanometer-thick superfluid 4He film [1,2]. Regions of high light intensity inside the resonator pull in more superfluid due to the optical radiation pressure force (see Fig. (b)), creating a spatially modulated refractive index grating, in turn scattering more light, leading to spontaneous Brillouin lasing (see Fig. (c)), where a pump photon is scattered into a lower energy Stokes photon and a phonon of frequency  $f_{BS}$  (the Brillouin shift) (see Fig. (d)).

In contrast to the commonly studied Brillouin scattering in solids, whereby the light intensity strains the material through electrostrictive forces, this superfluid based approach provides orders of magnitude larger gain. This dramatic enhancement can be intuited by comparing the difficulty of straining a high Young's modulus material such as silica, compared to the ease with which light can continuously deform a (super) fluid interface. This work brings the optical sensitivity of optomechanical systems to the fluid/soft-matter systems, and has applications in terms of on-chip ultra-narrow linewidth lasers and optical stirring of quantum fluids.

[1] Harris, G. I. et al. "Laser Cooling and Control of Excitations in Superfluid Helium." *Nature Physics* 12, 8, 2016.

[2] Baker, Christopher G. et al. "Theoretical Framework for Thin Film Superfluid Optomechanics: Towards the Quantum Regime." *New Journal of Physics* 18, 12, 2016.

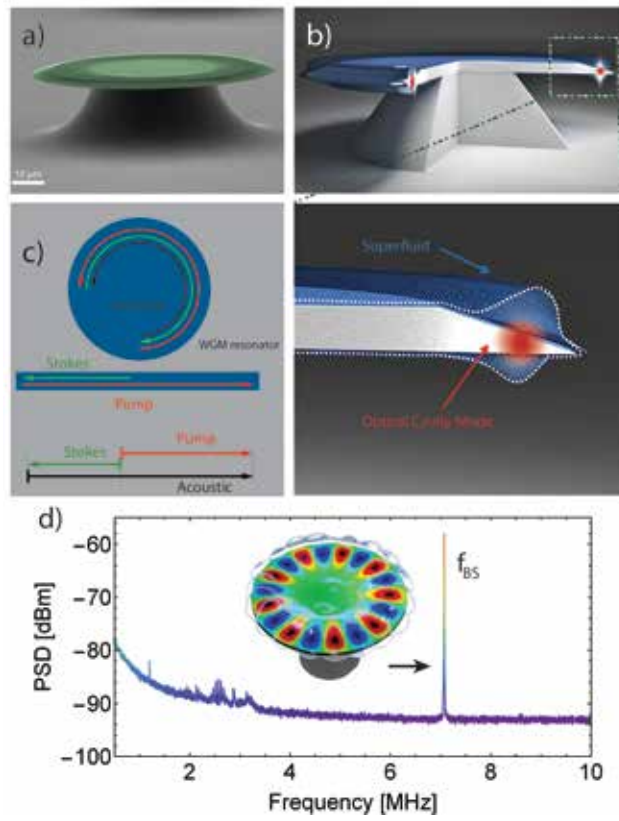


Figure.jpg

---

# The role of corners in the second harmonic scattering origin response from silver nanocubes

---

Wednesday, 3rd October @ 15:55: Nonlinear nano-optics (AUDITORIUM) - Oral - Abstract ID: 156

---

**Dr. christian jonin**<sup>1</sup>, **Dr. Isabelle Russier-antoine**<sup>1</sup>, **Prof. Emmanuel Benichou**<sup>1</sup>, **Prof. Pierre-françois Brevet**<sup>1</sup>, **Prof. Hye Jin Lee**<sup>2</sup>, **Dr. Alastair Wark**<sup>3</sup>, **Dr. Jérémy Butet**<sup>4</sup>, **Prof. Olivier Martin**<sup>5</sup>

1. university of Lyon, 2. Kyungpook National University, 3. University of Strathclyde, 4. Institute of Technology Lausanne, 5.

Swiss Federal Institute of Technology Lausanne

Fundamental studies on the nonlinear optical properties have been performed over the last years on a series of gold and silver nanoparticles with a special attention to the shape of the nanoparticles [1]. Among many others, nanospheres, nanorods or nanodecahedra have been closely investigated with the determination of their first hyperpolarizability, namely their cross-section for the SHG process [2-4]. A competition between the shape defect contribution and the field multipole modes has been identified while the nonlinearity can be assumed to originate from the surface itself. Unfortunately, no perfect centrosymmetric shape can be achieved and it is difficult to disentangle surface defects from field multipoles. Recently, it has nevertheless been demonstrated how polarization resolved measurements could achieve this operation [5].

To go further into this direction, nanocubes are investigated in the present work. It is indeed expected that, because the six cube facets can be easily identified, the nanocube shape will be close to the ideal shape, perhaps to a larger extent as compared to nanospheres to the spherical shape and nanorods to the ellipsoidal shape for instance.

We report here the second harmonic scattering (SHS) from silver nanocubes. We discuss the polarization analysis and disentangle the contribution from the surface defects and the field multipoles. These experimental results are presented in light of a surface integral method computations where a particular attention is given to the role of the rounding of edges and corners.

## References

- [1] J. Butet, P.F. Brevet, O.J.F. Martin, *ACS Nano*, 9 (2015) 10545-10562
- [2] I. Russier-Antoine, J. Duboisset, G. Bachelier, E. Benichou, C. Jonin, N. Del Fatti, F. Vallée, A. Sánchez-Iglesias, I. Pastoriza-Santos, L.M. Liz-Marzan, P.F. Brevet, *J. Phys. Chem. Lett.*, 1 (2010) 874-880.
- [3] I. Russier-Antoine, E. Benichou, G. Bachelier, C. Jonin, P. F. Brevet, *J. Phys. Chem. C*, 11
- [4] J. Butet, G. Bachelier, I. Russier-Antoine, Ch. Jonin, E. Benichou, P.F. Brevet, *Phys. Rev. Lett.*, 105 (2010) 0774011 (2007) 9044-9048.
- [5] Y. El Harfouch, E. Benichou, F. Bertorelle, I. Russier-Antoine, Ch. Jonin, N. Lascoux P.F. Brevet, *J. Phys. Chem. C*, 118 (2014) 609-616

---

## Raman spectroscopy of a single gold nanoparticle dimer

---

Wednesday, 3rd October @ 16:40: Nano-Optomechanics (ROOM 1) - Oral - Abstract ID: 162

---

**Dr. Adrien Girard**<sup>1</sup>, **Dr. Hélène Gehan**<sup>2</sup>, **Dr. Alain Mermet**<sup>2</sup>, **Dr. Christophe Bonnet**<sup>2</sup>, **Dr. Jean Lermé**<sup>2</sup>,  
**Dr. Alice Berthelot**<sup>2</sup>, **Dr. Emmanuel Cottancin**<sup>2</sup>, **Dr. Aurélien Crut**<sup>2</sup>, **Dr. Jeremie Margueritat**<sup>2</sup>

1. Goethe-Universität, 2. Université Claude Bernard Lyon 1

This paper reports the first measurement of ultra-low frequency Raman scattering by a single nano-system (an isolated gold nanoparticle embedded in a polymer matrix or a dimer of two such nanoparticles). This spectroscopy approach, avoiding the inhomogeneous broadening effects affecting experiments on nanoparticle assemblies, yields both the frequencies and damping rates of the detected acoustic modes, allowing a detailed analysis of the opto-mechanical response of a dimer of two close nanoparticles.

The Raman spectra of single dimers of close nanoparticles considerably differ from those of isolated gold nanoparticles, dominated by their quadrupolar vibration mode. Indeed, the frequency of this mode is modified, and additional modes become observable at both lower and higher frequencies. These observations are ascribed to mechanical (i.e., hybridization of the vibrational modes of nanoparticles in a dimer) and opto-mechanical (i.e., the fact that vibrations which do not affect the optical response of an isolated nanoparticle may modify that of a dimer, thus becoming Raman active) coupling effects. In particular, the two ultra-low frequency modes appearing in the Raman spectra of single dimers are interpreted as out-of-phase longitudinal and transverse (with respect to the dimer axis) quasi-translations of the nanoparticles. In the high frequency range, the dimer shape is also shown to enable Raman scattering by high angular momentum vibration modes, with an efficiency increasing with decreasing interparticle distance.

These results show that a gold dimer (or oligomer) constitutes a simple opto-mechanical resonator whose properties can be controlled by adjusting the morphology and number of composing nanoparticles, as well as the elastic properties of their surrounding matrix.



---

# Dynamics of electric dipoles in fluctuating light fields: From gravity-like interactions to accelerated expansion

---

Wednesday, 3rd October @ 16:57: Nano-Optomechanics (ROOM 1) - Oral - Abstract ID: 42

---

**Prof. M. I. Marques**<sup>1</sup>, **Dr. Jorge Luis-hita**<sup>1</sup>, **Mr. Victor Jose Lopez Pastor**<sup>2</sup>, **Dr. Nuno De Sousa**<sup>3</sup>, **Dr. Luis Froufe**<sup>4</sup>, **Prof. Frank Scheffold**<sup>4</sup>, **Prof. Rafael Delgado-Buscalioni**<sup>1</sup>, **Prof. J. J. Saenz**<sup>3</sup>

1. Universidad Autonoma de Madrid, 2. ICFO, 3. Donostia International Physics Center, 4. University of Fribourg

## INTRODUCTION

Fluctuating isotropic electromagnetic fields are obtained by considering a large group of plane waves with wave vectors, polarizations and phases randomly distributed and fluctuating on time. Due to the isotropic character of this electromagnetic field, the optical force induced on an electric dipole is, in average, equal to zero. However, the dynamics of electric dipoles on these kind of systems are far from being trivial. On the one hand, due to the nonzero value of the optical force fluctuations, super diffusive, diffusive and accelerated regimens are induced on a single dipole. On the other hand, when two particles are present, the isotropic symmetry breaks down and an interacting force between the two particles shows up. This interaction may lead to gravitational like potentials.

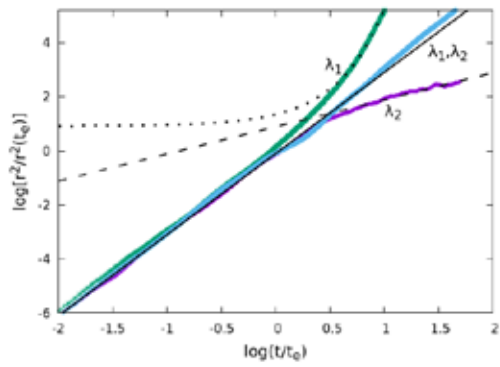
## RESULTS

In this work, the expressions for the optical random force fluctuations, the optical drag force, the equilibrium kinetic energy and mean square displacement are derived. The conditions to be fulfilled by the polarizability of the dipole in order to obtain a positive, a null, and a negative drag coefficient are analytically determined and checked against numerical simulations for the dynamics of a silver nanoparticle. Figure 1 shows a log-log plot of the mean square displacement of a silver nanoparticle versus time for different wavelengths, inducing a diffusive, superdiffusive and accelerated regime.

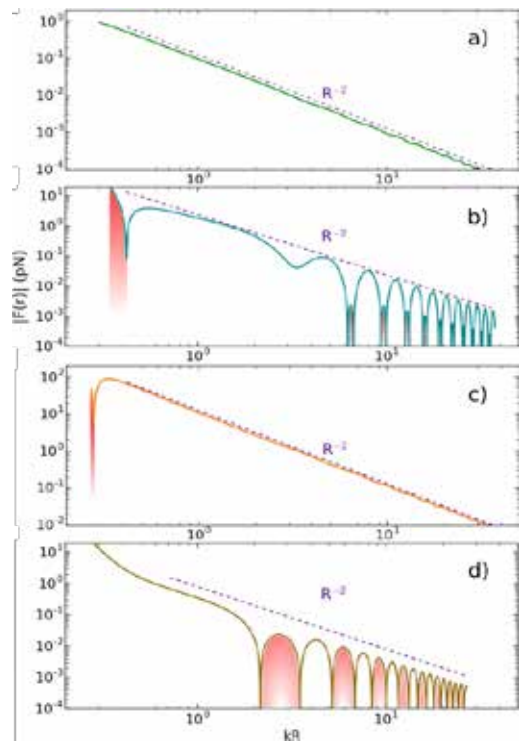
In addition, we predict the existence of Mock-Gravity attractive forces in a random light field, whenever the light frequency is tuned to an absorption line such that the real part of the particle's electric polarizability is zero. These interactions are scale independent, holding for both near and far-field separation distances. Figure 2 shows a log-log plot of the interaction force for two silver nanoparticles illuminated with a isotropic fluctuating random field with wavelengths (a) 317nm, (b) 337nm, (c) 352nm and (d) 470nm. Red shadowed regions indicate repulsive interaction forces.

## REFERENCES

- [1] Marqués M.I. Opt. Lett. 41, 796 (2016).
- [2] Marqués M.I. Phys. Rev. A 93, 063815 (2016).
- [3] López Pastor Víctor J, Marqués M.I. Submitted.
- [7] Luis-Hita J, Marqués M.I, Delgado-Buscalioni R., de Sousa N., Froufe-Pérez L.S, Scheffold F, Sáenz J.J. arXiv:1802.05648, 15 Feb 2018.



Meansquare.png



Gravityforce.png

# Optical Modulation of Flexible Pre-Structured Metallo-Dielectric Films

---

Wednesday, 3rd October @ 17:14: Nano-Optomechanics (ROOM 1) - Oral - Abstract ID: 496

---

***Mr. Ali El-Hadi Zeineddine<sup>1</sup>, Prof. Nazir Kherani<sup>1</sup>***

*1. University of Toronto*

Development of tunable materials is extremely important vis-a-vis their application to adaptive devices. Pliable metal thin-films have been investigated extensively within the framework of flexible electronics wherein the objective has been substantial preservation of electrical continuity under large strains. Recently our group has examined the influence of strain on the optical properties of nano-thin metal films deposited on polydimethylsiloxane. In particular, we have shown that a range of micro and nano length scale cracks develop in the strained metal films subject to the use of specific synthesis techniques. Further, a range of optical phenomena were observed under strain including surface plasmon resonances and optical scattering. In contrast, herein we report on investigating the potential of achieving specifically preferred optical response under strain through a-priori designed structuring of metal thin films on a pliable substrate. Our COMSOL study shows that a set of optical responses correspond to specific sets of micro and nano structured thin metal films under strain.

# Optomechanical Kerker effect

Wednesday, 3rd October @ 17:31: Nano-Optomechanics (ROOM 1) - Oral - Abstract ID: 262

*Dr. Alexander Poshakinskiy*<sup>1</sup>, *Dr. Alexander Poddubny*<sup>1</sup>

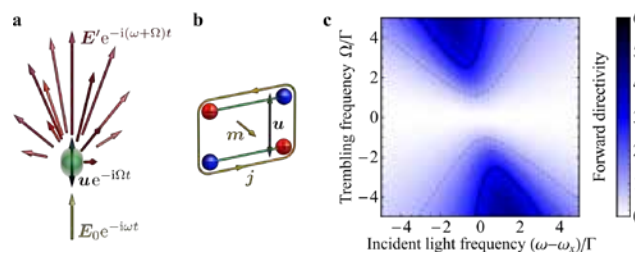
*1. Ioffe Institute*

The ability to control the direction, frequency, and polarization of the scattered light is essential for operation of antennas, routing of light, and design of topologically protected optical states. For visible light scattered on a particle, the directionality can be provided by the Kerker effect, exploiting the interference of electric and magnetic dipole emission patterns. However, magnetic optical resonances in the particles smaller than the light wavelength in the medium are relativistically weak.

Here, we put forward an optomechanical Kerker effect, where the tunable directional forward or backward inelastic scattering is achieved for a particle lacking magnetic resonances that trembles in space, see panel (a) of the Figure. Our concept is sketched in panel (b). The incident wave excites electric dipole polarization of the particle that oscillates in time. Trembling of the electric dipole in the direction transverse to its polarization induces the loop electric current with non-zero magnetic momentum as well as the electric quadrupole momentum. To describe this multipole conversion, we have developed a novel theoretical framework that incorporates rigorously the effect of the resonant dispersion of the moving medium on the multipolar emission and goes beyond previous approaches restricted to dielectric scatterers with non-resonant permittivity.

We found that the phase difference between electric and magnetic dipoles induced in the trembling particle is governed by the frequency dependence of the particle permittivity. For a particle with resonant permittivity, this enables control of the scattering direction via the detuning of light frequency from resonance. Panel (c) shows by color the forward directivity of the scattered light. The directivity can reach the values up to 5.25 that surpasses the limiting value of 3 for the classical Kerker effect, because the motion-induced electric quadrupole is additionally involved.

Our results apply to a variety of optomechanical systems based on the objects with resonant response, such as quantum dots, two-dimensional semiconductors, cold atoms, or superconducting qubits. We also put forward an optomechanical spin Hall effect, i.e., directional inelastic scattering of light depending on its circular polarization.



Optomech kerker.png

---

## Light Control using Microlens Arrays

---

Wednesday, 3rd October @ 16:40: Advanced imaging for photonic materials (ROOM 2) - Oral - Abstract ID: 379

---

***Prof. Nikolai Petrov<sup>1</sup>, Mrs. Galina Petrova<sup>1</sup>***

*1. Scientific and Technological Center of Unique Instrumentation of Russian Academy of Sciences*

Micro-optical elements are widely used in modern optical systems, such as light homogenizers, LEDs, displays, illumination systems, etc. Other application is the 3D image systems. Diffractive elements are the most powerful method for beam shaping, however, there are issues including the limitation to monochromatic illumination, limited divergence angles, and zero order, typically due to fabrication errors. A new class of beam shapers such as periodic microlens arrays has high transmission efficiency, controlled angular distribution and homogenized light [1].

In this paper, the analysis of the influence of the parameters of radiation source (wavelength, wavefront curvature, coherence, polarization) and micro-lens array (sag, lens size, refractive index, etc.) on the parameters of a diffracted beam is presented. The method combining wave propagation and ray-tracing procedures is proposed for the analysis of partially coherent light beams diffracted by micro-lens structures. The beam field at complicated surfaces is expanded into coherent states [2], representing elementary Gaussian beams with axis displacement and tilt angle.

Optical transmission efficiency depends on the polarization of incident light, and on the lens surface orientation relative to the light source. Influence of the randomization of the parameters of MLA on the intensity distribution is investigated.

In Fig. 1 the intensity distributions and radiation patterns for coherent (a, c) and low-coherent (b, d) sources are presented.

It is shown that it is possible to split the incident beam into a set of identical focused beams located at the same distances from each other (Fig. 2). In Fig. 3 the formation of independent beams during the propagation of light behind the MLA screen is shown. It is followed from the simulations that each of the beams propagate independently. The angular separation of the beams depends on the aspect ratio of MLA. For the considered values of  $R_L = 10 \mu\text{m}$  and  $R_{sc} = 3 \mu\text{m}$  the angular separation between spots is equal to 16.23 mrad.

Acknowledgement: The financial support by the Russian Science Foundation (project No. 17-19-01461) is highly appreciated.

### References

- [1] T.R.M. Sales, Opt. Eng. **42**, 3084-3085 (2003).
- [2] N.I. Petrov, G.N. Petrova, Optics Express **25**, No. 19, 22545-22564 (2017).

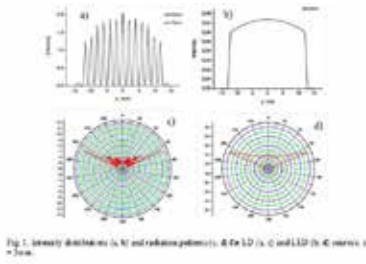
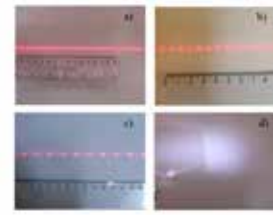
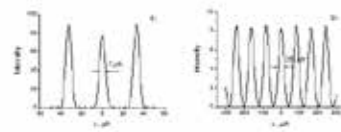


Fig1 mla.jpg



Measurement fig2.jpg



Simul mla fig3.jpg

---

# Surface profile 3D visualization from thickness map reconstruction of thin films using scattering of surface plasmon polaritons

---

Wednesday, 3rd October @ 16:57: Advanced imaging for photonic materials (ROOM 2) - Oral - Abstract ID: 268

---

*Dr. Rodolfo Cortés-Martínez*<sup>1</sup>, *Dr. César E. García-Ortiz*<sup>1</sup>, *Dr. Raúl Hernández-Aranda*<sup>2</sup>, *Dr. Felix Aguilar-Valdez*<sup>3</sup>, *Dr. Víctor M. Coello-Cárdenas*<sup>1</sup>

1. CICESE, Unidad Monterrey, 2. Tecnológico de Monterrey, 3. INAOE

We present a method to obtain wide ( $\sim\text{mm}^2$ ) three-dimensional (3D) thickness maps of dielectric thin films, with sub-nanometer precision, using the scattering produced by surface plasmon polaritons (SPPs). SPPs are electromagnetic modes coupled to electron plasma oscillations confined to the interface between a metal and a dielectric. We use the phenomenon of SP resonance to determine the thickness of a thin film. The experimental setup (Kretschmann configuration) with an imaging system was used to take images with a CCD camera of the same area of interest as the prism is rotated [Figure 1]. Optical images of the surface at different angles of excitation were achieved. Each pixel of the CCD as individual power detectors was used to register the intensity of the scattered light. By using an automated post-processing algorithm that runs a MATLAB script we find the thickness of the film at each point of the surface, corresponding to every pixel of the camera, using a semi-analytical numerical fit (Figure 2). Figure 3 shown scattering measurements obtained with the CCD camera and fitting (solid lines) for the four fabricated samples with flat surfaces. Figure 4 shown the full 3D reconstruction of the dielectric film thickness. The details of the logo are clearly visible. The inset shown an atomic force microscope topography measurement of a transverse section  $x$  along the edge of the structure. The samples consisted of thin magnesium fluoride ( $\text{MgF}_2$ ) coatings ( $< 100$  nm), deposited via thermal evaporation on top of a 45-nm-thick gold film on a glass substrate. The intensity of the scattered light was detected by SPPs decoupled by the local roughness of the films. We used the correlation coefficient  $R^2$  to fit the results as a figure of merit to determine the minimum amount of square pixels that would be necessary to average, in order to get a reliable experimental curve ( $R^2 > 0.9$ ). A value of  $R^2 = 0.9279$  was found for the  $3 \times 3$  array case. The resonances were analyzed through numerical fitting to find the thickness of dielectric films. This technique can be applied to investigate macroscopic inhomogeneities in dielectric thin films.

---

# Nanodisk lasers for internalisation by live cells

---

Wednesday, 3rd October @ 17:14: Advanced imaging for photonic materials (ROOM 2) - Oral - Abstract ID: 394

---

***Mr. Alasdair Fikouras<sup>1</sup>, Dr. Marcel Schubert<sup>1</sup>, Mr. Markus Karl<sup>1</sup>, Dr. Dinesh Kumar<sup>1</sup>, Dr. Simon Powis<sup>1</sup>, Dr. Andrea Di Falco<sup>1</sup>, Prof. Malte Gather<sup>1</sup>***

*1. University of St Andrews*

## Introduction

Biomedical imaging has driven research into intracellular light sources which can complement the functionality of presently used molecular dyes. These nanophotonic objects, such as quantum dots, are governed by spontaneous processes and as a result exhibit broad spectral features and limited signal to noise ratios. Inter-cellular laser emitters both overcome these limitations and present opportunities for spectral multiplexing and sensing, as illustrated in recent proof-of-concept studies [1,2]. However, these initial experiments were limited by the large laser sizes and thresholds [3]. Here, we report on design, high-throughput fabrication and application of semiconductor nanodisk lasers for this purpose. By exploiting the large optical gain and high refractive index of GaInP/AlGaInP quantum wells, we obtain lasers with volumes 1000-fold smaller than the eukaryotic nucleus ( $V_{\text{laser}} < 0.1 \mu\text{m}^3$ ), lasing thresholds 500-fold below the pulse energies typically used in two-photon microscopy ( $E_{\text{th}} \approx 0.13 \text{ pJ}$ ), and excellent spectral stability ( $< 50 \text{ pm}$  wavelength shift).

## Methods

Nanodisks were produced from an epitaxially grown quantum well structure. A resist was patterned using electron beam lithography and a two-step wet etch to deposit the nanolasers into petri-dishes ready for characterisation and cell culturing.

## Results and Discussion

A range of different cell types readily internalized nanodisk lasers via natural phagocytosis. Importantly, internalisation was also observed for T-cells and neurons which are too small to engulf the previously reported cell lasers and/or not specialised for phagocytosis, illustrating the importance of using sub- $\mu\text{m}$  sized lasers for cell internalisation. Additionally, due to the small size of our new lasers, each cell can internalise multiple nanodisk lasers without adding a heavy payload. The multiplexed emission spectrum from these lasers provides a highly characteristic optical barcode, thus allowing to uniquely label large numbers of cells. Furthermore, we demonstrate that the lasers do not encumber the cells and so can be used to track migration of cells through micro-pores, thus providing a powerful tool to study processes like cancer invasion.

## References

1. Gather, M. C. & Yun, S. H. Nature Photonics 5, 406-410 (2011).
2. Schubert, M. et al. Nano Letters 15, 5647-5652 (2015).
3. Hill, M. T. & Gather, M. C. Nature Photonics 8, 908-918 (2014).



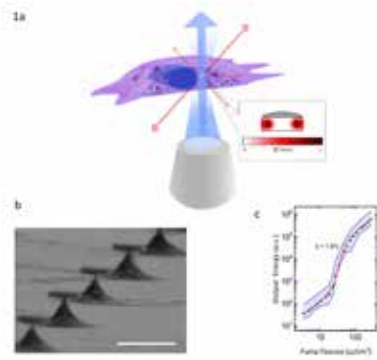


**Fig. 1 | Concept and characterisation of intracellular nanodisk lasers.** **a.** Illustration of a semiconductor nanodisk laser internalised by a eukaryotic cell. The disk is optically pumped through a microscope objective (blue) and the laser emission (red) is collected via the same objective. Inset shows the calculated profile of the lowest order mode for a 750 nm diameter disk made of a GaInP/AlGaInP quantum well structure. **b.** Scanning electron microscopy of an array of as fabricated nanodisks on a substrate. Scale bar, 1  $\mu\text{m}$ . **c.** Threshold characteristics for 10 detached nanodisk lasers in cell medium on a log-log plot of light intensity as a function of pump fluence (black symbols, average; blue lines, min-to-max range of all lasers) and fit to the data with rate-equation model (red line).

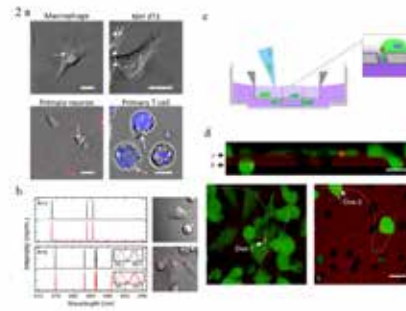


**Fig. 2 | Intracellular semiconductor nanodisks.** **a.** DIC microscopy of macrophage, M17 ST3 primary neuron and T cell with internalized nanodisks (overlaid red fluorescence, indicated by white arrows). Nucleus of T cell labelled by blue Hoechst dye. **b.** Demonstration of optical hysteresis of cells with 3 and 6 internalized nanodisk lasers, comparing spectra at the beginning of the experiment and after 1 h (left). DIC microscopy images of cells with overlaid red fluorescence from nanodisks (right). Inset for  $N = 6$  shows spectra collected for individual excitation of three lasers with similar emission spectra. **c.** Schematic cross-section of transmembrane migration assay. **d.** Live cell laser scanning confocal microscopy of membrane insert (weak red auto-fluorescence) with eGFP labelled cells (green) and nanodisk lasers (bright red). Arrows in top panel indicate the xy-slices shown in the bottom panels; dashed lines in bottom panels indicate the path of the cross-section in the top panel. Scale bars, 20  $\mu\text{m}$ .

C3d1d6b4-0029-48f8-a9d2-0cbdbd9cdb99.jpeg

7f389afa-1952-4034-a7ee-5bbceac8e24a.jpeg

---

# Dust particles contamination monitoring in the backscattering light experiment for the LISA mission

---

Wednesday, 3rd October @ 17:31: Advanced imaging for photonic materials (ROOM 2) - Oral - Abstract ID: 345

---

*Dr. Sibilla Di Pace*<sup>1</sup>, *Dr. Arwa Dabbech*<sup>2</sup>, *Mr. Vitalii Khodnevych*<sup>1</sup>, *Dr. Michel Lintz*<sup>1</sup>, *Dr. Nicoleta Dinu-jaeger*<sup>1</sup>

1. *Laboratoire Artemis, Université Cote d'Azur, OCA and CNRS, NICE*, 2. *Institute of Sensors, Signals and Systems, Heriot-Watt University, Edinburgh*

## Introduction

In the context of space-based optics, contamination of the optics due to particle deposition is inevitable and constitutes a critical issue. This gets more challenging for the sensitive heterodyne measurements of the Laser Interferometer Space Antenna (LISA), the space-based gravitational wave observatory to be launched in 2034. Therefore, table-top experiments need to be developed for a better understanding of how  $\mu\text{m}$ - to  $\text{mm}$ -size dust particles present on optical surfaces affect LISA measurements.

## Methods

We realised an experiment for constant monitoring of dust deposition on a mirror surface via a reflex camera and developed image processing methods to analyse the pictures. The set-up consists of a 12.5mm diameter mirror under test (MUT) placed on a micrometric translation stage and shined from the side (fig.1). We use a remotely controlled reflex camera with a macro objective constantly looking at the MUT and taking pictures. This set-up will be integrated to a homodyne Michelson interferometer designed to measure the coherent backscattering (CBS) from an optical surface with small roughness or contamination. Once integrated, the two experiments will allow to correlate the CBS signal with the physical properties of the dust particles identified on the MUT.

Dust particles are analysed via image processing techniques in MATLAB [1]. At a first instance, a sparse image composed of compact structures is estimated from the original image (fig.2) using convex optimisation theory and sparse representations framework. The constructed image is then analysed via MATLAB built-in functions where segmentation is performed, followed by the classification of the detected spots (size, position, flux, peak intensity). The smallest spot-diameter identified has a value of  $5\mu\text{m}$  (camera sensor pixel-size is  $3.9\mu\text{m}$ ) (fig.3). Spot-sizes range from  $5\mu\text{m}$  to  $390\mu\text{m}$ .

## Conclusion

This analysis applied on consecutive images helps to detect the apparition of dust. Improvements to reduce computational time and comparison with other image processing techniques are planned. The first results of the simultaneous measurements of the CBS signal and image processing on the pictures will be presented.

## Acknowledgments

This work is co-funded by: RegionPACA, Thales Alenia Space, Observatoire de la Cote d'Azur, CNES, CNRS

## Bibliography

1 A Dabbech *PhD Thesis* <https://tel.archives-ouvertes.fr/tel-01191496/document>

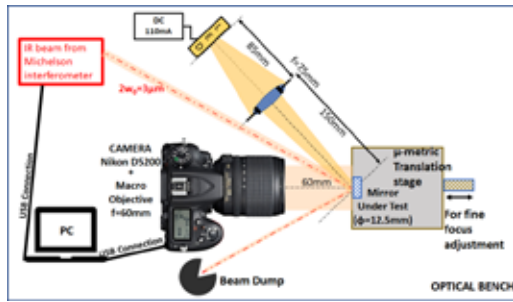


Figure1 scheme of the experimental set-up.png

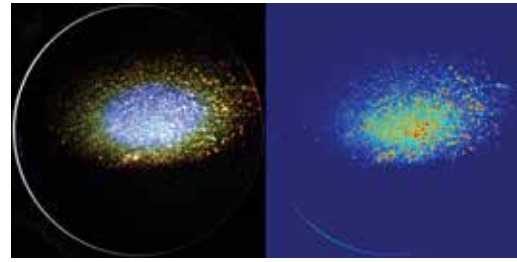


Figure2 example of a picture taken to the mirror under test left and the results of the image processing right .png

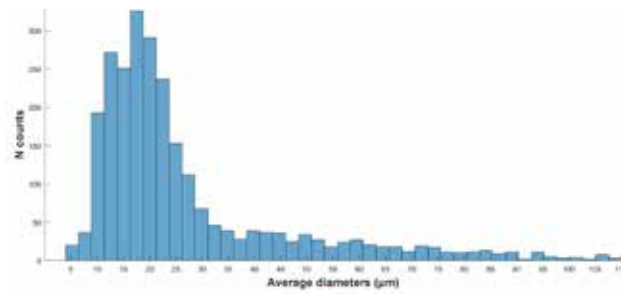


Figure3 histogram of the retrieved spot diameters in m plotted between values 5 m the smallest and 110 m. detected spot diameters range from 5 m to 390 m.png

## Localized surface plasmon studies on Au@Ag cuboids by electron energy-loss spectroscopy (EELS). Application to SERS experiments.

Wednesday, 3rd October @ 16:40: Enhanced spectroscopy and sensing (AUDITORIUM) - Oral - Abstract ID: 60

**Dr. Israa Haidar**<sup>1</sup>, **Dr. Guillaume Radtke**<sup>2</sup>, **Dr. Markus Krug**<sup>3</sup>, **Dr. Andreas Hohneau**<sup>3</sup>, **Dr. Viktor Kapetanovic**<sup>4</sup>, **Prof. Joachim. R. Krenn**<sup>3</sup>, **Dr. Matthieu Bugnet**<sup>5</sup>, **Prof. Gianluigi Botton**<sup>6</sup>, **Dr. Leïla Boubekour-lecaque**<sup>7</sup>, **Prof. Nordin Felidj**<sup>7</sup>

1. Université Paris Diderot, 2. university Pierre et Marie Curie, 3. University Karl Franzens, 4. McMaster University, 5. McMaster University / UCBL Lyon 1, 6. Mc Master University, 7. University Paris Diderot

The plasmonic response of metallic nanoparticles is frequently characterized using far-field and near-field optical techniques. Although these techniques are commonly used to investigate localized surface plasmon (LSP) modes, some relevant information cannot be provided such as dark modes (using for instance dark-field or extinction spectroscopies), or are limited by the spatial resolution to a few tens of nanometres using Near-field scanning optical microscopies. In this context, electron energy-loss spectroscopy (EELS) appears as a great tool, capable of probing bright and dark plasmonic modes at unprecedented spatial resolutions [1]. In particular, dark modes have great promise due to a strong confinement of energy. As a result of their vanishing dipole moments, inducing an inhibition of radiative losses, dark modes can store electromagnetic energy [2]. Such modes make them ideal candidates for surface enhanced spectroscopies such as surface enhanced Raman scattering (SERS) applications.

In this work, LSP mapping of Au@Ag cuboids are investigated by EELS. Different configurations of cuboids dimers are considered: end to end assembly, T and L shapes (Fig. 1, left). EELS mapping reveals LSP modes at various energies, including bright and dark modes, in excellent agreement with simulations done with the MNPBEM tool-box (Fig. 1, right) [3]. Captured by EELS, those modes should be a source of strong local electromagnetic field, of high interest in the context of SERS experiments.

Fig. 1. (left): SEM images of different configurations of Au@Ag nanorod dimers end to end assembly, T and L shapes; (right) experimental and calculated EELS mapping of a Au@Ag nanorods dimer end to end at 1.37 eV.

[1] Nelayah, J., Kociak, M., Stéphan, O., de Abajo, F.J.G., Tencé, M., Henrard, L., Taverna, D., Pastoriza-Santos, I., Liz-Marzán, L.M. and Colliex, C., 2007. Mapping surface plasmons on a single metallic nanoparticle. *Nature Physics*, 3(5), p.348.

[2] Bosman, M., Keast, V.J., Watanabe, M., Maarroof, A.I. and Cortie, M.B., 2007. Mapping surface plasmons at the nanometre scale with an electron beam. *Nanotechnology*, 18(16), p.165505.

[3] F. P. Schmidt, H. Ditlbacher, A. Hohenau, U. Hohenester, F. Hofer, and J.R. Krenn "Edge Mode Coupling within a Plasmonic Nanoparticle", *NanoLetters*, 16, 5152 (2016).

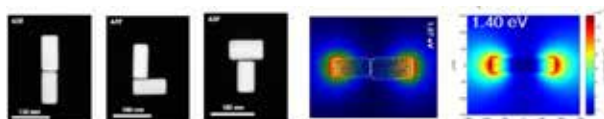


Fig eels.jpg

# Time-resolved four-wave mixing using Laguerre-Gauss modes

Wednesday, 3rd October @ 16:57: Enhanced spectroscopy and sensing (AUDITORIUM) - Oral - Abstract ID: 64

***Dr. Pierre Gilliot*<sup>1</sup>, *Mr. Marc Ziegler*<sup>1</sup>, *Prof. Bernd Hönerlage*<sup>2</sup>, *Dr. Mathieu Gallart*<sup>2</sup>**

*1. CNRS-IPCMS, 2. University of Strasbourg - IPCMS*

We perform four-wave mixing (FWM) experiments using Laguerre-Gauss (LG) beams and give a description of the signal generation.

Usual FWM setup use non-collinear beams that are characterized by their wave-vectors  $\mathbf{k}_2$  and  $\mathbf{k}_1$ . The emitted signal is discriminated by its propagation direction given by the phase matching condition  $\mathbf{k}_s=2\mathbf{k}_2-\mathbf{k}_1$ . This situation forbids a strong focusing which would need a large numerical aperture

The configuration we propose uses LG beams. They show a phase profile, which is associated to an orbital angular momentum (OAM) that is characterized through the quantized azimuthal number  $l$ . The FWM signal is discriminated using a new phase matching condition that writes  $l_s=2l_2-l_1$ . In particular,  $l_2=1$  and  $l_1=2$  beams show a donut spot profile with a zero-intensity at the center, where the  $l_s=0$  signal (which has a Gaussian beam profile) is emitted: it can thus be easily spatially filtered. It is then possible to use collinear beams that can thus be tighter focused. This method paves the way to nonlinear spectroscopy experiments performed with an improved spatial resolution that allows for a measurement of sample inhomogeneities.

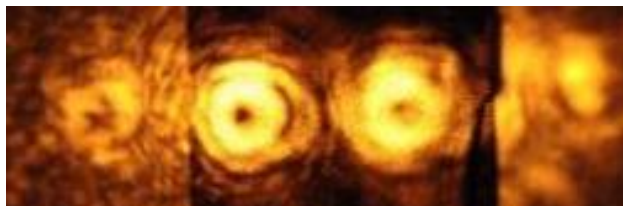
We have performed\* time-resolved experiments on CdTe quantum wells and compared the dynamics measured in a usual configurations with non-collinear Gaussians beams to that of the configuration involving collinear LG beams. The identical decay that is obtained shows that the OAM is transferred to and then conserved by the electronic excitations, allowing to measure their dynamics.

A general description of the interaction between LG modes or Hermite-Gauss (HG) modes can be also given. It involves the calculation of the spatial profile products as nonlinear processes are determined by the products of the incident electric fields. We exploit in particular the richness of the operatorial description of generalized Hermite-Laguerre-Gauss beams.

\* D. Persuy, M. Ziegler, O. Crégut, K. Kheng, M. Gallart, B. Hönerlage, and P. Gilliot, Phys. Rev. B 92, 115312 (2015)

*Figure caption: Beam profiles. Middle:  $l_b=2$  and  $l_a=1$  incident beams.*

*Left,  $l_{out}=2l_b-l_a=3$  and right,  $l_{out}=2l_b-l_a=0$  FWM signals*



Figureabstract.jpg

# Trigonal symmetric plasmonic array of standing wires for broadband, polarization insensitive molecular sensing.

Wednesday, 3rd October @ 17:14: Enhanced spectroscopy and sensing (AUDITORIUM) - Oral - Abstract ID: 469

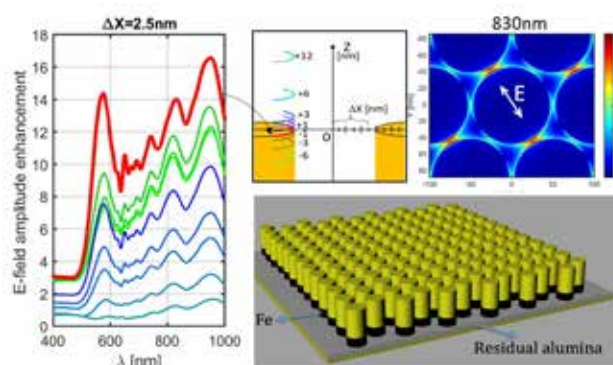
**Dr. Andrea Giugni<sup>1</sup>, Dr. Bruno Torre<sup>1</sup>, Dr. Marco Allione<sup>1</sup>, Dr. Giovanni Marinaro<sup>1</sup>, Dr. Gobind Das<sup>1</sup>, Prof. Jurgen Kosel<sup>1</sup>, Prof. Enzo Di Fabrizio<sup>1</sup>**

<sup>1</sup>. King Abdullah University of Science and Technology (KAUST), 23955-6900, Thuwal KSA

We present a simple and powerful standing nanowires array device developed for applications in surface-enhanced Raman spectroscopy (SERS). Plasmonic active gold wires grown on iron disks, and partially immersed in a supporting alumina matrix constitute it.

Looking for a cost-effective large area production technique, we designed a nanostructured device realizable by the galvanic bath and etching process. The elected fabrication method let the parallel growth of the nanowires directly in ordered pores of anodized alumina template with the possibility to select their gaps, size, diameter, and spatial arrangement from nano to microscale for the broadest spectral range scalability.

Extensive numerical calculations in the visible and NIR regimes have been used to characterize the spectroscopic properties versus its design, allowing a detailed description of the sensing abilities of the tool. The electromagnetic design analysis demonstrated a broadband plasmonic enhancement, effect useful for many standard excitation wavelengths in the visible and NIR. The trigonal pores arrangement impressed by the porous alumina and the cylindrical shape of the wire result in a plasmonic coupling efficiency weakly dependent on the polarization of the incident field. The devices, tested with 633 and 830 nm laser lines on two standards, physisorbed Rhodamine 6G and chemisorbed Benzenethiol show a significant Raman enhancement factor, up to around  $6 \times 10^4$ , with respect to the flat gold surface, used as a reference for the measurements of the investigated molecules. Optimizing the electrochemical technique allowed us to realize a large active area device, up to the  $\text{cm}^2$  range, for spectroscopic application with broadband spectral responses, weakly sensitive to polarization orientation, and high spatial homogeneity with respect the typical diffraction limited probe spot areas, appreciated properties in a plasmonic sensor for chemical analysis.



Plasmonic standing wires for broadband polarization insensitive sensing.jpg

---

## Low Frequency Raman spectroscopy of small gold clusters: limits of Lamb model ?

---

Wednesday, 3rd October @ 17:31: Enhanced spectroscopy and sensing (AUDITORIUM) - Oral - Abstract ID: 58

---

**Mr. Quentin Martinet**<sup>1</sup>, **Dr. Adrien Girard**<sup>2</sup>, **Dr. Alice Berthelot**<sup>1</sup>, **Dr. Baira Donoeva**<sup>3</sup>, **Ms. Clothilde Comby-zerbino**<sup>1</sup>, **Dr. Franck Bertorelle**<sup>1</sup>, **Ms. Marte Van Der Linden**<sup>3</sup>, **Dr. Nathalie Tarrat**<sup>4</sup>, **Prof. Nicolas Combe**<sup>4</sup>, **Dr. Jeremie Margueritat**<sup>1</sup>

1. Université Claude Bernard Lyon 1, 2. Goethe-Universität, 3. Utrecht University, 4. Université Paul Sabatier Toulouse 3

Metallic nanoclusters present interesting optical, vibrational, electronic and catalytic properties and explain why they have numerous fundamental research and applications. Properties of metallic clusters are due, like for nanocrystals, to their size and shape as well as to their discrete electronic structure alike organometallics systems. Therefore it is essentially to explain the correlation between the geometrical structure, i.e. the spatial confinement, and its properties. Studies of the vibrational behaviors of clusters are great approaches to accomplish this objective. The theory of elasticity by Horace Lamb regarding a free homogeneous sphere<sup>1</sup>, perfectly predicts the frequency of the vibration of a nanoparticle as a whole. These modes, coming from the confinement of the acoustic waves, allow to probe their size, shape, crystallinity and surrounding environment. Furthermore recent works<sup>2</sup> have shown that this theory based on the linear elastic theory is still valid for clusters as small as Au<sub>75</sub>. In this study, we investigate the vibrational modes of ultrasmall gold clusters (Au<sub>9</sub> and Au<sub>6</sub>), capped with phosphorous ligands, by acquiring their low frequency Raman scattering to determine if continuum mechanics remains still accurate for such sizes. Two distinct vibrational modes involving the gold core and depending on the size of the clusters have been identified and calculations taking into account the real position of the atoms have been developed. Moreover, another vibration due to the mechanical coupling<sup>3</sup> among clusters is observed for the first time in such sample.

### Reference:

- (1) Lamb, H. On the Vibrations of an Elastic Sphere. *Proc. London Math. Soc.* **1881**, s1-13, 189–212.
- (2) Saucedo, H. E.; Mongin, D.; Maioli, P.; Crut, A.; Pellarin, M.; Fatti, N. Del; Vallée, F.; Garzón, I. L. Vibrational Properties of Metal Nanoparticles: Atomistic Simulation and Comparison with Time-Resolved Investigation. *J. Phys. Chem. C* **2012**, *116*, 25147–25156.
- (3) Girard, A.; Gehan, H.; Crut, A.; Mermet, A.; Saviot, L.; Margueritat, J. Mechanical Coupling in Gold Nanoparticles Supermolecules Revealed by Plasmon-Enhanced Ultralow Frequency Raman Spectroscopy. *Nano Lett.* **2016**, *16*, 3843–3849.

# Authors Index

Abadal, S.	11	Baffa, O.	150
Abakumov, M.	35	Baidakova, N.	34
Abraham Ekeroth, R.	12	Bailly, M.	184
Abstreiter, G.	92	Baker, C.	254
Abu-Safe, H.	39	Bakker, R.	251
Adhlakha, N.	65	Bakr, O.	66
Adão, R.	53	Banzer, P.	69, 163
Agarwal, N.	98	Barbosa, A.	101
Agnoli, S.	46	Barczyk, R.	69
Aguilar-Valdez, F.	264	Barho, F.	87, 93
Ah, C.	134	Barois, P.	84
Ahmadi, A.	159	Baron, A.	84, 136, 142
Ahmadi, L.	184	Barreda, A.	40
Aimukhanov, A.	97	Bartolini, P.	193
Alarcón, E.	11	Baryshev, A.	182
Albella, P.	40	Baryshnikova, K.	79
ALI, H.	121	Bayle, M.	47
Allione, M.	17, 66, 112, 154, 271	Bedu, F.	122
Allsopp, D.	59	Belloeil, M.	74
Alonso, M.	211	Ben Sedrine, N.	74
Altug, H.	148	Bendix, P.	175
Alves, A.	74	Benichou, E.	256
Alves, E.	74, 78	Benoit, J.	137
Amer, M.	76	Berthelot, A.	137, 257, 272
Andersson, O.	52	Bertorelle, F.	272
Andreani, L.	30	Bessonov, V.	79
Andreotti, G.	72	Biccari, F.	72
Andrianov, E.	23	Bimberg, D.	1
AnferteV, V.	140	Birarda, G.	25
Angelini, A.	29	Bisio, F.	216
Anupama, Y.	128	Blondeau, J.	8
Apostolakis, A.	140	Boarino, L.	29
Appelt, C.	60	Bockowski, M.	74
Armin, R.	61	Bogdanowicz, J.	230
Asilevi, L.	184	Bomers, M.	93
Askes, S.	68, 192	Bonnet, C.	257
Assis, J.	173	Boonsin, R.	242
Astilean, S.	21, 166	Boschetti, A.	193
Aucélio, R.	101	Botchkova, E.	107
Aydındoğan, G.	123, 206	Botton, G.	269
		Boubekeur-lecaque, L.	269
B. Oddershede, L.	175	Bouhelier, A.	249



Bouteille, B.	136	Cohen, L.	190
Boutinaud, P.	242	Colas Des Francs, G.	137, 249
Bowen, W.	254	Coluccio, M.	14
Boyer, D.	242	Combe, N.	272
Bozio, R.	46	Comby-zerbino, C.	272
Brevet, P.	256	Comoretto, D.	146
Briere, G.	119	Compagnini, G.	246
Brioso Dias, E.	138	Condorelli, M.	246
Bryukhanov, V.	108	Consales, M.	99
Budner, B.	120	Conti, C.	250
Bugnet, M.	269	Correia, M.	74
Bunning, T.	177	Cortés-Martínez, R.	143, 264
Butet, J.	256	Cottancin, E.	257
Bychenko, M.	107	Coulon, P.	59
Bychkov, I.	105, 241	Cox, J.	157
Bürgi, T.	177	Cremona, M.	101
		Crut, A.	257
Cabellos-Aparicio, A.	11	Cuche, A.	249
Cabrini, S.	3	Cuda, G.	112
Calisi, N.	72	Cudney, R.	106
Campu, A.	21, 166	Cusano, A.	99, 152
Candeloro, P.	14	Czyszanowski, T.	81, 110
Canepa, M.	216		
Caporali, S.	72	D'orlando, A.	47
Carabelli, V.	248	D'urso, L.	246
Cardoso, J.	74	Dabbech, A.	267
Carmen, R.	38	Dadadzhyanov, D.	13
CASAS-RAMOS, M.	115	Danilov, V.	111
Castaldi, G.	99	Das, G.	271
Cataldi, U.	177	Daudin, B.	74
Caynak, S.	123	Dauer, C.	130
Cerea, A.	25	De Angelis, M.	112
Cerutti, L.	87, 93	De Beule, P.	173
Cesca, T.	46	De Cicco, S.	84
Chadeyron, G.	73, 242	De Leo, N.	29
Chen, Y.	165	De Liberato, S.	181
Cheng, P.	203	De Luca, A.	152
Cheon, S.	134	De Mello, J.	22
Cherpakova, Z.	44	De Sio, L.	177
Cheuveau, J.	238	De Sousa, N.	258
Cho, S.	134	Degiovanni, I.	248
Choi, D.	148, 234	Del Rosso, T.	101
Chou, J.	128	Delgado-Buscalioni, R.	258
Ciattoni, A.	187, 250	Della Sala, F.	180
Ciraci, C.	180	Demesy, G.	27, 126
Clarke, D.	150	Demin, M.	108
Clemens, M.	240	Demirdjian, B.	122
Coello-Cárdenas, V.	143, 264	Dems, M.	110

Dengler, S.	228	Fiutowski, J.	143
Descrovi, E.	29, 184	Flamant, Q.	84
Dezert, R.	136, 142	Fleischhauer, M.	130
Di Fabrizio, E.	14, 17, 66, 112, 154, 271	Focsan, M.	21, 166
Di Falco, A.	187, 265	Fornasari, L.	188
Di Gaspare, A.	65	Forneris, J.	248
Di Giulio, V.	170	Frascella, F.	29
Di Pace, S.	267	Freire Júnior, F.	101
Di Pietro, P.	65	Frosiniuk, A.	36
Diallo, B.	8	Froufe, L.	6, 258
Dinu-jaeger, N.	267	Frąckowiak, E.	70
Disseix, P.	73	Fu, Y.	251
Ditalia Tchernij, S.	248	Gabelloni, F.	72
Djemoui, L.	229	Galdi, V.	99
Donat, F.	242	Galeotti, F.	152
Donoeva, B.	272	Gallart, M.	270
Dore, C.	211	Garcia, A.	220
Drobczyński, S.	50	García De Abajo, J.	157
Dubourdieu, C.	60	García de Abajo, J.	138, 170, 196
Duguet, E.	84	García-Martín, A.	12
Dujardin, E.	249	García-Ortiz, C.	143, 264
Dzierzega, K.	8	García-Valenzuela, A.	231
Eberle, B.	228	Garnache, A.	237
Edelstein, S.	12	Garnett, E.	68, 192
Efremova, M.	35	Garshasbi, S.	164
Eggert, S.	130	Gather, M.	265
Einicker Lamas, M.	173	Gawlik, A.	230
El-Ghazawi, T.	61	Gehan, H.	257
Emani, N.	251	Generosi, A.	185
Enriquez, J.	106, 220	Genevet, P.	119, 238
Eremeeva, E.	125	Gennaro, S.	252
Espinha, A.	211	Genovese, M.	248
Evlyukhin, A.	127	Georg, N.	119
Fakhrullin, R.	202	George, J.	61
Falkner, M.	139	Georgiev, A.	227
Farias, R.	106, 220	Gerace, D.	30
Favero, I.	237	Gerlach, G.	116
Faye, D.	74	Ghiman, R.	21
Fedyanin, A.	79	Gibson, S.	159
Felici, M.	243	Gigli, C.	237
Felidj, N.	269	Gilliot, P.	270
Fernandes Pereira, M.	140	Girard, A.	257, 272
Fernandes, A.	173	Girard, C.	249
Ferraro, M.	238	Giudici, M.	238
Ferrera, M.	216	Giugni, A.	17, 66, 154, 271
Fikouras, A.	265	Golestanizadeh, T.	55
		Gomez-Correa, J.	143

Goni, A.	211	Hönerlage, B.	270
Gonzalez, F.	40	Ibrayev, N.	97, 225
Gonzalez, J.	106, 220	Ignatov, A.	83
Gonzalez-Posada Flores, F.	87, 93	Iida, T.	219
González, J.	74	Ilatovskii, D.	37
Gorbachevskii, M.	107, 171	Ion, M.	38
Gorczyca, A.	8	Iorsh, I.	155
Gozhyk, I.	136	Isic, G.	139
Gralak, B.	126	Ivanov, E.	171
Grodecki, K.	120	Jacquet, P.	136
Gubbin, C.	181	Jakob, T.	240
Gubin, M.	201	Jalali, T.	55
Guglielmelli, A.	177	Jang, J.	113
Guidelli, E.	150	Jarosz, D.	78
Gulkin, D.	79	Jauffred, L.	175
Gushchin, P.	107, 202	Jaworska, A.	20, 48
Gustafsson, A.	74	Jinuk, K.	95
Gómez Varela, A.	173	Jofre, L.	194
Görrn, P.	67, 236, 240	Joh, H.	232
Günther, M.	116	jonin, c.	256
Güven, K.	206	Jupille, J.	136
Gębski, M.	81, 110	Jörg, C.	130
Ha, S.	251	Kabgyun, J.	95
Haberko, J.	6, 132	Kamalieva, A.	16
Hadad, B.	79	Kang, M.	128
Haidar, I.	269	Kapetanovic, V.	269
Hao, Q.	151	Karabchevsky, A.	13, 79
Harea, D.	223	Karl, M.	265
He, J.	66	Karshi, K.	123
Henry, C.	122	Kasprowicz, D.	168
Hernández-Aranda, R.	264	Kazarkin, B.	224
Heyroth, F.	209	kellarev, A.	18
Hierro, A.	238	Khabushev, E.	182
Hirscher, M.	80	Khalid, M.	180
Hoff, B.	22	Kherani, N.	260
Hoffmann, V.	74	Khodnevych, V.	267
Hohneau, A.	269	Kildemo, M.	136
Hong, M.	217	Kim, D.	233
Hong, S.	232	Kim, J.	134
Hopkins, M.	59	KIM, M.	232
Horneber, A.	165	Kim, S.	134
Hu, J.	128	Kim, T.	134
Huang, S.	164	Kim, Y.	134
Humbert, b.	47	Kiselev, G.	37
Hwang, C.	134	Kivshar, Y.	148, 178
Hwang, J.	113	Kjaer, A.	175
Härtling, T.	116		

Klimov, V.	85	Lermé, J.	257
Klingberg, H.	175	Lerouge, F.	166
Koenderink, F.	198	Letscher, F.	130
Koeninger, T.	165	Leuchs, G.	163
Komar, P.	110	Lewins, C.	59
Konstantinova, E.	108	Li, B.	24
Kontoleta, E.	68, 192	Li, J.	80, 214
Kopitsyn, D.	107, 171	Li, X.	187
Kornovan, D.	155, 200	Li, Y.	190, 252
Kosel, J.	271	Li, Z.	24
Kotelev, M.	171	Lieberman, V.	128
Kozanecki, A.	78	Linden, S.	44
Krahne, R.	64	Lintz, M.	267
Krenn, J.	269	Lis, S.	59
Krivoshapkin, P.	37	Liu, M.	148
Krivoshapkina, E.	37	Liu, N.	80, 90, 214
Kroh, C.	116	Logvinenko, D.	202
Kropp, S.	240	Lopez Pastor, V.	258
Krug, M.	269	Lorenz, K.	74
Kryvyi, S.	78	Loshkarev, I.	34
Kröncke, H.	60	Lott, J.	81
Kuchierskaya, A.	171	Louarn, G.	47
Kudelski, A.	20, 48	Loukrezis, D.	119
Kumar, D.	265	Lova, P.	146
Kumar, U.	249	Lovergine, N.	63
Kuzmiak, V.	57	Lu, Y.	167
Kuzmin, D.	105, 241	Luis-hita, J.	258
Kuznetsov, A.	251	Luo, S.	22
Kymakis, E.	185	Lupi, S.	65
Kyuwon, P.	95	Lvov, Y.	202
		Lyatun, I.	108
Labbate, L.	243		
Lamperska, W.	50	Ma, L.	151
Langer, J.	70	Maack, J.	55
Langhammer, C.	52	Magalhaes, S.	78
Lanteri, S.	119	Magnozzi, M.	216
Lautru, J.	136	Mahiou, R.	73, 242
Laverdant, J.	137	Maier, S.	40, 190, 197, 252
Lazzari, R.	136	Majouga, A.	35
Le Boulbar, E.	59	Makarov, S.	178, 213
Lee, G.	113	Managò, S.	152
Lee, H.	256	Manso, M.	188
Lee, J.	134	Many, V.	84
Leitis, A.	148	Marabelli, F.	188
Leitão, J.	74	Marc, L.	5
Lemaitre, A.	91	Margueritat, J.	137, 257, 272
Leng, J.	84	Marichy, C.	6
Leo, G.	237	Marina, T.	38

Marinaro, G.	271	Nedelchev, L.	227
Marini, A.	187, 250	Nefedkin, N.	23
Marino, G.	237	Nemati, A.	217
Marques, M.	12, 258	Neshev, D.	148
Martin, O.	9, 256	Neugebauer, M.	163
Martinet, Q.	272	Neves, A.	74
Martinez, L.	106, 220	Nicolae, E.	38
Martyniuk, P.	120	Nicolet, A.	126
Martínez, E.	117	Nieder, J.	53
Masajada, J.	50	Nikiforov, A.	34
Mascart, R.	137	Nizamoğlu, S.	123
Mashanov, V.	34	Nouman, T.	113
Mateev, G.	227	Novikov, A.	107, 171, 202, 209
Matricardi, C.	211	Nurlianti, E.	66
Matsui, T.	190	NYALOSASO, J.	73
Mattei, G.	46		
Medvedskaya, P.	108	O'Faolain, L.	30
Mehrabian, A.	61	O'kane, S.	59
Meixner, A.	165	Oh, S.	65, 232
Melendez, E.	106	Olivero, P.	248
Mermet, A.	257	Omelyanchik, A.	35
Merzlikin, A.	83	Orlikovsky, N.	182
Meudt, M.	236, 240	Orzan, F.	166
Michalczewski, K.	120	Osewski, P.	168
Michieli, N.	46	Osmond, J.	211
Mihi, A.	211	Oulton, R.	190, 252
Milla Rodrigo, M.	93	Ozerov, I.	122
Miranda, A.	173		
Misiewicz, J.	230	Paci, B.	185
Mkhitarian, V.	170	Pacot, G.	93
Mohammed, M.	76	Palange, E.	187
Monteiro, T.	74	Pallerin, S.	8
Montes Bajo, M.	238	Pan, Z.	251
Morales-Luna, G.	231	Pandoli, O.	101
Moreno, F.	40	Paniagua-Dominguez, R.	251
Moretti, M.	112	Parola, S.	166
Moreva, E.	248	Passoni, M.	30
Mortensen, N.	55	Patanè, S.	98
Mukha, Y.	224	Pattelli, L.	193
Muller, N.	6	Pawlak, D.	168
Murawski, K.	120	Pazzagli, S.	158
Mutcu, S.	123	Pellacani, P.	188
Myslitskaya, N.	35	Pellerin, N.	8
		Penzo, E.	3
Nambannor, R.	221	Perozziello, G.	14
Nawrot, M.	132	Pertsch, T.	139
Nazarova, D.	227	Perucchi, A.	65
Nechayev, S.	69, 163	Peter, Y.	42

---

Petrov, M.	155, 200, 209	Reszka, A.	78
Petrov, N.	32, 111, 262	Rettori, C.	117
Petrova, G.	262	Ribeiro-andrade, R.	74
Petráček, J.	57	Richardson, K.	128
Pettinari, G.	243	Richetti, P.	84, 142
Piccirilli, F.	65	Rios, L.	220
Piccolo, F.	248	Rius, J.	194
Pieniazek, A.	78	Rizza, C.	187, 250
Pietrzyk, M.	78	Roberts, C.	128
pilot, R.	46	Robinson, P.	128
Pintea, A.	21	Rodionov, I.	182
Piotrowski, P.	168	Rodionova, V.	35
Pisano, E.	143	Rodrigues, J.	74
Pisco, M.	152	Rodriguez, C.	188
Pishimova, A.	182	Romeu, J.	194
Poddubny, A.	261	Roussey, M.	184
Podor, R.	136	Rozhina, E.	202
Polimeni, A.	243	Rubini, S.	243
Polywka, A.	67, 236, 240	Rugina, D.	21
Pong, P.	103, 207	Ruiz-cortes, V.	143
Ponsinet, V.	84	Runke, S.	240
Popov, V.	111	Ruschin, S.	18
Poshakinskiy, A.	261	Russier-antoine, I.	256
Potdevin, A.	73	Russo, M.	14
Pouresmaeil, F.	202	Russo, V.	46
Powis, S.	265	Rutckaia, V.	209
PRETE, P.	63	Ryu, H.	109, 134
Principe, M.	99	Réveret, F.	73
Prokhorov, A.	201	Römer, U.	119
Prucnal, P.	61	Sadecka, K.	168
Przeddziecka, E.	78	Sadeghi, S.	123
Puglisi, O.	246	Sadrieva, Z.	204
Pukhov, A.	23	Saenz, J.	12, 258
Pustovoit, V.	32	Sagnes, I.	237
Pyrak, E.	20, 48	Saija, R.	98
Pélisset, S.	184	Sajkowski, J.	78
Qarony, W.	203	Salmon, J.	84
Qin, K.	167	Salomé, P.	74
Quero, G.	152	Samadi, A.	175
Radtke, G.	269	Samusev, I.	35, 108
Ranguis, A.	122	Sandoval-romero, E.	115
Ratajczak, K.	70	Santamouris, M.	164
Ravaine, S.	84	Santschi, C.	9
Ravaux, J.	136	Sanvitto, D.	199
Reimer, M.	159	Savasta, S.	98
Renversez, G.	27	Savchuk, O.	53
		Savelev, R.	200, 245

---

Sawadsky, A.	254	Storici, P.	25
scardaci, v.	246	Stratakis, E.	185
Scheffold, F.	6, 258	Su, M.	247
Scheid, C.	119	Suffit, S.	237
Schilling, J.	209	Sun, Y.	213
Schmidt, O.	151	Sundarrajan, A.	221
Schmitt, N.	119	Szlachetko, K.	168
Schmitt, S.	60	Tabiryman, N.	177
Schneider, R.	242	Taghvaaee, H.	11
Scholz, C.	116	Talalaev, V.	209
Schubert, M.	265	Taliercio, T.	87, 93
Schulze, A.	230	Tamayo-Arriola, J.	238
Schwarzburg, K.	60	Tang, C.	203
Schwingenschloegl, U.	76	Tanyeli, I.	52
Scian, C.	46	Tarrat, N.	272
Sedlarik, V.	223	Taschin, A.	193
Selivertsova, E.	225	Tcibulnikova, A.	108
Semrau, M.	25	Teisseire, J.	136
Serena, P.	12	Teixeira, J.	74
Servida, A.	146	Temnov, V.	241
Shadrivov, I.	245	Teng, J.	217
Shalaginov, M.	128	TENG, Y.	103, 207
Shalin, A.	79	Terekhov, P.	79
Shamkhi, H.	79	Thangamuthu, M.	9
Sharonov, G.	182	Tiguntseva, E.	178
Shavrov, V.	105, 241	Timofeev, V.	34
Shaymanov, A.	182	Tittl, A.	148
Sherlekar, N.	159	Todescato, F.	46
Shibanuma, T.	40	Tokonami, S.	219
Shields, P.	59	Toma, A.	25
Shutsko, I.	67, 236	Toropov, N.	16
Signorini, R.	46	Torre, B.	17, 66, 154, 271
Siketanc, M.	173	Torre, R.	193
Silvestre, O.	53	Torres-costa, V.	188
Singh, A.	139	Tournié, E.	93
Slezhkin, V.	108	Traina, P.	248
Smirnov, A.	224	Treguer-delapierre, M.	84
Song, J.	134	Triolo, C.	98
Songki, M.	95	Trusso, S.	98
Sorger, V.	61	Tsang, Y.	203
Srinivasan, K.	221	Tückmantel, C.	67, 236
Stachowicz, M.	78	Ulkoski, D.	116
Stavitskaya, A.	202	Urbano, R.	117
Stegers, L.	240	Usievich, B.	111
Stella, U.	29	Usik, M.	105
Stepanov, A.	224	Vaccari, L.	25
Stockman, M.	89		

---

Vaks, V.	140	Yesilkoy, F.	148
Valverde, R.	173	Younghoon, S.	95
Van Den Berg, M.	165	Yu, P.	80
Van Der Linden, M.	272	Zacharchenya, I.	224
Vandervorst, W.	230	Zakhidov, A.	178
Varguet, H.	137	Zalogina, A.	245
Vartanyan, T.	13, 16	Zaman, Q.	101
Vasanelli, A.	238	Zang, M.	240
Viarbitskaya, S.	249	Zarifi, A.	55
Vinattieri, A.	72	zarrinkhat, F.	194
Vinichenko, A.	108	Zawadzki, W.	8
Vinogradov, A.	23, 125	Zednik, J.	223
Vinogradov, V.	36, 37, 125	Zeeshan, M.	159
Vinokurov, V.	171, 202	Zeineddine, A.	260
Von Freymann, G.	130	Zeng, S.	51
Vorndran, M.	163	Zhang, D.	165
Wang, X.	203	Zhang, S.	80
Wark, A.	256	Zhang, X.	154, 167
Wasiak, M.	110	Zhang, Y.	128
Wasylczyk, P.	50, 132	Zhao, X.	45
Weber Bargioni, A.	3	Zheludev, N.	2
Weyers, M.	74	Zhu, Y.	167
Wiersma, D.	193	Zhumabay, N.	225
Wiesner, S.	60	Zhumekenov, A.	66
Wilanowski, T.	20	Ziegler, M.	270
Wubs, M.	55	Zinkiewicz, L.	132
Wuchrer, R.	116	Zito, G.	152
Xin, H.	254	Zograf, G.	178
Yamamoto, Y.	219	Zoubi, H.	161
Yankovskii, G.	182	Zucchiatti, P.	25
Yaroshenko, V.	200	Zuev, D.	213, 245
		Zverev, A.	182
		Zyubin, A.	35, 108

---



**Prem** 

Conferences, Events & Workshops